RISK FACTORS AND OUTCOME PREDICATING BIOMARKER OF NEURODEGENERATIVE DISEASES

EDITED BY: Chaur-Jong Hu and Jean-Noël Octave

PUBLISHED IN: Frontiers in Neurology and Frontiers in Neuroscience and Frontiers in Psychiatry

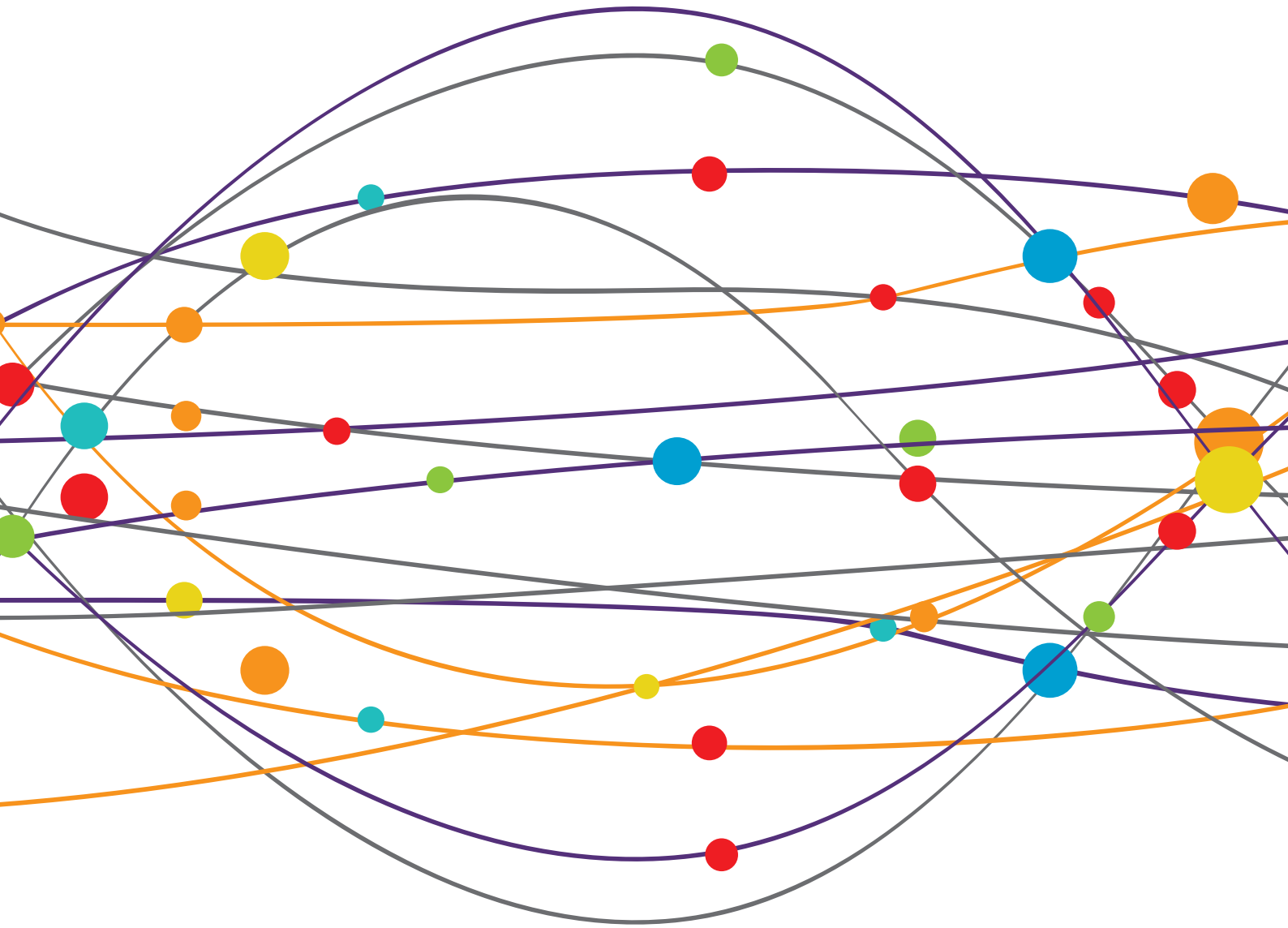

frontiers Research Topics

frontiers

ISSN 1664-8714
ISBN 978-2-88945-802-8
DOI 10.3389/978-2-88945-802-8

About Frontiers

Frontiers is more than just an open-access publisher of scholarly articles: it is a pioneering approach to the world of academia, radically improving the way scholarly research is managed. The grand vision of Frontiers is a world where all people have an equal opportunity to seek, share and generate knowledge. Frontiers provides immediate and permanent online open access to all its publications, but this alone is not enough to realize our grand goals.

Frontiers Journal Series

The Frontiers Journal Series is a multi-tier and interdisciplinary set of open-access, online journals, promising a paradigm shift from the current review, selection and dissemination processes in academic publishing. All Frontiers journals are driven by researchers for researchers; therefore, they constitute a service to the scholarly community. At the same time, the Frontiers Journal Series operates on a revolutionary invention, the tiered publishing system, initially addressing specific communities of scholars, and gradually climbing up to broader public understanding, thus serving the interests of the lay society, too.

Dedication to Quality

Each Frontiers article is a landmark of the highest quality, thanks to genuinely collaborative interactions between authors and review editors, who include some of the world's best academicians. Research must be certified by peers before entering a stream of knowledge that may eventually reach the public - and shape society; therefore, Frontiers only applies the most rigorous and unbiased reviews.
Frontiers revolutionizes research publishing by freely delivering the most outstanding research, evaluated with no bias from both the academic and social point of view. By applying the most advanced information technologies, Frontiers is catapulting scholarly publishing into a new generation.

What are Frontiers Research Topics?

Frontiers Research Topics are very popular trademarks of the Frontiers Journals Series: they are collections of at least ten articles, all centered on a particular subject. With their unique mix of varied contributions from Original Research to Review Articles, Frontiers Research Topics unify the most influential researchers, the latest key findings and historical advances in a hot research area! Find out more on how to host your own Frontiers Research Topic or contribute to one as an author by contacting the Frontiers Editorial Office: researchtopics@frontiersin.org

RISK FACTORS AND OUTCOME PREDICATING BIOMARKER OF NEURODEGENERATIVE DISEASES

Topic Editors:
Chaur-Jong Hu, Taipei Medical University, Taiwan
Jean-Noël Octave, Université catholique de Louvain, Belgium

Biomarkers for risk detection and outcome prediction of neurodegenerative diseases become more and more important for the clinical practise and neuroscience research. This eBook presents novel findings in this field, including amyotrophic lateral sclerosis, Alzheimer's disease, Parkinson's disease, Creutzfeldt-Jakob disease and application of neuroimaging, underlying mechanism of oxidative stress. The readers can catch new information about this emerging frontier of neurology with this eBook.

Citation: Hu, C.-J., and Octave, J.-N., eds. (2019). Risk Factors and Outcome Predicating Biomarker of Neurodegenerative Diseases. Lausanne: Frontiers Media. doi: 10.3389/978-2-88945-802-8

Table of Contents

frontiers in Neurology

EDITORIAL
published: 04 February 2019
doi: 10.3389/fneur.2019.00045

Editorial: Risk Factors and Outcome Predicating Biomarker of Neurodegenerative Diseases

Chaur-Jong Hu[1,2,3,4]* *and Jean-Noël Octave*[5]

[1] Department of Neurology, Shuang Ho Hospital, Taipei Medical University, New Taipei City, Taiwan, [2] Department of Neurology, School of Medicine, College of Medicine, Taipei Medical University, Taipei, Taiwan, [3] The Ph.D. Program for Neural Regenerative Medicine, College of Medical Science and Technology, Taipei Medical University, Taipei, Taiwan, [4] Taipei Neuroscience Institute, Taipei Medical University, New Taipei City, Taiwan, [5] Institute of Neuroscience, Catholic University of Louvain, Louvain-la-Neuve, Belgium

Keywords: neurodegeneration, Alzheimer's disease, Parkinson's disease, predication, biomarker

Editorial on the Research Topic

Risk Factors and Outcome Predicating Biomarker of Neurodegenerative Diseases

Neurodegenerative diseases, such as Alzheimer's disease (AD), Parkinson's disease (PD), and amyotrophic lateral sclerosis (ALS) are major public health issues in the aging population. The central nervous system undergoes considerable degeneration for years before the onset of cardinal neurodegenerative symptoms such as resting tremors in PD (1). Failure to identify highly disease-correlated risk factors or biomarkers delays the initiation of neuroprotective treatment; several clinical trials on disease modification in neurodegenerative disorders have failed because of this. The lack of reliable outcome-predicting biomarkers hinders the development of disease modification approaches (2). Epidemiological studies have presented significant risk factors for and biomarkers of neurodegenerative diseases that can be detected before diagnosis, such as mild cognitive impairment (MCI) for AD (3, 4) and rapid eye movement sleep behavioral disorder (RBD) for PD (5). Vascular risk factors accelerate AD progression (6); diabetes is associated with rapid deterioration in PD (7). However, this knowledge does not facilitate robust prediction of neurodegenerative diseases and outcomes or early initiation of neuroprotective treatment in clinical trials.

In this special issue, we have gathered eight original articles regarding biomarkers of neurodegenerative diseases. A review article explores the role of neuroimaging in neurodegenerative diseases. Articles in this special issue address three topics: clinical disease biomarkers for neurodegenerative diseases, biomarkers from animal models of neurodegenerative diseases, and biomarkers as therapeutic indicators.

CLINICAL DISEASE BIOMARKERS FOR NEURODEGENERATIVE DISEASES

Dolatshahi et al. used the database of the Parkinson's Progression Markers Initiative project for analyzing the levels of alpha-synuclein (α-syn), total tau (t-tau), phosphorylated tau (p-tau), and beta-amyloid (Aβ1–42) in cerebrospinal fluid (CSF) to determine associations between the levels of each protein and baseline clinical manifestations; Aβ1–42 levels did not differ significantly between PD and control cohorts at any time; t-tau and α-syn levels differed significantly. Only the baseline RBD questionnaire scores were predictive of temporal alterations in the α-syn levels. Longitudinal changes in the levels of CSF proteins are mutually related, and RBD is a promising prognostic predictor of PD progression. Joo et al. investigated body mass index (BMI) and the risk of progression from MCI to AD, and effects of BMI on progression to AD with age, sex, cognitive intervention, and chronic diseases as variables. Clinical data obtained from 388 patients

OPEN ACCESS

Edited and reviewed by:
Einar M. Sigurdsson,
New York University, United States

***Correspondence:**
Chaur-Jong Hu
chaurjongh@tmu.edu.tw

Specialty section:
This article was submitted to Neurodegeneration, a section of the journal Frontiers in Neurology

Received: *16 October 2018*
Accepted: *14 January 2019*
Published: *04 February 2019*

Citation:
Hu C-J and Octave J-N (2019) Editorial: Risk Factors and Outcome Predicating Biomarker of Neurodegenerative Diseases. Front. Neurol. 10:45. doi: 10.3389/fneur.2019.00045

with MCI over 36.3 ± 18.4 months of follow-up indicated that the underweight patients with MCI had a relatively high risk of AD conversion. Subgroup analysis showed that this effect was strongly observed among patients who were female, at least ≥75 years old, did not receive cognitive intervention, and had hypertension. Being underweight was a potential biomarker for a high MCI risk. Cho et al. investigated baseline serum vitamin B12 levels and the progression of cognitive impairment in patients with AD who received cholinesterase inhibitors (ChEI). In 165 Taiwanese patients with mild to moderate AD who received ChEI for at least 2 years, the rates of cognitive decline were significantly lower in the patients with optimal (above the median level) than in those with suboptimal baseline vitamin B12 levels. After adjusting for several variables, the suboptimal baseline serum vitamin B12 level was a significant predictor of cognitive decline. Hsieh et al. retrospectively reviewed the medical records of patients with sporadic Creutzfeldt–Jacob disease (sCJD) to identify predictive variables for early initiation of artificial feeding, which indicates swallowing failure; the presence of myoclonus in the early stages and the elevated CSF levels of 14-3-3 protein were associated with early artificial feeding, which may indicate rapid deterioration in sCJD. Stanga et al. analyzed amyloid precursor protein (APP) processing by measuring the levels of its soluble nonamyloidogenic fragments (sAPPα and sAPPβ), amyloid-β (Aβ peptides), and glial cell line–derived neurotrophic factor (GDNF) levels in the CSF and serum samples obtained from patients with ALS and healthy controls; alterations in GDNF and sAPPα levels in the samples were associated with a moderate and rapid progression of ALS. GDNF levels were markedly lower in the serum of the patients with ALS, while sAPPα levels were higher than those in the healthy controls. Shimizu et al. reviewed the role of neuroimaging for biomarkers of neurodegenerative diseases. This review describes magnetic resonance imaging, single photon emission computed tomography, positron emission tomography, amyloid imaging, dopamine transporter imaging, and 123I-metaiodobenzyl-guanidine myocardial scintigraphy, for biomarkers of AD, PD, and progressive supranuclear palsy.

BIOMARKERS FROM THE ANIMAL MODELS OF NEURODEGENERATIVE DISEASES

Huang et al. considered circadian rhythm dysfunction (CRD) and the progression of ALS in SOD1G93A ALS model mice; cCRD accelerated ALS onset and progression and increased the loss of motor neurons, activated gliosis, and nuclear factor κB-mediated inflammation in the spinal cord. CRD also resulted in an increase in the abundance of enteric cyanobacteria in the ALS model mice, which may be involved in the pathogenesis of ALS. Lu et al. used 1-Methyl-4-phenyl-1,2,3,6-tetrahydropyridine (MPTP)-induced PD mice to explore the cerebral metabolic bases of the occurrence and development of PD. The alteration of metabolite levels in the striatum and substantia nigra of the mice on days 1, 7, and 21 after MPTP injection were assessed through ^{1}H nuclear magnetic resonance spectroscopy; in the striatum, the glutamate levels increased significantly and persistently after PD induction; N-acetylaspartate levels increased transiently after PD induction but soon declined and were identical with the controls. Key enzymes in the glutamate–glutamine cycle increased significantly in the PD mice. Stanga et al. considered animal models of ALS; the results indicated that both GDNF and APP levels increased in the hind limb muscles of the transgenic ALS mouse models at the onset of motor deficits.

BIOMARKERS AS THERAPEUTIC INDICATORS

Oxidative stress is a major pathogenic factor of neurodegenerative diseases; oxidative stress markers can be used to evaluate the therapeutic effect of antioxidants. Al-Amin et al. investigated the antioxidative effects of risperidone on lipopolysaccharide (LPS)-induced oxidative stress in mice; risperidone significantly reduced the LPS-induced increase in the levels of the lipid peroxidation product malondialdehyde, advanced protein oxidation products, and nitric oxide in the cortex. Risperidone attenuated LPS-induced neuronal oxidative damage in the cortex through its ability to reduce reactive oxidative stress.

Biomarkers are essential for all types of neurodegenerative diseases. Determination of either clinical or experimental biomarkers provides additional knowledge about disease mechanisms, outcome prediction, and selection of therapeutic targets.

AUTHOR CONTRIBUTIONS

All authors listed have made a substantial, direct and intellectual contribution to the work, and approved it for publication.

REFERENCES

1. Hindle JV. Ageing, neurodegeneration and Parkinson's disease. *Age Ageing* (2010) 39:156–61. doi: 10.1093/ageing/afp223
2. Streffer JR, Grachev ID, Fitzer-Attas C, Gomez-Mancilla B, Boroojerdi B, Bronzova J, et al. Prerequisites to launch neuroprotective trials in Parkinson's disease: an industry perspective. *Movement Disord.* (2012) 27:651–5. doi: 10.1002/mds.25017
3. Flicker C, Ferris SH, Reisberg B. Mild cognitive impairment in the elderly: predictors of dementia. *Neurology* (1991) 41:1006–9.
4. Michaud TL, Su D, Siahpush M, Murman DL. The risk of incident mild cognitive impairment and progression to dementia considering mild cognitive impairment subtypes. *Dement Geriatr Cogn Disord Extra* (2017) 7:15–29. doi: 10.1159/000452486
5. Postuma RB, Gagnon J-F, Bertrand J-A, Génier Marchand D, Montplaisir JY. Parkinson risk in idiopathic REM sleep

behavior disorder: preparing for neuroprotective trials. *Neurology* (2015) 84:1104–13. doi: 10.1212/WNL.0000000000001364

6. Helzner EP, Luchsinger JA, Scarmeas N, Cosentino S, Brickman AM, Glymour MM, et al. Contribution of vascular risk factors to the progression in alzheimer disease. *Arch Neurol.* (2009) 66:343–8. doi: 10.1001/archneur.66.3.343
7. Pagano G, Polychronis S, Wilson H, Giordano B, Ferrara N, Niccolini F, et al. Diabetes mellitus and Parkinson disease. *Neurology* (2018) 90:e1654–62. doi: 10.1212/WNL.0000000000005475

Conflict of Interest Statement: The authors declare that the research was conducted in the absence of any commercial or financial relationships that could be construed as a potential conflict of interest.

frontiers in Neurology

ORIGINAL RESEARCH
published: 30 May 2018
doi: 10.3389/fneur.2018.00384

A Role for GDNF and Soluble APP as Biomarkers of Amyotrophic Lateral Sclerosis Pathophysiology

Serena Stanga[1], Liliana Brambilla[2], Bernadette Tasiaux[1], Anh H. Dang[3], Adrian Ivanoiu[4], Jean-Noël Octave[1], Daniela Rossi[2†], Vincent van Pesch[3,4†] and Pascal Kienlen-Campard[1]**

[1] Alzheimer Research Group, Institute of Neuroscience, Université Catholique de Louvain, Brussels, Belgium, [2] Laboratory for Research on Neurodegenerative Disorders, Istituti Clinici Scientifici Maugeri SpA SB - IRCCS, Pavia, Italy, [3] Unité de Neurochimie, Institute of Neuroscience, Université Catholique de Louvain, Brussels, Belgium, [4] Neurology Department, Cliniques Universitaires Saint-Luc, Brussels, Belgium

OPEN ACCESS

Edited by:
Tibor Hortobágyi,
University of Debrecen, Hungary

Reviewed by:
Vanessa Xiuwen Tan,
Faculty of Medicine & Health Sciences, Macquarie University, Australia
Savina Apolloni,
Fondazione Santa Lucia (IRCCS), Italy
Massimiliano Filosto,
Asst degli Spedali Civili di Brescia, Italy

***Correspondence:**
Serena Stanga
serena.stanga@uclouvain.be
Pascal Kienlen-Campard
pascal.kienlen-campard@uclouvain.be

† These authors have contributed equally to this work.

Specialty section:
This article was submitted to Neurodegeneration, a section of the journal Frontiers in Neurology

Received: 28 February 2018
Accepted: 11 May 2018
Published: 30 May 2018

Citation:
Stanga S, Brambilla L, Tasiaux B, Dang AH, Ivanoiu A, Octave J-N, Rossi D, van Pesch V and Kienlen-Campard P (2018) A Role for GDNF and Soluble APP as Biomarkers of Amyotrophic Lateral Sclerosis Pathophysiology. Front. Neurol. 9:384. doi: 10.3389/fneur.2018.00384

The current inability of clinical criteria to accurately identify the "at-risk group" for Amyotrophic Lateral Sclerosis (ALS) development as well as its unknown etiology are fueling the interest in biomarkers aimed at completing clinical approaches for the diagnosis. The Glial cell line-derived neurotrophic factor (GDNF) is a diffusible peptide critically involved in neuronal differentiation and survival. GDNF is largely studied in various neurological and neuromuscular diseases, with a great interest in the peripheral nervous system (PNS). The recent discovery of Amyloid Precursor Protein (APP)-dependent GDNF regulation driving neuro-muscular junctions' formation in APP null transgenic mice, prompts to study whether neurodegeneration relies on loss or gain of APP function and suggests that it could affect peripheral processes. Here, we explored a brand-new aspect of the loss of trophic support in ALS by measuring GDNF, APP, soluble APP fragments and Aβ peptides levels in $SOD1^{WT}$ or $SOD1^{G93A}$ transgenic mouse models of ALS and in human biological fluids [i.e. serum and cerebrospinal fluid (CSF)] from ALS patients and control subjects. Our results show that both GDNF and soluble APP fragments levels are altered at the onset of motor deficits in mice and that their levels are also modified in patient samples. This study indicates that both GDNF and soluble APPα represent possible biomarkers for ALS.

Keywords: biomarker, neurodegeneration, glial cell line-derived neurotrophic factor (GDNF), amyloid precursor protein (APP), amyotrophic lateral sclerosis (ALS)

INTRODUCTION

Amyotrophic lateral sclerosis (ALS) is a neurodegenerative disease characterized by the selective and progressive loss of motor neurons from the motor cortex, brain stem, and spinal cord leading to muscle atrophy, irreversible paralysis and eventually death within 3–5 years from symptom onset as a result of respiratory failure. Most patients are aged between 50 and 75 years at diagnosis and ALS is mostly sporadic with 90% of the cases occurring without a family history of the disease. Although the disease is considered a rare type of motor neuron neurodegeneration, by 2040 it has been estimated that around 400,000 patients will be diagnosed with ALS worldwide (1). Currently approved treatments for the disease, i.e. Riluzole and Edaravone, extend survival by few months and only mildly improve motor function. The inefficacy of the available treatments may be

attributed to the fact that ALS is a heterogeneous disease. Furthermore, the process of diagnosis is often delayed, mainly because many parameters need to meet diagnostic criteria.

Understanding the pathophysiology of both familial and sporadic ALS and finding specific biomarkers to accelerate diagnosis could help in developing more effective treatments. Trophic factors have been largely studied as potential therapeutic targets for ALS because of their essential role in neuronal development, motor neuron maintenance and survival (2). Difficulties for growth factor-based therapies relate to the fact that therapeutic intervention mostly occurs after the diagnosis, thereby resulting as ineffective in counteracting the already ongoing neurodegenerative process. In this regard, trophic factors' levels would rather be useful as biomarkers for diagnosis and/or prognosis.

Interestingly, aside from their synthesis in the local spinal/muscular microenvironment, trophic factors play important roles in the nourishing feedback during which originating neurons receive trophic input from their target tissues (3). In ALS, it has been proposed that the failure of muscle cells to release neurotrophic factors that maintain the favorable physiological context for spinal motor neurons may lead to the loss of that neuronal cell population (4).

The glial cell line-derived neurotrophic factor (GDNF) is one of the factors produced by muscles and Schwann cells. The absence of GDNF alters the location of developing spinal motor neurons that innervate the limbs (5) and selectively affects the innervation of intrafusal muscle spindles in mice (6). Interestingly, the overexpression of this factor in muscle during development causes a hyperinnervation of neuromuscular junctions (7), while GDNF heterozygous mice (+/−) exhibit locomotor deficiencies (8), suggesting that GDNF dosage plays a key role in neuromuscular function. When GDNF is administered directly in muscles, it preserves the muscle-nerve synapse and promotes motor neuron function and survival in a familial rat model of ALS (9). Furthermore, overexpression of GDNF in muscle extends lifespan in ALS mice (10). Interestingly, GDNF can be retrogradely transported along motor neuronal axons (11), thereby enabling to explore the relevance of the intramuscular delivery route to act on both somas and nerve endings.

Recently, we demonstrated that the Amyloid Precursor Protein (APP) controls GDNF transcription in mouse embryonic fibroblasts (MEFs) and muscles with an important impact on muscular trophy and on the formation of neuromuscular contacts (12). Together with others, our study suggests that defects in APP function might be directly related not only to Alzheimer's disease (AD), but also to other neurodegenerative diseases involving muscle denervation, such as ALS. Indeed, APP is upregulated in muscle from mouse models of familial ALS as well as from patients with ALS, where APP upregulation correlates with clinical symptoms (13, 14).

In this study, we investigated in parallel the expression levels of GDNF and APP and its metabolites in muscles from non-transgenic mice and transgenic mice overexpressing the wild-type human isoform of the Cu/Zn superoxide dismutase 1 ($SOD1^{WT}$) enzyme or the mutant $SOD1^{G93A}$ protein, the latter animals recapitulating much of the pathophysiology of ALS. We analyzed APP processing by measuring the levels of its soluble non-amyloidogenic fragments (sAPPα and sAPPβ) and amyloid-β (Aβ peptides), together with GDNF levels, in cerebrospinal fluid (CSF) and serum from ALS patients and healthy controls.

We found that both GDNF and APP levels are increased in hindlimbs muscles of the transgenic $SOD1^{G93A}$ mouse model of ALS at the onset of motor deficits. Alterations in GDNF and sAPPα levels have been observed also in human biological fluids from patients with a moderate and fast progression of the disease. More precisely, GDNF levels are importantly decreased in the serum of ALS patients while sAPPα levels are increased in the same fluid, compared to healthy controls.

Altogether, our results suggest that both GDNF and sAPPα, which are clearly involved in neuromuscular pathologies, represent possible biomarkers for ALS pathophysiology.

MATERIALS AND METHODS

Mouse Models and Genotyping

Transgenic mice expressing human $SOD1^{WT}$ [B6SJL-Tg(SOD1) 2Gur/J–002298] or $SOD1^{G93A}$ [B6SJL-TgN(SOD1-G93A) 1Gur/J–002726] were purchased from The Jackson Laboratories. Animal care and handling were performed according to the European Council Directive 2010/63/EU and to the Italian and Belgian Animal Welfare Act for the use and care of laboratory animals and approved by the Animal Ethics Committee of the Universite Catholique of Louvain.

Genotyping and Tissue Processing

Genomic DNA was extracted from mouse tail biopsies and used as DNA template in genotyping PCR analysis. Offspring positive for the $SOD1^{G93A}$ transgene were identified using the following primers: SOD1, forward 5′-CATCAGCCCTAATCC ATCTGA-3′ and reverse 5′-CGCGACTAACAATCAAAGTGA-3′ as described in Brambilla et al. (15). Hindlimbs muscles (gastrocnemius and tibialis anterior) from transgenic mice were snap frozen in liquid nitrogen and stored at −80°C until further use (RNA isolation for RT-qPCR and Western blotting).

RNA Preparation, RT-PCR, and Quantitative PCR

RNAs were extracted from tissues in TRIzol Reagent and reverse transcribed using an iScript cDNA Synthesis Kit (Bio-Rad). Real-time quantitative PCR (qPCR) analysis was performed on 2ng cDNA template by using iQ SYBR Green Supermix in an iCycler IQ Multicolor Real-Time PCR Detection System (Bio-Rad). qPCR conditions were typically 95°C for 30 s, followed by 40 cycles of 30 s at 95°C, 45 s at 60°C, and 15 s at 79°C and ended by 71 cycles of 30 s at 60°C. The relative changes in the target gene: glyceraldehyde 3-phosphate dehydrogenase mRNA ratio were determined by the $2^{(-\Delta\Delta Ct)}$ calculation.

The sequences for qPCR primers are the following: GDNF, forward 5′-TTAATGTCCAACTGGGGGTCT-3′ and reverse 5′-GCCGAGGGAGTGGTCTTC-3′; and glyceraldehyde 3-phosphate dehydrogenase, forward 5′-ACCCAGAAGACTGTG GATGG-3′ and reverse 5′-ACACATTGGGGGTAGGAACA-3′.

Western Blotting

Muscles were homogenized in 10 volumes of lysis buffer [50 mM Tris (pH 7.5), 150 mM NaCl, 0.05 mM EDTA, 1% Triton X-100, and 0.1% sodium dodecyl sulfate] with Complete Protease Inhibitor Cocktail on ice using a Ultraturax homogenizer 3 × 10 s for each sample and in between 30 s (or more) on ice to cool down. After 1h at 4°C with continuous rotation, samples were centrifuged at 10,000 g for 10 min at 4°C and the supernatants were collected. Protein concentration was determined by the BCA Protein Assay Kit (Bio-Rad). A total of 15 μg protein was heated for 10 min at 70°C in loading buffer (lysis buffer containing 0.5 M DTT and staining NuPAGE blue), loaded and separated onto NuPAGE4–12% Bis-TrisGel, and then transferred for 2 h at 30 V onto PVDF membranes. After blocking (5% nonfat milk in PBS-Tween 0.05%), membranes were incubated overnight at 4°C with the primary antibodies, washed, and incubated with the secondary antibody coupled to peroxidase prior to ECL detection (GEHealthcare). ECL signals were quantified with a GelQuantNET software. Primary antibodies included anti-APP Y188 (1:5,000) or $GAPDH_2$ (1:25,000) in 5% nonfat milk in PBS-Tween 0.05%. Secondary antibody included anti-rabbit (1:10,000).

Study Group and Sampling

Venous serum samples and CSF were obtained from a group of subjects consisting of 7 patients with sporadic ALS and 7 healthy age-matched controls (CTR); clinical and demographic features are summarized in **Table 1**. All the subjects were examined by a senior neurologist and diagnosis of ALS was made according to the El Escorial criteria (16). ALS was diagnosed based upon symptom evaluation, neurological examination, laboratory and brain and/or spinal cord magnetic resonance imaging. Disease progression rates have been calculated as the ratio between the functional scale and disease duration in months; < 0.5 is considered slow; 0.5–1: moderate and >1: fast progression.

Control subjects were individuals with subjective complaints but with no diagnosis of neurological or psychiatric disease. None of the subjects selected in this study was affected by neoplastic or autoimmune disease when the blood and CSF samples were taken.

The patients had undergone a lumbar puncture and blood sampling in the Neurology department of the Cliniques Universitaires Saint-Luc (Brussels, Belgium) as part of the routine diagnostic procedure. Patients admitted to this hospital sign an internal regulatory document, stating that left-overs from biological samples used for routine diagnostic procedures can be used for retrospective academic studies, without an additional informed consent (ethics committee approval 2007/10SEP/233). Haemorrhagic CSF samples were excluded. CSF sample collection and storage were carried out in accordance with the consensus protocol proposed by Teunissen et al. (17). For serum studies, blood samples were collected in S-Monovette® 7.5 ml Serum Z tube (ref. 01-1601, Sarstedt). Both blood and CSF were centrifuged at 3600 rpm for 6 min. Serum and cell-free CSF were respectively aliquoted and stored at −80°C for later analysis.

GDNF, sAPP, and Aβ Measurements

Secreted GDNF levels were quantified in serum and CSF from the study group by ELISA following the manufacturer's instructions (Promega). sAPPα and β and Aβ38, Aβ40, and Aβ42 peptides were quantified using a sAPPα/sAPPβ multiplex and an Aβ multiplex electro-chemiluminescence immunoassay ECLIA (Meso Scale Discovery), respectively. sAPPα and β and Aβ were quantified according to the manufacturer's instructions.

Statistical Analysis

The number of samples in each experimental condition is indicated in the figure legends. Data were analyzed using GraphPad Prism software (GraphPad Software, La Jolla, CA, USA) by unpaired Student's *t*-test (2 experimental conditions) or by ANOVA followed by Bonferroni's multiple comparison tests (>2 experimental conditions).

RESULTS

We analyzed GDNF mRNA levels in hindlimbs muscles from non-transgenic (NTg) or transgenic $SOD1^{WT}$ and $SOD1^{G93A}$ mice at 30 (asymptomatic stage), ∼100 (onset of motor deficits) and ∼130 days of age (symptomatic stage) (**Figure 1**). GDNF mRNA levels remained below the detection limit at the asymptomatic stage in all the mouse genotypes (data not shown). A significant increase in GDNF mRNA levels in $SOD1^{G93A}$ mice vs. NTg and $SOD1^{WT}$ mice was observed only at the onset of motor deficits at 100 days (**Figure 1A**), and diminished thereafter.

In the same tissues, we measured by Western blotting APP levels, which showed a significant increase in its expression in $SOD1^{G93A}$ mice at the onset of motor deficits. More specifically, we found a 3.5-fold increase in APP levels in the hindlimb muscles at 100 days of age in $SOD1^{G93A}$ mice compared to both NTg and $SOD1^{WT}$ mice (**Figures 1B,C**). To note, the maturation profile of APP was also sharply pronounced at this stage (APP appearing as a doublet). This increase in APP expression levels was not detectable in animals aged 30 days or 130 days. By contrast, in NTg or $SOD1^{WT}$ APP levels remained low and constant throughout the lifespan (**Figures 1B,C**).

Since ALS transgenic mouse models mimic the clinical situation observed in patients, we analyzed both GDNF and soluble APP fragments in biological fluids from controls subjects and ALS patients. Group characteristics of study population are shown in **Table 1**. The mean age of the control group was 58.6 ± 9.9 years (range 43–75 years) and that of ALS group was 64.1 ± 13.5 years (range 38–81 years). There was no significant statistical difference between the groups ($p = 0.398$). The mean duration of disease in ALS patients was 13.4 ± 15.7 months; the mean ALSFRS-R and the Progression rate calculated at the diagnosis were 41.7 ± 3 and 9.9 ± 15.1 respectively, indicating that ALS patients were all fast progressors, with one intermediate and no slow progressors.

We measured GDNF concentration in CSF and serum from healthy subjects and ALS patients to follow their expression in biological fluids reflecting the biochemical changes ongoing in the brain and in the peripheral tissues, respectively. The median

TABLE 1 | Demographic and clinical variables of the study group.

Patients	Age range at collection (years)	Onset	L.O.I. until diagnosis (months)	ALSFRS-R score	Progression rate (point/month)
Control 1	56–61	NA	NA	NA	NA
Control 2	60–65	NA	NA	NA	NA
Control 3	40–45	NA	NA	NA	NA
Control 4	60–65	NA	NA	NA	NA
Control 5	70–75	NA	NA	NA	NA
Control 6	50–55	NA	NA	NA	NA
Control 7	50–55	NA	NA	NA	NA
ALS 1	56–61	Bulbar	1	44	44
ALS 2	36–41	Bulbar + hemiparesis	6	43	7.2
ALS 3	66–71	Paraparesis	48	38	0.8
ALS 4	60–65	Bulbar + hemiparesis	8	37	4.6
ALS 5	70–75	Paraparesis	11	43	3.9
ALS 6	70–75	Bulbar	12	42	3.5
ALS 7	80–85	Paraparesis	8	45	5.6

L.O.I., Length of Illness; ALSFRS-R, ALS Functional Rating Scale-Revised; NA, Not applicable. Both the ALSFRS-R and the Progression rate were calculated at the diagnosis. The references for the Progression Rate are: slow < 0.5, intermediate 0.5–1.0, fast >1.0.

of GDNF levels in CSF was higher in ALS patients (33.1 ± 20.5 pg/ml) compared to CTR (21.2 ± 4.3 pg/ml), but the statistical significance was reached only in serum, where ALS patients showed clearly lower levels of GDNF when compared to CTR (107.3 ± 37.7 pg/ml vs. 198.1 ± 41 pg/ml, respectively). These results (**Figures 2A,B**) were consistent with the decrease in GDNF expression oberserved in $SOD1^{G93A}$ mouse muscles at the advanced stage (**Figure 1A**). APP holoprotein cannot be tracked in extracellular media. In order to analyse a potential correlation with the amount of soluble APP levels in subjects' biological fluids and GDNF levels, we measured by ECLIA the soluble non-amyloidogenic fragments of APP: sAPPα and β, both in CSF and serum (**Figures 3A–D**) and their ratio (**Figures 3E,F**) that provides additional information about the equilibrium between non-amyloidogenic and amyloidogenic APP processing. Interestingly, the levels of sAPPα were increased only in serum of ALS patients compared to controls. No differences were observed in CSF. To note, neither sAPPβ levels nor sAPPα/β ratio was affected in serum or CSF of patients with ALS. Concerning the levels of Aβ38, Aβ40, and Aβ42, in both CTR and ALS patients, Aβ peptides were detectable only in CSF (**Figure 4A**), while in serum Aβ levels were very low (**Figure 4B**). No significant differences were observed in Aβ42/Aβ40 ratio (**Figure 4C**).

DISCUSSION

The lack of clinical criteria to accurately identify the "at-risk group" for ALS development together with the unknown etiology of the disease are fueling the interest in biomarkers aimed at completing clinical approaches for the diagnosis and suitable as new therapeutic targets. In this study, we explored specifically if the loss of trophic support in neurodegenerative diseases could provide *bona fide* biomarkers for ALS. We measured GDNF, APP as well as soluble APP fragments and Aβ peptides levels, in mouse models of ALS and in human biological fluids (i.e., serum and CSF) from patients and control subjects.

Glial cell line-derived neurotrophic factor is a diffusible peptide critically involved in neuronal differentiation and survival and it has been identified in an unbiased proteomic assay as potential AD biomarker (18, 19). It has been evaluated for symptomatic treatment of Parkinson's disease (PD) (20), and shown to be able to reverse some aspects of aging in monkeys (21). Importantly, GDNF is particularly involved in the pathophysiology of various neurological and neuromuscular diseases, with a great interest in the peripheral nervous system (PNS). GDNF has been reported to preserve motor neurons from dying by using neural progenitor cells delivery (22) or muscle-derived GDNF (23), suggesting that therapies targeting GDNF could be efficient to cope with ALS. Here, we have reported a clear alteration of GDNF levels both in muscles from ALS mouse models and serum from ALS patients. We found an increase in GDNF levels in muscle from mice expressing the mutant isoform of $SOD1^{G93A}$ at the onset of symptoms (100 days). Other groups observed an increased expression of GDNF mRNA in skeletal muscle from patients (24–26). The increment in GDNF mRNA levels in SOD1G93A mice is concomitant to the onset of ALS symptoms (denervation) but it is temporary. As it has been demonstrated in patients; GDNF levels increase contemporary to denervation aiming to promote potential reinnervation, but the reaction may be transient. We believe that the decrease in GDNF mRNA levels observed at day 130 might be due to the reduction in the total number of muscle fibers, the low number of fibers in acute stages of neurogenic atrophy and replacement of muscle fibers by connective tissue occurring in later stages of the disease. The fact that a similar reduction in GDNF mRNA levels is detected in SOD1wt mice can be explained by the presence of motor neuron pathology and skeletal muscle atrophy also in these animals (27, 28).

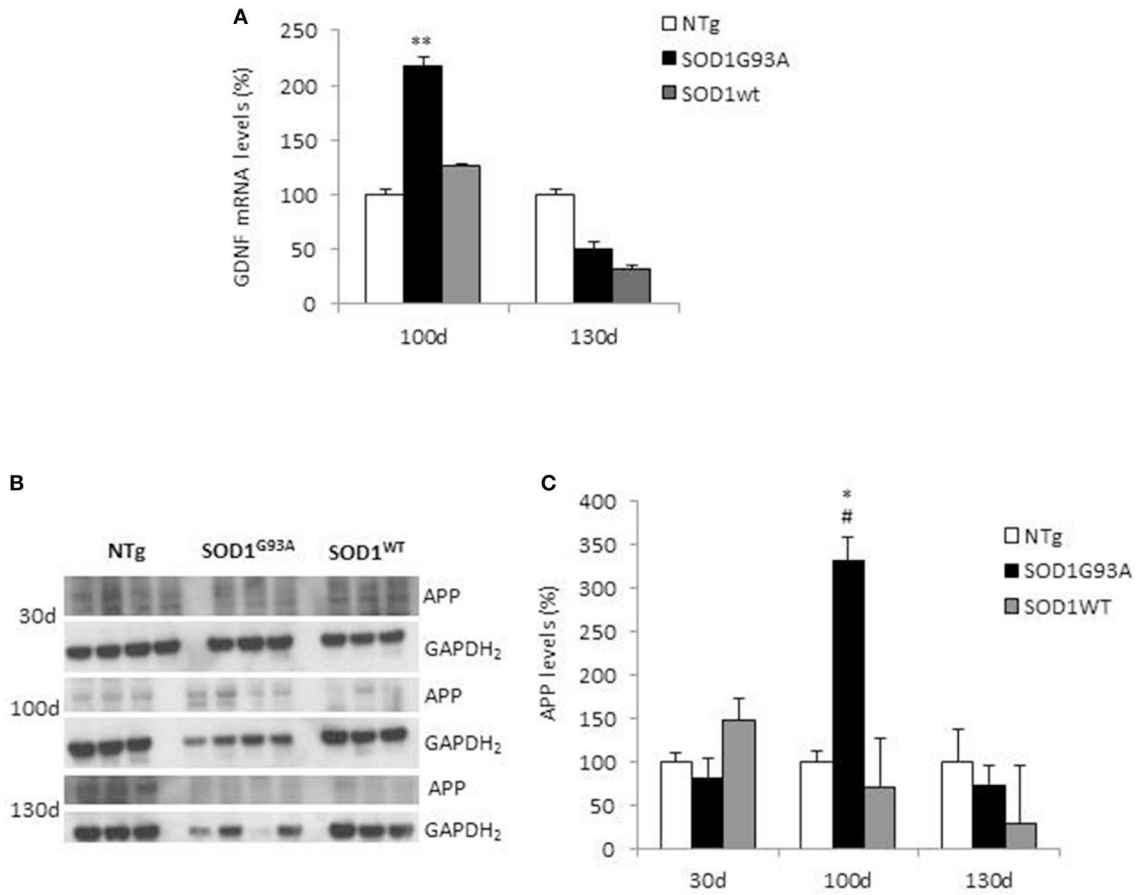

FIGURE 1 | GDNF and APP levels in non-transgenic and SOD1 transgenic mice models. **(A)** GDNF mRNA levels were analyzed in hindlimbs muscles from non-transgenic (NTg), $SOD1^{WT}$ and $SOD1^{G93A}$ mice at ∼100 (onset of motor deficits) and ∼130 days of age (symptomatic stage). Values (mean ± SEM) are expressed as percentage of age-matched NTg mice. $^{**}P < 0.01$, ANOVA followed by Bonferroni *post-hoc* test, $n = 3$–4 mice per genotype and age. **(B)** APP levels were analyzed by Western blotting in the same muscles' lysates at 100 and 130 days, plus at 30 days (asymptomatic stage) in NTg, $SOD1^{WT}$ and $SOD1^{G93A}$ mice; $GAPDH_2$ was used as a loading control probe. Quantifications are shown in **(C)**. Values (mean ± SEM) are expressed as percentage of expression level of age-matched NTg mice. $^{*}P < 0.05$ and $^{\#}P < 0.05$ vs. 100-day-old genotype-matched mice NTg and $SOD1^{WT}$; ANOVA followed by Bonferroni *post-hoc* test, $n =$ 3–4 mice per genotype and age.

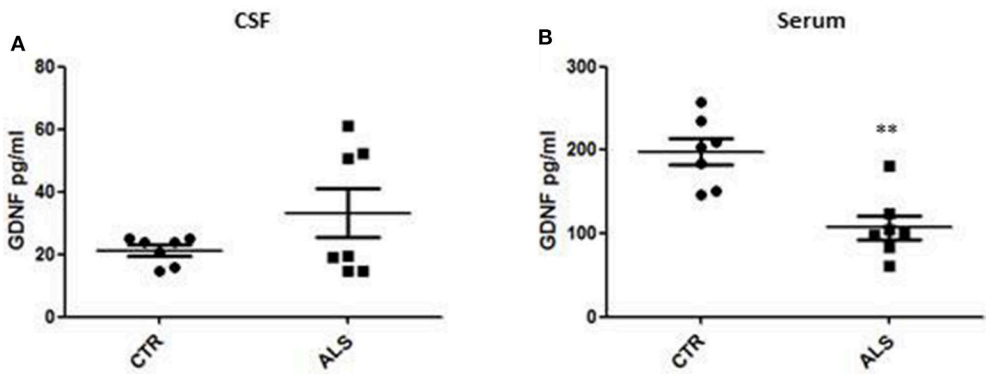

FIGURE 2 | GDNF levels in biological fluids from CTR subjects and ALS patients. GDNF levels were quantified by ELISA in the CSF **(A)** and serum **(B)** of controls without neurological disease and ALS patients. Values are given in picograms per milliliter (pg/ml). Each dot corresponds to one subject studied; the horizontal bar indicates the mean in each group. $^{**}P < 0.001$, Student's *t*-test ($n = 7$/group).

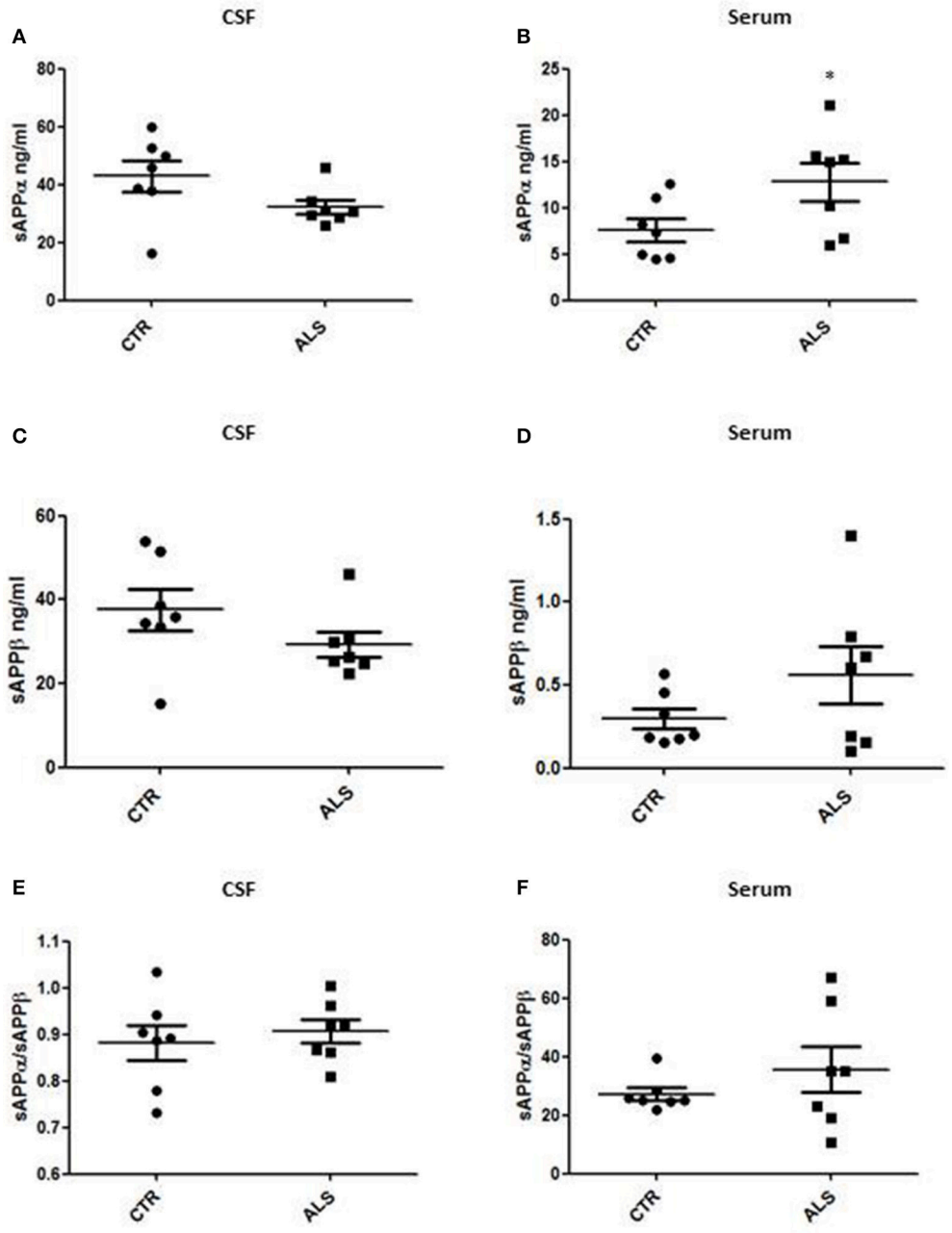

FIGURE 3 | CSF and serum sAPPα, β and their ratio in CTR and ALS patients. sAPP α levels **(A,B)** and sAPP β **(C,D)** were quantified by ECLIA in the CSF and serum of controls without neurological disease and ALS patients. sAPP α / sAPP β ratio have been showed for both CSF **(E)** and Serum **(F)**. Values are given in nanograms per milliliter (ng/ml). Each dot corresponds to one subject studied; the horizontal bar indicates the mean in each group. *$P < 0.05$, Student's *t*-test ($n = 7$/group).

All together, these findings suggest that GDNF is importantly synthetized by muscles to sustain the increased demand for trophic factors by motor neurons, which are prone to degenerate in ALS. Interestingly, we observed also a significant increment in APP levels in mice expressing the mutant isoform of $SOD1^{G93A}$ at the stage of disease onset (100 days). This is in line with previously published work (13, 14). We recently found that APP controls GDNF transcription in muscles, supporting the neuromuscular phenotype observed in APP knock-out (KO) mice (12). This result suggests that changes in APP expression observed herein and in muscles of patients with ALS (14), could directly affect muscular GDNF expression and release. Thus, APP could not only be a biomarker of ALS progression, but it could be involved in the pathways controlling trophic supply that are impaired in the ALS pathology.

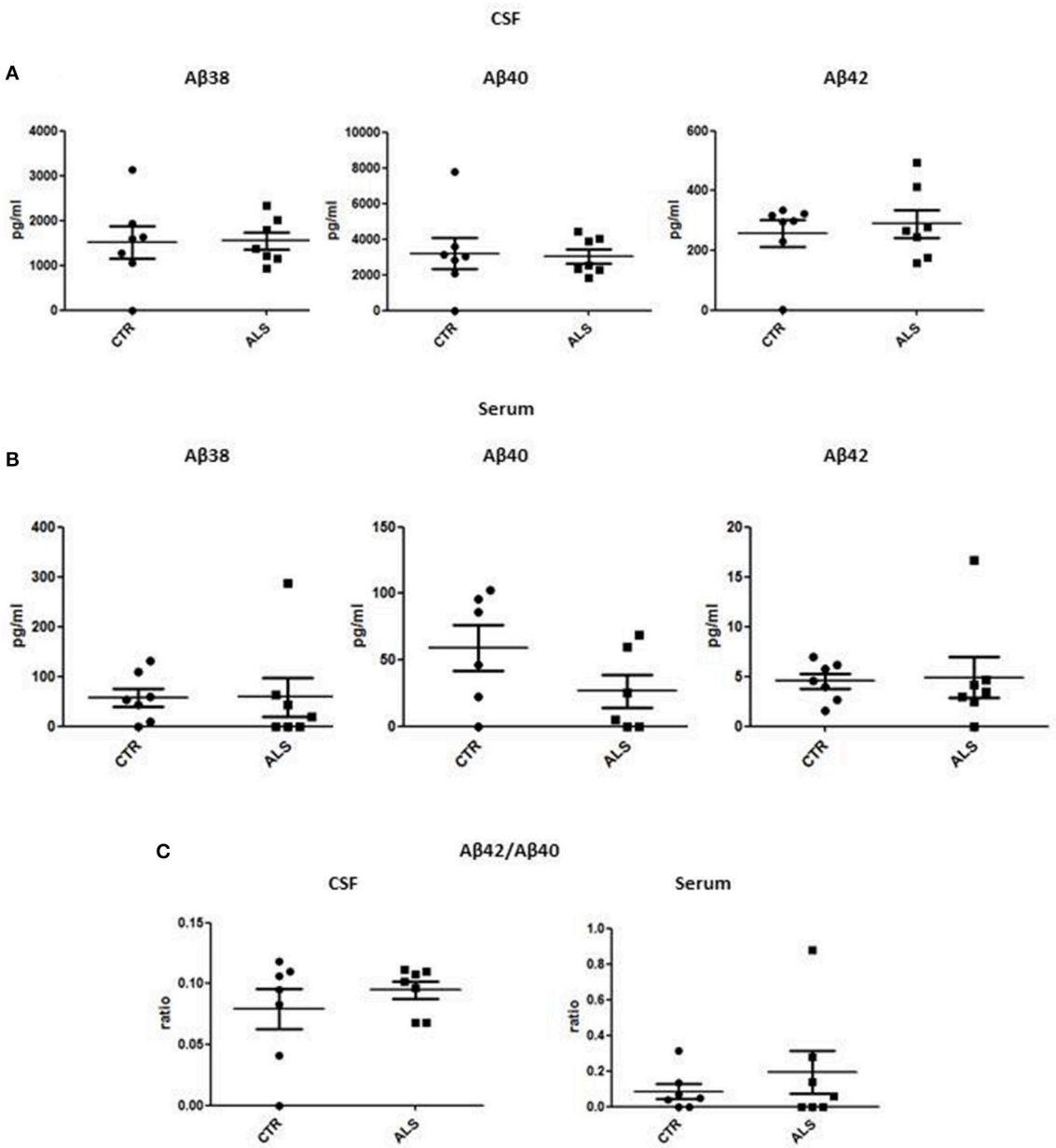

FIGURE 4 | CSF and serum Aβ38, Aβ40, and Aβ42 and Aβ42/Aβ40 ratio in CTR and ALS patients. Soluble monomeric Aβ38, Aβ40, and Aβ42 were quantified by ECLIA in the CSF **(A)** and serum **(B)** of controls without neurological disease and ALS patients. **(C)** Aβ42/Aβ40 ratio have been showed for both CSF and Serum. Values are given in nanograms per milliliter (ng/ml). Each dot corresponds to one subject studied ($n = 7$/group); the horizontal bar indicates the mean in each group.

In human samples, we observed significant and clear-cut results in serum while we measured only tendencies of impairment for both GDNF and APP metabolites in CSF. More specifically, we recorded a trend of GDNF levels to increase in the CSF of only 3 over 7 ALS patients, while a uniform and significant decrease in serum from ALS patients was detected. Our results indicate that peripheral GDNF (serum) is decreased as consequence to the fact that the regulatory system of GDNF production, likely involving APP, is no more functional and therefore reflected by a decrease of GDNF in serum. This is a peripheral process since central GDNF (CSF) is not significantly affected in the pathology. In parallel, we studied APP metabolite levels in the patient samples and we observed a trend to decrease of sAPPα levels in the CSF of ALS patients and a significant increase in sAPPα levels in serum from patients. Interestingly, sAPPα has been suggested to have potent neuroprotective capacities (29). Alterations in sAPPα levels in peripheral fluids from patients could indicate that peripheral mechanisms involving APP-dependent GDNF regulation may be implicated in the disease. Same observations, though not

statistically significant, hold true for sAPPβ while no differences have been detected neither in sAPPα/sAPPβ ratio nor in Aβ levels.

Aβ levels are one of the most extensively evaluated markers of sporadic AD, since GDNF was identified as potential AD biomarker (18, 19), could we suggest it as a general biomarker of neurodegenerative diseases? The question is open. What is clear is that in AD Aβ levels are importantly high, while in ALS there are no alterations compared to age-matched control subjects at any stage of the disease. This suggests that very likely, APP and GDNF are linked in different neurodegenerative diseases but the mechanistic aspects are peculiar to the specific disease and still need to be decipher.

It is at this stage difficult to make clear-cut correlations between GDNF and APP soluble fragments in human samples because of the reduced number of ALS patients enrolled in the study, the variability existing between them and especially because of the peculiarity of disease history. Large scale studies on bigger cohorts would be useful to elaborate on the observations we made here. Clearly, both GDNF and soluble sAPPα levels are altered in fluids from patients with intermediate and fast progression of the disease, indicating that GDNF and soluble APP are biomarkers of ALS pathophysiology. The unequivocal observations in mouse muscles and serum from patients strongly suggest that changes in APP and GDNF levels result from peripheral processes. Assessing biomarkers in blood has the great advantage of minimal invasiveness when compared to measurement in CSF samples.

Changes in GDNF and sAPPα in serum go in opposite directions leaving open the following question: is APP-dependant GDNF expression involved in ALS progression, or are they independent biomarkers? The correlation between APP-related and GDNF changes, and their contribution to ALS pathways need to be fully elucidated, in order to consider them as possible targets for therapeutic approaches.

In conclusion, we suggest that the combined analysis of GDNF and sAPPα that we propose as possible predictive peripheral biomarkers for ALS, could help for the comprehension of the etiopathogenesis and the improved precision of the diagnosis of ALS.

AUTHOR CONTRIBUTIONS

SS and PK-C designed the research study. SS conducted experiments, LB, BT, and AD offered technical help. VvP enrolled subjects and conducted the clinical diagnosis. SS wrote the paper with fundamental input of J-NO, DR, and P-KC. All the authors analyzed data, read and approved the final manuscript.

FUNDING

This work was supported by a grant of the Foundation for Research on Alzheimer's disease (PK-C), by the Interuniversity Attraction Pole Programme-Belgian Sate-Belgian Science Policy (IAP-P7/16 and IAP-P7/13) to J-NO and PK-C, by the Action de Recherche Concertée (ARC 14/19-059) to PK-C.

ACKNOWLEDGMENTS

We are grateful to Giulia Guidotti (Laboratory for Research on Neurodegenerative Disorders, Istituti Clinici Scientifici Maugeri SpA SB, Pavia, Italy) for the helpful technical assistance.

REFERENCES

1. Hardiman O, van den Berg LH, Kiernan MC. Clinical diagnosis and management of amyotrophic lateral sclerosis. *Nat Rev Neurol.* (2011) **7**:639–49. doi: 10.1038/nrneurol.2011.153
2. Ekestern E. Neurotrophic factors and amyotrophic lateral sclerosis. *Neurodegener Dis.* (2004) **1**:88–100. doi: 10.1159/000080049
3. Tovar-Y-Romo LB, Ramírez-Jarquín UN, Lazo-Gómez R, Tapia R. Trophic factors as modulators of motor neuron physiology and survival: implications for ALS therapy. *Front Cell Neurosci.* (2014) **8**:61. doi: 10.3389/fncel.2014.00061
4. Loeffler JP, Picchiarelli G, Dupuis L, Gonzalez De Aguilar JL. The role of skeletal muscle in amyotrophic lateral sclerosis. *Brain Pathol.* (2016) **26**:227–36. doi: 10.1111/bpa.12350
5. Kramer ER, Knott L, Su F, Dessaud E, Krull CE, Helmbacher F et al. Cooperation between GDNF/Ret and ephrinA/EphA4 signals for motor-axon pathway selection in the limb. *Neuron* (2006) **50**:35–47. doi: 10.1016/j.neuron.2006.02.020
6. Gould TW, Yonemura S, Oppenheim RW, Ohmori S, Enomoto H. The neurotrophic effects of glial cell line-derived neurotrophic factor on spinal motoneurons are restricted to fusimotor subtypes. *J Neurosci.* (2008) **28**:2131–46. doi: 10.1523/JNEUROSCI.5185-07.2008
7. Nguyen QT, Parsadanian AS, Snider WD, Lichtman JW. Hyperinnervation of neuromuscular junctions caused by GDNF overexpression in muscle. *Science* (1998) **279**:1725–9. doi: 10.1126/science.279.5357.1725
8. Littrell OM, Pomerleau F, Huettl P, Surgener S, McGinty JF, Middaugh LD, et al. Enhanced dopamine transporter activity in middle-aged Gdnf heterozygous mice. *Neurobiol Aging* (2012) **33**:427.e1–14. doi: 10.1016/j.neurobiolaging.2010.10.013
9. Suzuki M, McHugh J, Tork C, Shelley B, Hayes A, Bellantuono I, et al. Direct muscle delivery of GDNF with human mesenchymal stem cells improves motor neuron survival and function in a rat model of familial ALS. *Mol Ther.* (2008) **16**:2002–10. doi: 10.1038/mt.2008.197
10. Mohajeri MH, Figlewicz DA, Bohn MC. Intramuscular grafts of myoblasts genetically modified to secrete glial cell line-derived neurotrophic factor prevent motoneuron loss and disease progression in a mouse model of familial amyotrophic lateral sclerosis. *Hum Gene Ther.* (1999) **10**:1853–66. doi: 10.1089/10430349950017536
11. Leitner ML, Molliver DC, Osborne PA, Vejsada R, Golden JP, Lampe PA, et al. Analysis of the retrograde transport of glial cell line-derived neurotrophic factor (GDNF), neurturin, and persephin suggests that *in vivo* signaling for the GDNF family is GFRalpha coreceptor-specific. *J Neurosci.* (1999) **19**:9322–31. doi: 10.1523/JNEUROSCI.19-21-09322.1999
12. Stanga S, Zanou N, Audouard E, Tasiaux B, Contino S, Vandermeulen G, et al. APP-dependent glial cell line-derived neurotrophic factor gene expression drives neuromuscular junction formation. *FASEB J.* (2016) **30**:1696–711. doi: 10.1096/fj.15-278739
13. Bryson JB, Hobbs C, Parsons MJ, Bosch KD, Pandraud A, Walsh FS, et al. Amyloid precursor protein (APP) contributes to pathology in the SOD1(G93A) mouse model of amyotrophic lateral sclerosis. *Hum Mol Genet.* (2012) **21**:3871–82. doi: 10.1093/hmg/dds215
14. Koistinen H, Prinjha R, Soden P, Harper A, Banner SJ, Pradat PF, et al. Elevated levels of amyloid precursor protein in muscle of patients with amyotrophic

lateral sclerosis and a mouse model of the disease. *Muscle Nerve* (2006) **34**:444–450. doi: 10.1002/mus.20612
15. Brambilla L, Guidotti G, Martorana F, Iyer AM, Aronica E, Valori CF, et al. Disruption of the astrocytic TNFR1-GDNF axis accelerates motor neuron degeneration and disease progression in amyotrophic lateral sclerosis. *Hum Mol Genet*. (2016) **25**:3080–95. doi: 10.1093/hmg/ddw161
16. Brooks BR, Miller RG, Swash M, Munsat TL. World federation of neurology group on motor neuron diseases. el escorial revisited: revised criteria for the diagnosis of amyotrophic lateral sclerosis. *Amyotroph Lateral Scler Other Motor Neuron Disord.* (2000) **1**:293–9. doi: 10.1080/146608200300079536
17. Teunissen CE, Petzold A, Bennett JL, Berven FS, Brundin L, Comabella M, et al. A consensus protocol for the standardization of cerebrospinal fluid collection and biobanking. *Neurology* (2009) **73**:1914–22. doi: 10.1212/WNL.0b013e3181c47cc2
18. Ray S, Britschgi M, Herbert C, Takeda-Uchimura Y, Boxer A, Blennow K, et al. Classification and prediction of clinical Alzheimer's diagnosis based on plasma signaling proteins. *Nat Med.* (2007) **13**:1359–62. doi: 10.1038/nm1653
19. Straten G, Eschweiler GW, Maetzler W, Laske C, Leyhe T. Glial cell-line derived neurotrophic factor (GDNF) concentrations in cerebrospinal fluid and serum of patients with early Alzheimer's disease and normal controls. *J Alzheimers Dis.* (2009) **18**:331–7. doi: 10.3233/JAD-2009-1146
20. Taylor H, Barua N, Bienemann A, Wyatt M, Castrique E, Foster R, et al. Clearance and toxicity of recombinant methionyl human glial cell line-derived neurotrophic factor (r-metHu GDNF) following acute convection-enhanced delivery into the striatum. *PLoS ONE* (2013) **8**:e56186. doi: 10.1371/journal.pone.0056186
21. Ai Y, Markesbery W, Zhang Z, Grondin R, Elseberry D, Gerhardt GA, et al. Intraputamenal infusion of GDNF in aged rhesus monkeys: distribution and dopaminergic effects. *J Comp Neurol.* (2003) **461**:250–61. doi: 10.1002/cne.10689
22. Suzuki M, McHugh J, Tork C, Shelley B, Klein SM, Aebischer P, et al. GDNF secreting human neural progenitor cells protect dying motor neurons, but not their projection to muscle, in a rat model of familial ALS. *PLoS ONE* (2007) **2**:e689. doi: 10.1371/journal.pone.0000689
23. Li W, Brakefield D, Pan Y, Hunter D, Myckatyn TM, Parsadanian A. Muscle-derived but not centrally derived transgene GDNF is neuroprotective in G93A-SOD1 mouse model of ALS. *Exp Neurol.* (2007) **203**:457–71. doi: 10.1016/j.expneurol.2006.08.028
24. Grundström E, Askmark H, Lindeberg J, Nygren I, Ebendal T, Aquilonius SM. Increased expression of glial cell line-derived neurotrophic factor mRNA in muscle biopsies from patients with amyotrophic lateral sclerosis. *J Neurol Sci.* (1999) **162**:169–73. doi: 10.1016/S0022-510X(98)00333-5
25. Lie DC, Weis J. GDNF expression is increased in denervated human skeletal muscle. *Neurosci Lett.* (1998) **250**:87–90. doi: 10.1016/S0304-3940(98)00434-0
26. Yamamoto M, Mitsuma N, Inukai A, Ito Y, Li M, Mitsuma T, et al. Expression of GDNF and GDNFR-alpha mRNAs in muscles of patients with motor neuron diseases. *Neurochem Res.* (1999) **24**:785–90. doi: 10.1023/A:1020739831778
27. Jaarsma D, Haasdijk ED, Grashorn JA, Hawkins R, van Duijn W, Verspaget HW, et al. Human Cu/Zn superoxide dismutase (SOD1) overexpression in mice causes mitochondrial vacuolization, axonal degeneration, and premature motoneuron death and accelerates motoneuron disease in mice expressing a familial amyotrophic lateral sclerosis mutant SOD1. *Neurobiol Dis.* (2000) **7**:623–43. doi: 10.1006/nbdi.2000.0299
28. Wong M, and Martin LJ. Skeletal muscle-restricted expression of human SOD1 causes motor neuron degeneration in transgenic mice. *Hum Mol Genet*. (2010) **19**:2284–302. doi: 10.1093/hmg/ddq106
29. Chasseigneaux S, and Allinquant B. Functions of Aβ, sAPPα and sAPPβ : similarities and differences. *J Neurochem.* (2012) **120** (Suppl. 1):99–108. doi: 10.1111/j.1471-4159.2011.07584.x.2011.07584.x

Conflict of Interest Statement: The authors declare that the research was conducted in the absence of any commercial or financial relationships that could be construed as a potential conflict of interest.

frontiers in Neurology

ORIGINAL RESEARCH
published: 24 April 2018
doi: 10.3389/fneur.2018.00218

Circadian Rhythm Dysfunction Accelerates Disease Progression in a Mouse Model With Amyotrophic Lateral Sclerosis

Zhilin Huang[1†], Qiang Liu[2†], Yu Peng[2], Jiaying Dai[3], Youna Xie[1], Weineng Chen[1], Simei Long[1], Zhong Pei[1], Huanxing Su[2] and Xiaoli Yao[1*]*

[1] Department of Neurology, National Key Clinical Department and Key Discipline of Neurology, Guangdong Key Clinical Laboratory for Diagnosis and Treatment of Major Neurological Diseases, The First Affiliated Hospital, Sun Yat-sen University, Guangzhou, China, [2] State Key Laboratory of Quality Research in Chinese Medicine, Institute of Chinese Medical Sciences, University of Macau, Macao, China, [3] Comprehensive Department, Sun Yat-sen Memorial Hospital affiliated to Sun Yat-sen University, Guangzhou, China

OPEN ACCESS

Edited by:
Chaur-Jong Hu,
Taipei Medical University, Taiwan

Reviewed by:
Savina Apolloni,
Fondazione Santa Lucia (IRCCS), Italy
Shinghua Ding,
University of Missouri, United States

***Correspondence:**
Huanxing Su
huanxingsu@umac.mo;
Xiaoli Yao
yaoxiaol@mail.sysu.edu.cn

[†]These authors have contributed equally to this article and should be considered co-first authors.

Specialty section:
This article was submitted to Neurodegeneration, a section of the journal Frontiers in Neurology

Received: 05 December 2017
Accepted: 21 March 2018
Published: 24 April 2018

Citation:
Huang Z, Liu Q, Peng Y, Dai J, Xie Y, Chen W, Long S, Pei Z, Su H and Yao X (2018) Circadian Rhythm Dysfunction Accelerates Disease Progression in a Mouse Model With Amyotrophic Lateral Sclerosis. Front. Neurol. 9:218. doi: 10.3389/fneur.2018.00218

Amyotrophic lateral sclerosis (ALS) is a fatal neurodegenerative disease caused by interactions between environmental factors and genetic susceptibility. Circadian rhythm dysfunction (CRD) is a significant contributor to neurodegenerative conditions such as Alzheimer's disease and Parkinson's disease. However, whether CRD contributes to the progression of ALS remains little known. We performed behavioral and physiological tests on SOD1G93A ALS model mice with and without artificially induced CRD, and on wild-type controls; we also analyzed spinal cord samples histologically for differences between groups. We found that CRD accelerated the disease onset and progression of ALS in model mice, as demonstrated by aggravated functional deficits and weight loss, as well as increased motor neuron loss, activated gliosis, and nuclear factor κB-mediated inflammation in the spinal cord. We also found an increasing abundance of enteric cyanobacteria in the ALS model mice shortly after disease onset that was further enhanced by CRD. Our study provides initial evidence on the CRD as a risk factor for ALS, and intestinal cyanobacteria may be involved.

Keywords: circadian rhythm dysfunction, amyotrophic lateral sclerosis, inflammation, NF-κB, cyanobacteria

INTRODUCTION

Amyotrophic lateral sclerosis (ALS) is a fatal neurodegenerative disease that impairs motor neurons (MNs) in the brain and spinal cord, normally causing death within 3–5 years of onset (1). Although the precise mechanisms remain unclear, the consensus is that ALS is the pathological outcome of a combination of genetic and environmental factors. So far, more than 180 potential genetic risk factors have been identified, including mutations in SOD1 (Cu/Zn superoxide dismutase 1), TDP-43 (TAR DNA-binding protein 43), FUS (fused in sarcoma/translated in liposarcoma), and an increased number of repeats in C9ORF72 (2). Numerous studies have sought to identify ALS-related environmental factors, such as excessive exercise, mercury and heavy metal toxicity, geographical clustering, electromagnetic fields, head injuries, and neurotoxins (3, 4). Specifically, sleep disorders including nocturnal hypoventilation, restless legs syndrome, mood disorders,

sleep-disordered breathing, and circadian disturbances occur frequently in ALS patients (5, 6). Some studies suggest that circadian rhythm dysfunction (CRD) alters molecular, cellular, or physiologic functions that favor the development of neurodegenerative conditions (7–9).

The circadian system is considered to be a complex network of positive and negative feedback loops consisting of clock genes (clock and bmal1; per1-3 and cry1-2) and their transcriptional products (BMAL1-CLOCK complexes; PER1-3 and CRY1-2) and regulated by posttranslational events, such as phosphorylation and dephosphorylation (10, 11). The suprachiasmatic nucleus (SCN) is the core circadian clock, and is entrained by a zeitgeber ("time giver"), a signal such as the light–dark (diurnal) cycle transduced through the retinohypothalamic tract (12). Studies have shown that peripheral cells and tissues also have their own rhythmicity in the immune (13), cardiovascular (14), and digestive systems (15) with time. The SCN can synchronize both central nervous system rhythms and those of peripheral tissues through neural and humoral controls (16). Accumulating evidence demonstrates that CRD contributes to the progression of neurodegenerative diseases such as Alzheimer's disease (AD) and Parkinson's disease (PD) (7–9, 17, 18). Several mechanisms of functional impairment by abnormal circadian clocks have been proposed, including epigenetic signals, cellular metabolic changes, and inflammation (19). Gliosis play crucial roles in MN death *via* non-cell-autonomous mechanisms (20). A large body of evidence indicates that nuclear factor κB (NF-κB)-mediated signaling plays an important role in neuronal survival in many pathological conditions [for a review see Ref. (21)]. The p65 subunit is considered the most important NF-κB subunit in the nervous system, and the activation of NF-κB has been shown to involve the phosphorylation of p65 (p-p65) and IκB kinase (p-IKK) (22).

The gut and its microbiome are also regulated by the SCN circadian clock in a complex way. Although the digestive system cannot perceive illumination, the SCN, driven by the light zeitgeber, regulates digestive rhythms in a distinct way, by affecting the intestinal bacterial compositions of the host (23). However, other signals, such as feeding and drinking, were also found to act as zeitgebers for digestive clocks. Thus, it is quite possible for an enteric clock to be desynchronized from the SCN clock rhythm, an event that can result in broad-spectrum disorders like metabolic diseases (24). Indeed, a recent study has stated that the intestinal microbiome can regulate host transcriptomic oscillations through regulating rhythmic biogeography and the metabolome (25).

Increasing evidence suggests that disturbances in the gut microbiota contribute to the development of neurological diseases. For example, colonization with microbiota from patients with PD enhances motor impairments in animal models of PD (26). It has also been hypothesized that an unknown toxin produced by gut microbes causes ALS through the gut–microbe–brain axis (27, 28). Cyanobacteria (formerly known as blue-green algae) are common in water, cycads, and intestinal flora. Epidemiological studies suggest that the areas near rivers and lakes with cyanobacteria blooms, including Wisconsin, New Hampshire, and Southern France, had a higher incidence of ALS (29). Interestingly, cyanobacteria possess an internal clock system with a three-protein (Kai A/B/C) oscillator that maintains rhythmicity in certain biological activities, such as nitrogen fixation. Kai B folds into two different three-dimensional structures that can drive the internal transition between day and night (30). In addition, nitrogen starvation of cyanobacteria can trigger the production of β-*N*-methylamino-L-alanine (BMAA), a neurotoxin which inhibits MN growth (31). Very little information on the relationship between circadian rhythms, cyanobacteria, and ALS progression is available, particularly regarding alterations in gut microbiome compositions and the abundance of cyanobacteria at different stages in the progression of ALS. Therefore, the present study investigated whether CRD could alter either cyanobacteria abundance in gut microbiome compositions or disease progression in adult ALS model mice, or both.

MATERIALS AND METHODS

Animals and Circadian Dysfunction

Transgenic mice overexpressing human SOD1 were obtained from the Nanjing Biomedical Research Institute of Nanjing University, and the genotypes of their offspring were identified by polymerase chain reaction (PCR) using a standard protocol (32). Male transgenic [B6SJL-Tg (SOD1-G93A) 1GurJ] mice and their wild-type (WT) littermates were randomly divided into four groups: a SOD1G93A group with a light-induced CRD (ALS + CRD, $n = 19$), a SOD1G93A group with a normal light/dark cycle (ALS, $n = 18$), a WT group with a light-induced CRD (WT + CRD, $n = 20$), and a WT group with a normal light/dark cycle (WT, $n = 15$). All of the animals in CRD (altered rhythm) groups lived under a 20/4-h light/dark cycle from the age of 42 days until they were sacrificed; the animals in the other two groups lived under a normal 12/12-h light/dark cycle. Mice were sacrificed at the ages of 60, 90, or 120 days. All animals were provided *ad libitum* access to food and water in a temperature (25°C) and humidity (45–55%) -controlled environment. All experiments were performed according to the policies for the care and use of experimental animals and were approved by the Animal Ethical Committee at Sun Yat-Sen University, China. All animals were used only for one procedure and were humanely sacrificed under anesthesia after the completion of the experiment.

Body Weight and Motor Function Assessments

The mice were transferred to the new light/dark environments and adapted for 1 week before measurement of body weight and motor function. Body weight and motor function measurements were performed every 3 days from the age of 50 days to one of the above three time points by a trained observer blinded to the experimental conditions. The final time point was set at the age of 120 days because ALS mice begin to die at this age. Using the widely accepted 4-point evaluation system for motor deficits in SOD1G93A mice (33), we defined the day of disease onset as the day on which hind limb tremors were evident when suspending the mouse in the air by its tail. Impending terminal impairment was defined as the day on which a mouse was unable to right itself

within 30 s, and survival rate was calculated as a percentage of mice that had not reached the terminal stage.

Fecal Bacteria Analysis

Gene sequencing of 16S ribosomal RNA (rRNA) was performed to characterize the distal gut microbiota (22,800 ± 35,017 trimmed sequences per sample). At each of the three time points, fresh fecal samples were collected in sterile 1.5-ml Eppendorf tubes at approximately 0900–1100 and immediately frozen in liquid nitrogen for 5 min. The fresh fecal samples were then transferred to −80°C until further processing. Microbial genomic DNA was extracted from stools, and the V4 region of the 16S rRNA gene was PCR-amplified using the following primers: 515F, GTGCCAGCMGCCGCGGTAA, and 806R, GGACTAC-HVGGGTWTCTAAT. The PCR products were sequenced on an Illumina Hiseq 2 × 300 bp platform (TinyGene Bio-Tech Co. Ltd.; Shanghai, China). The comparisons of relative abundance of bacterial taxa were performed based on the total number of classified reads for each sample.

Immunolabeling

At the end of each time point, the mice were deeply anesthetized and transcardially perfused with ice-cold normal saline and followed by 4% paraformaldehyde. Then the spinal cords were carefully extracted, fixed in 4% paraformaldehyde for 24 h, and successively cryoprotected by immersion in 20 and 30% sucrose overnight. The cervical and lumbar enlargements were cut into 20-μm sections on a cryostat. Selected slices were blocked with 10% normal donkey serum (Beyotime) for 1 h at room temperature, and then incubated with primary antibodies to detect MNs (anti-choline acetyltransferase [ChAT], 1:400, OmnimAbs), astrocytes [anti-glial fibrillary acidic protein (GFAP), 1:400, Sigma], and microglia [anti-ionized calcium binding adaptor molecule 1 (Iba1), 1:200, Millipore] overnight at 4°C. Species-specific secondary antibodies were then added to incubate the slices at 37°C for 1 h in the dark. Images were captured using a Leica SP5 confocal microscope. The anterior horns of labeled sections were visualized and imaged with a laser scanning confocal microscope (Leica TCS SP5MP).

Western Blotting

Mice were deeply anesthetized and transcardially perfused with ice-cold normal saline and the spinal cords were carefully removed. Total protein was extracted from each sample using the extraction protocol (Pierce). The extraction buffer contained protease and phosphatase inhibitors. Equal amounts of protein (10 μg) were loaded onto 8 or 10% sodium dodecyl sulfate polyacrylamide gel electrophoresis gel (SDS-PAGE) and separated. The proteins were transferred onto 0.22-μm polyvinylidene difluoride membranes (Millipore). Non-specific binding was blocked using 5% bovine serum albumin for 1 h at room temperature. The blots were subsequently incubated overnight at 4°C in primary antibodies with mild agitation. The primary antibodies used were rabbit anti-ChAT (1:1,000, OmnimAbs), rabbit anti-GFAP (1:1,000, Sigma), rabbit anti-Iba1 (1:1,000, Millipore), rabbit anti-p65 (1:1,000, CST), rabbit anti-p-p65 (1:1,000, CST), rabbit anti-p-Ikkα/β (1:1,000, CST), rabbit anti-β-actin (1:2,000, Sigma), and rabbit anti-GAPDH (1:2,000, Sigma). The membranes were washed three times for 10 min with Tris-buffered saline containing Tween-20 (TBS/T) and incubated with goat anti-rabbit secondary antibody (1:2,000, abcam) for 1 h at room temperature. The membranes were subsequently washed four times for 10 min with TBS/T. Immunoreactive proteins were visualized using the chemiluminescent horseradish peroxidase substrate (Pierce) and scanned using image analyzer software (Bio-Rad, Image lab 4.1).

Analysis of MN Survival and Inflammation Activation in the Spinal Cord

Previous reports indicate that MNs in the cervical and lumbar segments of ALS model mice have very similar characteristics. We, therefore, studied sections from the cervical segment as representative of the spinal cord in the ALS model mice. About five sections per mice were labeled, and five fields of the ventral horn per slice were randomly selected at 250× magnification. We counted the numbers of ChAT-positive cells in these sections to assess the survival of MNs in the cervical spinal cord. We only counted ChAT-expressing cells clearly displaying a nucleolus located in the ventral horns of spinal sections. The number of surviving ventral horn MNs was described quantitatively as a percentage of the number counted in the WT controls. The luminescence intensity values of western blot bands were calculated by integrating the signals using ImageJ software. The normalized value of p-p65 is represented by the ratio of p65. All expression levels of gliosis and NF-κB are shown as rates of values in the WT controls.

Statistical Analysis

All the data are presented as the means ± SEM. The comparisons of the relative abundances of microflora were analyzed using the Differentially Abundant Features program (Metastats, http://metastats.cbcb.umd.edu). A one-way of analysis of variance followed by Bonferroni's *post hoc* test for multiple comparisons was used to analyze MN survival and glial activation. The comparisons between two groups were made using GraphPad Prism 5 (GraphPad Prism; La Jolla, CA, USA). p-Values < 0.05 were considered significant.

RESULTS

CRD Accelerated Disease Onset and Progression in ALS Model Mice

As shown in **Figure 1A**, the 42-day-old ALS model and WT mice were housed in a 20/4-h light/dark (ALS + CRD and WT + CRD groups) and a regular 12/12-h light/dark cycle (ALS and WT groups). Body weight and behavioral assessments were acquired every 3 days until euthanasia at days 60, 90, and 120. Symptom onset, as assessed based on motor function tests, occurred at 74.00 ± 2.60 days of age in the ALS group ($n = 14$). The end stage occurred at 130.00 ± 3.662 days of age in the ALS model mice ($n = 7$). In contrast, symptom onset was significantly advanced in the ALS + CRD group, occurring 12 days earlier than in the ALS group (**Figure 1B**; ALS + CRD: 62.00 ± 0.78 days of age, $n = 15$, $p < 0.01$); CRD also significantly

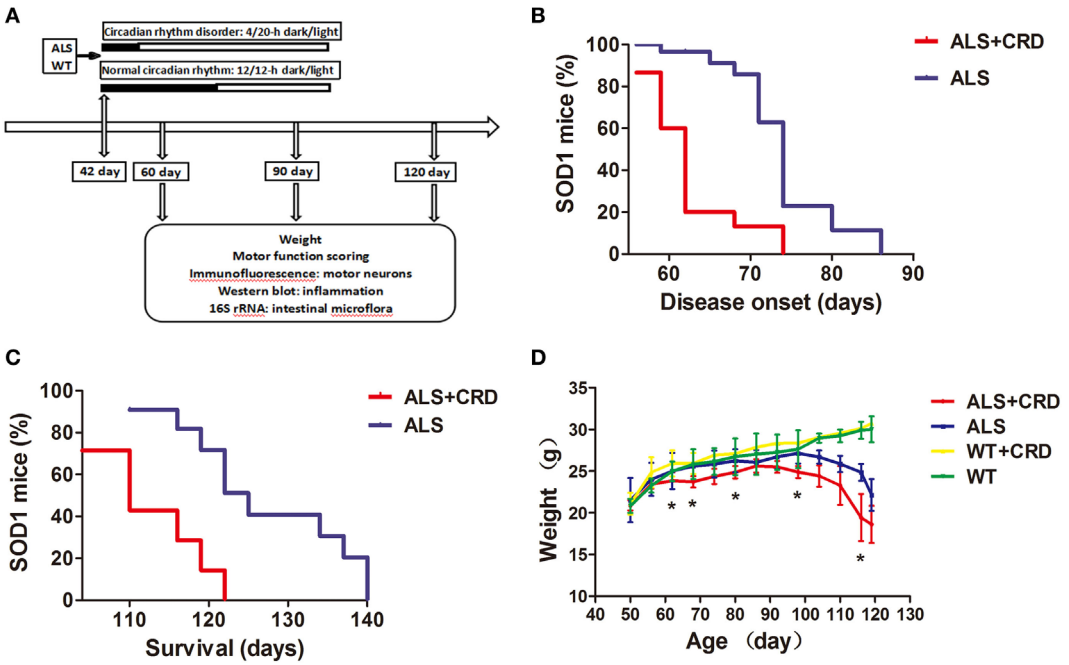

FIGURE 1 | Circadian rhythm dysfunction (CRD) accelerated disease onset and progression in *SOD1G93A* mice. **(A)** A schematic showing the experimental procedures. **(B,C)** Survival curves: disease onsets and disease progression in the ALS + CRD and the ALS group. **(D)** Body weights loss of four groups starting from the day 50 to the day 119. $N = 4$–6 animals per group, $^*p < 0.05$. Error bars represent SEM.

shortened the lifespan of ALS mice (**Figure 1C**; ALS + CRD: 116.00 ± 3.00 days of age, $n = 7$, $p < 0.05$). We measured the change in body weight of the mice over time because body weight is a reliable index of disease progression in ALS (33). All mice in both the ALS and ALS + CRD groups demonstrated weight loss over time. A rapid and significant drop in body weight was found in the ALS group at the age of 83 days compared to the WT group (**Figure 1D**, $p < 0.05$). Notably, CRD accelerated the body weight loss of the ALS model mice such that the weight loss in the ALS + CRD group was significantly worse than that in the ALS group beginning at about 62 days of age (**Figure 1D**, $p < 0.05$). In contrast, WT mice gained weight during the experimental period; CRD did not affect body weight in the WT mice (**Figure 1D**, $p > 0.05$). Taken together, these results suggested that CRD accelerated the onset and progression of the ALS in the model mice.

CRD Aggravated Neurodegeneration and Induced Inflammation in SOD1G93A Mice

The most typical pathological feature of ALS is the degeneration of spinal MNs. As shown in **Figure 2A**, there were no significant differences in the numbers of ChAT-positive cells at any time point between the WT + CRD group and WT groups, suggesting that chronic CRD did not lead to MN death in WT mice. In comparison, the percentage of remaining ChAT-positive cells in the ALS + CRD group was significantly lower than that of the ALS group at the 60-day time point (**Figures 2A–C**; $p < 0.01$) and the 90-day time point (**Figures 2A–C**; $p < 0.05$); the difference between the two groups at the 120-day time point was not significant because of the paucity of cells remaining in both the ALS + CRD and ALS groups at that time. Glial activation was assessed using both immunofluorescence and western blot measurements of GFAP and Iba1. Significantly more intense GFAP expression was detected in the ALS + CRD group relative to the ALS group at the 60- and 90-day time points (**Figures 2A,D,F**; $p < 0.05$). There were similar differences in Iba1 intensity between the ALS + CRD and ALS groups, although these differences were significant only at the 90-day and 120-day time points (**Figures 2B,E,F**; $p < 0.01$). The mice in the WT + CRD group also had a slight increase in GFAP and Iba1 expression when compared to those in the WT group. We measured the expression levels of p65, p-p65, and p-IKK, which are important constituents of the classical NF-κB inflammatory pathway. The expression levels of p-p65 and p-IKK were all slight increased in the ALS + CRD group when compared to the ALS group at each time point, but only had significance in p-p65 at days 90 and 120. A increase trend was observed in the WT + CRD group when compared to the WT group (**Figures 3A–C**, $p < 0.05$). All of the inflammatory markers assessed in the ALS group were increased significantly in association with disease progression. These data suggest that CRD exacerbated MNs loss and increased the numbers of gliosis and NF-κB inflammatory responses in the spinal anterior horn in transgenic ALS mice.

CRD Increased Enteric Cyanobacteria Abundance in SOD1G93A Mice

Ribosomal RNA analyses allowed for a phylum-level description of the intestinal flora in the different experimental groups.

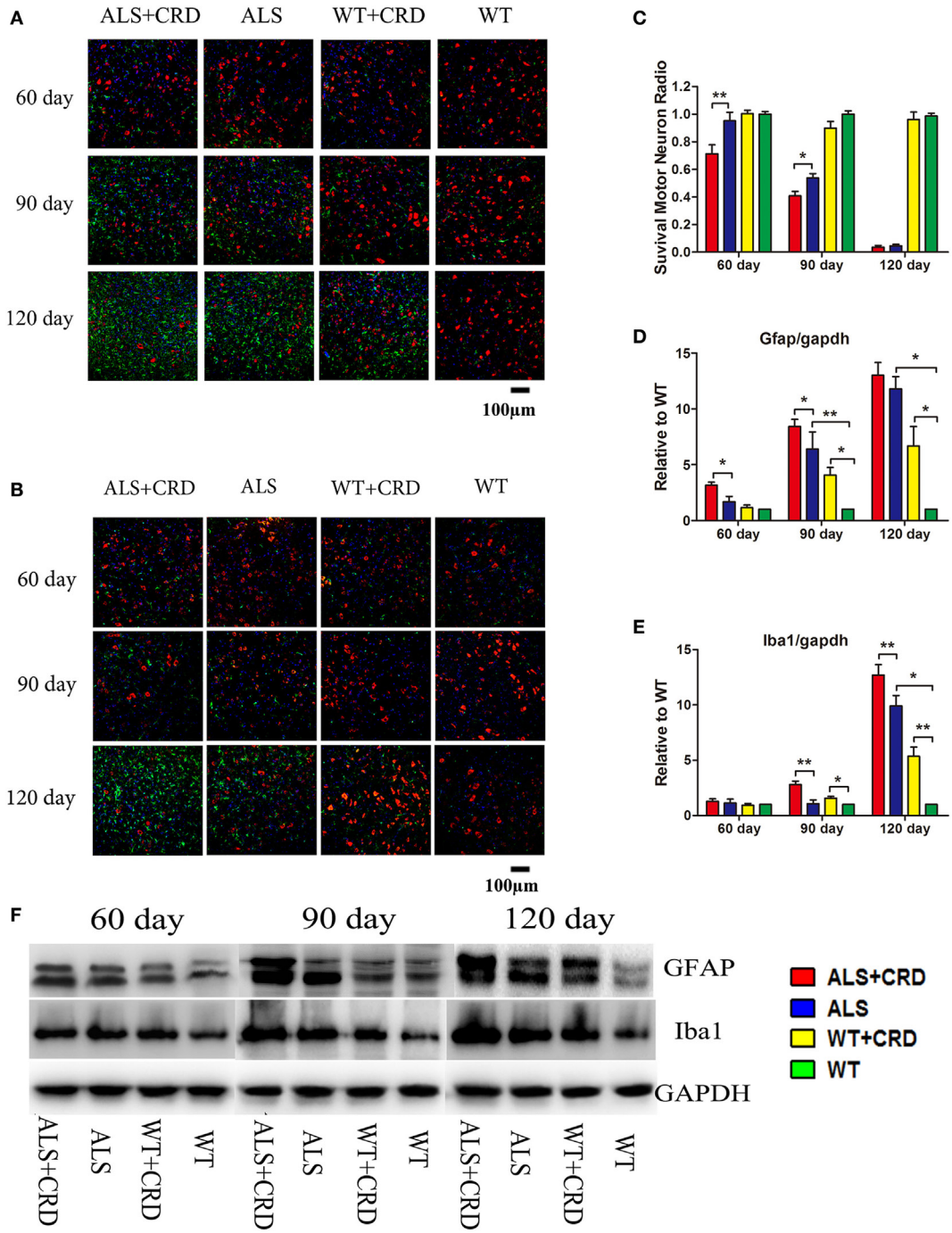

FIGURE 2 | Circadian rhythm dysfunction (CRD) aggravated motor neuron (MN) loss and activated glial cells in *SOD1G93A* mice. **(A)** MNs [choline acetyltransferase (ChAT)-positive cells, red] and astrocytes [glial fibrillary acidic protein (GFAP)-positive cells, green] expression in four groups for three stages. **(B)** MNs (ChAT-positive cells, red) and microcytes (Iba1-positive cells, green) expression in four groups for three stages. Scale bars represent 100 μm. **(C)** Statistical evaluation of surviving MNs radio by counting the number of ChAT-positive cells. $^{**}p < 0.01$; $^{*}p < 0.05$ (one-way ANOVA, $n = 4$–6 animals per group). **(D,E)** GFAP and Iba1 expression was quantified at three stages by western blotting (one-way ANOVA, $n = 2$–3 animals per group). **(F)** Expression of GFAP and Iba1 in the spinal cord. $^{**}p < 0.01$; $^{*}p < 0.05$. Error bars represent SEM.

The microbial gut compositions of the four groups at the three time points are presented in **Figure 4A**. The most abundant fecal microbes found in all four groups at all time points belonged to the phyla Bacteroidetes, Firmicutes, Proteobacteria, Verrucomicrobia, Deferribacteres, and Cyanobacteria (**Figure 4A**). Principle component analysis identified evident cluster differences

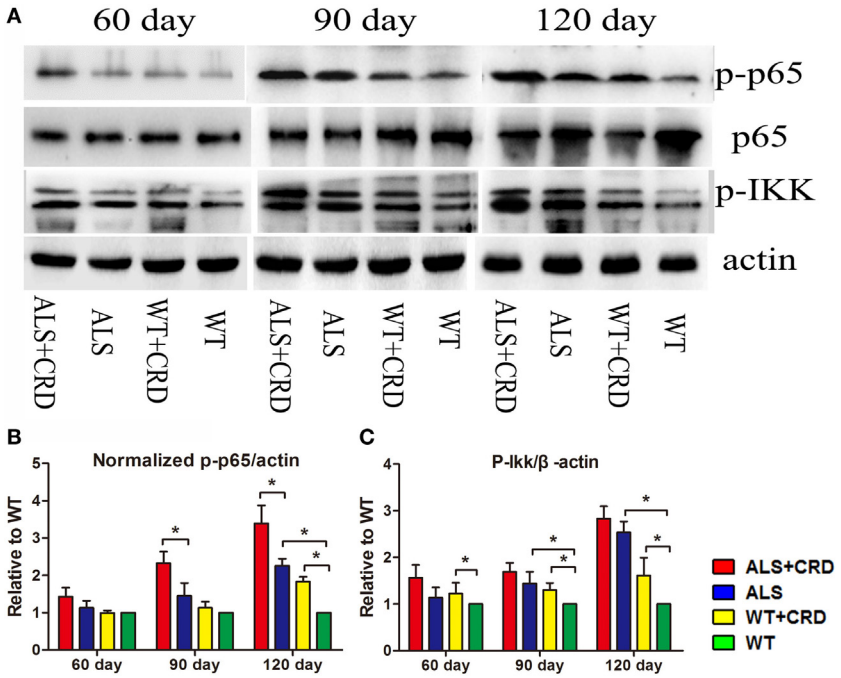

FIGURE 3 | Circadian rhythm dysfunction (CRD) aggravated nuclear factor κB-mediated inflammation in *SOD1G93A* mice. **(A)** Expression of p65, p-p65, and p-IKK in the spinal cord. **(B,C)** Expression of p-IKK and normalized p-p65 was quantified at three stages by western blotting (one-way ANOVA, $n = 2$–3 animals per group). $^{**}p < 0.01$; $^{*}p < 0.05$. Error bars represent SEM.

in the compositions of gut flora between the ALS + CRD and ALS groups at both the 60- and 90-day time points (**Figure 4B**). Because epidemiological studies suggest that an increased abundance of cyanobacteria is associated with a higher incidence of ALS (29). Therefore, we focused our attention on the possible relationship between CRD and the abundance of enteric cyanobacteria. A significant increase in the relative quantity of cyanobacteria in the ALS model mice vs. the WT mice was found at the 90-day time point (**Figure 4C**, 0.8807 ± 0.3429% reads in the ALS group vs. 0.1180 ± 0.0264% reads in the WT group, $p < 0.05$). CRD significantly increased the cyanobacteria abundance beyond that of the ALS group at the 60-day time point (**Figure 4C**; day 60: 0.3512 ± 0.0743% reads in the ALS + CRD group vs. 0.1471 ± 0.0406% reads in the ALS group, $p < 0.05$), but only a slight increase at day 90-day time point (**Figure 4C**; day 90: 1.886 ± 0.5680% reads in the ALS + CRD group vs. 0.8807 ± 0.3429% reads in the ALS group, $p > 0.05$). These data showed that CRD might enrich the proportion cyanobacteria in the gut of ALS model mice. CRD did not lead to significant changes in the cyanobacteria levels in the WT mice at any of the three time points (**Figure 4C**; day 60: 0.2222 ± 0.1624% reads in the WT + CRD group vs. 0.0898 ± 0.0086% reads in the WT group, $p > 0.05$; day 90: 1.1689 ± 0.6295% reads in the WT + CRD group vs. 0.118 ± 0.0264% reads in the WT group, $p > 0.05$; day 120: 0.1892 ± 0.0579% reads in the WT + CRD group vs. 0.3335 ± 0.1574% reads in the WT group, $p > 0.05$). Moreover, no significant difference in the cyanobacteria levels was found between the ALS + CRD group and the WT + CRD group at any of the three time points (**Figure 4C**; day 60: 0.3512 ± 0.0743% reads in the ALS + CRD group vs. 0.2222 ± 0.1624% reads in the WT + CRD group, $p > 0.05$; day 90: 1.8862 ± 0.5680% reads in the ALS + CRD group vs. 1.1689 ± 0.6295% reads in the WT + CRD group, $p > 0.05$; day 120: 0.2222 ± 0.0973% reads in the ALS + CRD group vs. 0.1892 ± 0.0579% reads in the WT + CRD group, $p > 0.05$).

DISCUSSION

Accumulating evidence suggests that disturbed circadian rhythms contribute to the progression of several neurodegenerative diseases such as AD and PD, and here, we provide evidence that CRD could contribute to ALS progression as well. We found that CRD exacerbated the degeneration of MNs in the spinal ventral horn, increased the numbers of glial cells, activated the NF-κB inflammatory pathway, increased the numbers of gut cyanobacteria, and accelerated both the onset and progression of the disease in the presence of an SOD1 mutation.

Disturbed circadian rhythms are comorbid with psychiatric abnormalities including stress, anxiety, depression, schizophrenia, and suicide (34). Transgenic animal models of clock disruptions such as PER1Brdm1−/−, CRY1−/−, and CRY2−/− mutant mice displayed evident depression or anxiety-like behaviors, as well as arrhythmic feeding behavior and impaired glucose tolerance (35). Interestingly, several of the above pathological states have been observed in patients and/or animals with ALS. Persistent exposure to intense stress led to more activation of astrocytes and

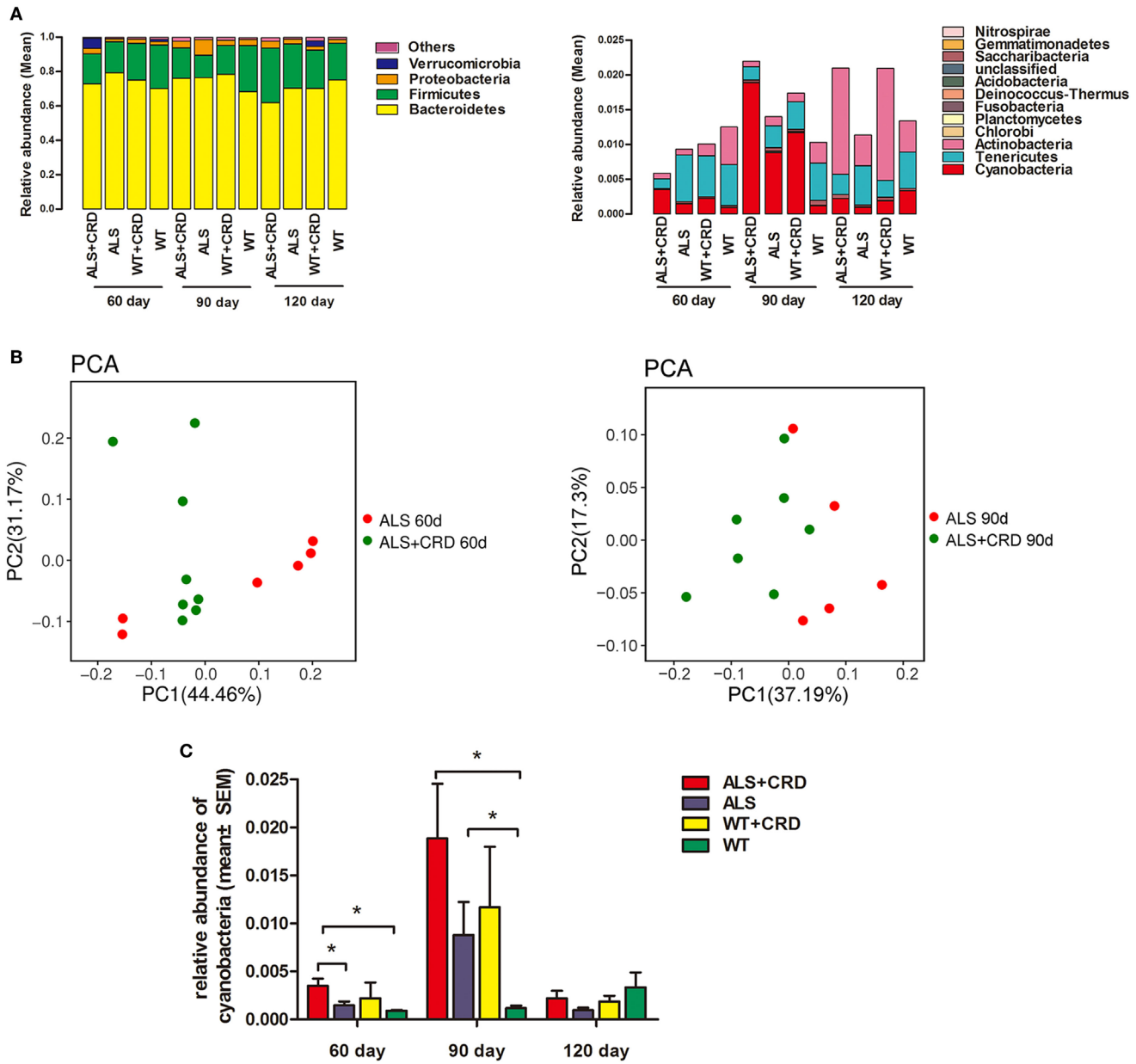

FIGURE 4 | Circadian rhythm dysfunction (CRD) increased enteric cyanobacteria abundance in *SOD1G93A* mice. **(A)** Intestinal bacterial abundance profiles at the level of phylum among the four groups at three time points using 16S high throughput sequencing. Flora were presented in the form of averages. Sample capacity of each group was 4–8. **(B)** Differences and distances of each sample between the amyotrophic lateral sclerosis (ALS) + CRD group and the ALS group at day 60 and 90, respectively, reflected by Principle Component Analysis (PCA). **(C)** Comparisons of relative abundances of cyanobacteria among the four groups at different disease stages. $N = 4–6$ per group per time point, $^*p < 0.05$. Error bars represent SEM.

microglia in the spinal cord, accelerated symptoms, and shortened the median survival period in mouse models with ALS (36). Disturbed eating behaviors and metabolic dysfunction worsened disease progression and prognosis of ALS (37). Additionally, the glial immune reactions that are crucial components of the process underlying ALS were found to follow a circadian variation in the mouse SCN, and could mediate peripheral signals being sent to the central circadian clock (38). Here, astrocytic and microglial activation in the spinal cord accompanying the disruption of circadian rhythmicity may support the role of glial immune reactions in ALS.

Many immunohistochemistry studies have shown that NF-κB is activated in glia in patients with familial and sporadic ALS and in animal models of the disease (39, 40). Consistent with these findings, we found a gradual increase in the activation of the constituents of the NF-κB pathway in the spinal

cord in association with disease progress in SOD1G93A ALS mice. More direct evidence indicates that inappropriate NF-κB activation is the pathogenic mechanism underlying optineurin mutation-related ALS (41, 42). The circadian clock controls many physiological changes mediated by activation of the transcription factor NF-κB (43). In our study, activation of the NF-κB pathway in the spinal cord caused by circadian rhythm disorder further confirmed that NF-κB-induced inflammation mediates the connection between abnormal circadian rhythm and neuronal death in ALS model mice. Microglia, but not astrocytes, can induce MN death *via* the classical NF-κB pathway in ALS (44). Therefore, whether the effects of the abnormal circadian rhythm were mainly mediated by microglia or astrocytes requires further investigation, as both cell types were activated in our study. More intense inflammatory reactions were also seen in WT mice exposed to the unusual circadian rhythm, although such inflammatory changes were not sufficient to cause neuronal death in WT mice. We thus conclude that circadian rhythm disorder catalyzes pathological progress in individuals with ALS due to genetic mutations, although it is not a causative factor. If this is true, then prophylactic treatments to adjust the circadian rhythm might be required for patients with familiar ALS. Although our work defines CRD as a risk factor for ALS progression, the exact mechanisms linking the circadian clock and MNs, and the subsequent upregulation of inflammatory responses requires further in-depth studies.

The gut microbiome and the SCN circadian clock may interact reciprocally in complex ways (23–25). We, therefore, hypothesize that the negative effects of CRD on the progression of ALS result from multifaceted mechanisms involving the intestinal microbiota. The recent study regarding the colonization of microbiota from patients with PD cited in the Section "Introduction" demonstrates the importance of gut microbes in PD (26). Furthermore, constipation is a common and early non-motor symptom in patients with PD that can be improved by treatment with *Lactobacillus casei* Shirota (45). However, similar studies on the effects of gut microbes in ALS are rare, although gut health-related problems, such as eating difficulties, lower physical activity, and mood disorders, are common in patients with ALS (46). The use of 16S rRNA sequencing has improved the correlative analysis of gut microflora and disease. Recently, shifts in the intestinal microbiome and aberrant intestinal homeostasis were reported to be associated with ALS pathophysiology in SOD1G93A mice following 454 pyrosequencing (47). The oral administration of butyrate restored intestinal microbiota homeostasis, and thus delayed disease onset and progression in the SOD1G93A mice (47).

The prevalence of ALS is greater in areas with abundant cyanobacteria or high levels of BMAA (48, 49). We found a remarkable increase of the cyanobacteria abundance at day 90, shortly after disease onset in the ALS model mice, which hints a link between intestinal cyanobacteria and the onset and progression of ALS. Gut microflora are vulnerable to the changes of host diet, circadian clock, genotype, age, sex, medicine, and other conditions (50). In this study, the relative abundance of cyanobacteria was enriched by CRD in the ALS model mice at the day 60. However, there were no statistically significant differences in intestinal cyanobacteria in the terminal stages among the four groups. We suspect that this may be due to extremely disordered floral changes due to many different factors, such as an inability to eat or move at the end stages of the disease in ALS mice. Thus, it is tempting to conclude that CRD gradually desynchronizes the intestinal activity of cyanobacteria in the early stage of ALS progression. Cyanobacteria generate BMAA, which has been shown to be neurotoxic and correlated with the higher incidence of ALS-related neurodegenerative disease in Guam (48). Additionally, a recent study found that neonatal mice treated with BMAA had long-term learning impairments (51). Another study analyzing the gut in SOD1G93A mice demonstrated deficits in the tight junction protein zonula occludens-1 leading to increased gut permeability. The above report thus highlights a putative mechanism by which neurotoxins can move from the gut to the brain (52). Our results provide evidence that circadian rhythm disorders promote ALS disease onset and progression, possibly by increasing the abundance of gut cyanobacteria in the mice. However, assessments of the levels of BMAA and other cyanobacterial neurotoxins, such as saxitoxin and anatoxin (53–55), will be necessary in determining the mechanisms underlying the effects of gut cyanobacteria on disease onset and progression in ALS.

ETHICS STATEMENT

This study was carried out in accordance with the institutional recommendations for the care and use of experimental animals of the research and ethics committee. The protocol was approved by the Animal Ethical Committee at Sun Yat-Sen University, China.

AUTHOR CONTRIBUTIONS

ZH, HS, and XY contributed to the conception and design of the study; ZH, QL, YP and SL organized the database; JD, YX and WC performed the statistical analysis; ZH, HS and XY wrote the first draft of the manuscript; QL and ZP wrote sections of the manuscript. All authors contributed to manuscript revision, read and approved the submitted final version.

FUNDING

This study was supported by the grants from Science and Technology Program of Guangzhou (No. 2014J4500031); Fundamental Research Funds for Central Universities (No.15ykcj15b); National Key Research and Development Program of China (No. 2017YFC0907703); National Key Research and Development Program of China (No. 2017YFA0105104); Guangdong Provincial Key Laboratory for Diagnosis and Treatment of Major Neurological Disease (No. 2014B030301035); The Southern China International Cooperation Base for Early Intervention and Functional Rehabilitation of Neurological Diseases (No. 2015B050501003); Guangzhou Clinical Research and Translational Center for Major Neurological Disease (No. 201604020010); and Guangdong Provincial Engineering Center for Major Neurological Disease Treatment.

REFERENCES

1. Gordon PH. Amyotrophic lateral sclerosis: an update for clinical features, pathophysiology, management and therapeutic trials. *Aging Dis* (2013) 4:295–310. doi:10.14336/AD.2013.0400295
2. Taylor JP, Brown RH, Cleveland DW. Decoding ALS: from genes to mechanism. *Nature* (2016) 539:197–206. doi:10.1038/nature20413
3. Al-Chalabi A, Hardiman O. The epidemiology of ALS: a conspiracy of genes, environment and time. *Nat Rev Neurol* (2013) 9:617–28. doi:10.1038/nrneurol.2013.203
4. Zufiría M, Gil-Bea FJ, Fernández-Torrón R, Poza JJ, Muñoz-Blanco JL, Rojas-García R, et al. ALS: a bucket of genes, environment, metabolism and unknown ingredients. *Prog Neurobiol* (2016) 142:104–29. doi:10.1016/j.pneurobio.2016.05.004
5. Ahmed RM, Newcombe RE, Piper AJ, Lewis SJ, Yee BJ, Kiernan MC, et al. Sleep disorders and respiratory function in amyotrophic lateral sclerosis. *Sleep Med Rev* (2016) 26:33–42. doi:10.1016/j.smrv.2015.05.007
6. Bourke SC, Shaw PJ, Gibson GJ. Respiratory function vs sleep-disordered breathing as predictors of QOL in ALS. *Neurology* (2001) 57:2040–2. doi:10.1212/WNL.57.11.2040
7. Musiek ES, Holtzman DM. Mechanisms linking circadian clocks, sleep, and neurodegeneration. *Science* (2016) 354:1004–8. doi:10.1126/science.aah4968
8. Roh JH, Huang YF, Bero AW, Kasten T, Stewart FR, Bateman RJ, et al. Disruption of the Sleep-Wake Cycle and Diurnal Fluctuation of Amyloid-β in Mice with Alzheimer's Disease Pathology. *Sci Transl Med* (2012) 4:122–50. doi:10.1126/scitranslmed.3004291
9. Breen DP, Vuono R, Nawarathna U, Fisher K, Shneerson JM, Reddy AB, et al. Sleep and circadian rhythm regulation in early Parkinson disease. *JAMA Neurol* (2014) 71:589–95. doi:10.1001/jamaneurol.2014.65
10. Gallego M, Virshup DM. Post-translational modifications regulate the ticking of the circadian clock. *Nature Rev Mol Cell Biol* (2007) 8:139–48. doi:10.1038/nrm2106
11. Welsh DK, Takahashi JS, Kay SA. Suprachiasmatic nucleus: cell autonomy and network properties. *Annu Rev Physiol* (2010) 72:551–77. doi:10.1146/annurev-physiol-021909-135919
12. Golombek DA, Rosenstein RE. Physiology of circadian entrainment. *Physiol Rev* (2009) 90:1063–102. doi:10.1152/physrev.00009.2009
13. Yu X, Rollins D, Ruhn KA, Stubblefield JJ, Green CB, Kashiwada M, et al. TH17 cell differentiation is regulated by the circadian clock. *Science* (2013) 342:727–30. doi:10.1126/science.1243884
14. Storch KF, Lipan O, Leykin I, Viswanathan N, Davis FC, Wong WH, et al. Extensive and divergent circadian gene expression in liver and heart. *Nature* (2002) 417:78–83. doi:10.1038/nature744
15. Scheving LA, Russell WE. It's about time: clock genes unveiled in the gut. *Gastroenterology* (2007) 133:1373–6. doi:10.1053/j.gastro.2007.08.068
16. Yamazaki S, Numano R, Abe M, Hida A, Takahashi R, Ueda M, et al. Resetting central and peripheral circadian oscillators in transgenic rats. *Science* (2000) 288:682–5. doi:10.1126/science.288.5466.682
17. Karatsoreos IN, Bhagat S, Bloss EB, Morrison JH, McEwen BS. Disruption of circadian clocks has ramifications for metabolism, brain, and behavior. *Proc Natl Acad Sci U S A* (2011) 108:1657–62. doi:10.1073/pnas.1018375108
18. Lauretti E, Di, Meco A, Merali S, Praticò D. Circadian rhythm dysfunction: a novel environmental risk factor for Parkinson's disease. *Mol Psychiatry* (2017) 22:280–6. doi:10.1038/mp.2016.47
19. Masri S, Sassone-Corsi P. The circadian clock: a framework linking metabolism, epigenetics and neuronal function. *Nat Rev Neurosci* (2013) 14:69–75. doi:10.1038/nrn3393
20. Clement AM, Nguyen MD, Roberts EA, Garcia ML, Boillée S, Rule M, et al. Wildtype nonneuronal cells extend survival of SOD1 mutant motor neurons in ALS mice. *Science* (2003) 302:113–7. doi:10.1126/science.1086071
21. Mincheva-Tasheva S, Soler RM. NF-κB signaling pathways: role in nervous system physiology and pathology. *Neuroscientist* (2013) 19:175–94. doi:10.1177/1073858412444007
22. Mattson MP, Meffert MK. Roles for NF-κB in nerve cell survival, plasticity, and disease. *Cell Death Differ* (2006) 13:852–60. doi:10.1038/sj.cdd.4401837
23. Liang X, Bushman FD, FitzGerald GA. Rhythmicity of the intestinal microbiota is regulated by gender and the host circadian clock. *Proc Natl Acad Sci U S A* (2015) 112:10479–84. doi:10.1073/pnas.1501305112
24. Landgraf D, Tsang AH, Leliavski A, Koch CE, Barclay JL, Drucker DJ, et al. Oxyntomodulin regulates resetting of the liver circadian clock by food. *Elife* (2015) 4:e06253. doi:10.7554/eLife.06253
25. Thaiss CA, Levy M, Korem T, Dohnalová L, Shapiro H, Jaitin DA, et al. Microbiota diurnal rhythmicity programs host transcriptome oscillations. *Cell* (2016) 167:1495–510. doi:10.1016/j.cell.2016.11.003
26. Sampson TR, Debelius JW, Thron T, Janssen S, Shastri GG, Ilhan ZE, et al. Gut microbiota regulate motor deficits and neuroinflammation in a model of Parkinson's disease. *Cell* (2016) 167:1469–80. doi:10.1016/j.cell.2016.11.018
27. Longstreth WT, Meschke JS, Davidson SK, Smoot LM, Smoot JC, Koepsell TD. Hypothesis: a motor neuron toxin produced by a clostridial species residing in gut causes ALS. *Med Hypotheses* (2005) 64:1153–6. doi:10.1016/j.mehy.2004.07.041
28. Kaneko K, Hachiya NS. Hypothesis: gut as source of motor neuron toxin in the development of ALS. *Med Hypotheses* (2006) 66:438–9. doi:10.1016/j.mehy.2005.09.012
29. Bradley WG, Borenstein AR, Nelson LM, Codd GA, Rosen BH, Stommel EW, et al. Is exposure to cyanobacteria an environmental risk factor for amyotrophic lateral sclerosis and other neurodegenerative diseases? *Amyotroph Lateral Scler Frontotemporal Degener* (2013) 14:325–33. doi:10.3109/21678421.2012.750364
30. Chang YG, Cohen SE, Phong C, Myers WK, Kim YI, Tseng R, et al. Circadian rhythms. A protein fold switch joins the circadian oscillator to clock output in cyanobacteria. *Science* (2015) 349:324–8. doi:10.1126/science.1260031
31. Downing S, Banack SA, Metcalf JS, Cox PA, Downing TG, et al. Nitrogen starvation of cyanobacteria results in the production of β-N-methylamino-L-alanine. *Toxicon* (2011) 58:187–94. doi:10.1016/j.toxicon.2011.05.017
32. Gurney ME, Pu H, Chiu AY, Dal Canto MC, Polchow CY, Alexander DD, et al. Motor neuron degeneration in mice that express a human Cu,Zn superoxide dismutase mutation. *Science* (1994) 264(5166):1772–5. doi:10.1126/science.8209258
33. Weydt P, Hong SY, Kliot M, Moller T. Assessing disease onset and progression in the *SOD1* mouse model of ALS. *Neuroreport* (2003) 14:1051–4. doi:10.1097/01.wnr.0000073685.00308.89
34. Lamont EW, Legault-Coutu D, Cermakian N, Boivin DB. The role of circadian clock genes in mental disorders. *Dialogues Clin Neurosci* (2007) 9:333–42.
35. Barandas R, Landgraf D, McCarthy MJ, Welsh DK. Circadian clocks as modulators of metabolic comorbidity in psychiatric disorders. *Curr Psychiatry Rep* (2015) 17:98. doi:10.1007/s11920-015-0637-2
36. Fidler JA, Treleaven CM, Frakes A, Tamsett TJ, McCrate M, Cheng SH, et al. Disease progression in a mouse model of amyotrophic lateral sclerosis: the influence of chronic stress and corticosterone. *FASEB J* (2011) 25:4369–77. doi:10.1096/fj.11-190819
37. Ahmed RM, Irish M, Piguet O, Halliday GM, Ittner LM, Farooqi S, et al. Amyotrophic lateral sclerosis and frontotemporal dementia: distinct and overlapping changes in eating behaviour and metabolism. *Lancet Neurol* (2016) 15:332–42. doi:10.1016/S1474-4422(15)00380-4
38. Leone MJ, Marpegan L, Bekinschtein TA, Costas MA, Golombek DA. Suprachiasmatic astrocytes as an interface for immune-circadian signalling. *J Neurosci Res* (2006) 84:1521–7. doi:10.1002/jnr.21042
39. Prell T, Lautenschlager J, Weidemann L, Ruhmer J, Witte OW, Grosskreutz J. Endoplasmic reticulum stress is accompanied by activation of NF-kappa B in amyotrophic lateral sclerosis. *J Neuroimmunol* (2014) 270:29–36.
40. Swarup V, Phaneuf D, Dupré N, Petri S, Strong M, Kriz J, et al. Deregulation of TDP-43 in amyotrophic lateral sclerosis triggers nuclear factor kB-mediated pathogenic pathways. *J Exp Med* (2011) 208:2429–47. doi:10.1084/jem.20111313
41. Maruyama H, Morino H, Ito H, Izumi Y, Kato H, Watanabe Y, et al. Mutations of optineurin in amyotrophic lateral sclerosis. *Nature* (2010) 465:223–6. doi:10.1038/nature08971
42. Akizuki M, Yamashita H, Uemura K, Maruyama H, Kawakami H, Ito H, et al. Optineurin suppression causes neuronal cell death via NF-κB pathway. *J Neurochem* (2013) 126:699–704. doi:10.1111/jnc.12326
43. Spenglera ML, Kuropatwinski KK, Comas K, Gasparian V, Fedtsova N, Gleiberman AS, et al. Core circadian protein CLOCK is a positive regulator of NF-κB–mediated transcription. *Proc Natl Acad Sci U S A* (2012) 109(37):E2457–65. doi:10.1073/pnas.1206274109
44. Frakes AE, Ferraiuolo L, Haidet-Phillips AM, Schmelzer L, Braun L, Miranda CJ, et al. Microglia induce motor neuron death via the classical NF-kB pathway in amyotrophic lateral sclerosis. *Neuron* (2014) 81:1009–23. doi:10.1016/j.neuron.2014.01.013

45. Cassani E, Privitera G, Pezzoli G, Pusani C, Madio C, Iorio L, et al. Use of probiotics for the treatment of constipation in Parkinson's disease patients. *Minerva Gastroenterol Dietol* (2011) 57:117–21.
46. Forshew DA, Bromberg MB. A survey of clinicians' practice in the symptomatic treatment of ALS. *Amyotroph Lateral Scler Other Motor Neuron Disord* (2003) 4:258–63. doi:10.1080/14660820310017344
47. Zhang YG, Wu SP, Yi JX, Xia YL, Jin DP, Zhou JS, et al. Target intestinal microbiota to alleviate disease progression in amyotrophic lateral sclerosis. *Clin Ther* (2017) 39:322–36. doi:10.1016/j.clinthera.2016.12.014
48. Cox PA, Banack SA, Murch SJ. Biomagnification of cyanobacterial neurotoxins and neurodegenerative disease among the Chamorro people of Guam. *Proc Natl Acad Sci U S A* (2003) 100:13380–3. doi:10.1073/pnas.2235808100
49. Kuzuhara S. Revisit to Kii ALS – the innovated concept of ALS-Parkinsonism-dementia complex, clinicopathological features, epidemiology and etiology. *Brain Nerve* (2007) 59:1065–74.
50. Maurice CF, Knowles SC, Ladau J, Pollard KS, Fenton A, Pedersen AB, et al. Marked seasonal variation in the wild mouse gut microbiota. *ISME J* (2015) 9:2423–34. doi:10.1038/ismej.2015.53
51. Karlsson O, Roman E, Brittebo EB. Long-term cognitive impairments in adult rats treated neonatally with beta-N-methylamino-L-alanine. *Toxicol Sci* (2009) 112:185–95. doi:10.1093/toxsci/kfp196
52. Wu SP, Yi JX, Zhang YG, Zhou JS, Sun J. Leaky intestine and impaired microbiome in an amyotrophic lateral sclerosis mouse model. *Physiol Rep* (2015) 3:e12356. doi:10.14814/phy2.12356
53. Kerrin ES, White RL, Quilliam MA. Quantitative determination of the neurotoxin β-N-methylamino-L-alanine (BMAA) by capillary electrophoresis-tandem mass spectrometry. *Anal Bioanal Chem* (2017) 409:1481–91. doi:10.1007/s00216-016-0091-y
54. Lajeunesse A, Segura PA, Gélinas M, Hudon C, Thomas K, Quilliam MA, et al. Detection and confirmation of saxitoxin analogues in freshwater benthic Lyngbya wollei algae collected in the St. Lawrence River (Canada) by liquid chromatography-tandem mass spectrometry. *J Chromatogr A* (2012) 6:93–103. doi:10.1016/j.chroma.2011.10.092
55. Dittmann E, Fewer DP, Neilan BA. Cyanobacterial toxins: biosynthetic routes and evolutionary roots. *FEMS Microbiol Rev* (2013) 37:23–43. doi:10.1111/j.1574-6976.2012.12000.x

Conflict of Interest Statement: The authors declare that the research was conducted in the absence of any commercial or financial relationships that could be construed as a potential conflict of interest.

frontiers in Psychiatry

ORIGINAL RESEARCH
published: 17 April 2018
doi: 10.3389/fpsyt.2018.00142

Body Mass Index in Mild Cognitive Impairment According to Age, Sex, Cognitive Intervention, and Hypertension and Risk of Progression to Alzheimer's Disease

*Soo Hyun Joo[1], Se Hee Yun[2], Dong Woo Kang[1], Chang Tae Hahn[3], Hyun Kook Lim[4] and Chang Uk Lee[1]**

[1] Department of Psychiatry, Seoul St. Mary's Hospital, College of Medicine, The Catholic University of Korea, Seoul, South Korea, [2] Seocho Center for Dementia, Seoul, South Korea, [3] Department of Psychiatry, Daejeon St. Mary's Hospital, College of Medicine, The Catholic University of Korea, Seoul, South Korea, [4] Department of Psychiatry, Yeouido St. Mary's Hospital, College of Medicine, The Catholic University of Korea, Seoul, South Korea

OPEN ACCESS

Edited by:
Chaur-Jong Hu,
Taipei Medical University, Taiwan

Reviewed by:
Xifei Yang,
Shenzhen Center for Disease Control and Prevention, China
Soichiro Shimizu,
Tokyo Medical University, Japan

***Correspondence:**
Chang Uk Lee
jihan@catholic.ac.kr

Specialty section:
This article was submitted to Neurodegeneration, a section of the journal Frontiers in Psychiatry

Received: *06 November 2017*
Accepted: *03 April 2018*
Published: *17 April 2018*

Citation:
Joo SH, Yun SH, Kang DW, Hahn CT, Lim HK and Lee CU (2018) Body Mass Index in Mild Cognitive Impairment According to Age, Sex, Cognitive Intervention, and Hypertension and Risk of Progression to Alzheimer's Disease. Front. Psychiatry 9:142. doi: 10.3389/fpsyt.2018.00142

Introduction: Mild cognitive impairment (MCI) is a prodromal stage of dementia. The association of body mass index (BMI) and progression to Alzheimer's disease (AD) in MCI subjects according to age, sex, and cognitive intervention remains unknown. We investigated the relationship between BMI and the risk of progression to AD in subjects with MCI, as well as the effect of BMI on progression to AD depending on age, sex, cognitive intervention, and chronic diseases.

Methods: Three hundred and eighty-eight MCI subjects were followed for 36.3 ± 18.4 months, prospectively. They underwent neuropsychological testing more than twice during the follow-up period. The MCI subjects were categorized into underweight, normal weight, overweight, and obese subgroups. The associations between baseline BMI and progression to AD over the follow-up period were estimated using Cox proportional hazard regression models. Data were analyzed after stratification by age, sex, cognitive intervention, and chronic diseases.

Results: After adjustment for the covariates, the underweight MCI group had a higher risk of progression to AD [hazard ratio (HR): 2.38, 95% confidence interval (CI): 1.17–4.82] relative to the normal weight group. After stratifying by age, sex, cognitive intervention, and chronic diseases, this effect remained significant among females (HR: 3.15, 95% CI: 1.40–7.10), the older elderly ≥75 years old (HR: 3.52, 95% CI: 1.42–8.72), the non-intervention group (HR: 3.06, 95%CI: 1.18–7.91), and the hypertensive group (HR: 4.71, 95% CI: 1.17–18.99).

Conclusion: These data indicate that underweight could be a useful marker for identifying individuals at increased risk for AD in MCI subjects. This association is even stronger in females, older elderly subjects, the non-cognitive intervention group, and the hypertensive group.

Keywords: body mass index, mild cognitive impairment, Alzheimer's disease, intervention, CERAD

INTRODUCTION

Mild cognitive impairment (MCI) is a prodromal stage of dementia. According to epidemiological studies, approximately 5–15% of individuals with MCI will progress to dementia each year [1, 2]. Furthermore, there is no disease-modifying treatment for AD. Therefore, identifying risk factors at the MCI stage is critical because correcting modifiable risk factors can lower the incidence of dementia and the identification of non-modifiable risk factors can predict the progression of MCI to Alzheimer disease (AD).

Recently, there has been increasing evidence of the relationship between the body mass index (BMI) of normal cognitive individuals and risk of dementia. There are differences in the association between midlife BMI and dementia compared to late-life BMI and dementia. Being overweight or obese in mid-life is a risk factor for dementia [3–5], but in late-life being underweight is a risk factor [5–7]. However, there are few studies on the relationship between BMI and AD in MCI subjects. A recent study of 228 MCI subjects reported that the overweight or obese group had a reduced risk of both dementia and AD, while the underweight group had a higher risk of dementia but not AD, compared to the normal weight group [8]. Other study has investigated this relationship in MCI subjects, suggesting that, the underweight group had a higher risk while the obese group had a lower risk of AD compared to the normal weight group [9]. However, these two studies did not consider the heterogeneity of MCI subjects. The MCI group is composed of individuals with various demographics characteristics and life-styles. We suspected that BMI might have a different impact depending on individual's age, sex, cognitive intervention status, or chronic diseases, unlike finding from the two recent studies described above. In particular, cognitive intervention may improve cognitive reserve and prevent progression to dementia [10]. Therefore, the impact of BMI on the onset of AD may be different in individuals who have received cognitive intervention compared to a non-intervention group.

We hypothesized that BMI in MCI subjects can predict the progression to AD, and BMI may have a different effect depending on age, sex, cognitive intervention status, and chronic diseases. Therefore, we followed a cohort of MCI subjects prospectively to investigate the relationship between baseline BMI status and the risk of progression to AD in MCI subjects, as well as the effect of BMI on progression to AD depending on age, sex, cognitive intervention status, and chronic diseases.

MATERIALS AND METHODS

Study Population

We recruited MCI subjects at the Seocho Center for Dementia, which is one of the 25 regional dementia support centers in Seoul, South Korea. Each participant underwent a detailed clinical interview and standardized neuropsychological battery, namely the Korean version of the Consortium to Establish a Registry for Alzheimer's disease (CERAD-K). Then, the psychiatrist employed a common standardized diagnostic assessment protocol that included measures for the diagnoses of normal cognition, MCI, and dementia. Participants diagnosed with MCI were eligible to take the CERAD-K test at least once every 6 months. Participants diagnosed with dementia were sent to the hospital for further evaluation. After diagnosis, participants could choose to attend cognitive intervention programs according to their particular cognitive level.

Enrollment started in September 2008 and ended in February 2015. The calculation of the follow-up period for each subject of the cohort was equal to the interval between enrollment and the diagnosis of dementia or end of follow-up. We screened 1,905 participants. We excluded 833 participants who were initially diagnosed with normal cognition or dementia. 684 participants were excluded because they did not follow-up. The final cohort consisted of 388 MCI participants who underwent neuropsychological testing more than twice. All participants were over 60 years old.

Diagnostic Assessments

A diagnosis of MCI was made by criteria recommended by the international working group [11]. Objective cognitive impairment of MCI was defined as a performance score of 1.5 *SD* below the respective age-, education-, and gender-specific normative means in at least one of the cognitive test included in the CERAD-K neuropsychological battery. This battery consisted of verbal fluency (VF), the 15-item Boston Naming Test (BNT), the Mini Mental Status Examination (MMSE), word list memory (WLM), constructional praxis (CP), word list recall (WLR), word list recognition (WLRc), and constructional recall (CR) [12]. All MCI subjects had an overall Clinical Dementia Rating of 0.5.

Dementia was defined as by the criteria of the fourth edition of the Diagnostic and Statistical Manual of Mental Disorders (DSM-IV) and required objective evidence of cognitive deficits (confirmed by neuropsychological testing) and social and/or occupational dysfunction (confirmed by impairments in ADL). We used the criteria of the National Institute of Neurological and Communicative Disorders and Stroke (NINCDS) and the Alzheimer's Disease and Related Disorders Association (ADRDA) for a diagnosis of AD [13].

BMI Categories

The weights and heights of all MCI subjects were measured using standard scales while the subjects were dressed in indoor clothing without shoes; using these data, BMI (kilograms/meters squared) was calculated at baseline. MCI subjects were categorized into four BMI subgroups based on the World Health Organization's (WHO) recommendations for Asian populations: underweight (BMI: $<$18.5 kg/m2), normal weight (18.5–22.9 kg/m2), overweight (23.0–24.9 kg/m2), and obese (BMI $\geq$ 25 kg/m2) [14–16].

Cognitive Intervention

Cognitive intervention is defined as engagement in a range of activities aimed at general enhancement of cognitive and social functioning in a nonspecific manner [10]. This term is a concept that includes cognitive training, cognitive rehabilitation, and cognitive stimulation. Our cognitive intervention includes group programs consisting of memory training, recreational activities

TABLE 1 | Baseline clinical characteristics of MCI subjects according to BMI category (line No. 191).

	All subjects	Underweight	Normal	Overweight	Obese	*p*-value
Number	388	24	160	120	84	
Female, *n* (%)	257 (66.2)	18 (75.0)	112 (70.0)	69 (57.5)	58 (69.1)	0.101
Baseline age, years	74.5 ± 7.6	77.1 ± 7.0	75.2 ± 8.3	74.4 ± 6.9	72.7 ± 6.9	0.029
<75, *n* (%)	200 (51.6)	7 (29.2)	76 (47.5)	66 (55.0)	51 (60.7)	0.026
≥75, *n* (%)	188 (48.5)	17 (70.8)	84 (52.5)	54 (45.0)	33 (39.3)	
Education, years	9.3 ± 5.0	10.4 ± 5.4	9.0 ± 4.8	9.4 ± 5.1	9.3 ± 5.1	0.445
Hypertension, *n* (%)	199 (51.7)	8 (33.3)	69 (44.0)	71 (59.2)	51 (60.7)	0.006
Diabetes mellitus, *n* (%)	70 (18.2)	1 (4.2)	29 (18.5)	26 (21.7)	14 (16.7)	0.232
Hyperlipidemia, *n* (%)	80 (20.8)	6 (25.0)	32 (20.4)	27 (22.5)	15 (17.9)	0.819
Heart disease, *n* (%)	46 (12.0)	3 (12.5)	13 (8.3)	14 (11.8)	16 (19.1)	0.110
Cerebrovascular disease, *n* (%)	28 (7.3)	1 (4.2)	10 (6.4)	8 (6.7)	9 (10.7)	0.557
Follow-up duration, months	36.3 ± 18.4	36.5 ± 22.1	37.1 ± 18.5	35.5 ± 18.7	36.0 ± 16.7	0.905
MMSE score	21.1 ± 4.1	20.4 ± 3.0	20.4 ± 4.4	21.8 ± 3.9	21.6 ± 3.8	0.007
CERAD-K total score	51.0 ± 14.1	48.0 ± 12.0	48.7 ± 15.3	52.6 ± 12.4	54.0 ± 13.8	0.014
Cognitive intervention						
Absent	236 (60.8)	19 (79.2)	106 (66.3)	58 (48.3)	53 (63.1)	0.004
Attended	152 (39.2)	5 (20.8)	54 (33.8)	62 (51.7)	31 (36.9)	

Data are presented as the mean ± standard deviation or frequency (percentage). P-values were calculated by the Kruskal-Wallis test or chi square test. MCI, mild cognitive impairment; BMI, body mass index; MMSE, Mini-Mental Status Examination; CERAD-K, Korean version of the Consortium to Establish a Registry for Alzheimer's Disease.

TABLE 2 | Cox proportional hazard regression for risk of AD in MCI subjects according to baseline BMI (line No. 206).

	Unadjusted		Model 1		Model 2	
	Crude HR (95% CI)	*p*-value	Adjusted HR (95% CI)	*p*-value	Adjusted HR (95% CI)	*p*-value
BMI						
Underweight	**2.09 (1.11–3.92)**	**0.023**	**2.00 (1.03–3.86)**	**0.039**	**2.38 (1.17–4.82)**	**0.017**
Normal weight	Reference		Reference		Reference	
Overweight	0.62 (0.35–1.10)	0.099	0.66 (0.37–1.17)	0.150	0.78 (0.42–1.45)	0.434
Obese	0.51 (0.25–1.06)	0.069	0.59 (0.28–1.23)	0.160	0.71 (0.33–1.53)	0.380

Model 1: Adjusted for age, sex, and education; Model 2: Adjusted for Model 1 plus CERAD-K total score, cognitive intervention, hypertension, diabetes mellitus, hyperlipidemia, heart disease, and cerebrovascular disease. AD, Alzheimer's disease; MCI, mild cognitive impairment; BMI, body mass index; HR, hazard ratio; CI, confidence interval. Statistically significant values are shown in bold.

(games, crafts, and learning to play musical instruments), and physical training implemented by the Seocho Center for Dementia. Each intervention was performed 2–3 times per week for 1 h. The presence of cognitive intervention was defined as attending one of these programs during the follow-up period.

Statistical Analyses

All analyses were performed with SPSS version 24 (SPSS Inc., Chicago, IL, USA). We compared demographic data using the Kruskal-Wallis test, or Chi-square test. The associations between BMI and progression to dementia over the follow-up period were estimated using Cox proportional hazard regression models and are shown as hazard ratios (HRs) with 95% confidence intervals (CIs). The multivariable models were as follows: First, we analyzed the associations without any adjustment. In Model 1, the independent effects of baseline BMI were evaluated after controlling for age, sex, and education. In Model 2, the CERAD-K total score, the presence of cognitive intervention, and the presence of each disease (hypertension, diabetes mellitus, hyperlipidemia, heart disease, or cerebrovascular disease) were added to Model 1. Finally, we divided the subjects into two groups by age (according to the median age), sex, the presence of cognitive intervention, and chronic diseases, separately. Statistical significance was defined as a p-value of 0.05. Values are presented as the mean ± standard deviation or frequency (percentage) as appropriate. Cumulative hazard curves according to BMI were derived from Model 2.

Ethics Statement

All participants voluntarily attended this study and gave written informed consent participate in the study. The Institutional Review Board of Catholic Medical Center approved this study protocol (KC17RESI0150).

RESULTS

Baseline Demographic Characteristics

The baseline demographic characteristics of the 388 MCI subjects according to BMI category are summarized in **Table 1**. At

baseline, 24 subjects were underweight, 160 normal weight, 120 overweight, and 84 obese. The mean age was 74.5 years and women were predominant (66.2%). The mean follow-up duration from the diagnosis of MCI was 36.3 months. 152 subjects attended cognitive intervention programs.

Relationship Between BMI and the Progression to AD

Of the MCI subjects, 12 of 24 underweight subjects (54.2%), 40 of 160 normal weight subjects (25.0%), 17 of 120 overweight subjects (14.2%), and 9 of 84 obese subjects (10.7%) progressed to AD. Prior to adjustment for covariates, the results of the Cox proportional hazard model showed that the underweight group had a higher risk of progression to AD (hazard ratio [HR]: 2.09, 95% confidence interval [CI]: 1.11–3.92) relative to the normal weight group. Adjusting for all covariates (Model 2) accentuated the risk of progression to AD (HR: 2.38, 95% CI: 1.17–4.82) (**Table 2**, **Figure 1**).

Effects of Sex and Age on the Relationship Between BMI and Progression to AD

After stratifying by sex, underweight female had a higher risk of progression to AD (HR: 3.15, 95% CI: 1.40–7.10) than normal weight female in the fully adjusted model (Model 2). On the other hand, in male, there were no differences in the risk of progression to AD among the four BMI groups (**Table 3**).

Age was divided into two groups according to the median age. Stratification of the full model by age revealed that the four BMI groups had no differences in the risk of progression to AD in younger elderly group (age < 75), while the underweight group had a higher risk of progression to AD (HR: 3.52, 95% CI: 1.42–8.72) than the normal weight group in older elderly group (age ≥ 75) (**Table 4**).

Effects of Cognitive Intervention on the Relationship Between BMI and Progression to AD

Stratification of the full model by cognitive intervention revealed the negative effect of underweight to be limited to the non-intervention group (Model 2, **Table 5**). In the cognitive intervention group, the underweight group had no risk of progression to AD while the overweight group had a lower risk of progression to AD (HR: 0.37, 95% CI: 0.14–0.99) than the normal weight group. On the other hand, in group without cognitive intervention underweight group had a higher risk of progression to AD (HR: 3.06, 95% CI: 1.18–7.91) than the normal weight group.

Effects of Chronic Diseases on the Relationship Between BMI and Progression to AD

After stratifying by hypertension, underweight hypertensive group had a higher risk of progression to AD (HR: 4.71, 95% CI: 1.17–18.99) than normal weight hypertensive group in the fully adjusted model (Model 2). On the other hand, there were no differences in the risk of progression to AD among the four BMI groups in group without hypertension (**Table 6**).

After stratifying by DM, underweight non-diabetic group had a higher risk of progression to AD (HR: 2.35, 95% CI: 1.12–4.95) than normal weight non-diabetic group in the fully adjusted model (Model 2). On the other hand, there were no differences in the risk of progression to AD among the four BMI groups in group with DM. However, statistical power was very low because the sample size of underweight subjects with DM was too small ($N = 1$). Other chronic diseases such as hyperlipidemia, heart disease, and cerebrovascular disease did not affect the relationship between underweight and progression to AD in MCI subjects.

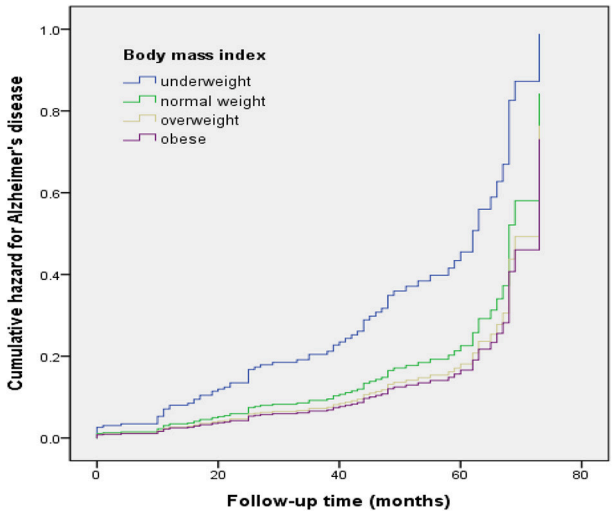

FIGURE 1 | Cumulative risk curves of the effects of baseline body mass index categories on progression to Alzheimer's disease. The figure was derived from model 2 (adjusted for age, sex, education, CERAD-K total score, cognitive intervention, hypertension, diabetes mellitus, hyperlipidemia, heart disease, and cerebrovascular disease).

DISCUSSION

This is the first prospective clinical study to confirm the relationship between BMI and AD considering the heterogeneity of MCI subjects. Our major findings were as follows: First, underweight MCI subjects had a higher risk of progression to AD relative to the normal weight group. Second, the negative effects of underweight on progression to AD were even stronger in females, older elderly, the non-cognitive intervention group and the hypertensive group.

Our first finding that underweight MCI subjects had a higher risk of progression to AD is in line with previous findings [8, 9, 17]. There are various explanations about the relationship between underweight and AD. Aging itself is associated with weight loss; however, weight loss may be accelerated before diagnosis of AD [18]. In other words, weight loss may be either a potential cause of dementia or it may be an early manifestation of an underlying dementia. Lower BMI may reflect

TABLE 3 | Cox proportional hazard regression for risk of AD in MCI subjects according to baseline BMI stratified by sex (line No. 225).

	Unadjusted		Model 1		Model 2	
	Crude HR (95% CI)	***p*-value**	**Adjusted HR (95% CI)**	***p*-value**	**Adjusted HR (95% CI)**	***p*-value**
Males			*n* = 129			
BMI						
Underweight	1.01 (0.21–4.80)	0.992	0.91 (0.19–4.40)	0.906	0.52 (0.09–2.99)	0.465
Normal weight	Reference		Reference		Reference	
Overweight	0.77 (0.30–1.99)	0.585	0.75 (0.28–2.02)	0.573	0.60 (0.20–1.86)	0.379
Obese	0.75 (0.20–2.79)	0.665	0.92 (0.24–3.53)	0.899	1.20 (0.26–5.55)	0.818
Females			*n* = 257			
BMI						
Underweight	**2.58 (1.29–5.16)**	**0.008**	**2.57 (1.23–5.38)**	**0.012**	**3.15 (1.40–7.10)**	**0.006**
Normal weight	Reference		Reference		Reference	
Overweight	0.53 (0.25–1.11)	0.094	0.57 (0.27–1.21)	0.145	0.82 (0.37–1.84)	0.632
Obese	0.44 (0.18–1.07)	0.070	0.51 (0.21–1.24)	0.135	0.64 (0.25–1.63)	0.351

Model 1: Adjusted for age, sex, and education; Model 2: Adjusted for Model 1 plus CERAD-K total score, cognitive intervention, hypertension, diabetes mellitus, hyperlipidemia, heart disease, and cerebrovascular disease. AD, Alzheimer's disease; MCI, mild cognitive impairment; BMI, body mass index; HR, hazard ratio; CI, confidence interval. Statistically significant values are shown in bold.

TABLE 4 | Cox proportional hazard regression for risk of AD in MCI subjects according to baseline BMI stratified by age (<75, ≥75) (line No. 234).

	Unadjusted		Model 1		Model 2	
	Crude HR (95% CI)	***p*-value**	**Adjusted HR (95% CI)**	***p*-value**	**Adjusted HR (95% CI)**	***p*-value**
Age<75			*n* = 198			
BMI						
Underweight	**3.29 (1.04–10.45)**	**0.043**	2.90 (0.88–9.62)	0.082	0.81 (0.18–3.73)	0.788
Normal weight	Reference		Reference		Reference	
Overweight	0.55 (0.19–1.55)	0.256	0.58 (0.20–1.65)	0.309	0.47 (0.15–1.48)	0.197
Obese	0.63 (0.20–1.99)	0.429	0.69 (0.22–2.19)	0.530	0.48 (0.14–1.63)	0.238
Age≥75			*n* = 183			
BMI						
Underweight	1.63 (0.76–3.49)	0.212	1.77 (0.80–3.94)	0.160	**3.52 (1.42–8.72)**	**0.007**
Normal weight	Reference		Reference		Reference	
Overweight	0.70 (0.35–1.40)	0.315	0.79 (0.39–1.59)	0.505	1.17 (0.53–2.58)	0.693
Obese	0.54 (0.21–1.40)	0.204	0.54 (0.21–1.42)	0.214	0.93 (0.34–2.56)	0.893

Model 1: Adjusted for age, sex, education; Model 2: Adjusted for Model 1 plus CERAD-K total score, cognitive intervention, hypertension, diabetes mellitus, hyperlipidemia, heart disease, and cerebrovascular disease. AD, Alzheimer's disease; MCI, mild cognitive impairment; BMI, body mass index; HR, hazard ratio; CI, confidence interval. Statistically significant values are shown in bold.

a decrease in muscle mass or a decrease in fat. Some studies have shown that cognitive decline is associated with muscle loss [19, 20]. Poor nutritional status associated with reduced production of leptin, lack of vitamins, and essential fatty acids, can lead to oxidative damage to neuronal cells, and consequential acceleration of neurodegenerative processes [21]. Level of serum leptin, an adipocyte-derived peptide hormone have been lower in AD patients with BMI <20 compared to those with BMI >25 [22]. Another possible explanation is the degeneration of the mesial temporal cortex because limbic structures within the mesial temporal lobe are involved in appetite, feeding behaviors, memory, and emotional regulation all of which could potentially affected to body weight [23].

In our study, the association between underweight and progression to AD was restricted in females, and was not found in males. While these findings require further study and confirmation, one possible explanation for the observed gender difference may be hormonal factors. It is suggested that lower estrogen levels are potentially associated with AD in studies based on the association between estrogen replacement therapy in postmenopausal women [24, 25]. Because adipose tissue contributes to the production of estrogen, the circulating levels of estrogen are lower in women with less adipose tissue. Estrogens may affect cognition by binding to estrogen receptors that are located throughout the brain, especially in regions such as the hippocampus

TABLE 5 | Cox proportional hazard regression for risk of AD in MCI subjects according to baseline BMI stratified by cognitive intervention (line No. 251).

	Unadjusted		Model 1		Model 2	
	Crude HR (95% CI)	***p*-value**	**Adjusted HR (95% CI)**	***p*-value**	**Adjusted HR (95% CI)**	***p*-value**
Cognitive intervention-absent			*n* = 230			
BMI						
Underweight	**2.33 (1.07–5.09)**	**0.033**	**2.50 (1.09–5.69)**	**0.030**	**3.06 (1.18–7.91)**	**0.021**
Normal weight	Reference		Reference		Reference	
Overweight	0.89 (0.42–1.88)	0.7604	1.02 (0.47–2.18)	0.966	1.64 (0.71–3.78)	0.247
Obese	0.53 (0.20–1.39)	0.1946	0.62 (0.23–1.67)	0.347	0.87 (0.29–2.59)	0.803
Cognitive intervention-attended			*n* = 139			
BMI						
Underweight	1.91 (0.63–5.76)	0.250	1.74 (0.56–5.38)	0.338	3.59 (0.91–14.17)	0.068
Normal weight	Reference		Reference		Reference	
Overweight	**0.34 (0.14–0.82)**	**0.016**	**0.32 (0.13–0.80)**	**0.015**	**0.37 (0.14–0.99)**	**0.048**
Obese	0.47 (0.16–1.40)	0.172	0.50 (0.16–1.57)	0.237	0.51 (0.17–1.59)	0.249

Model 1: Adjusted for age, sex, and education; Model 2: Adjusted for Model 1 plus CERAD-K total score, cognitive intervention, hypertension, diabetes mellitus, hyperlipidemia, heart disease, and cerebrovascular disease. AD, Alzheimer's disease; MCI, mild cognitive impairment; BMI, body mass index; HR, hazard ratio; CI, confidence interval. Statistically significant values are shown in bold.

TABLE 6 | Cox proportional hazard regression for risk of AD in MCI subjects according to hypertension (line No. 265).

	Unadjusted		Model 1		Model 2	
	Crude HR (95% CI)	***p*-value**	**Adjusted HR (95% CI)**	***p*-value**	**Adjusted HR (95% CI)**	***p*-value**
Hypertension-no			*n* = 184			
BMI						
Underweight	1.90 (0.88–4.10)	0.105	1.78 (0.81–3.94)	0.154	1.94 (0.78–4.83)	0.153
Normal weight	Reference		Reference		Reference	
Overweight	0.54 (0.24–1.21)	0.133	0.53 (0.24–1.18)	0.119	0.41 (0.17–1.00)	0.050
Obese	0.25 (0.06–1.06)	0.060	0.27 (0.06–1.15)	0.077	0.25 (0.06–1.07)	0.062
Hypertension-yes			*n* = 197			
BMI						
Underweight	2.88 (0.90–9.21)	0.074	2.91 (0.80–10.60)	0.106	**4.71 (1.17–18.99)**	**0.030**
Normal weight	Reference		Reference		Reference	
Overweight	1.01 (0.41–2.47)	0.990	1.27 (0.51–3.15)	0.605	1.86 (0.68–5.04)	0.224
Obese	1.00 (0.39–2.57)	0.993	1.25 (0.47–3.29)	0.657	1.38 (0.49–3.85)	0.544

Model 1: Adjusted for age, sex, and education; Model 2: Adjusted for Model 1 plus CERAD-K total score, cognitive intervention, hypertension, diabetes mellitus, hyperlipidemia, heart disease, and cerebrovascular disease. AD, Alzheimer's disease; MCI, mild cognitive impairment; BMI, body mass index; HR, hazard ratio; CI, confidence interval. Statistically significant values are shown in bold.

and amygdala which are involved in learning and memory [26].

We also found that age affected the relationship between underweight and progression to AD in MCI subjects. In the older elderly group, underweight predicted higher progression to AD, but not in the younger elderly group. In previous studies, there was a difference in the effect of BMI on the onset of dementia according to age. Obesity in midlife is associated with incident AD [3, 5], whereas underweight in the elderly is associated with AD [6, 7]. This finding highlights the importance of stratifying subjects by age in studies of BMI and dementia and suggests that the older elderly should be considered a separate population from the larger majority of elderly younger than 75.

Our other finding was that the impact of BMI on the progression to AD was different according to the presence or absence of cognitive intervention. The effect of cognitive intervention may be explained by neuroplasticity. Neuroplasticity is defined as the brain's ability to adapt to changes in the environment through modification, reorganization, and creation of neural connections [27]. Many cognitive intervention programs attempt to enhance neuroplasticity of the brain. Therefore, cognitive intervention has a beneficial effect on cognitive decline in MCI subjects [28–30]. In the present study, cognitive intervention did not affect the progression of MCI to AD. However, we found that cognitive intervention affects the relationship between BMI and the progression to AD in MCI

subjects. Underweight still increased the risk of progression to AD in the non-intervention group, while overweight had a protective effect on the progression to AD in the intervention group. It may be an inaccurate interpretation that cognitive intervention contributes to reducing the impact of underweight on the progression to AD, therefore further studies on the impact of cognitive intervention are needed.

Finally, we also found that the association between underweight and progression to AD was stronger in hypertensive group, and was not found in non-hypertensive group. In the study by Sakakura et al. leanness in hypertensive elderly patients was associated with poor cognitive function [31]. The mechanism of cognitive decline in lean hypertensive patients is not clear. However, it is well known that hypertension affects cognitive decline in elderly subjects [32, 33]. There are evidences that white matter medullary arterioles are vulnerable to hypertension, it can cause microvascular dysfunction and narrowing, which can lead to cerebral hypoperfusion [34, 35]. Recent study found that hypertension was associated with worse cognitive function and hippocampal hypometabolism in AD patients [36]. Because underweight and hypertension are risk factors for AD, MCI patients with underweight and hypertension may be highly likely to progress to AD.

This study has several limitations. First, we did not specify MCI diagnosis by amnestic MCI, non-amnestic MCI, single domain MCI, or multi-domain MCI. Second, amyloid imaging, CSF analysis, or pathological studies were not performed to determine on AD diagnosis. Third, the APOE genotype may modify the association between BMI and cognitive decline; however, we could not investigate this association because more than half of the participants did not undergo APOE genotyping. Fourth, this study only analyzed the presence or absence of cognitive intervention without taking the type of cognitive intervention and the duration of attendance into consideration. Fifth, we performed stratification analysis based on chronic diseases which may affect BMI, but we could not found the potential effects of chronic diseases such as DM on MCI and the progression to AD because of the small sample size. Furthermore, we did not investigate the treatment of chronic diseases. Sixth, Muscle loss is also known to be related to cognitive decline, but we could not consider sarcopenic obesity because we didn't investigate muscle mass. Finally, we did not measure longitudinal changes of BMI over time. Nonetheless, this study has several strengths. This study not only identified an effect of underweight on the progression to AD in MCI, but was also the first study to analyze the effects of sex, age, cognitive intervention, and chronic diseases on the relationship between BMI and progression to AD in MCI subjects. Other strength of this study is that the CERAD-K, which is a more accurate cognitive function assessment tool than the MMSE, was used to diagnose MCI and AD. Also, the CERAD-K total score and cognitive intervention attendance, which may affect progression to AD in MCI, were used covariates in this study, which was not done in previous studies. Furthermore, BMI is a biomarker that can be measured easily in clinical practice, so this outcome will be useful to clinicians.

In conclusion, although it is not known whether underweight is the cause of AD or preclinical symptom, these data indicate that low baseline BMI could be a useful marker for identifying individuals at increased risk for AD in MCI subjects. This result is stronger in females, older elderly, the non-cognitive intervention group, and the hypertensive group. Therefore, age and sex specific BMI control might be needed for delaying progression to AD in MCI subjects, and individuals who do not receive cognitive intervention or who have hypertension might need more BMI control.

AUTHOR CONTRIBUTIONS

CL planned the design and carried out the supervision of all parts of this study; SJ recruited participants, analyzed the data and drafted the manuscript; SY managed participants and collected the data; DK, CH, and HL collected the data and performed statistical analysis. All authors read and approved the final manuscript.

FUNDING

This research was supported by the Ministry of Trade, Industry and Energy (MOTIE, Korea) under Industrial Technology Innovation Program No. 10062378.

ACKNOWLEDGMENTS

We thank the members of Seocho Center for Dementia for collecting data.

REFERENCES

1. Mitchell AJ, Shiri-Feshki M. Rate of progression of mild cognitive impairment to dementia–meta-analysis of 41 robust inception cohort studies. *Acta Psychiatr Scand.* (2009) **119**:252–65. doi: 10.1111/j.1600-0447.2008.01326.x
2. Roberts R, Knopman DS. Classification and epidemiology of MCI. *Clin Geriatr Med.* (2013) **29**:753–72. doi: 10.1016/j.cger.2013.07.003
3. Whitmer RA, Gunderson EP, Barrett-Connor E, Quesenberry CP Jr, Yaffe K. Obesity in middle age and future risk of dementia: a 27 year longitudinal population based study. *BMJ* (2005) **330**:1360. doi: 10.1136/bmj.38446.466238.E0
4. Xu WL, Atti AR, Gatz M, Pedersen NL, Johansson B, Fratiglioni L. Midlife overweight and obesity increase late-life dementia risk: a population-based twin study. *Neurology* (2011) **76**:1568–74. doi: 10.1212/WNL.0b013e3182190d09
5. Fitzpatrick AL, Kuller LH, Lopez OL, Diehr P, O'Meara ES, Longstreth WT Jr, et al. Midlife and late-life obesity and the risk of dementia: cardiovascular health study. *Arch Neurol.* (2009) **66**:336–42. doi: 10.1001/archneurol.2008.582
6. Anstey KJ, Cherbuin N, Budge M, Young J. Body mass index in midlife and late-life as a risk factor for dementia: a meta-analysis of prospective studies. *Obes Rev.* (2011) **12**:e426–37. doi: 10.1111/j.1467-789X.2010.00825.x
7. Burns JM, Johnson DK, Watts A, Swerdlow RH, Brooks WM. Reduced lean mass in early Alzheimer disease and its association with brain atrophy. *Arch Neurol.* (2010) **67**:428–33. doi: 10.1001/archneurol.2010.38

8. Cova I, Clerici F, Maggiore L, Pomati S, Cucumo V, Ghiretti R, et al. Body mass index predicts progression of mild cognitive impairment to dementia. *Dement Geriatr Cogn Disord.* (2016) **41**:172–80. doi: 10.1159/000444216
9. Ye BS, Jang EY, Kim SY, Kim EJ, Park SA, Lee Y, et al. Unstable body mass index and progression to probable Alzheimer's disease dementia in patients with amnestic mild cognitive impairment. *J Alzheimers Dis.* (2015) **49**:483–91. doi: 10.3233/JAD-150556
10. Buschert V, Bokde AL, Hampel H. Cognitive intervention in Alzheimer disease. *Nat Rev Neurol.* (2010) **6**:508–17. doi: 10.1038/nrneurol.2010.113
11. Winblad B, Palmer K, Kivipelto M, Jelic V, Fratiglioni L, Wahlund LO, et al. Mild cognitive impairment–beyond controversies, towards a consensus: report of the International Working Group on Mild Cognitive Impairment. *J Intern Med.* (2004) **256**:240–6. doi: 10.1111/j.1365-2796.2004.01380.x
12. Lee JH, Lee KU, Lee DY, Kim KW, Jhoo JH, Kim JH, et al. Development of the Korean version of the consortium to establish a registry for Alzheimer's disease assessment packet (CERAD-K): clinical and neuropsychological assessment batteries. *J Gerontol B Psychol Sci Soc Sci.* (2002) **57**:P47–53. doi: 10.1093/geronb/57.1.P47
13. McKhann G, Drachman D, Folstein M, Katzman R, Price D, Stadlan EM. Clinical diagnosis of Alzheimer's disease: report of the NINCDS-ADRDA work group under the auspices of department of health and human services task force on Alzheimer's disease. *Neurology* (1984) **34**:939–44. doi: 10.1212/WNL.34.7.939
14. Thandassery RB, Appasani S, Yadav TD, Dutta U, Indrajit A, Singh K, et al. Implementation of the Asia-Pacific guidelines of obesity classification on the APACHE-O scoring system and its role in the prediction of outcomes of acute pancreatitis: a study from India. *Dig Dis Sci.* (2014) **59**:1316–21. doi: 10.1007/s10620-013-3000-7
15. Bhardwaj S, Misra A, Misra R, Goel K, Bhatt SP, Rastogi K, et al. High prevalence of abdominal, intra-abdominal and subcutaneous adiposity and clustering of risk factors among urban Asian Indians in North India. *PLoS ONE* (2011) **6**:e24362. doi: 10.1371/journal.pone.0024362
16. WHO Expert Consultation. Appropriate body-mass index for Asian populations and its implications for policy and intervention strategies. *Lancet* (2004) **363**:157–63. doi: 10.1016/S0140-6736(03)15268-3
17. Sobow T, Fendler W, Magierski R. Body mass index and mild cognitive impairment-to-dementia progression in 24 months: a prospective study. *Eur J Clin Nutr.* (2014) **68**:1216–9. doi: 10.1038/ejcn.2014.167
18. Johnson DK, Wilkins CH, Morris JC. Accelerated weight loss may precede diagnosis in Alzheimer disease. *Arch Neurol.* (2006) **63**:1312–7. doi: 10.1001/archneur.63.9.1312
19. Nourhashemi F, Andrieu S, Gillette-Guyonnet S, Reynish E, Albarede JL, Grandjean H, et al. Is there a relationship between fat-free soft tissue mass and low cognitive function? Results from a study of 7,105 women. *J Am Geriatr Soc.* (2002) **50**:1796–801. doi: 10.1046/j.1532-5415.2002.50507.x
20. Spauwen PJ, Murphy RA, Jonsson PV, Sigurdsson S, Garcia ME, Eiriksdottir G, et al. Associations of fat and muscle tissue with cognitive status in older adults: the AGES-Reykjavik Study. *Age Ageing* (2017) **46**:250–7. doi: 10.1093/ageing/afw219
21. Sergi G, De Rui M, Coin A, Inelmen EM, Manzato E. Weight loss and Alzheimer's disease: temporal and aetiologic connections. *Proc Nutr Soc.* (2013) **72**:160–5. doi: 10.1017/S0029665112002753
22. Power DA, Noel J, Collins R, O'Neill D. Circulating leptin levels and weight loss in Alzheimer's disease patients. *Dement Geriatr Cogn Disord.* (2001) **12**:167–70. doi: 10.1159/000051252
23. Grundman M, Corey-Bloom J, Jernigan T, Archibald S, Thal LJ. Low body weight in Alzheimer's disease is associated with mesial temporal cortex atrophy. *Neurology* (1996) **46**:1585–91. doi: 10.1212/WNL.46.6.1585
24. LeBlanc ES, Janowsky J, Chan BK, Nelson HD. Hormone replacement therapy and cognition: systematic review and meta-analysis. *JAMA* (2001) **285**:1489–99. doi: 10.1001/jama.285.11.1489
25. Waring SC, Rocca WA, Petersen RC, O'Brien PC, Tangalos EG, Kokmen E. Postmenopausal estrogen replacement therapy and risk of AD: a population-based study. *Neurology* (1999) **52**:965–70. doi: 10.1212/WNL.52.5.965
26. McEwen BS, Akama KT, Spencer-Segal JL, Milner TA, Waters EM. Estrogen effects on the brain: actions beyond the hypothalamus via novel mechanisms. *Behav Neurosci.* (2012) **126**:4–16. doi: 10.1037/a0026708
27. Kraft E. Cognitive function, physical activity, and aging: possible biological links and implications for multimodal interventions. *Neuropsychol Dev Cogn B Aging Neuropsychol Cogn.* (2012) **19**:248–63. doi: 10.1080/13825585.2011.645010
28. Belleville S. Cognitive training for persons with mild cognitive impairment. *Int Psychogeriatr.* (2008) **20**:57–66. doi: 10.1017/S104161020700631X
29. Kinsella GJ, Mullaly E, Rand E, Ong B, Burton C, Price S, et al. Early intervention for mild cognitive impairment: a randomised controlled trial. *J Neurol Neurosurg Psychiatry* (2009) **80**:730–6. doi: 10.1136/jnnp.2008.148346
30. Troyer AK, Murphy KJ, Anderson ND, Moscovitch M, Craik FI. Changing everyday memory behaviour in amnestic mild cognitive impairment: a randomised controlled trial. *Neuropsychol Rehabil.* (2008) **18**:65–88. doi: 10.1080/09602010701409684
31. Sakakura K, Hoshide S, Ishikawa J, Momomura S, Kawakami M, Shimada K, et al. Association of body mass index with cognitive function in elderly hypertensive Japanese. *Am J Hypertens* (2008) **21**:627–32. doi: 10.1038/ajh.2008.157
32. Kivipelto M, Helkala EL, Laakso MP, Hanninen T, Hallikainen M, Alhainen K, et al. Midlife vascular risk factors and Alzheimer's disease in later life: longitudinal, population based study. *BMJ* (2001) **322**:1447–51. doi: 10.1136/bmj.322.7300.1447
33. Peila R, White LR, Masaki K, Petrovitch H, Launer LJ. Reducing the risk of dementia: efficacy of long-term treatment of hypertension. *Stroke* (2006) **37**:1165–70. doi: 10.1161/01.STR.0000217653.01615.93
34. Hiroki M, Miyashita K, Oda M. Tortuosity of the white matter medullary arterioles is related to the severity of hypertension. *Cerebrovasc Dis.* (2002) **13**:242–50. doi: 10.1159/000057850
35. Faraco G, Iadecola C. Hypertension: a harbinger of stroke and dementia. *Hypertension* (2013) **62**:810–7. doi: 10.1161/HYPERTENSIONAHA.113.01063
36. Moonga I, Niccolini F, Wilson H, Pagano G, Politis M. Hypertension is associated with worse cognitive function and hippocampal hypometabolism in Alzheimer's disease. *Eur J Neurol.* (2017) **24**:1173–82. doi: 10.1111/ene.13374

Conflict of Interest Statement: The authors declare that the research was conducted in the absence of any commercial or financial relationships that could be construed as a potential conflict of interest.

frontiers in Neurology

ORIGINAL RESEARCH
published: 09 May 2018
doi: 10.3389/fneur.2018.00325

Suboptimal Baseline Serum Vitamin B12 Is Associated With Cognitive Decline in People With Alzheimer's Disease Undergoing Cholinesterase Inhibitor Treatment

Hsiao Shan Cho[1†], Li Kai Huang[1,2†], Yao Tung Lee[3,4], Lung Chan[1,5] and Chien Tai Hong[1,5]*

[1] Department of Neurology, Shuang Ho Hospital, Taipei Medical University, New Taipei City, Taiwan, [2] Graduate Institute of Humanities in Medicine, Taipei Medical University, Taipei, Taiwan, [3] Department of Psychiatry, Shuang Ho Hospital, Taipei Medical University, New Taipei City, Taiwan, [4] Department of Psychiatry, School of Medicine, College of Medicine, Taipei Medical University, Taipei, Taiwan, [5] Department of Neurology, School of Medicine, College of Medicine, Taipei Medical University, Taipei, Taiwan

OPEN ACCESS

Edited by:
Jean-Noël Octave, Université catholique de Louvain, Belgium

Reviewed by:
Diego Albani, Istituto Di Ricerche Farmacologiche Mario Negri, Italy
Antonio Gambardella, Università degli studi Magna Graecia di Catanzaro, Italy

***Correspondence:**
Chien Tai Hong
ct.hong@tmu.edu.tw

[†]These authors have contributed equally to this work.

Specialty section:
This article was submitted to Neurodegeneration, a section of the journal Frontiers in Neurology

Received: 02 October 2017
Accepted: 24 April 2018
Published: 09 May 2018

Citation:
Cho HS, Huang LK, Lee YT, Chan L and Hong CT (2018) Suboptimal Baseline Serum Vitamin B12 Is Associated With Cognitive Decline in People With Alzheimer's Disease Undergoing Cholinesterase Inhibitor Treatment. Front. Neurol. 9:325. doi: 10.3389/fneur.2018.00325

Objectives: Cholinesterase inhibitors (ChEIs) are the mainstream treatment for delaying cognitive decline in Alzheimer's disease (AD). Low vitamin B12 is associated with cognitive dysfunction, and its supplementation has been applied as the treatment for certain types of reversible dementia. The present study hypothesized that baseline serum vitamin B12 is associated with the deterioration of cognitive function in people with AD undergoing ChEI treatment.

Materials and methods: Between 2009 and 2016, medical records from 165 Taiwanese with mild to moderate AD who underwent ChEI treatment for at least 2 years were reviewed. Their baseline serum vitamin B12 levels were measured before treatment initiation. Their cognitive function was assessed using the Mini–Mental State Examination (MMSE) and Cognitive Abilities Screening Instrument (CASI). Student's *t* test and multivariable logistic regression were used to analyze the association between cognitive decline and vitamin B12 level. Statistical analyses were performed using SPSS 19.0.

Results: Overall, 122 participants were women. Their median age was 76 years (ranging from 54 to 91). For people with optimal baseline vitamin B12 (above the median level of 436 ng/L), the rates of MMSE and CASI decline were 0.78 ± 1.28 and 2.84 ± 4.21 per year, respectively, which were significantly slower than those with suboptimal vitamin B12 (1.42 ± 1.67 and 4.94 ± 5.88 per year; $p = 0.007$ and 0.009, respectively). After adjustment for age, sex, education level, hypertension, diabetes, history of stroke, and baseline cognitive function, the baseline serum vitamin B12 level was negatively associated with MMSE and CASI decline.

Conclusion: Suboptimal baseline serum vitamin B12 level is associated with cognitive decline in people with AD undergoing ChEI treatment.

Keywords: cholinesterase inhibitors, Alzheimer's disease, vitamin B12, cognition, Mini–Mental State Status Examination, Cognitive Abilities Screening Instrument

INTRODUCTION

Alzheimer's disease (AD) is the most common cause of dementia. Estimates have revealed that in 2050, the number of people with AD aged 65 years and older will be triple (1). Presently, no curative treatment is available for AD. The most effective symptomatic pharmacological treatment for AD is cholinesterase inhibitors (ChEIs), which delay the progress of cognitive dysfunction (2). However, the response to ChEI treatment is variable. Higher cognitive profile, a previous intellectual occupation, healthier lifestyles, being married and not living alone, a higher degree of autonomy, and lower degree of brain atrophy at baseline were associated with better response to ChEI (3). The genotype of apolipoprotein E (ApoE), a cholesterol-transporting enzyme is strongly associated with AD. However, whether ApoE genotype affects the response to ChEI in people with AD is controversial. It had been demonstrated that ApoE ε4 allele carriers were poor responders to tacrine (4); nevertheless, other studies revealed that this detrimental genotype carriers exhibited better response to donepezil (5, 6). Evidence from several prospective, randomized, placebo-controlled trials with large samples were consistent with that ApoE was not a good predictor of response to ChEIs (7–10).

Vitamin B12 has been identified to be associated with cognitive function. Vitamin B12 deficiency because of a vegetarian diet, gastric surgery, malnutrition, or alcoholism results in cognitive dysfunction, and vitamin B12 supplementation can be applied as a rescue treatment for "reversible dementia" (11). A low vitamin B12 level is associated with increasing risks of AD and behavioral and psychological symptoms of dementia in people with AD (12, 13). Although a previous study reported that vitamin B12 supplementation failed to demonstrate neuroprotection in AD (14), the significance of vitamin B12 in AD should not be underestimated.

According to the Taiwan National Health Insurance (NHI) guideline, the insurance-coverage of ChEI treatment is only available to people with AD after vitamin B12 deficiency has been ruled out. Therefore, baseline serum vitamin B12 level measurements were available for all people with approval for the ChEI prescription. The present study investigated whether the baseline vitamin B12 level was associated with the deterioration of cognitive function in Taiwanese people with AD undergoing ChEI treatment.

MATERIALS AND METHODS

Patient Selection

This retrospective study was approved by the Joint Institutional Review Board of Taipei Medical University (TMU-JIRB) (Approval No. N201707049) and waived of informed consent was agreed by TMU-JIRB due to (1) the risk of participants is minimal and (2) waiving of informed consent is no harmful for the right of participants. Medical records from Shuang Ho Hospital between August 2009 and December 2016 were reviewed. During this period, there were 165 people with mild to moderate AD [baseline Mini–Mental State Examination (MMSE) between 10 and 26] who (1) underwent NHI-approved ChEI treatment (2) regular follow-up through cognitive function tests for at least two years. To avail of the insurance-coverage of ChEI treatment, the Taiwan NHI requires that patients should fulfill the following criteria: 1. AD diagnosis (DSM-IV diagnostic criteria of AD) and without any comorbidity affecting cognitive function, such as obvious vascular insults, vitamin B12 (≥206 ng/L), or folate deficiency, or metabolic disorder; 2. a review process to assess all medical records of the patient. The review is conducted by an NHI committee consisting of either neurologists or psychiatrists. After receiving NHI approval for ChEI treatment, patients are required to receive at least annual follow-up through the MMSE, and ChEI treatment would be discontinued for patients with MMSE decline of more than 2 points year-by-year.

The present study collected baseline medical and personal records, including age; sex; education years; medical history of hypertension, diabetes, and cerebrovascular accident (CVA); and serum vitamin B12 and folate. Since vitamin B12 level is known to be affected by several drugs (colchicine, proton pump inhibitors, histamine H2-receptor antagonists, metformin, and antiepileptic agents) and medical conditions (alcohol consumption, peptic ulcer, or gastric operation), specific drug and medical history were also recorded. All patients received MMSE and Cognitive Abilities Screening Instrument (CASI) tests at least three times: at the baseline, first follow-up, and second follow-up, with a 1-year interval. The longest follow-up period was 8 years. For ChEI treatment, donepezil (5 and 10 mg) and rivastigmine (1.5 and 4.5-mg pill and 10-mg patch) were available in Shuang Ho Hospital. People with AD were allowed to switch medications if side effects were intolerable. The deterioration of MMSE and CASI was determined by calculating the ratio of the difference in scores between the baseline and last cognitive tests (unit: score) to the time interval between two tests (unit: year).

Statistical Analyses

All statistical analyses were performed using SPSS for Windows 10 (version 19; SPSS Inc., Chicago, IL, USA). Continuous variables are presented as mean ± SD, and categorical variables are presented as percentages with corresponding 95% confidence intervals. The differences were analyzed using Student's *t* test. The multivariate logistic regression model was adjusted for the following variables: age; sex; education level; initial cognitive function test (either the MMSE or CASI); history of hypertension, diabetes, and CVA; and baseline folate level. A *p*-value of <0.05 was considered statistically significant.

RESULTS

All 165 people with AD underwent ChEI treatment for at least 2 years and were followed through annual cognitive examination (the MMSE and CASI). Their median age was 76 years (ranging from 54 to 91) while initiating treatment; 112 of them were women; and their median education years was 6 years (ranging from 0 to 16). The median level of vitamin B12 was 436 ng/L (ranging from 206 to 5,454). The distribution of serum vitamin B12 was a two-tailed normal distribution pattern (Figure S1 in Supplementary Material).

Furthermore, people with AD were categorized into two groups based on their baseline vitamin B12 levels: the group with optimal baseline vitamin B12 level (above median, 436 ng/L, $n = 82$) and suboptimal baseline vitamin B12 level ($n = 83$) (**Table 1**). Comparison between these two groups revealed no significant difference in most of the background demographic characteristics, including age, education years, major medical history, and baseline MMSE and CASI scores. However, more women (65 versus 47, $p = 0.003$) were in the optimal vitamin B12 group. Moreover, patients in the optimal B12 group had a significantly higher folate level. In both groups, donepezil was the main choice of ChEI treatment and the dosage of donepezil among the majority of them were titrated up to 10 mg daily. Only few of participants in both groups were exposure to drugs which may affect vitamin B12, mainly metformin.

TABLE 1 | Demographic data of all patients categorized into optimal vitamin B12 (>436 ng/L) and suboptimal (≤436 ng/L) groups.

	Optimal vitamin B12 ($n = 82$)	Suboptimal vitamin B12 ($n = 83$)	*p*-Value
Women (%)	65 (79.3)	47 (56.6)	0.003
Age (years)	76.01 ± 6.93	75.41 ± 8.46	0.618
Education (years)	5.46 ± 4.81	7.10 ± 4.23	0.019
Hypertension (%)	30 (36.6)	38 (45.8)	0.269
Diabetes (%)	17 (20.7)	25 (30.1)	0.211
CVA (%)	9 (11.0)	9 (10.8)	1.000
Folate (ng/mL)	15.79 ± 10.52	11.14 ± 10.46	0.005
Baseline MMSE	18.33 ± 5.00	19.28 ± 4.38	0.197
Baseline CASI	60.30 ± 16.57	64.83 ± 13.67	0.057
ChEIs	Donepezil 5 mg, $n = 12$ Donepezil 10 mg, $n = 50$ Rivastigmine, $n = 20$	Donepezil 5 mg, $n = 21$ Donepezil 10 mg, $n = 43$ Rivastigmine, $n = 19$	0.253
Medications affecting Vitamin B12	Metformin, $n = 7$ PPI, $n = 4$ AED, $n = 1$ H2 blockers, $n = 1$	Metformin, $n = 11$ AED, $n = 3$ Colchicine, $n = 1$	
MMSE decline/year	0.78 ± 1.28	1.42 ± 1.67	0.007
CASI decline/year	2.84 ± 4.21	4.95 ± 5.88	0.009

CVA, cerebrovascular accident; MMSE, Mini–Mental State Examination; CASI, Cognitive Abilities Screening Instrument; ChEI, cholinesterase inhibitor; PPI, proton pump inhibitor; AED, antiepileptic drug; H2, histamine H2 receptors.

The present study aimed to investigate the effect of baseline vitamin B12 on the response to ChEI treatment for cognitive decline in people with AD. After the first 2-year treatment, participants in both groups demonstrated a decline in the MMSE and CASI with highly variable results of cognitive function test within the group (**Figure 1**). However, if extending the follow-up period to the end of ChEI treatment (maximum follow-up period: 8 years), for patients with optimal vitamin B12 level, the corresponding cognitive decline was significantly slower than suboptimal vitamin B12 group of patients (MMSE decline: 0.78 ± 1.28 versus 1.42 ± 1.67 point/year, $p = 0.007$; CASI decline: 2.84 ± 4.21 versus 4.95 ± 5.88 point/year, $p = 0.009$) (**Table 1**).

If further categorized all the patients into four groups by first, second, and third quartile, the results demonstrated a similar pattern that people with higher baseline vitamin B12 level demonstrated less cognitive decline (Table S1 in Supplementary Material).

Because several factors affect cognitive decline, including age, education years, comorbidities, and baseline cognitive function before treatment, we applied a multivariable regression model to investigate the association between the baseline serum vitamin B12 level and cognitive decline. After adjustment for the aforementioned factors, the baseline vitamin B12 level was significantly and negatively associated with cognitive decline (MMSE decline, $p = 0.009$; CASI decline, $p = 0.014$) (**Table 2**).

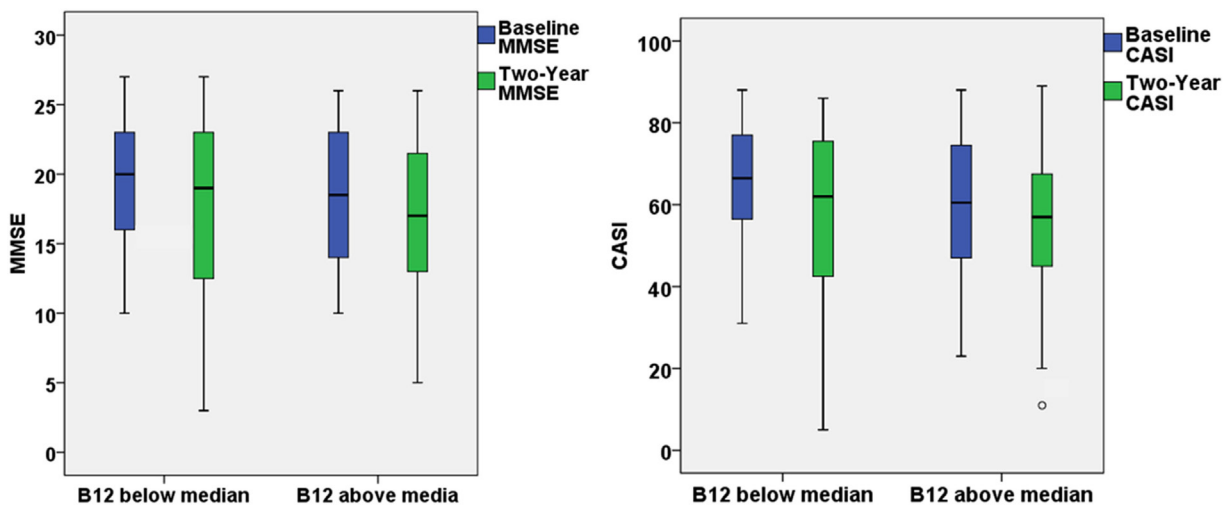

FIGURE 1 | The box plots demonstrated the results of Mini–Mental State Examination (MMSE) and Cognitive Abilities Screening Instrument (CASI) at baseline and 2-year follow-up for patients with optimal (>436 ng/L) or suboptimal baseline vitamin B12 level.

TABLE 2 | Multivariable regression model of the association between high vitamin B12 level and deterioration of cognitive function.

	Deterioration of Mini–Mental State Examination (MMSE)		Deterioration of Cognitive Abilities Screening Instrument (CASI)	
	Normalized beta coefficient	*p*-Value	Normalized beta coefficient	*p*-Value
Vitamin B12	−0.214	0.009	−0.195	0.014

The model was adjusted for age; sex; education level; initial cognitive function test (either MMSE or CASI); history of diabetes, and CVA; and baseline folate level.

DISCUSSION

The present study showed that the baseline vitamin B12 level was negatively associated with cognitive decline in people with AD undergoing ChEI treatment. The deterioration of cognitive function, as assessed by the MMSE and CASI, was significantly slower in patients with optimal baseline vitamin B12 level. Moreover, after adjustment of age, sex, education level, comorbidity, and baseline cognitive function, the baseline vitamin B12 level was negatively associated with cognitive decline. The results demonstrate that the suboptimal baseline vitamin B12 level was associated with poorer response to ChEI treatment in people with AD.

Vitamin B12 deficiency is associated with damage to the white matter in the spinal cord and in the brain, which adversely affects neuronal function. The exact mechanism underlying this association remains unknown. Damage to myelin as a result of defective methylation of myelin basic protein (MBP) has been postulated as an underlying mechanism. MBP accounts for approximately one-third of myelin protein, and demyelination in the setting of vitamin B12 deficiency may explain many of the neurologic findings, including the association with cognitive decline (15, 16). Another hypothesis is the alteration of the concentrations of cytokines, such as tumor necrosis factor-α or epidermal growth factor (17). A low vitamin B12 status leads to *S*-adenosylmethionine deficiency, which results in defective methylation reactions in the central nervous system (18). In a longitudinal study, the serum holotranscobalamin level was found to be related to cognitive performance 7 years later, even in elderly subjects without dementia, and a higher holotranscobalamin level tended to be related to higher performance in executive functions and psychomotor speed (19). Another study conducted in participants aged 45–69 years showed that participants whose vitamin B12 level was in the highest quartile had significantly higher verbal fluency scores (20). The Framingham Heart Study that included community-dwelling individuals aged 74.8 ± 4.6 years showed that plasma vitamin B12 levels ranging from 187 to 256.8 pmol/L predicted cognitive decline (21). Cohort studies have also demonstrated the association of low vitamin B12 status with cognitive dysfunction and cognitive decline (22, 23). A longitudinal cohort study that included 97 people with AD also revealed that baseline homocysteine levels showed a concentration–response relationship with the subsequent rate of decline in cognitive tests (24). However, in clinical practice, it was found that people with cognitive impairment, which is associated with vitamin B12 deficiency, did not always improve on treatment, whereas those with obvious dementia usually showed no improvement (25). Connelly suggested that the isolated use of B vitamins and folic acid is ineffective in improving cognition in people with AD, although homocysteine levels were normal or mildly increased (26). In a systematic review of four randomized controlled trials, vitamin B supplementation was found to be effective in reducing serum homocysteine levels but not in facilitating cognitive improvement (27). In a meta-analysis of 11 randomized trials involving 22,000 participants, Clarke et al. argued that 5-year dietary supplementation with B vitamins did not have any effect on cognitive domains, global cognitive function, or cognitive aging in older people (28).

The present study has some limitations. Although the medical chart review could identify numerous useful information, it was shortage of certain valuable factors for research. For instance, the present study failed to provide the ApoE genetic information, which is the strongest genetic determinant of AD. However, as aforementioned, whether ApoE genotype affects the response of ChEI was controversial. In addition, activities of daily living and instrumental activities of daily living assessments were not routinely performed in the clinical setting, so authors were not able to provide this information. On the other hand, according to the NHI guidelines about the insurance-coverage ChEI treatment, all people with AD with approved ChEI treatment are required to receive the cognitive function test annually. However, this treatment may be discontinued in patients with cognitive decline of more than 2 points in MMSE year-by-year; thus, the follow-up of cognitive function may stop. Our patients received ChEI treatment for at least 2 years, indicating that they were not the early non-responders to ChEI treatment in the first 12 months. Patients with a longer follow-up duration had a more benign course of AD. Therefore, this population was not exactly real-world people with AD but a group of partial or good responders to ChEI treatment. In addition, the vitamin B12 level of the study patients was not followed up annually. Without follow-up, no information was available to determine the correlation between the change in vitamin B12 and cognitive function and the effect of vitamin B12 supplementation on cognitive decline.

In conclusion, the present study demonstrated that suboptimal baseline serum vitamin B12 level was associated with rapid cognitive decline in people with AD undergoing ChEI treatment. Additional studies are required to delineate whether the alteration of the vitamin B12 level during the ChEI treatment period is correlated with cognitive change and to identify the specific people with AD who may be the responders to vitamin B12 supplementation.

ETHICS STATEMENT

This retrospective study was approved by the Joint Institutional Review Board of Taipei Medical University (TMU-JIRB) (Approval No. N201707049) and waived of informed consent was agreed by TMU-JIRB.

AUTHOR CONTRIBUTIONS

Conception or design of the work: YL, LC, and CH. The acquisition, analysis: HC and LH. Interpretation of data for the work: HC, LH, and YL. Drafting the work or revising it critically for important intellectual content, final approval of the version to be published, agreement to be accountable for all aspects of the work in ensuring that questions related to the accuracy or integrity of any part of the work are appropriately investigated and resolved: HC, LH, YL, LC, and CH. HC and LH: both authors contributed equally to this study.

FUNDING

The study was a PI-initiated, non-funded study.

SUPPLEMENTARY MATERIAL

The Supplementary Material for this article can be found online at https://www.frontiersin.org/articles/10.3389/fneur.2018.00325/full#supplementary-material.

REFERENCES

1. Alzheimer's Association. 2016 Alzheimer's disease facts and figures. *Alzheimers Dement* (2016) 12:459–509. doi:10.1016/j.jalz.2016.03.001
2. Rabins PV, Blacker D, Rovner BW, Rummans T, Schneider LS, Tariot PN, et al. American Psychiatric Association practice guideline for the treatment of patients with Alzheimer's disease and other dementias. Second edition. *Am J Psychiatry* (2007) 164:5–56.
3. Gallucci M, Spagnolo P, Arico M, Grossi E. Predictors of response to cholinesterase inhibitors treatment of Alzheimer's disease: date mining from the TREDEM registry. *J Alzheimers Dis* (2016) 50:969–79. doi:10.3233/JAD-150747
4. Sjögren M, Hesse C, Basun H, Köl G, Thostrup H, Kilander L, et al. Tacrine and rate of progression in Alzheimer's disease – relation to ApoE allele genotype. *J Neural Transm (Vienna)* (2001) 108:451–8. doi:10.1007/s007020170066
5. Petersen RC, Smith GE, Waring SC, Ivnik RJ, Tangalos EG, Kokmen E. Mild cognitive impairment: clinical characterization and outcome. *Arch Neurol* (1999) 56:303–8. doi:10.1001/archneur.56.3.303
6. Bizzarro A, Marra C, Acciarri A, Valenza A, Tiziano FD, Brahe C, et al. Apolipoprotein E epsilon4 allele differentiates the clinical response to donepezil in Alzheimer's disease. *Dement Geriatr Cogn Disord* (2005) 20:254–61. doi:10.1159/000087371
7. Wilcock GK, Lilienfeld S, Gaens E. Efficacy and safety of galantamine in patients with mild to moderate Alzheimer's disease: multicentre randomised controlled trial. Galantamine International-1 Study Group. *BMJ* (2000) 321:1445–9. doi:10.1136/bmj.321.7274.1445
8. Aerssens J, Raeymaekers P, Lilienfeld S, Geerts H, Konings F, Parys W. APOE genotype: no influence on galantamine treatment efficacy nor on rate of decline in Alzheimer's disease. *Dement Geriatr Cogn Disord* (2001) 12:69–77. doi:10.1159/000051238
9. Winblad B, Engedal K, Soininen H, Verhey F, Waldemar G, Wimo A, et al. A 1-year, randomized, placebo-controlled study of donepezil in patients with mild to moderate AD. *Neurology* (2001) 57:489–95. doi:10.1212/WNL.57.3.489
10. Farlow MR, Cyrus PA, Nadel A, Lahiri DK, Brashear A, Gulanski B. Metrifonate treatment of AD: influence of APOE genotype. *Neurology* (1999) 53:2010–6. doi:10.1212/WNL.53.9.2010
11. Health Quality Ontario. Vitamin B12 and cognitive function: an evidence-based analysis. *Ont Health Technol Assess Ser* (2013) 13:1–45.
12. Chan A, Paskavitz J, Remington R, Rasmussen S, Shea TB. Efficacy of a vitamin/nutriceutical formulation for early-stage Alzheimer's disease: a 1-year, open-label pilot study with an 16-month caregiver extension. *Am J Alzheimers Dis Other Demen* (2008) 23:571–85. doi:10.1177/1533317508325093
13. Shen L, Ji HF. Associations between homocysteine, folic acid, vitamin B12 and Alzheimer's disease: insights from meta-analyses. *J Alzheimers Dis* (2015) 46:777–90. doi:10.3233/JAD-150140
14. Sun Y, Lu CJ, Chien KL, Chen ST, Chen RC. Efficacy of multivitamin supplementation containing vitamins B6 and B12 and folic acid as adjunctive treatment with a cholinesterase inhibitor in Alzheimer's disease: a 26-week, randomized, double-blind, placebo-controlled study in Taiwanese patients. *Clin Ther* (2007) 29:2204–14. doi:10.1016/j.clinthera.2007.10.012
15. Scott JM. Folate and vitamin B12. *Proc Nutr Soc* (1999) 58:441–8. doi:10.1017/S0029665199000580
16. Ikram MA, Vrooman HA, Vernooij MW, den Heijer T, Hofman A, Niessen WJ, et al. Brain tissue volumes in relation to cognitive function and risk of dementia. *Neurobiol Aging* (2010) 31:378–86. doi:10.1016/j.neurobiolaging.2008.04.008
17. Scalabrino G, Veber D, Mutti E. Experimental and clinical evidence of the role of cytokines and growth factors in the pathogenesis of acquired cobalamin-deficient leukoneuropathy. *Brain Res Rev* (2008) 59:42–54. doi:10.1016/j.brainresrev.2008.05.001
18. Weir DG, Scott JM. Brain function in the elderly: role of vitamin B12 and folate. *Br Med Bull* (1999) 55:669–82. doi:10.1258/0007142991902547
19. Hooshmand B, Solomon A, Kåreholt I, Rusanen M, Hänninen T, Leiviskä J, et al. Associations between serum homocysteine, holotranscobalamin, folate and cognition in the elderly: a longitudinal study. *J Intern Med* (2012) 271:204–12. doi:10.1111/j.1365-2796.2011.02484.x
20. Horvat P, Gardiner J, Kubinova R, Pajak A, Tamosiunas A, Schöttker B, et al. Serum folate, vitamin B-12 and cognitive function in middle and older age: the HAPIEE study. *Exp Gerontol* (2016) 76:33–8. doi:10.1016/j.exger.2016.01.011
21. Morris MS, Selhub J, Jacques PF. Vitamin B-12 and folate status in relation to decline in scores on the mini-mental state examination in the Framingham heart study. *J Am Geriatr Soc* (2012) 60:1457–64. doi:10.1111/j.1532-5415.2012.04076.x
22. Nie T, Lu T, Xie L, Huang P, Lu Y, Jiang M. Hyperhomocysteinemia and risk of cognitive decline: a meta-analysis of prospective cohort studies. *Eur Neurol* (2014) 72:241–8. doi:10.1159/000363054
23. O'Leary F, Allman-Farinelli M, Samman S. Vitamin B 12 status, cognitive decline and dementia: a systematic review of prospective cohort studies. *Br J Nutr* (2012) 108:1948–61. doi:10.1017/S0007114512004175
24. Oulhaj A, Refsum H, Beaumont H, Williams J, King E, Jacoby R, et al. Homocysteine as a predictor of cognitive decline in Alzheimer's disease. *Int J Geriatr Psychiatry* (2010) 25:82–90. doi:10.1002/gps.2303
25. Malouf R, Areosa Sastre A. Vitamin B12 for cognition. *Cochrane Database Syst Rev* (2003):CD004326. doi:10.1002/14651858.CD004326
26. Connelly P. High dose vitamin B supplementation does not slow cognitive decline in mild to moderate Alzheimer's disease. *Evid Based Ment Health* (2009) 12:86. doi:10.1136/ebmh.12.3.86
27. Zhang D-M, Ye J-X, Mu J-S, Cui X-P. Efficacy of vitamin B supplementation on cognition in elderly patients with cognitive-related diseases: a systematic review and meta-analysis. *J Geriatr Psychiatry Neurol* (2017) 30:50–9. doi:10.1177/0891988716673466
28. Clarke R, Bennett D, Parish S, Lewington S, Skeaff M, Eussen SJ, et al. Effects of homocysteine lowering with B vitamins on cognitive aging: meta-analysis of 11 trials with cognitive data on 22,000 individuals. *Am J Clin Nutr* (2014) 100:657–66. doi:10.3945/ajcn.113.076349

Conflict of Interest Statement: The authors declare that the research was conducted in the absence of any commercial or financial relationships that could be construed as a potential conflict of interest.

frontiers in Neurology

ORIGINAL RESEARCH
published: 11 July 2018
doi: 10.3389/fneur.2018.00560

Longitudinal Alterations of Alpha-Synuclein, Amyloid Beta, Total, and Phosphorylated Tau in Cerebrospinal Fluid and Correlations Between Their Changes in Parkinson's Disease

*Mahsa Dolatshahi[1], Shayan Pourmirbabaei[1], Aida Kamalian[1], Amir Ashraf-Ganjouei[1], Mehdi Yaseri[2] and Mohammad H. Aarabi[1]**

[1] Faculty of Medicine, Tehran University of Medical Sciences, Tehran, Iran, [2] Department of Epidemiology and Biostatistics, School of Public Health, Tehran University of Medical Sciences, Tehran, Iran

OPEN ACCESS

Edited by:
Chaur-Jong Hu,
Taipei Medical University, Taiwan

Reviewed by:
Fabiana Novellino,
Consiglio Nazionale Delle Ricerche (CNR), Italy
Chien Tai Hong,
Taipei Medical University, Taiwan

***Correspondence:**
Mohammad Aarabi
mohammadhadiarabi@gmail.com

Specialty section:
This article was submitted to Neurodegeneration, a section of the journal Frontiers in Neurology

Received: 19 February 2018
Accepted: 21 June 2018
Published: 11 July 2018

Citation:
Dolatshahi M, Pourmirbabaei S, Kamalian A, Ashraf-Ganjouei A, Yaseri M and Aarabi MH (2018) Longitudinal Alterations of Alpha-Synuclein, Amyloid Beta, Total, and Phosphorylated Tau in Cerebrospinal Fluid and Correlations Between Their Changes in Parkinson's Disease. Front. Neurol. 9:560. doi: 10.3389/fneur.2018.00560

Background: Parkinson's disease (PD) is characterized by proteinopathies and these proteinopathies seem to interact synergistically and lead to protein aggregations and changes in protein cerebrospinal fluid (CSF) levels. In this study, we aimed to explore the longitudinal changes of CSF a lpha-synuclein (α-syn), total tau (t-tau), phosphorylated tau (p-tau), and beta-amyloid ($A\beta_{1-42}$) and their relationships with each other and with baseline clinical entities like REM sleep behavior disorder (RBD), cognitive impairment, motor symptoms, and olfaction dysfunction.

Method: One hundred and twelve non-demented PD patients and 110 controls were recruited from Parkinson's Progression Markers Initiative (PPMI).We used a linear mixed model within groups to assess longitudinal protein changes over 6 and 12 months and a random regression coefficient within the linear mixed model to investigate the correlation between proteins and their baseline clinical characteristics.

Results: P-tau was lower in PDs only at baseline, but during a year, p-tau increased more rapidly in PDs than controls. $A\beta_{1-42}$ was not significantly different between groups at any separate timepoint; however, when assessed longitudinally, $A\beta_{1-42}$ showed significant changes in both groups. Conversely, t-tau and α-syn differed significantly between groups, but their longitudinal changes were not significant in either of the groups. Moreover, all proteins' baseline levels, except p-tau, could determine estimated longitudinal tau changes. Baseline RBDSQ scores but not UPDRS III, MoCA, or UPSIT scores were predictive of longitudinal increase in α-syn levels.

Conclusion: Longitudinal changes in levels of CSF proteins are related to each other and could help researchers further understand PD pathology. In addition, RBD seems to be a potential prognostic factor for PD progression. However, in order to reach a consensus, longer follow-up times are required.

Keywords: Parkinson's disease, Cerebrospinal fluid (CSF), Longitudinal, alpha-synuclein, tau, beta-amyloid

INTRODUCTION

As the life expectancy of population increases, neurodegenerative diseases like Parkinson's disease (PD) become the spotlight in medicine (1). PD is characterized by several pathological mechanisms like lysosomal damage, oxidative stress, and most importantly protein aggregation. The main form of proteinopathy in PD has long been considered to be synucleinopathy, i.e., intraneuronal inclusions of alpha-synuclein in the form of Lewy bodies and Lewy neurites. However, recent research has indicated the accompanying role of other AD-associated proteinopathies like tauopathy and beta-amyloidopathy (2).

Moreover, it is known that PD symptoms progress heterogeneously (3) which can be mainly attributed to the variations in the predominant pathological mechanisms (4, 5). These variations can make a great difference in manifestations of PD symptoms such as cognitive dysfunction and contribute to disease heterogeneity. For example, concomitant AD-pathology (tau and beta-amyloid aggragations) is a more common observation in PD dementia (PDD) (6, 7). On the other hand, recently it has been revealed that the predominant clinical manifestations which patients are presented with at baseline might be a predictor for progression of disease, both from a pathophysiological and clinical point of view. More importantly, these differences in the type and severity of underlying proteinopathies determine the most effective therapeutic procedure for each person, which is the cornerstone of personalized medicine. Thus, clinicians would benefit from a method to detect the main pathological pathways leading to dopaminergic neuron loss and PD symptoms in each individual, in association with their different clinical entities, for both diagnostic and curative purposes (8, 9).

On the other hand, many studies have reached the notion that mutual interactions between different proteins promote the aggregation of these proteins *in vivo* and accelerate cognitive dysfunction (10). Most notably, alpha-synuclein induces polymerization, and aggregation of tau and thereby promotes the formation of intracellular amyloid–tau inclusions (11, 12). It also engages in cross-seeding with tau proteins so they tend to co-exist in intracellular inclusions (13).

Importantly, these proteinopathies are mirrored in changes of CSF protein concentrations, which can be easily measured in clinic. Unfortunately, despite the large number of studies, the diagnostic utility of CSF biomarkers has been unsatisfactory (14).

Numerous studies have assessed the concentration of CSF biomarkers in PD. However, most of these studies were cross-sectional and just a few studies assessed longitudinal changes of CSF markers and lead to inconsistant results. These cross-sectional studies have mostly shown decreased CSF levels of alpha-synuclein (α-syn) in PD and other synucleinopathies compared to healthy controls (15–20). In addition, the levels of Alzheimer's disease (AD) biomarkers such as total tau (t-tau), phosphorylated tau (p-tau), and beta-amyloid 1-42 ($A\beta_{1-42}$) have been previously shown to be decreased or normal in PD patients (17–21). Apart from the mentioned findings, there has been some different observations. For example, in the study conducted by Montine et al., one third of non-demented PD patients and half of PDD patients showed higher CSF tau levels compared to healthy controls (17). Moreover, the study of Parkinson Progression Markers Initiative (PPMI) (200 healthy controls and 400 PDs) showed non-significantly changed levels of $A\beta_{1-42}$ compared to controls at baseline (20). Specific patterns of changes in levels of these proteins in different groups of PD patients with various PD symptoms have been observed, which are reviewed elsewhere (22, 23).

Longitudinal studies that evaluated longitudinal changes of CSF proteins (α-syn, t-tau, p-tau, and $A\beta_{1-42}$) levels in PD patients have reached heterogeneous results e.g., the study conducted by Hall et al. has shown significantly increasing levels of all proteins except $A\beta_{1-42}$ during a two-year follow-up, in which increase of p-tau was associated with motor symptoms aggravation and cognitive decline (21). Another study done by Majbour et al. revealed no significant change in levels of t-tau, p-tau, $A\beta_{40}$, and $A\beta_{42}$ but an increase in total and oligomeric α-syn levels and a decrease in serine129 phosphorylated α-syn during a two-year follow-up (24). The study conducted by Stewart et al. has shown a decline in alpha-synuclein over a 2-year follow-up in patients of DATATOP cohort who received medication, which was associated with an improvement in cognitive abilities but was not correlated with motor symptoms (25). On the other hand, a recent study by Forland et al. showed nonsignificant changes of CSF alpha-synuclein in a 4-year follow-up (26). Another study done by Boungiorno et al. has shown a longitudinal decline in CSF Aβ but an increase in t-tau levels during 18 months, which were not significantly associated with cognitive decline (27). On the whole, these studies have shown quite inconsistent results regarding longitudinal changes of CSF proteins.

Thus, it seems that conducting studies with a large sample size in ongoing cohorts with drug-naïve cases like PPMI can be helpful in interpretation of these heterogeneous results and complementing our knowledge about this cohort. Furthermore, investigating the correlations between baseline levels of proteins and their changes in association with clinical manifestations facilitates estimation of patients' prognoses and can lead to a better understanding of PD pathogenesis.

In this study, we used a relatively large sample size in recent-onset, drug-naive, non-demented patients recruited from PPMI cohort to investigate the longitudinal changes in CSF protein levels and also their association with each other, with baseline levels of each protein, and also the clinical entities. These longitudinal assessments might elucidate the interaction between pathological mechanisms during disease progression and whether they have any associations with heterogeneous clinical manifestations.

METHODS

Participants

The participants of this study were recruited from the Parkinson Progression Markers Initiative (PPMI) database freely available at http://www.ppmi-info.org/. PPMI cohort comprises 400 recently

Abbreviations: CSF, cerebrospinal fluid; PD, Parkinson's disease; HC, healthy controls; α-syn, alpha-synuclein; Aβ, beta-amyloid; t-tau, total tau; p-tau, phosphorylated tau.

diagnosed PD and 200 healthy subjects followed longitudinally for biomarker assessment at 21 clinical sites using standard data acquisition protocols (28). The PPMI study was approved by the Institutional Review Board of all participating sites and all participants were given written informed consent before inclusion in the study. PD subjects of PPMI study were recruited at disease threshold, meaning that they had been diagnosed within 2 years while they were drug-naïve at baseline. The clinical criteria for PD diagnosis included asymmetric resting tremor and/or asymmetric bradykinesia. In addition, all subjects underwent dopamine transporter (DAT) imaging and DAT deficit was considered necessary for PD diagnosis. The subjects were assessed for motor symptoms using Unified Parkinson's Disease Rating Scale part III (UPDRS III), cognitive impairment using Montreal Cognitive Assessment (MoCA). REM sleep Behavior Disorder (RBD) and olfaction dysfunction were assessed using REM Sleep Behavior Disorder Screening Questionnaire (RBDSQ) and University of Pennsylvania Smell Identification Test (UPSIT), respectively. Healthy subjects were required to have no significant neurologic dysfunction, no first-degree family member with PD and MoCA >26 (2011). In PPMI cohort longitudinal data for CSF samples were available only for a portion of the patients. Thus, we selected the subjects for which longitudinal CSF data were available at baseline (BL), the second visit (V02) i.e., 6 months after recruitment, and the fourth visit (V04) i.e., one year after recruitment. We excluded the patients who met the criteria for PD dementia (PDD) at baseline and those who had recently received medications to have a clinically homogenous sample. In the end, 112 PD patients and 110 matched healthy subjects with the above-mentioned properties were included in the study. Complementary data on disease duration, age, gender, and UPDRS III score at different time points is provided in Supplementary Tables 1–4.

CSF Samples Collection and Analysis

CSF was collected by using standardized lumbar puncture procedures. CSF was collected into siliconized polypropylene tubes and the first 1–2 mL of CSF of sent to the site's local laboratory for routine testing for cell count, total protein level, and glucose level. An additional 15–20 mL of CSF was transferred into 15-mL conical propylene tubes at room temperature, mixed gently, centrifuged at 2,000 g for 10 min at room temperature, and transferred into 1.5-mL pre-cooled siliconized polypropylene aliquot tubes followed by immediate freezing on dry ice. The frozen aliquots of CSF were shipped overnight to the PPMI Biorepository Core Laboratories on dry ice and then thawed, aliquoted into 0.5-mL siliconized polypropylene tubes, refrozen once, and stored at −80°C. The coded frozen aliquots of CSF were transferred from the PPMI Biorepository Core laboratories to the University of Pennsylvania and to Covance for analyses. CSF Aβ1-42, t-tau and p-tau were measured using the xMAP-Luminex platform with INNOBIA AlzBio3 immunoassay kit-based reagents (Fujirebio-Innogenetics, Ghent, Belgium). CSF α-syn and CSF hemoglobin levels were analyzed using appropriate commercially available sandwich type ELISA kits (Covance, Dedham, MA) [2011; (19, 20)].

Statistical Analysis

We used Kolmogorov-Smirnov test as well as a Q-Q plot to check for the normal distribution of data. To present data, we used mean, standard deviation, median, and range. To find the difference between the two groups during the study period, we used the Mann-Whitney test. To assess the changes within each group (PD, controls) considering the correlation of measurements (CSF protein concentrations, age, disease duration), we used a linear mixed model within each group. In this analysis, multiple comparison corrections were performed by Bonferroni method. Other linear mixed models with the interaction of time and groups were used to test the difference of trends in parameters during the study course between the two groups. Correlation of different parameters and their changes during the study course was assessed with Pearson correlation. To adjust for the probable confounding effect of age, sex, and disease duration (in PD group) we used partial correlation coefficient. Finally, to evaluate the effect of baseline values of biomarkers on their own changes and the changes of other biomarkers, we used a two-step procedure: in the first step, we obtained the estimated mean change of each parameter on each subject with the use of random regression coefficients of a linear mixed model. In the next step, we used correlation coefficient to evaluate the relation of these estimations with baseline values of all parameters. Also, the correlation of different biomarkers' estimated changes was calculated. All statistical analyses were performed by R (R Foundation for Statistical Computing, Vienna, Austria), http://www.R-project.org/. A p-value of < 0.05 was considered statistically significant.

RESULTS

Demographics

Demographics and clinical scores of study participants and their comparison are given in **Table 1**. UPDRS III, MoCA, and UPSIT scores were significantly lower in PD compared to controls at baseline and after a year (for MoCA and UPDRS III). MoCA and UPDRS III scores were significantly lower at V04 compared to baseline in PD patients. However, in controls, only MoCA scores were lower at V04 compared to baseline. RBDSQ scores, however, not only showed no difference between PD and control groups, but also they were not different at baseline compared to V04.

On the whole, age and disease duration were correlated with levels of some CSF biomarkers at different time points in PD and controls.

Values of $A\beta_{1-42}$ were correlated with age in the control group and levels of t-tau showed correlation with age in PD group at all time points. Percentage of changes in levels of t-tau and $A\beta_{1-42}$ were correlated with age in both groups.

Baseline values of p-tau and t-tau in PD groups were correlated with disease duration. Also, percentage of changes of p-tau and $A\beta_{1-42}$ during 6 months was correlated with disease duration. Percentage of changes during one year, only for t-tau and $A\beta_{1-42}$, was correlated with disease duration.

TABLE 1 | Demographics and clinical tests including Unified Parkinson's Disease Rating Scale part III (UPDRS III), Montreal Cognitive Assessment (MoCA), REM sleep Behavior Disorder Questionnaire (RBDSQ), and University of Pennsylvania Smell Identification Test (UPSIT) scores at Baseline (BL) and after a year, visit 04 (V04) in Parkinson's disease (PD) and control subjects.

	PD ($n = 112$)	Control ($n = 110$)	*P*-value (PD, control) [two-sample *t*-test]	*P*-value (BL, V04) [paired sample *t*-test]
Age (years) (mean ± SD)	60.89 ± 10.46	61.54 ± 10.03	0.6381[a]	–
Gender (Male Number/ %)	80 M/71.42%	69 M/62.72%	0.2465[b]	–
Disease duration (months) (mean ± SD)	14.23 ± 14.08	–	–	–
UPDRS III (BL) (mean ± SD)	19.15 ± 8.16	2.41 ± 1.39	0.0000[a]	0.0027[c](*PD*)
UPDRS III (V04) (mean ± SD)	22.98 ± 10.52	3.12 ± 1.92	0.0000[a]	0.1555[c](*control*)
MoCA (BL) (mean ± SD)	27.03 ± 2.10	28.22 ± 1.06	0.0000[a]	0.0031[c](*PD*)
MoCA (V04) (mean ± SD)	26.34 ± 2.42	27.29 ± 2.10	0.0023[a]	0.0000[c](*control*)
RBDSQ (BL) (mean ± SD)	4.17 ± 2.89	3.95 ± 2.89	0.5358[a]	0.3394[c](*PD*)
RBDSQ (V04) (mean ± SD)	3.99 ± 2.82	3.60 ± 2.99	0.6371[a]	0.5694[c](*control*)
UPSIT baseline (mean ± SD)	20.77 ± 8.03	33.99 ± 4.69	0.0000[a]	–

n, number; SD, standard deviation.
[a]*p-values obtained by independent samples t-test.*
[b]*p-values obtained by chi-square independence test.*
[c]*p-values obtained by paired samples t-test (difference between clinical scores at baseline and after 1-year follow-up).*

Difference Between PD and Control in Biomarker Levels at Different Time Points

The levels of α-syn and t-tau were significantly lower in PD group than controls at baseline, after six months, and after one year. P-tau level was significantly lower in PD group at baseline, but not after 6 months and one year. Levels of $A\beta_{1-42}$ showed no significant difference between the two groups at any time point. (**Table 2**).

Longitudinal Changes Over 6 Months and One Year in CSF Biomarker Levels in PD and Control Groups

The levels of α-syn showed no significant change after 6 months and one year in neither of the groups. P-tau level had not significantly changed after 6 months in either group; however, its level had significantly risen after one year in PD group but not in controls. T-tau showed no significant change after 6 months and one year in control. T-tau levels had decreased significantly after 6 months in PD group, but no significant change was observed from baseline to visit 4 (after one year). $A\beta_{1-42}$ had not significantly changed after 6 months, but it had significantly increased after one year in both control and PD groups.

On the whole, the pattern of changes (increase or decrease) of biomarkers was not different between controls and PD group, except for total tau for which there was a different pattern of change between the two groups. Also, the trend of changes based on interaction analysis of time and group, within the linear mixed model, was not significantly different between the two groups. (**Table 2**, **Figure 1**).

Correlation Between Levels of Different CSF Biomarkers at Different Time Points

None of the CSF biomarkers showed any significant correlation with each other in control group when adjusted for age and sex although several significant correlations were observed in control group when not adjusted. Correlations between levels of the same biomarker at different time points were significant in the PD group whether adjustment for age, gender, and disease duration was done or not. However, there were some exceptions for t-tau.

Correlation of Baseline Values of Each Biomarker With Estimated Changes of Different Biomarkers During Study Period

Baseline values of all biomarkers were correlated with their own estimated changes, except for p-tau. Additionally, baseline values of all biomarkers were correlated with estimated changes of t-tau and baseline values of α-syn correlated to estimated changes of $A\beta_{1-42}$ ($P = 0.002$). (**Table 3**, **Figure 2**).

Correlation of Estimated Changes of Different Biomarkers During Study Period With Each Other

Estimated changes of p-tau and t-tau were positively correlated to each other ($P = 0.002$). Moreover, estimated changes of p-tau and $A\beta_{1-42}$ were correlated positively ($P < 0.001$). (**Table 3**, **Figure 3**).

Correlation of Baseline Values of MoCA, RBDSQ, UPSIT, and UPDRS III Scores With Estimated Changes of Different Biomarkers During Study

Using linear mixed models for changes of p-tau, t-tau, α-syn, and Aβ CSF levels, with interaction of baseline UPDRS III, RBDSQ, UPSIT, and MoCA scores, no significant association between these clinical scores with estimated

TABLE 2 | Biomarker changes in PD and control group within a linear mixed model.

Parameter	Control		PD		Group difference	P of trend with interaction of time and group
	Mean ± SD	Median (range)	Mean ± SD	Median (range)	$P^{\dagger}$	diff[$]
α-synuclein						0.950
Value at baseline	2,163 ± 976	1,950 (593 to 5,238)	1,783 ± 700	1,704 (333 to 5,174)	0.007	
Value at 6 months	2,196 ± 924	2,070 (659 to 5,209)	1,822 ± 700	1,770 (680 to 4,659)	0.001	
Crude change till 6 months	33 ± 623	7 (-1,913 to 2,258)	40 ± 317	34 (−674 to 837)	0.948	
Change% till 6 months	8 ± 37	0 (−61 to 257)	6 ± 27	2 (−40 to 192)	0.943	
P[§]-within linear mixed model till 6 months	1.000		0.774			
Value at 1 year	2,166 ± 964	2,037 (729 to 5,295)	1,812 ± 712	1,700 (782 to 4,633)	0.004	
Crude change till 1 year	3 ± 589	−5 (−2,292 to 1,748)	30 ± 406	11 (−1,612 to 1,284)	0.872	
Change% till 1 year	5 ± 34	0 (−55 to 161)	6 ± 31	1 (−46 to 202)	0.737	
P[§]-within linear mixed model till 1 year	1.000		1.000			
P-tau						0.654
Value at baseline	17 ± 9	14 (6 to 59)	15 ± 8	12 (6 to 40)	0.032	
Value at 6 months	16 ± 8	13 (6 to 53)	15 ± 9	11 (5 to 56)	0.221	
Crude change till 6 months	−1 ± 9	0 (−24 to 39)	0 ± 10	0 (−22 to 40)	0.421	
Change% till 6 months	0 ± 0	0 (−2 to 1)	0 ± 1	0 (−2 to 2)	0.433	
P[§]-within linear mixed model till 6 months	0.983		1.000			
Value at 1 year	20 ± 13	16 (6 to 90)	19 ± 11	15 (5 to 58)	0.622	
Crude change till 1 year	3 ± 15	1 (−30 to 75)	4 ± 13	3 (−27 to 47)	0.365	
Change% till 1 year	0 ± 1	0 (−2 to 4)	0 ± 1	0 (−2 to 3)	0.256	
P[§]-within linear mixed model till 1 year	0.094		0.003			
T-tau						0.240
Value at baseline	52 ± 26	45 (18 to 188)	45 ± 18	39 (22 to 121)	0.047	
Value at 6 months	51 ± 24	45 (17 to 181)	43 ± 18	37 (16 to 135)	0.002	
Crude change till 6 months	−1 ± 9	0 (−27 to 35)	−2 ± 6	−2 (−15 to 22)	0.037	
Change% till 6 months	0 ± 0	0 (−1 to 2)	0 ± 0	0 (−2 to 2)	0.006	
P[§]-within linear mixed model till 6 months	1.000		0.007			
Value at 1 year	53 ± 27	45 (19 to 216)	44 ± 18	39 (19 to 129)	0.002	
Crude change till 1 year	1 ± 10	1 (−28 to 40)	−1 ± 6	−1 (−28 to 15)	0.047	
Change% till 1 year	0 ± 0	0 (−1 to 3)	0 ± 0	0 (−1 to 2)	0.025	
P[§]-within linear mixed model till 1 year	0.893		0.459			
$A\beta_{1-42}$						0.785
Value at baseline	368 ± 103	379 (89 to 680)	362 ± 84	368 (140 to 627)	0.561	
Value at 6 months	374 ± 100	374 (98 to 610)	364 ± 95	374 (129 to 687)	0.245	
Crude change till 6 months	6 ± 54	5 (−230 to 152)	2 ± 52	4 (−122 to 205)	0.404	
Change% till 6 months	0 ± 3	0 (−18 to 8)	0 ± 4	0 (−28 to 19)	0.484	
P[§]-within linear mixed model till 6 months	0.835		1.000			
Value at 1 year	388 ± 106	392 (95 to 691)	382 ± 105	379 (144 to 733)	0.376	
Crude change till 1 year	20 ± 64	20 (−265 to 190)	20 ± 71	6 (−161 to 317)	0.370	
Change% till 1 year	1 ± 4	1 (−12 to 16)	1 ± 4	0 (−8 to 14)	0.428	
P[§]-within linear mixed model till 1 year	0.022		0.043			

[†]*P-value of comparing the groups at each timepoint based on Mann-Whitney test; however, the 95% Confidence Intervals are based on t-statistics.*
[§]*Longitudinal changes within the liner mixed model in each group, multiple comparison correction performed by Bonferroni method.*
[$]*Comparison between the trend of changes in groups based on interaction analysis of time and group, within a linear mixed model.*

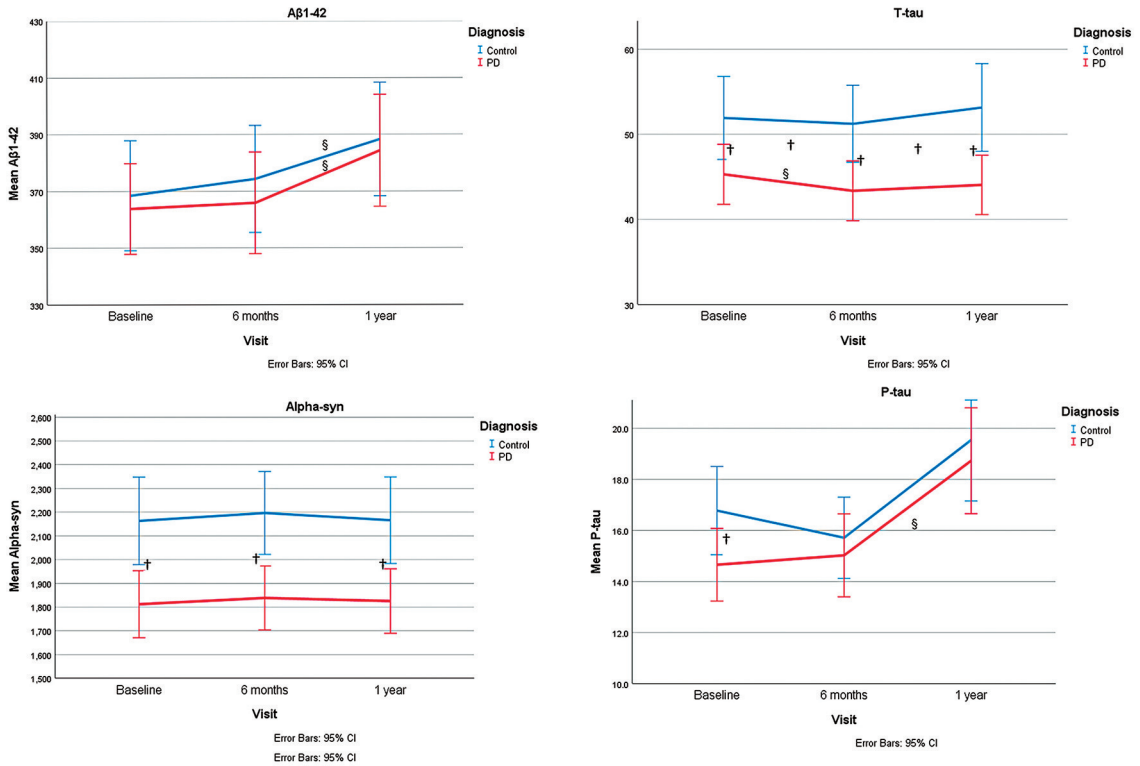

FIGURE 1 | Representation of α-syn, P-tau, T-tau, and Aβ 1-42 levels at different time points and the trend of changes during study period. [§]shows significant changes during time within each group within a linear mixed model. [†]shows the significant group differences for CSF levels of markers at each time point or their changes (from baseline to 6 months or from baseline to 1 year).

changes of each CSF marker was observed except for the significant correlation between estimated changes in alpha-synuclein level and RBDSQ scores ($p = 0.0013$) (data not shown).

DISCUSSION

In this study, we explored baseline levels and longitudinal changes of CSF markers and evaluated their association with each other in drug-naïve, non-demented PD patients of PPMI cohort who were at the early stage of their disease. In addition, we evaluated the power of baseline clinical scores (UPDRS III, MoCA, UPSIT, RBDSQ) in prediction of longitudinal changes of CSF markers in PD patients. In brief, all CSF markers were lower in PDs compared to controls except $A\beta_{1-42}$ at baseline, which was similar to the results of the previously mentioned cross-sectional study in PPMI cohort. In longitudinal assessment, $A\beta_{1-42}$ and p-tau concentrations showed an increase in PD patients with the former also increasing in control subjects. Correlations between baseline concentrations of each of the CSF markers with their own estimated changes were significant except for p-tau. Furthermore, longitudinal changes of p-tau levels were positively correlated to t-tau and $A\beta_{1-42}$ longitudinal changes.

Difference Between PD and Control in Biomarker Levels at Different Time Points and Their Changes During Time

This study has shown a reduced level of α-syn and t-tau at all time-points and p-tau only at baseline in patients' CSF compared to healthy controls'. This observation is in line with the most recent studies (16, 20, 21); however, some studies observed higher or unchanged CSF t-tau or p-tau levels in PD patients (17, 29–31).

P-tau levels were significantly lower in the PD group compared to controls and rose significantly during the 1-year follow-up time, only in the PD group. Therefore, the p-tau level differences between PD and control groups vanished at the 6-month and one-year time points. On the other hand, t-tau levels were different between the two groups at all time points despite their non-significant longitudinal changes. In the study by Boungiorno et al., t-tau but not p-tau longitudinal increase was significant. Hall et al., however, found an increase in both. Thus, due to the high rate of p-tau changes during the disease course, at least in some time points, there would be an overlap with p-tau levels in controls, which challanges its diagnostic value. Thus, we hypothesize that CSF t-tau is a better candidate as a diagnostic tool than p-tau, which needs to be further investigated.

Our study does not provide the means to discover the underlying mechanism of these protein level differences;

TABLE 3 | The correlation and regression coefficient of estimated changes and baseline values with estimated change of different factors during study periods, obtained within linear mixed model.

Estimated		Estimated changes per year*				Baseline values			
Change per year*		α-synuclein	P-tau	T-tau	Aβ42	α-synuclein	P-tau	T-tau	Aβ42
α-synuclein	r		0.015	0.092	0.096	−0.310	−0.036	−0.125	0.042
	B		0.309	27.400	0.429	−0.020	−0.211	−0.306	0.022
	P		0.871	0.335	0.314	0.001	0.708	0.190	0.663
P-tau	r	0.015		−0.220	0.387	0.129	0.030	0.228	−0.068
	B	0.001		−3.286	0.087	0.000	0.009	0.028	−0.002
	P	0.871		0.020	0.000	0.175	0.750	0.016	0.476
T–tau	r	0.092	−0.220		−0.159	−0.762	−0.399	−0.983	−0.193
	B	0.000	−0.015		−0.002	0.000	−0.008	−0.008	0.000
	P	0.335	0.020		0.094	0.000	0.000	0.000	0.041
Aβ1-42	r	0.096	0.387	−0.159		0.297	−0.052	0.127	0.635
	B	0.021	1.731	−10.599		0.004	−0.068	0.070	0.075
	P	0.314	0.000	0.094		0.002	0.587	0.182	0.000

r, Correlation coefficient.

B, Linear regression coefficient.

**Estimated changes were calculated for each subject based on the regression coefficient of each subject within a linear mixed model.*

The correlations were assessed between different biomarkers in the study. One single biomarker could not have a correlationship with itself and they were marked black.

however, we speculate that at the very early stages of PD, i.e., at our baseline, there is an accumulation of toxic p-tau in form of neurofibrillary tangles (NFTs) in neurons, which causes absorption of more functional tau molecules from extracellular space as a compensatory mechanism in order to reverse back the function of neuronal trafficking. The similar mechanisms are the case for α-syn. In contrast, it has been shown that due to the altered processing of α-syn and occasionally increased transcription of SNCA gene, neurons secrete exosomal α-syn and propagate PD pathology (32, 33). Maybe, the observed changes of α-syn in different studies vary based on the weight of such mechanisms. This phenomenon causes a decrease in t-tau, p-tau, and α-syn levels in CSF. In later phases of the disease, due to axonal damage, p-tau and α-syn molecules accumulated in form of NFTs and Lewy bodies are released into CSF and the levels of p-tau and α-syn will increase. However, α-syn longitudinal changes are not significant in the time points we have studied, which is in line with some of the previous studies (26). One theory is that in PD the accelerated injury to neuronal plasma membrane which causes an increase in CSF α-syn, is contradicted by the more α-syn intracellular accumulation (34). Thus, variability in rates of axonal degeneration is one of the important factors in this regard and probably α-syn change is not an appropriate diagnostic tool for PD (35). We reckon that levels of t-tau and α-syn might have already fallen in earlier stages (because of absorption of these molecules into neurons as a compensation) and in the follow-up time due to the floor effect, no longitudinal decrease could be observed, although heterogeneity in disease duration makes such assumptions non-applicable. Maybe, longer follow-up times could allow significant longitudinal changes.

It is worthy of note that in AD, CSF tau levels are elevated from the earliest phases of the disease (36, 37) except for the subgroups of patients with the concomitant alpha-synucleinopathy, i.e., Dementia with Lewy Bodies (DLB) (37). This common observation in synucleinopathies might refer to the colocalization of tau molecules with α-syn, which contributes to their reduction in CSF.

On the other hand, $A\beta_{1-42}$ levels were not significantly different between the two groups at any time point although significant longitudinal increase of $A\beta_{1-42}$ was observed in both groups. However, the study done by Buongiorno et al. has shown the opposite, i.e., a decrease in Aβ levels during 18 months, which was associated with cognitive decline in non-demented PD patients (27). In addition, in the study done by Hall et al. the changes in Aβ levels in PD patients with long disease durations were non-significant during 2 years. Herein, we checked for levels of whole CSF Aβ ($A\beta_{1-42}$) in contrast to the mentioned study, which evaluated the level of $A\beta_{42}$, and this might explain the discrepancies in results. The progressive reduction of $A\beta_{1-42}$ levels in other studies (both in AD and PD) can be mainly attributed to its extracellular accumulation but we can not justify the observed increase in $A\beta_{1-42}$ in our study.

On the whole, it seems that the difference in clinical and pathophysiological characteristics contributes to variability in disease progression and different results of such studies.

Variables which affect the results of these studies include the rate of axonal damage, clinical endophenotypes, the stage of the disease, and whether compensatory mechanisms are working properly. For instance, it is shown that significantly increased levels of CSF α-syn and t-tau is a common phenomenon in the ones who develop PD dementia (PDD) (16). This is similar to the observation of increased α-syn and t-tau in AD patients compared to healthy controls (36–38). Herein, we excluded the patients fulfilling the criteria for PDD at baseline, and this might explain the reason why t-tau and α-syn did not increase during

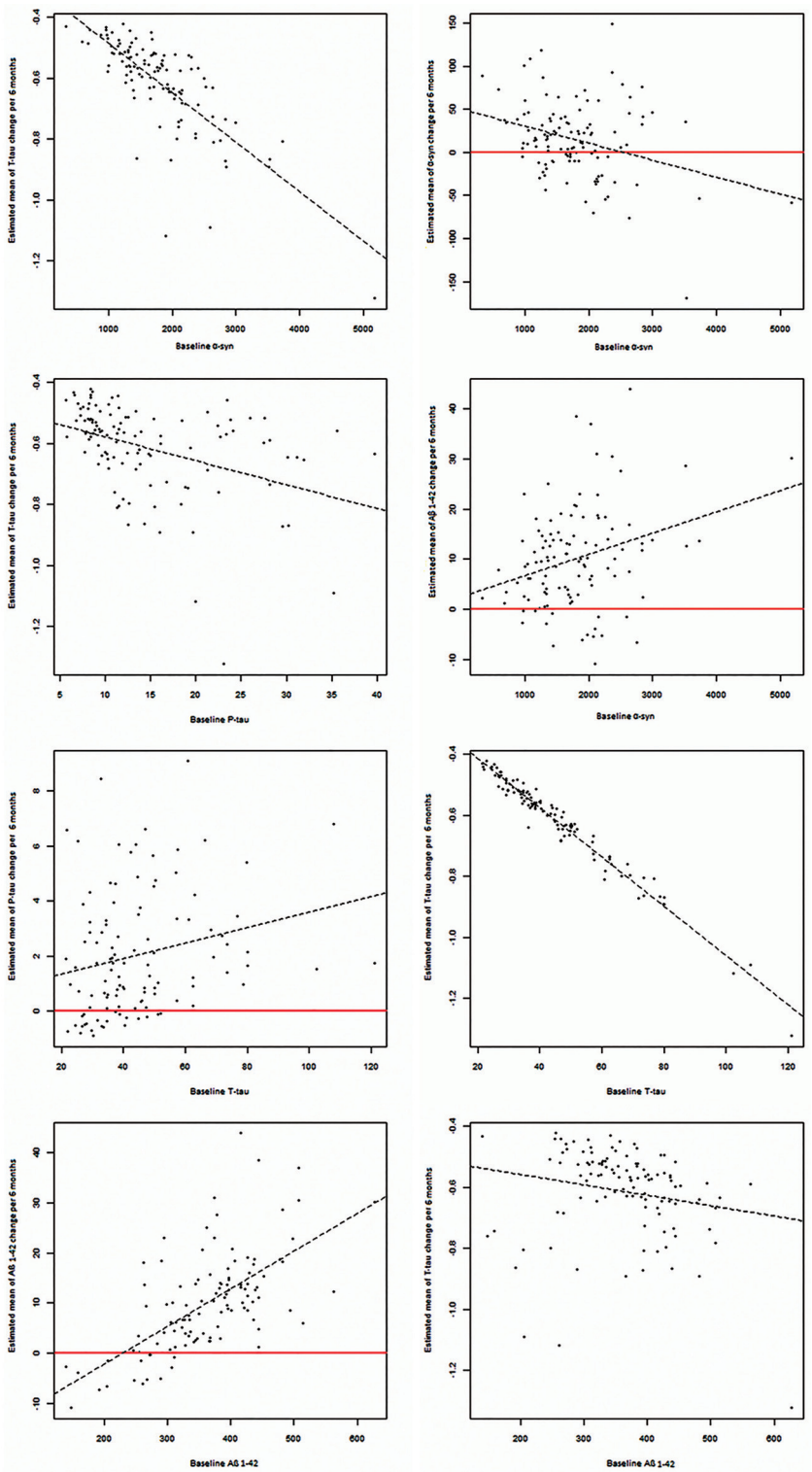

FIGURE 2 | Significant correlations between baseline CSF levels of α-syn, P-tau, T-tau, and $A\beta_{1-42}$ with estimated changes of α-syn, P-tau, T-tau, and $A\beta_{1-42}$.

the course of the disease in our sample. Moreover, it seems that as the disease duration increases, higher levels of α-syn in patients compared to HC is encountered in CSF samples as opposed to the lower levels of this protein in early-stage PD cases such as ours. This is in line with the previous longitudinal assessment done by Hall et al. in which despite significant increases in all

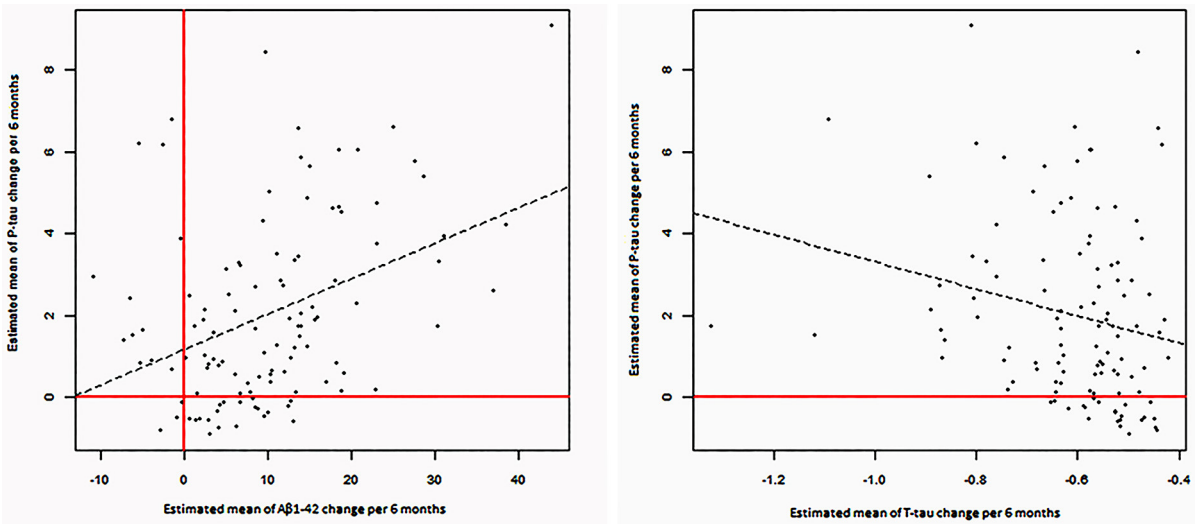

FIGURE 3 | Significant correlations between estimated changes in CSF levels of α-syn, P-tau, T-tau, and Aβ 1- 42.

CSF markers except $A\beta_{42}$, non-significantly changed level of CSF proteins in patients with short disease duration (<5 years from diagnosis) and controls were observed (21). Similarly, all patients in our study had short disease duration (<2 years) and also due to shorter follow-up time in our study, the time required for significant changes in some of the biomarkers was not provided.

Correlation Between Levels of Different CSF Biomarkers at Different Time Points and Between Their Estimated Changes

This study showed the correlation between different CSF markers adjusted for age and gender at different time points in PD patients. No significant correlation found in control group when adjusted for age and gender. In addition, lower baseline levels of p-tau, t-tau, and α-syn were correlated with lower rate of estimated decrease of t-tau within a linear mixed model.

The disappearance of any association between CSF biomarkers in controls after adjusting for age and gender made us infer that any observed correlation between protein concentrations in healthy people was confounded by age and gender. However, in PD group correlations remained significant after this adjustment; meaning that there must be a pathological and disease-specific link between these proteinopathies. Therefore, we suspect that any correlation observed between levels of different biomarkers in control cases of previous PPMI studies was the result of not adjusting them for age and gender (20).

Probably the most distinctive part of this study was the assessment of correlation between "estimated" changes of biomarkers within a linear mixed model and baseline values of different biomarkers. Lower p-tau, t-tau, and α-syn levels at baseline were predictive of the higher rate of t-tau level decrease in the next year. The power of lower α-syn levels at baseline for estimation of lower rate of *t*-tau decrease might be due to lower baseline α-syn CSF levels being associated with more toxic α-syn accumulation in Lewy bodies. Actually, accumulation of α-syn in Lewy body has a seeding effect on tau oligomerization and accumulation (11–13). In addition, accumulation of tau itself propagates its accumulation in neurofibrillary tangles. These protein accumulations (α-syn and tau) inhibit release of tau into CSF (39). Although, these phenomena necessitate more tau absorption into neurons as a compensatory mechanism, in later stages such mechanisms do not seem to function and there is lower rate of decrease in tau levels (making these changes were not significant in a one-year follow-up due to the floor effect or short follow-up time).

On the other hand, lower levels of $A\beta_{1-42}$ were predictive of the lower rate of tau decrease in CSF. We suppose that lower level of CSF $A\beta_{1-42}$ means more accumulation of Aβ in extracellular amyloid plaques and lead to lower free (intracellular) Aβ level, which is necessary for tau phosphorylation and accumulation (40).

On the whole, these results show that changes of t-tau CSF levels may be the convergence point of PD pathology. However, because amyloidopathy and synucleinopathy have opposing effects on the rate of CSF tau level changes, assessing CSF t-tau levels can not reflect the severity of underlying proteinopathies and thus, the rate of t-tau CSF level changes may be quite small and need a long time to change. Therefore, in short follow-up times, like in our study, its changes would not be significant.

Another finding was that lower CSF α-syn levels at baseline were predictive of slower $A\beta_{1-42}$ increase after one year. One explanation is that α-syn accumulation propagates Aβ accumulations and its lower CSF concentrations. For instance, a recent study has shown that non-amyloid beta component of human alpha-synuclein oligomers induces the formation of new Aβ oligomers (41).

Correlation Between Baseline Clinical Entities of PD Patients and Longitudinal Changes of CSF Markers

It has been suggested that Rapid Eye Movement (REM) sleep Behavior Disorder (RBD) can be a clue to early diagnosis of neurodegenerative diseases (42), specifically it can help with early detection of PD (19, 43, 44). Affliction of brainstem structures which control REM sleep with alpha-synuclein protein inclusions in early phases of PD seems to be the underlying mechanism responsible for RBD (45).

In this study, we detected significant increase in CSF levels of alpha-synuclein in PD-RBD patients. Although a previous cross-sectional study in PD patients have revealed no association between CSF alpha-synuclein levels and RBD (46), prior investigations have revealed that CSF Prion Proteins (PrPs) are significantly elevated in PD patients with RBD compared to PD patients without sleep disorders (47), which might be suggestive of accelerated neuronal degeneration in PD-RBD patients and thus, introduce RBD as potentially the most appropriate clinical predictive marker of neuronal degeneration and disease progression in PD, as shown previously (48).

Importantly, changes in other CSF protein levels were not associated with UPDRS III, MoCA, and UPSIT scores. This might refer to the fact that motor symptoms, cognitive impairment, and olfaction dysfunction are not appropriate predictors of progression of neuronal degeneration in PD patients. In this study we have not assessed progression of different PD symptoms in association with the baseline clinical scores and it is worthy of note that although these CSF biomarkers pattern of changes in patients with various clinical entities at baseline might elucidate the speed of neurodegeneration to some extent, it does not necessarily mean that clinical manifestations progress is in line with CSF marker changes. However, it might help identify the speed of neurodegeneration at a molecular level and design more targeted therapies.

CONCLUSION

Although there are some positive points to this study like recruitment of drug-naïve patients, it suffers from some limitations like short follow-up time. To reach a more comprehensive conclusion, further longitudinal assessments regarding the predictive role of CSF proteins and their different species in patients at different stages of the disease and with longer follow-ups are suggested.

In addition, the patients in this study were quite heterogeneous in terms of disease duration which renders this study to some limitations; for instance, the patterns of CSF protein changes of different subgroups at different disease stages may be different.

In addition, in the manuscript we have assumed that lower CSF concentration of proteins is due to their accumulation in extracellular and intracellular spaces. This assumption might not be the case and several undiscovered mechanisms may play a role in determining the CSF concentrations of these proteins. There are some other limitations such as various degrees of CSF concentrations due to altered states of hydration and the position of proteins in a caudo-rostral column from the lumbar region to the cerebral origin. Moreover, clinical application of the difficult and invasive procedure of lumbar puncture to determine CSF markers as a way to follow-up the patients suffering from neurodegenerative diseases seems unlikely and such studies may just help enlighten the pathological mechanisms of proteinopathies.

In sum, it seems that α-syn, t-tau, p-tau, and Aβ play a role in PD pathology and have bidirectional interactions with each other, which mostly converge on tau pathology and lead to changes of CSF tau levels. Most noticeably, colocalization of α-syn and t-tau molecules in intracellular inclusions cause a reduction in CSF α-syn and t-tau levels, in contrast to AD without synucleinopathies which is associated with higher levels of CSF tau.

Importantly, among the clinical measures we applied, only RBD was predictive of α-syn increase during time. This might refer to the fact that evaluating patients for RBD at baseline is far more important than motor, olfaction, or cognitive assessment for prognostic purposes.

We suggest that different subtypes of PD patients progress heterogeneously. Thus, conducting similar studies in patient subtypes with various clinical symptoms and genetic, epigenetic, and environmental predispositions may be helpful.

In addition, most of the studies have shown the role of lower Aβ levels at baseline in predicting cognitive decline in the future (49). However, recently, predictive roles for tau levels in cognitive decline have been shown in other neurodegenerative diseases like Alzheimer's disease (50) and Huntington's disease (51). This observation in AD has been attributed to the later position of tau in the preclinical phase of the disease. To the best of our knowledge, there has been no evidence about the temporality of changes in tau and Aβ pathology in PD, i.e., whether CSF tau levels start to rise (or maybe fall) in later stages of the disease compared to Aβ or not. Thus, it seems that conducting longitudinal studies are necessary to discover whether changes in Aβ or tau is a more appropriate predictor of cognitive decline in the future.

ETHICS STATEMENT

All procedures performed here, including human participants were in accordance with the ethical standards of the institutional research committee and with the 1964 Helsinki declaration and its later amendments or comparable ethical standards.

INFORMED CONSENT

Informed consent was obtained from all individual participants included in the study.

AUTHOR CONTRIBUTIONS

MD, MA, AA-G, SP, AK contributed to the conception and design of the study; MY, AA-G, MD, SP contributed to data collection

and analysis; and MD, SP, AK, AA-G contributed to writing the manuscript.

ACKNOWLEDGMENTS

This work was funded by grants from the Michael J Fox Foundation for Parkinson's Research, the W Garfield Weston Foundation, and the Alzheimer's Association, the Canadian Institutes for Health Research, and the Natural Sciences and Engineering Research Council of Canada. We thank Christian Beckmann and Simon Eickhoff for their advice on data analysis. Data used in this article were obtained from the Parkinsons Progression Markers Initiative (PPMI) database (www.ppmi-info.org/data). For up-to-date information on the study, visit www.ppmi-info.org. PPMI is sponsored and partially funded by the Michael J Fox Foundation for Parkinsons Research and funding partners, including AbbVie, Avid Radiopharmaceuticals, Biogen, Bristol-Myers Squibb, Covance, GE Healthcare, Genentech, GlaxoSmithKline (GSK), Eli Lilly and Company, Lundbeck, Merck, Meso Scale Discovery (MSD), Pfizer, Piramal Imaging, Roche, Servier, and UCB (http://www.ppmi-info.org/about-ppmi/who-we-are/study-sponsors/).

SUPPLEMENTARY MATERIAL

The Supplementary Material for this article can be found online at: https://www.frontiersin.org/articles/10.3389/fneur.2018.00560/full#supplementary-material

REFERENCES

1. Rodriguez M, Rodriguez-Sabate C, Morales I, Sanchez A, Sabate M. Parkinson's disease as a result of aging. *Aging Cell* (2015) 14:293–308. doi: 10.1111/acel.12312
2. Bourdenx M, Koulakiotis NS, Sanoudou D, Bezard E, Dehay B, Tsarbopoulos A. Protein aggregation and neurodegeneration in prototypical neurodegenerative diseases: Examples of amyloidopathies, tauopathies and synucleinopathies. *Prog Neurobiol.* (2015) 155:171–93. doi: 10.1016/j.pneurobio.2015.07.003.
3. Thenganatt MA, Jankovic J. Parkinson disease subtypes. *JAMA Neurol.* (2014) 71:499–504. doi: 10.1001/jamaneurol.2013.6233
4. Halliday GM, Holton JL, Revesz T, Dickson DW. Neuropathology underlying clinical variability in patients with synucleinopathies. *Acta Neuropathol.* (2011) 122:187–204. doi: 10.1007/s00401-011-0852-9
5. Petrou M, Dwamena BA, Foerster BR, MacEachern MP, Bohnen NI, Muller ML, et al. Amyloid deposition in Parkinson's disease and cognitive impairment: a systematic review. *Mov Disord.* (2015) 30:928–35. doi: 10.1002/mds.26191
6. Sabbagh MN, Adler CH, Lahti TJ, Connor DJ, Vedders L, Peterson LK, et al. Parkinson disease with dementia: comparing patients with and without Alzheimer pathology. *Alzheimer Dis Assoc Disord.* (2009) 23:295–7. doi: 10.1097/WAD.0b013e31819c5ef4
7. Irwin DJ, White MT, Toledo JB, Xie SX, Robinson JL, Van Deerlin V, et al. Neuropathologic substrates of Parkinson disease dementia. *Ann Neurol.* (2012) 72:587–98. doi: 10.1002/ana.23659
8. Smirnova L, Harris G, Delp J, Valadares M, Pamies D, Hogberg HT, et al. A LUHMES 3D dopaminergic neuronal model for neurotoxicity testing allowing long-term exposure and cellular resilience analysis. *Arch Toxicol.* (2015) 90:2725–43. doi: 10.1007/s00204-015-1637-z
9. Bellou V, Belbasis L, Tzoulaki I, Evangelou E, Ioannidis JP. Environmental risk factors and Parkinson's disease: an umbrella review of meta-analyses. *Parkinsonism Relat Disord.* (2016) 23:1–9. doi: 10.1016/j.parkreldis.2015.12.008
10. Clinton LK, Blurton-Jones M, Myczek K, Trojanowski JQ, LaFerla FM. Synergistic Interactions between Abeta, tau, and alpha-synuclein: acceleration of neuropathology and cognitive decline. *J Neurosci.* (2010) 30:7281–9. doi: 10.1523/JNEUROSCI.0490-10.2010
11. Waxman EA, Giasson BI. Induction of intracellular tau aggregation is promoted by alpha-synuclein seeds and provides novel insights into the hyperphosphorylation of tau. *J Neurosci.* (2011) 31:7604–18. doi: 10.1523/JNEUROSCI.0297-11.2011
12. Oikawa T, Nonaka T, Terada M, Tamaoka A, Hisanaga S, Hasegawa M. Alpha-synuclein fibrils exhibit gain of toxic function, promoting tau aggregation and inhibiting microtubule assembly. *J Biol Chem.* (2016) 291:15046–56. doi: 10.1074/jbc.M116.736355
13. Sengupta U, Guerrero-Munoz MJ, Castillo-Carranza DL, Lasagna-Reeves CA, Gerson JE, Paulucci-Holthauzen AA, et al. Pathological interface between oligomeric alpha-synuclein and tau in synucleinopathies. *Biol Psychiatry* (2015) 78:672–83. doi: 10.1016/j.biopsych.2014.12.019
14. Parnetti L, Castrioto A, Chiasserini D, Persichetti E, Tambasco N, El-Agnaf O, et al. Cerebrospinal fluid biomarkers in Parkinson disease. *Nat Rev Neurol.* (2013) 9:131–40. doi: 10.1038/nrneurol.2013.10
15. Hong Z, Shi M, Chung KA, Quinn JF, Peskind ER, Galasko D, et al. DJ-1 and alpha-synuclein in human cerebrospinal fluid as biomarkers of Parkinson's disease. *Brain* (2010) 133(Pt 3):713–26. doi: 10.1093/brain/awq008
16. Montine TJ. CSF Aβ(42) and tau in Parkinson's disease with cognitive impairment. *Mov Disord.* (2010) 25:2682–5. doi: 10.1002/mds.23287
17. Mollenhauer B, Locascio JJ, Schulz-Schaeffer W, Sixel-Doring F, Trenkwalder C, Schlossmacher MG. alpha-Synuclein and tau concentrations in cerebrospinal fluid of patients presenting with parkinsonism: a cohort study. *Lancet Neurol.* (2011) 10:230–40. doi: 10.1016/S1474-4422(11)70014-X
18. Hall S, Ohrfelt A, Constantinescu R, Andreasson U, Surova Y, Bostrom F, et al. Accuracy of a panel of 5 cerebrospinal fluid biomarkers in the differential diagnosis of patients with dementia and/or parkinsonian disorders. *Arch Neurol.* (2012) 69:1445–52. doi: 10.1001/archneurol.2012.1654
19. Kang JH, Irwin DJ, Chen-Plotkin AS, Siderowf A, Caspell C, Coffey CS, et al. Association of cerebrospinal fluid beta-amyloid 1-42, T-tau, P-tau181, and alpha-synuclein levels with clinical features of drug-naive patients with early Parkinson disease. *JAMA Neurol* (2013) 70:1277–1287. doi: 10.1001/jamaneurol.2013.3861
20. Kang JH, Mollenhauer B, Coffey CS, Toledo JB, Weintraub D, Galasko DR, et al. CSF biomarkers associated with disease heterogeneity in early Parkinson's disease: the Parkinson's Progression Markers Initiative study. *Acta Neuropathol.* (2016) 131:935–49. doi: 10.1007/s00401-016-1552-2
21. Hall S, Surova Y, Ohrfelt A, Blennow K, Zetterberg H, Hansson O. Longitudinal Measurements of Cerebrospinal Fluid Biomarkers in Parkinson's Disease. *Mov Disord.* (2016) 31:898–905. doi: 10.1002/mds.26578
22. Irwin DJ, Lee V. MY, Trojanowski JQ. Parkinson's disease dementia: convergence of α-synuclein, tau and amyloid-β pathologies. *Nat Rev Neurosci.* (2013) 14:626–36. doi: 10.1038/nrn3549
23. Kang J. H. Cerebrospinal Fluid Amyloid beta1-42, Tau, and alpha-synuclein predict the heterogeneous progression of cognitive dysfunction in Parkinson's Disease. *J Mov Disord.* (2016) 9:89–96. doi: 10.14802/jmd.16017
24. Majbour NK, Vaikath NN, Eusebi P, Chiasserini D, Ardah M, Varghese S, et al. Longitudinal changes in CSF alpha-synuclein species reflect Parkinson's disease progression. *Mov Disord.* (2016) 31:1535–42. doi: 10.1002/mds.26754
25. Stewart T, Liu C, Ginghina C, Cain KC, Auinger P, Cholerton B, et al. Cerebrospinal fluid alpha-synuclein predicts cognitive decline in Parkinson disease progression in the DATATOP cohort. *Am J Pathol.* (2014) 184:966–75. doi: 10.1016/j.ajpath.2013.12.007
26. Forland MG, Ohrfelt A, Dalen I, Tysnes OB, Blennow K, Zetterberg H, et al. Evolution of cerebrospinal fluid total alpha-synuclein in Parkinson's disease. *Parkinsonism Relat Disord.* (2018) 49:4–8. doi: 10.1016/j.parkreldis.2018.01.018

27. Buongiorno M, Antonelli F, Compta Y, Fernandez Y, Pavia J, Lomena F, et al. Cross-Sectional and Longitudinal Cognitive Correlates of FDDNP PET and CSF Amyloid-beta and Tau in Parkinson's Disease1. *J Alzheimers Dis.* (2017) 55:1261–72. doi: 10.3233/JAD-160698
28. Parkinson Progression Marker Initiative. The Parkinson Progression Marker Initiative (PPMI) *Prog Neurobiol.* (2011) 95:629–35. doi: 10.1016/j.pneurobio.2011.09.005
29. Parnetti L, Tiraboschi P, Lanari A, Peducci M, Padiglioni C, D'Amore C, et al. Cerebrospinal fluid biomarkers in Parkinson's disease with dementia and dementia with Lewy bodies. *Biol Psychiatry* (2008) 64:850–5. doi: 10.1016/j.biopsych.2008.02.016
30. Alves G, Bronnick K, Aarsland D, Blennow K, Zetterberg H, Ballard C, et al. CSF amyloid-beta and tau proteins, and cognitive performance, in early and untreated Parkinson's disease: the Norwegian ParkWest study. *J Neurol Neurosurg Psychiatry* (2010) 81:1080–6. doi: 10.1136/jnnp.2009.199950
31. Parnetti L, Chiasserini D, Bellomo G, Giannandrea D, De Carlo C, Qureshi MM, et al. Cerebrospinal fluid Tau/alpha-synuclein ratio in Parkinson's disease and degenerative dementias. *Mov Disord.* (2011) 26:1428–35. doi: 10.1002/mds.23670
32. Emmanouilidou E, Melachroinou K, Roumeliotis T, Garbis SD, Ntzouni M, Margaritis LH, et al. Cell-produced alpha-synuclein is secreted in a calcium-dependent manner by exosomes and impacts neuronal survival. *J Neurosci.* (2010) 30:6838–51. doi: 10.1523/JNEUROSCI.5699-09.2010
33. Danzer KM, Kranich LR, Ruf WP, Cagsal-Getkin O, Winslow AR, Zhu L, et al. Exosomal cell-to-cell transmission of alpha synuclein oligomers. *Mol Neurodegener* (2012) 7:42. doi: 10.1186/1750-1326-7-42
34. Mollenhauer B, Cullen V, Kahn I, Krastins B, Outeiro TF, Pepivani I, et al. Direct quantification of CSF alpha-synuclein by ELISA and first cross-sectional study in patients with neurodegeneration. *Exp Neurol.* (2008) 213:315–25. doi: 10.1016/j.expneurol.2008.06.004
35. Mollenhauer B, Parnetti L, Rektorova I, Kramberger M, Pikkarainen M J., Schulz-Schaeffer W, et al. Biological confounders for the values of cerebrospinal fluid proteins in Parkinson's disease and related disorders. *J Neurochem.* (2015) 139(Suppl. 1):290–317. doi: 10.1111/jnc.13390
36. Hansson O, Zetterberg H, Buchhave P, Londos E, Blennow K, Minthon L. Association between CSF biomarkers and incipient Alzheimer's disease in patients with mild cognitive impairment: a follow-up study. *Lancet Neurol.* (2006) 5:228–34. doi: 10.1016/S1474-4422(06)70355-6
37. Toledo JB, Korff A, Shaw LM, Trojanowski JQ, Zhang J. CSF alpha-synuclein improves diagnostic and prognostic performance of CSF tau and Abeta in Alzheimer's disease. *Acta Neuropathol.* (2013) 126:683–97. doi: 10.1007/s00401-013-1148-z
38. Sonnen JA, Montine KS, Quinn JF, Kaye JA, Breitner JC, Montine TJ. Biomarkers for cognitive impairment and dementia in elderly people. *Lancet Neurol.* (2008) 7:704–14. doi: 10.1016/S1474-4422(08)70162-5
39. Parnetti L, Farotti L, Eusebi P, Chiasserini D, De Carlo C, Giannandrea D, et al. Differential role of CSF alpha-synuclein species, tau, and Aβ42 in Parkinson's Disease. Front Aging Neurosci (2014) 6:53. doi: 10.3389/fnagi.2014.00053
40. Stancu IC, Vasconcelos B, Terwel D, Dewachter I. Models of β-amyloid induced Tau-pathology: the long and "folded" road to understand the mechanism. *Mol Neurodegener.* (2014) 9:51. doi: 10.1186/1750-1326-9-51
41. Atsmon-Raz Y, Miller Y. Non-Amyloid-beta Component of Human alpha-Synuclein Oligomers Induces Formation of New AbetaOligomers: insight into the mechanisms that Link Parkinson's and Alzheimer's Diseases. *ACS Chem Neurosci.* (2016) 7:46–55. doi: 10.1021/acschemneuro.5b00204
42. Ferini-Strambi L, Marelli S, Galbiati A, Rinaldi F, Giora E. REM Sleep Behavior Disorder (RBD) as a marker of neurodegenerative disorders. *Arch Ital Biol.* (2014) 152:129–46. doi: 10.12871/000298292014238
43. Postuma RB, Gagnon JF, Rompre S, Montplaisir JY. Severity of REM atonia loss in idiopathic REM sleep behavior disorder predicts Parkinson disease. *Neurology* (2010) 74:239–44. doi: 10.1212/WNL.0b013e3181ca0166
44. Prashanth R, Dutta Roy S, Mandal PK, Ghosh S. High-Accuracy Detection of Early Parkinson's disease through multimodal features and machine learning. *Int J Med Inform.* (2016) 90:13–21. doi: 10.1016/j.ijmedinf.2016.03.001
45. Howell MJ, Schenck CH. Rapid eye movement sleep behavior disorder and neurodegenerative disease. *JAMA Neurol.* (2015) 72:707–12. doi: 10.1001/jamaneurol.2014.4563
46. Goldman JG, Andrews H, Amara A, Naito A, Alcalay RN, Shaw LM, et al. Cerebrospinal fluid, plasma, and saliva in the BioFIND study: relationships among biomarkers and Parkinson's disease features. *Mov Disord.* (2018) 33:282–8. doi: 10.1002/mds.27232
47. Zhang WJ, Shang XL, Peng J, Zhou MH, Sun WJ. Expression of prion protein in the cerebrospinal fluid of patients with Parkinson's disease complicated with rapid eye movement sleep behavior disorder. *Genet Mol Res.* (2017) 16. doi: 10.4238/gmr16019022
48. Mollenhauer B, Zimmermann J, Sixel-Doring F, Focke NK, Wicke T, Ebentheuer J, et al. Monitoring of 30 marker candidates in early Parkinson disease as progression markers. *Neurology* (2016) 87:168–77. doi: 10.1212/WNL.0000000000002651
49. Leaver K, Poston KL. Do CSF Biomarkers Predict Progression to Cognitive Impairment in Parkinson's disease patients? A systematic review. *Neuropsychol Rev.* (2015) 25:411–23. doi: 10.1007/s11065-015-9307-8
50. Brier MR, Gordon B, Friedrichsen K, McCarthy J, Stern A, Christensen J, et al. Tau and Abeta imaging, CSF measures, and cognition in Alzheimer's disease. *Sci Transl Med.* (2016) 8:338ra366. doi: 10.1126/scitranslmed.aaf2362
51. Rodrigues FB, Byrne L, McColgan P, Robertson N, Tabrizi SJ, Leavitt BR, et al. Cerebrospinal fluid total tau concentration predicts clinical phenotype in Huntington's disease. *J Neurochem.* (2016) 139:22–5. doi: 10.1111/jnc.13719

Conflict of Interest Statement: The authors declare that the research was conducted in the absence of any commercial or financial relationships that could be construed as a potential conflict of interest.

The reviewer CH and handling Editor declared their shared affiliation.

frontiers in Neuroscience

ORIGINAL RESEARCH
published: 20 February 2018
doi: 10.3389/fnins.2018.00090

Metabolic Disturbances in the Striatum and Substantia Nigra in the Onset and Progression of MPTP-Induced Parkinsonism Model

Yi Lu[1,2†], Xiaoxia Zhang[1,2†], Liangcai Zhao[2], Changwei Yang[2], Linlin Pan[2], Chen Li[2], Kun Liu[1], Guanghui Bai[1], Hongchang Gao[2] and Zhihan Yan[1*]*

[1] Department of Radiology, The Second Affiliated Hospital and Yuying Children's Hospital of Wenzhou Medical University, Wenzhou, China, [2] Institute of Metabonomics & Medical NMR, School of Pharmaceutical Sciences, Wenzhou Medical University, Wenzhou, China

Metabolic confusion has been linked to the pathogenesis of Parkinson's disease (PD), while the dynamic changes associated with the onset and progression of PD remain unclear. Herein, dynamic changes in metabolites were detected from the initiation to the development of 1-Methyl-4-phenyl-1,2,3,6-tetrahydropyridine (MPTP) -induced Parkinsonism model to elucidate its potential metabolic mechanism. *Ex vivo* ^{1}H nuclear magnetic resonance (NMR) spectroscopy was used to measure metabolite changes in the striatum and substantia nigra (SN) of mice at 1, 7, and 21 days after injection of MPTP. Metabolomic analysis revealed a clear separation of the overall metabolites between PD and control mice at different time points. Glutamate (Glu) in the striatum was significantly elevated at induction PD day 1 mice, which persisted to day 21. N-acetylaspartate (NAA) increased in the striatum of induction PD mice on days 1 and 7, but no significant difference was found in striatum on day 21. Myo-Inositol (mI) and taurine (Tau) were also disturbed in the striatum in induction PD day 1 mice. Additionally, key enzymes in the glutamate-glutamine cycle were significantly increased in PD mice. These findings suggest that neuron loss and motor function impairment in induction PD mice may be linked to overactive glutamate-glutamine cycle and altered membrane metabolism.

Keywords: Parkinson's disease, ^{1}H NMR, striatum, metabolism, neurotransmitter

OPEN ACCESS

Edited by:
Chaur-Jong Hu,
Taipei Medical University, Taiwan

Reviewed by:
Petr A. Slominsky,
Institute of Molecular Genetics, Russia
Márcia Liz,
Instituto de Biologia Molecular e Celular, Portugal

***Correspondence:**
Hongchang Gao
gaohc27@wmu.edu.cn
Zhihan Yan
zhihanyan@hotmail.com
† Co-first authors.

Specialty section:
This article was submitted to Neurodegeneration, a section of the journal Frontiers in Neuroscience

Received: *25 October 2017*
Accepted: *05 February 2018*
Published: *20 February 2018*

Citation:
Lu Y, Zhang X, Zhao L, Yang C, Pan L, Li C, Liu K, Bai G, Gao H and Yan Z (2018) Metabolic Disturbances in the Striatum and Substantia Nigra in the Onset and Progression of MPTP-Induced Parkinsonism Model. Front. Neurosci. 12:90. doi: 10.3389/fnins.2018.00090

INTRODUCTION

Parkinson's disease (PD) is one of the most common neurodegenerative diseases found in the aging population. As the worldwide population ages and life expectancy increases, the number of people with PD is expected to rise by more than 50% by 2030 (Kalia and Lang, 2015). The attendant motor disorders, such as resting tremor, rigidity, bradykinesia or slowness, gait disturbance, and postural instability, significantly decrease the quality of life (Fasano et al., 2012). As individuals have an increased life span, increased PD and its treatment can lead to a severe burden to patients, caregivers, and social health institutions (Nagy et al., 2012).

A metabolic abnormality was previously implicated in the pathogenesis of PD. Dopamine (DA) and its metabolites, 3, 4-dihydroxyphenylacetic (DOPAC), and homovanillic acid (HVA), are critical in the physiopathology of PD with motor dyskinesia and were used to validate the

pharmacology of L-Dopa and other therapies (Smith et al., 2014). Tryptophan, serotonin, and the serotonin metabolite 5-HIA were also thought to be related to the psychiatric symptoms of PD (Hatano et al., 2016). However, dopamine modulators can cause serious side effects and often lose effectiveness. The discovery of other metabolites that are altered in the pathogenesis of the neurodegeneration may be involved in the underlying molecular pathways of PD, such as oxidative stress, inflammation, and glial reactions (Dawson and Dawson, 2003; Niranjan, 2014).

Wen et al. (2015) found in a PD rat model with 6-hydroxydopamine (6-OHDA) lesions showed significantly decreased acetylcholine (ACh) and moderately decreased noradrenaline (NA) concentrations in the ventrolateral thalamic nucleus. Ma et al. (2015) revealed that regional glucose metabolism changed in parkinsonism non-human primates by FDG PET. Alterations in the bilirubin-to-biliverdin ratio and ergothioneine in the serum indicate altered oxidative stress intensity, suggesting elevated oxidative stress and/or insufficient ability for scavenging free radicals, as was shown in the work of Hatano et al. (2016). Therefore, studying metabolic changes in cerebral metabolites at the molecular level could uncover novel pathophysiologic mechanisms involved in PD.

Proton nuclear magnetic resonance (^{1}H NMR)-based metabolomics, a powerful approach to study the brain energy metabolism and neurotransmission, has been widely used in psychosis (Chitty et al., 2015), brain tumor (Zhang et al., 2014), and other cerebral diseases. Compared to other metabolomics analytical techniques, NMR has some unique advantages, such as minimal sample processing, robust reproducibility, and high throughput (Lei and Powers, 2013). Using this approach, our previous work showed disturbances of glutamate (Glu), glutamine (Gln), and γ-Aminobutyric acid (GABA) in the Gln-Glu-GABA cycle (GGC) in the striatum of PD rats (Zheng et al., 2015). Although the metabolic abnormality had been previously found to be involved in the pathogenesis of PD, dynamic changes associated with the onset and progression of PD remain to be investigated.

To comprehensively profile changes in metabolites associated with the onset and progression of PD, we used 1-Methyl-4-phenyl-1,2,3,6-tetrahydropyridine (MPTP)-induced PD mice, the most widely accepted dopaminergic neurotoxin used in rodents for studying the progression and mechanisms involved in PD (Jackson-Lewis and Przedborski, 2007). With the goals of exploring the cerebral metabolic bases of the occurrence and development of PD, NMR-based metabolomics was performed to study the kinetic changes in metabolites in the striatum and substantia nigra (SN) of MPTP-induced PD mice.

RESULTS

TH Neuronal Contents and Behavioral Performance

Tyrosine hydroxylase (TH) can be used to label dopaminergic afferents and is commonly used to verify the success of a PD model (Jackson-Lewis and Przedborski, 2007). Microscopic examinations identified representative TH-positive neurons in the SN and striatum from control and induction PD day 1 mice (**Figure 1A**). MPTP administration led to a significant reduction in the number of TH-positive cells in the SN compared with the control group (1,142 ± 122 vs. 3,213 ± 348, $p < 0.001$), demonstrating the successful establishment of the PD model (**Figure 1B**).

Mice were subjected to an open field test 1 day before modeling, and then 1 and 7 days after the injection of MPTP or normal saline (**Figure 2A**). Significant reductions in the movement path, activity time, and total distance were observed in the PD group at different time points (**Figures 2B–D**). In addition, the immobility time in the PD group was significantly increased compared to control mice (**Figure 2E**). These behavioral findings are consistent with the formation of lesions and motor symptoms in MPTP-induced Parkinsonism mice model.

NMR-Based Metabolic Profiling of the Striatum of Mice

To further characterize dynamic changes of metabolites that occur during PD progression, we performed an unbiased metabolic analysis of striatum and SN tissues from control and induction PD mice at different time points. Representative ^{1}H NMR spectra of striatum extracts obtained from control and induction PD mice are shown in **Figure 3**. Assignments presented in **Figure 3D** were based on our previously published work (Gao et al., 2007) using the 600 MHz library of Chenomx NMR suite 7.0 (Chenomx Inc., Edmonton, Canada). The ^{1}H NMR spectra of brain tissue extracts allows for the simultaneous measurement of the numbers of endogenous metabolites, including Glu, GABA, Gln, lactate (Lac), alanine (Ala), N-acetyl aspartate (NAA), succinate (Suc), aspartate (Asp), creatine (Cre), choline (Cho), taurine (Tau), glycine (Gly), and myo-inostitol (mI).

NMR spectra were normalized to the internal standard TSP concentration to evaluate the relative content of metabolites and binned to reduce data dimensions for further metabolomic analyses. We conducted a Partial Least Squares-Discriminant Analysis (PLS-DA), a method that incorporates elements from principal component analysis, regression, and linear discriminant analysis, which revealed a clear separation of the overall metabolite levels in the right striatum between induction PD mice and control mice on days 1, 7, and 21 (**Figure 4**). Further evaluation of the metabolome using a corresponding loading plot, shown with color-coded correlation coefficients (|r|) of metabolites, revealed changed levels of Glu, Gln, NAA, Asp, mI, Cre, and Ala, indicating that neurotransmitter regulation and other metabolites disturbances could be involved in the progression of PD.

Metabolite Changes in Various Brain Regions

For univariate statistical analysis, relative concentrations of specific metabolites were calculated for each subject by subtracting the integrals of the signals. Levels of all identified metabolites in the right striatum and SN are shown in **Figure 5**.

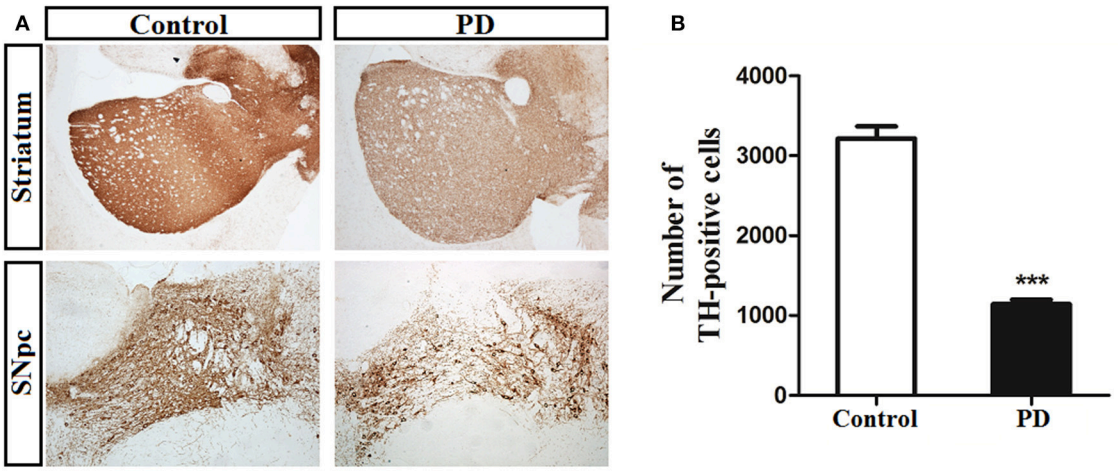

FIGURE 1 | Immunohistochemical staining of tyrosine hydroxylase (TH) in the substantia nigra pars compacta (SNpc) and striatum. **(A)** Illustration of toxicity of MPTP on TH in both SNpc and striatum at the first day after the last treatment. **(B)** MPTP administration induced a significant decrease (64%) number of TH-positive neurons in SNpc of PD group compared with control group (3,213 ± 348 vs. 1,142 ± 122). Bar represented means ± *SD* of three mice per group (***$p < 0.001$).

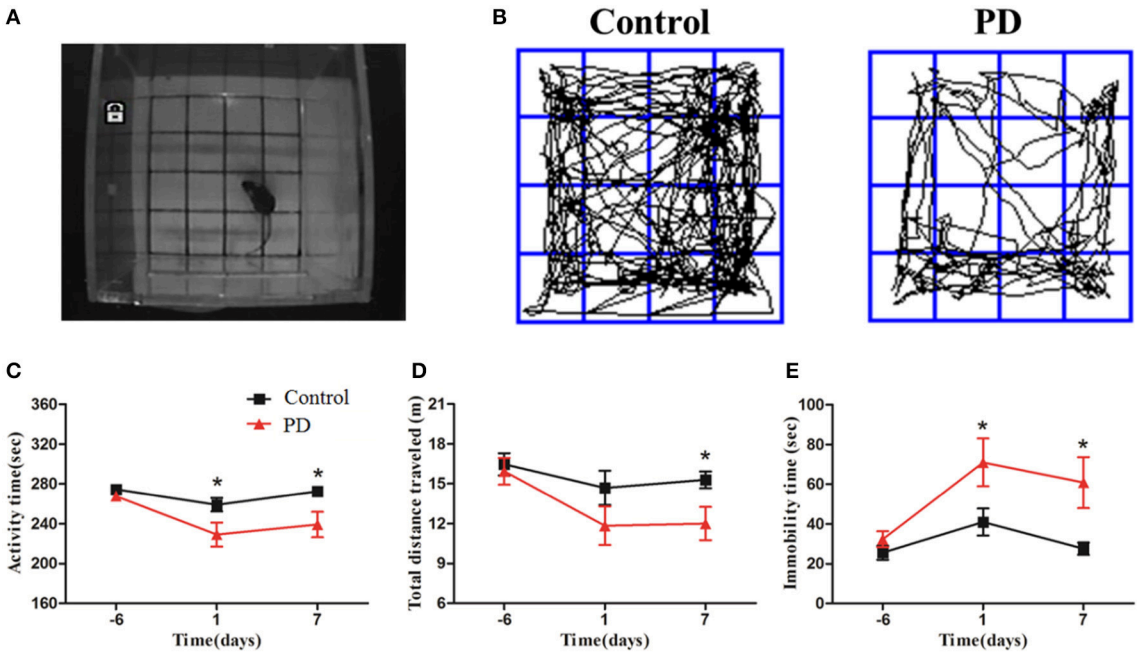

FIGURE 2 | MPTP deteriorated Behavioral alteration of mice in the open field test. **(A)** The open field test was conducted in the chamber measuring 25 × 25 × 45 cm with an automated video tracking system. **(B)** Representative examples of movement path was selected at 1 day after last treatment. The activity time, total distance traveled and immobility time **(C–E)** were recorded and analyzed at 3 time points (6 days before the last treatment, 1 and 7 days after the last treatment). All data were shown as means ± SEM, *$p < 0.05$.

In the right striatum of induction PD mice at day 1 (**Figure 5A**), compared with the control group we found higher levels of neurotransmitters, including Glu (32.72 ± 2.90 vs. 29.55 ± 1.59, $p = 0.041$) and Gln (20.46 ± 1.97 vs. 17.78 ± 0.53, $p = 0.009$), the neuronal marker NAA (28.73 ± 2.93 vs. 25.30 ± 2.07, $p = 0.041$) and the antioxidant Tau (39.99 ± 0.91 vs. 37.39 ± 2.30, $p = 0.027$). By contrast, levels of the energy-related metabolite Ala decreased (5.16 ± 0.32 vs. 6.03 ± 0.51, $p = 0.006$). In the induction PD day 7 group (**Figure 5B**), metabolic profiles revealed higher levels of NAA (32.23 ± 1.64 vs. 29.34 ± 1.91, $p = 0.014$), Glu (36.00 ± 1.15 vs. 33.38 ± 2.34, $p = 0.024$), and Asp (6.32 ± 0.40 vs. 5.86 ± 0.23, $p = 0.033$). In addition, higher levels of Glu (35.25 ± 2.54 vs. 31.98 ± 1.84, $p = 0.029$) and Tau (40.42 ± 1.08 vs. 37.53 ± 1.86, $p = 0.008$) were detected in the

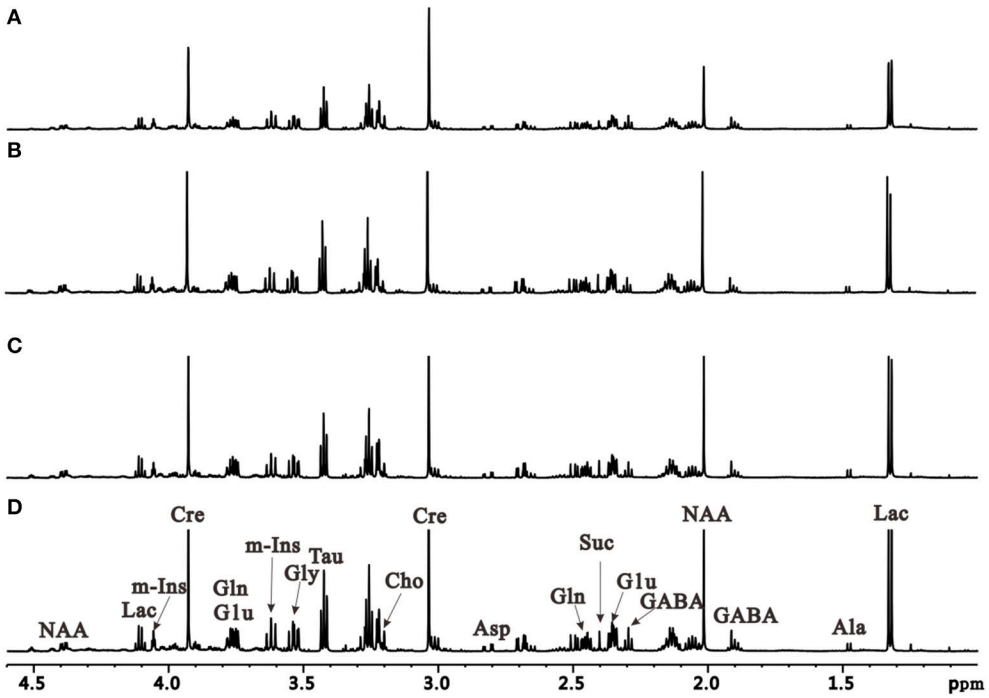

FIGURE 3 | Representative 1H NMR spectra of the right striatum extracts obtained from the control group at the first day after administration **(A)** and induction PD group, respectively at 1 day **(B)**, 7 days **(C)**, and 21 days **(D)**.

induction PD day 21 group (**Figure 5C**). In the SN, PD mice were marked by high concentrations of NAA (38.55 ± 0.93 vs. 37.55 ± 0.47, $p = 0.048$) and Gln (21.55 ± 1.53 vs. 19.72 ± 0.80, $p = 0.031$; **Figure 5D**).

Changes in the levels of NAA, Glu, and Gln in the striatum throughout the progression of MPTP-induced Parkinsonism are shown in **Figure 6**. NAA levels were significantly higher in the induction PD day 1 and 7 groups compared to the control group, while no difference was observed at induction PD day 21. Meanwhile, Glu levels were elevated at day 1, then reached a maximum at day 7, and remained elevated until day 21. In addition, Gln levels were significantly elevated at day 1, but not at days 7 or 21.

Key Enzymes in the Glutamate-Glutamine Cycle

The metabolic changes in Glu and Gln in PD mice suggested that the GGC was involved in the progression of MPTP-induced Parkinsonism. To further explore the reasons whereby GGC influenced PD in mice, levels of selected key enzymes involved in this cycle, including GS and GLS, were measured. GS, an ubiquitous enzyme present in the astroglial cytoplasm and involved in the formation of Gln from Glu (Hertz et al., 1999), was shown to be elevated in the subcortex of PD mice (**Figure 7**). In addition, a similar result was shown in the GLS, which was consistent with the increased conversion of Gln into Glu. Collectively, these findings suggest that an overactive GGC could be observed during the progression of MPTP-induced PD in mice.

DISCUSSION

PD, a multi-centric neurodegenerative disorder, has been shown to be associated with disturbed systemic metabolism (Bogdanov et al., 2008). However, variations in brain metabolites at different time points during the progression remain to be firmly established. In this present study, we used MPTP-induced PD mice to investigate dynamic changes in metabolite levels using high resolution *ex vivo* ^{1}H NMR spectroscopy. Metabolomics analysis showed that multiple time- and region-dependent neurochemical metabolite perturbations occurred, including NAA, Glu, Gln, mI, and Tau in the striatum and SN. These changes could be involved in the initiation and development of PD pathogenesis.

NAA has been widely used as a marker of neuronal density as its concentration is reduced in cases of neuronal loss (Delli Pizzi et al., 2013). However, in this present study, we found that MPTP administration significantly elevated NAA in the striatum in induction PD day 1 and 7 mice, as well as in the SN in induction PD day 1 mice. Previously, we showed (Gao et al., 2013) that 6-OHDA rats showed a trend for increased NAA in the striatum. This present study went a step further and showed that NAA returned to normal levels in the striatum in induction PD day 21 mice by assessing metabolite changes at different time points during PD progression. The recovery of NAA was consistent with early studies in both people with PD and PD model animals (Lewis et al., 2012; Groger et al., 2013; Zhou et al., 2014). It is possible that temporary increase in NAA levels may be a consequence of the stress response to the drug or, more

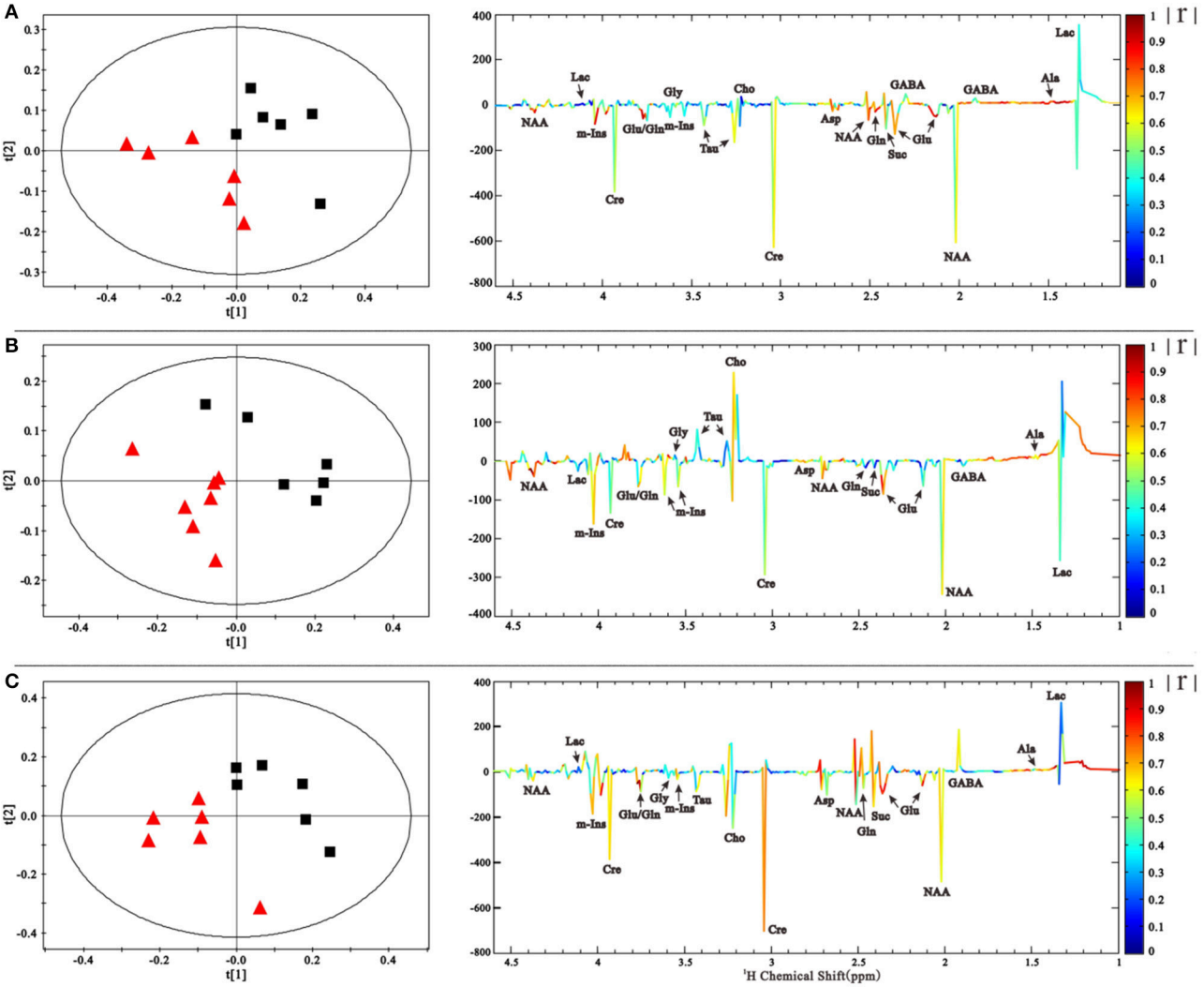

FIGURE 4 | PLS-DA scores plot based on the ^{1}H NMR spectra of the right striatum samples showed that PD group (▲) is clearly separated from control group (■) at 1, 7, and 21 days **(A–C)**. The coefficient-coded loading plots corresponding to PLS-DA revealed the metabolites with large intensities responsible for the discrimination of the corresponding score plots.

specifically, might compensate for the loss of dopaminergic neurons.

Glu is the major excitatory neurotransmitter in the mammalian central nervous system (CNS), which can be functionally invoked in virtually all activities of the nervous system (Lewerenz and Maher, 2015). In our present study, Glu levels in the striatum of induction PD day 1, 7, and 21 mice and the SN of induction PD day 1 mice were significantly increased compared with control rats. Similarly, our previous study also reported increased synthesis of Glu in the striatum of 6-OHDA rats (Gao et al., 2013). Both higher or lower levels of Glu can be noxious, as excessive Glu can stimulate activation of the N-methyl-D-aspartic acid (NMDA) receptor and induce excitatory toxicity (Grohm et al., 2012). In neurons, acute exposure to glutamate causes Parkin translocation to mitochondria in a calcium- and N-methyl-D-aspartate (NMDA) receptor-dependent manner, which disrupts some dynamic properties of mitochondria (Van Laar et al., 2015). Many studies in people with PD and animal models of PD have shown that mitochondrial dysfunction might be a defect that occurs early in the pathogenesis of PD (Subramaniam and Chesselet, 2013). Thus, we assume that the excitatory toxicity of Glu accumulation impairs mitochondrial function, and represents one of the potential metabolic mechanisms of PD.

GGC is one of the most important pathways involved in the metabolic coupling of astrocytes and neurons (Gallo and Ghiani, 2000). Changes in astrocyte-mediated GGC have been reported to be involved in the etiology of several neurodegenerative diseases, including epilepsy (Barker-Haliski and White, 2015), amyotrophic lateral sclerosis (ALS) (Sako et al., 2016), Alzheimer's disease (AD) (Chen et al., 2016), and Huntington's disease (HD) (Buren et al., 2016). Our present

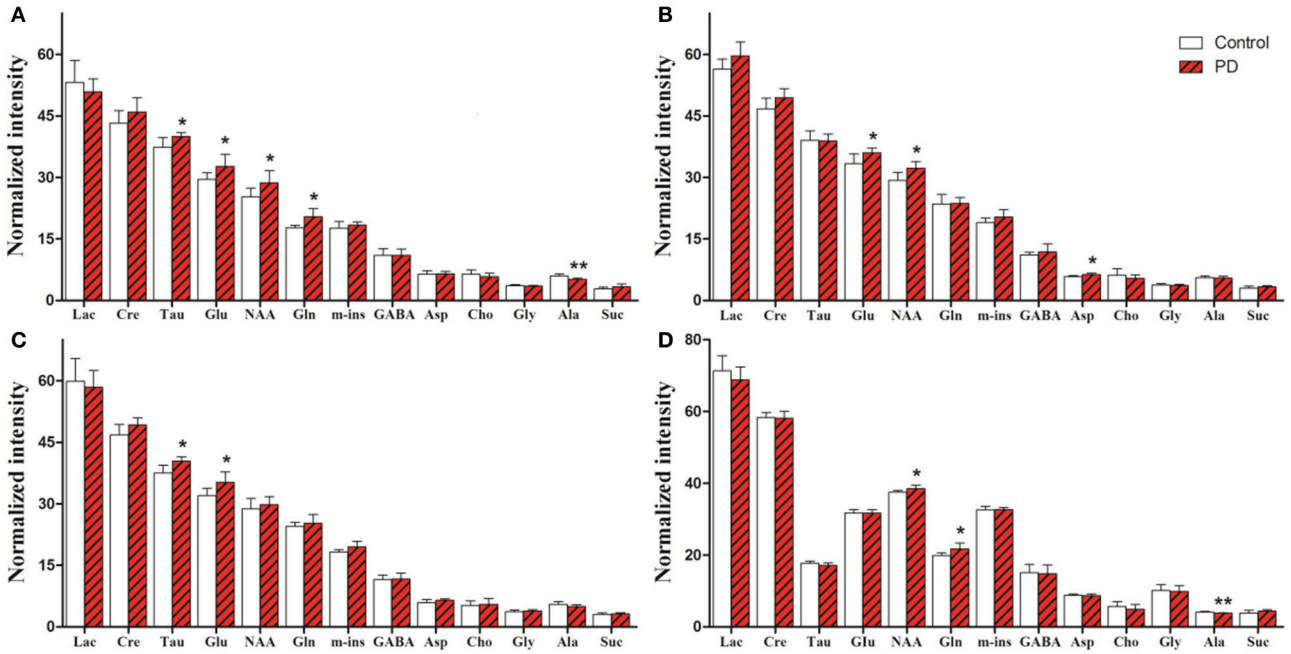

FIGURE 5 | Metabolic alterations obtained from the striatum of induction PD day 1, 7, 21 group **(A–C)** and the substantia nigra of induction PD day 1 group **(D)**, respectively. The results are expressed as mean ± *SD*, $^{*}p < 0.05$, $^{**}p < 0.01$.

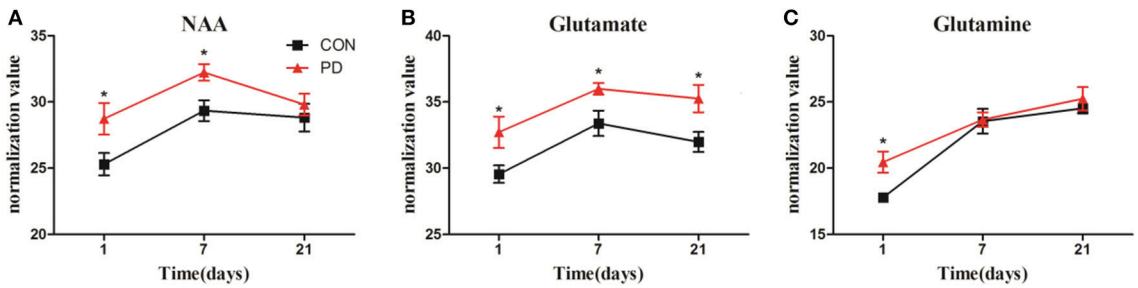

FIGURE 6 | Changes in the levels of NAA **(A)**, Glu **(B)**, and Gln **(C)** obtained from ^{1}H NMR spectra of right striatum samples collected from PD and control group of 1, 7, and 21 days after last administration. The results were expressed as means ± SD, $^{*}p < 0.05$.

findings showed that levels of Gln significantly increased in induction PD day 1 mice, while no significant change in Gln levels were observed in induction PD day 7 and 21 mice in the striatum or SN. Meanwhile, the cycle-related enzymes (i.e., both GLS and GS) in the subcortex were significantly increased. We, therefore, hypothesize that this phenomenon could serve as a temporary strategy to protect neurons from Glu excitotoxic injury after the injection of MPTP when the balance of the GGC was rapidly compromised, as Glu levels only increased in the striatum. Considering previous studies and our current measurements of metabolites and enzymes, we speculate that the GGC is involved in metabolism mechanisms related to PD, and could be a potential target in the treatment or prevention of neuron loss and/or motor function impairment in PD.

Myoinositol (MI), one of most abundant metabolites in the human brain, acts to maintain glial cell volumes as an osmolyte. Additionally, activated glia with enlarged cell volumes tends to have an elevated mI (Chang et al., 2013). Although there was no significant change in mI between the PD and control group mice, we found the normalized mI value was always slightly higher in the striatum of MPTP-induced PD mice, especially in induction PD day 21 mice ($p = 0.067$). This finding suggested that glia may be activated at later stages in the MPTP-induced Parkinsonism model, which is in accord with the opinion of Niranjan (2014) that a glial reaction participates in the cascade of events leading to neuronal degeneration in PD.

Tau is considered the major organic osmolyte, in addition to mI, that can regulate brain osmotic adaption (Lien et al., 1991). Our study showed that Tau is significantly elevated in the striatum and SN by MPTP in induction PD day 1 and 21 mice. Additionally, the changes in Tau

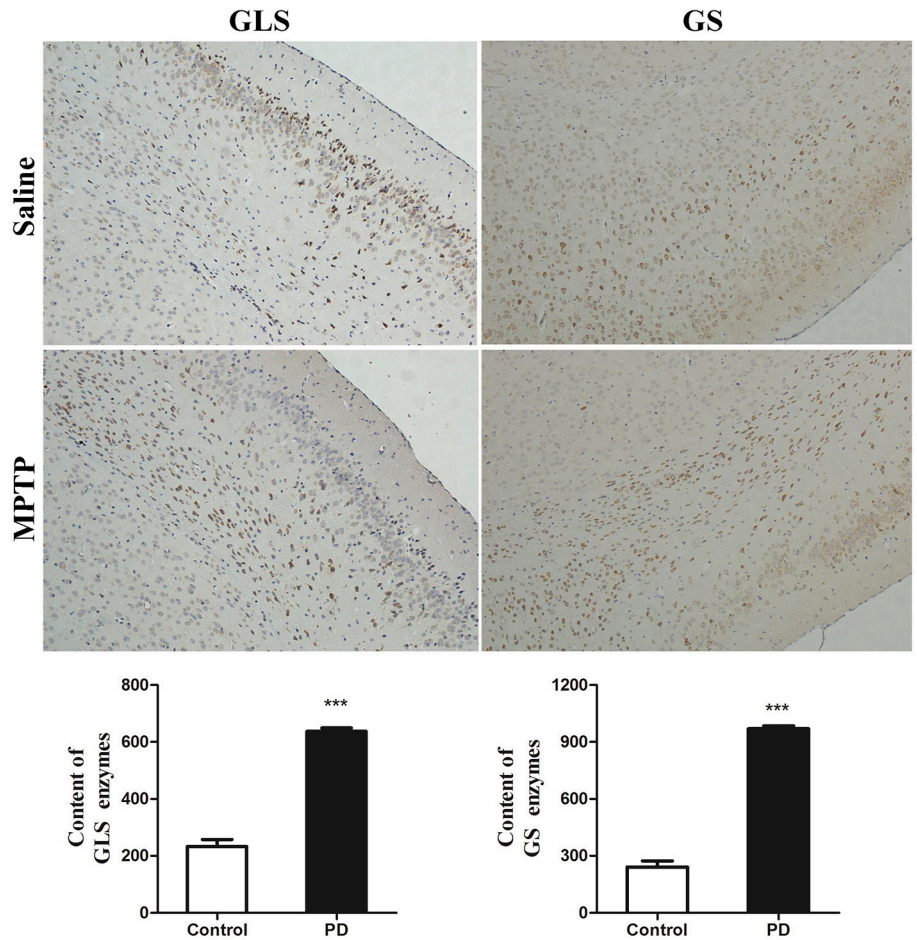

FIGURE 7 | Key enzymes were disturbed by MPTP in the disordered cycle of Glu-Gln-GABA. The deep dyed brown cytoplasm was represented as GLS and GS enzymes, by immunohistochemical staining. Content of GLS and GS enzymes were expressed as means ± SD, ***$p < 0.001$.

and mI indicated that osmolarity disorder occurs in the brain of PD mice. Furthermore, Tau was thought to have antioxidant properties and be able to reduce oxidative stress (Di Leo et al., 2004). These changes may represent a defense mechanism whereby increased Tau protects against the toxicity of MPTP, which can destroy the function of mitochondria and result in oxidative damage in the pathogenesis of PD.

Our study had several potential limitations for obtaining insights into the dynamic pathological mechanism leading to the development of PD. Indeed, people with PD at different severity levels would be the ideal subjects. However, the differentiation of these patients is not usually clinically feasible. In this present study, the MPTP mice model was used as an alternative to investigate changes in the metabolites underlying PD in a longitudinal study, from the initial to the final stages, which made it easy to control for the uniform state of disease. In addition, this present study adopted *in vitro* ^{1}H NMR for metabolomics analyses of mice brain, as it allowed for straightforward comparisons with the *in vivo* MRS results. Further work will be required to confirm whether these dynamic alterations of metabolism occur in the brains of people with PD, from the proximal to the distal stages, using *in vivo* MRS.

In conclusion, our results demonstrate that the neuron loss and motor function impairment related with PD might be linked to an overactive GGC and altered membrane metabolism. The increased Glu, accompanied by an overactive GGC, can induce excitatory toxicity and impaired mitochondrial function in the brain, which may be strongly associated with the pathogenesis of PD. The change in NAA was more likely to have occurred to compensate for the loss of dopaminergic neurons. In addition, altered osmolality and activated glia may also be involved in the mechanism driving the onset of PD, as reflected by the changes in mI and Tau. Notably, more evidence is needed to identify the exact mechanisms involved that lead to the observed changes in Glu, Gln, and GABA concentrations, and to test those metabolites as novel therapeutic targets to arrest or ameliorate PD progression.

MATERIALS AND METHODS

Animals

Male C57BL/6 mice (the SLAC Laboratory Animal Co. Ltd. Shanghai, China), weighing between 20 and 26 g, were housed 5 per cage under the standard laboratory conditions (controlled temperature/humidity condition, a normal 12/12-h light/dark schedule with the lights on at 08:00 a.m.). They were given free access to standard chow and water during whole experimental process. All animal handling and surgery were performed in accordance with standard animal protection guidelines and were approved by the Institutional Animal Care and Use Committee of Wenzhou Medical College (wydw2016-0128).

Preparation and Treatment

After adapting to the environment for a week, 60 mice were randomly divided into control and PD groups. Mice in PD groups were injected intraperitoneally (i.p.) 30 mg/kg MPTP-HCl (M0896, Sigma-Aldrich) daily for 5 consecutive days (Jackson-Lewis and Przedborski, 2007), while the mice in control group received equal volume of normal saline. At 1, 7, and 21 days after the last injection, the mice were sacrificed and samples were harvested immediately. All brain tissues were frozen using liquid nitrogen and stored at −80°C until analysis.

Behavioral Test

Open-field test was performed to evaluate locomotor activity when mice were exposed to the novel environment. Standard protocol was conducted in a dark sound-attenuating apparatus to avoid outside interference. Activity was limited in the test chamber (25 × 25 × 45 cm) with white smooth floor divided by black lines into 16 equal squares 4 × 4. Behavior test was carried out between 19:00 and 21:00. Mice from control 21 day and induction PD day 21 groups were gently placed in the center of the chamber and allowed to move freely for 5 min. The total distance traveled, number of activity, activity time and immobility time were analyzed using an automated video tracking system DigBehv Animal Behavior Video-tracking System (Shanghai Jiliang Software Technology Co. Ltd. China) (Jing et al., 2011).

Immunohistochemical Staining

Three mice of subgroup were processed for immunohistochemical studies. The brains were carefully removed and serial coronal sections (5 μm) of striatum and substantia nigra (SN) were mounted on slides. The stained was handled in accordance with the instruction of immunohistochemical Kit (KIT-9710, Fuzhou Maixin Biotech. Co. Ltd. Fujian, China). Primary antibodies were: Tyrosine Hydroxylase (TH, as marker of DA terminals, 1:750, ab112, abcam), Glutaminase (GS, 1:50, ab156876, abcam), and Glutamine synthetase (GLS, 1:50, SCB). Images were obtained and analyzed using a fluorescence microscope (Nikon, Tokyo, Japan). Control sections in which primary antibodies or secondary antibodies were omitted showed no labeled cells.

Sample Preparation

Mice were sacrificed by decapitation, specimens of mesencephalon and bilateral striatum were dissected rapidly, snap-frozen in liquid nitrogen, and stored at −80°C until analysis. The metabolite extraction was referred to our previous method (ref). The frozen tissues were weighed into an Eppendorf tube. Following the homogenization by electric homogenizer with ice-cold methanol (4.0 mL/g) and ultrapure water (0.85 mL/g; (Beckonert et al., 2007)), the mixture was homogenized again with 2 mL/g of chloroform and 0.85 mL/g of ultrapure water using a vortex mixer, placed on ice for 15 min, and centrifuged at 10,000 g for 15 min at 4°C. Finally, the supernatant was carefully transferred into a new Eppendorf tube, lyophilized for 24 h, and stored at −80°C until NMR analysis.

NMR Spectroscopy

The lyophilized extract was redissolved in 0.5 mL of D_2O containing 0.2 mM of TSP for NMR spectroscopy. D_2O provided a field-frequency lock, and TSP was used as the chemical shift reference. ^{1}H NMR spectra was acquired on a Bruker AVANCE III 600 MHz NMR spectrometer with a 5-mm TXI probe (Bruker BioSpin, Rheinstetten, Germany) at 298 K. The one-dimensional 1H NMR spectra of right striatum and SN were acquired using a standard single-pulse sequence with water signal presaturation (ZGPR). The acquisition time was 2.65 s per scan, and an additional 6 s relaxation delay was used to ensure full relaxation 128 transients were collected into 64 K data points with a spectral width of 12,000 Hz.

Data Processing of NMR Spectra and Multivariate Pattern Recognition

In all NMR spectra, the phase and baseline were corrected manually and referenced to the chemical shift of the methyl peak of lactate (CH_3, 1.33 ppm) using Topspin (v2.1 pl4, Bruker Biospin, Germany). The spectra (5.90–4.50 ppm) containing the residual peak from the suppressed water resonance was set to the zero integral in the analysis. The remaining spectral segments were normalized to the total sum of the spectral intensity to partially compensate for differences in concentration of the many metabolites in the samples. Then spectra (0.5–10.0 ppm) were data-reduced to 1,100 integrated regions of 0.01 ppm width for multivariate pattern recognition analysis by SIMCA-P+ 12.0 software (Umetrics, Umea, Sweden).The supervised projection to latent structure discriminant analysis, Partial least squares-discriminant analysis (PLS-DA), was carried out for classifying the samples according to their common spectral characteristics as described previously (Liu et al., 2013). And another data-reduced to 7,334 integrated regions of 0.0015 ppm width corresponding to the region of δ 10 to 0.5 for quantitative analysis.

Statistical Analysis

Metabolite intensities relative to the sum of the total spectral integral among groups were calculated. Repeated measures ANOVA were used to compare the data from control and PD mice at different time points. For statistical comparison between two groups, Independent sample *t*-test was used. Statistical analyses were performed using SPSS (version 22, IBM, USA). The

normality was assessed by the Kolmogorov–Smirnov test. Data are expressed as mean ± SE, and a significance level of 0.05 was used.

AUTHOR CONTRIBUTIONS

YL and XZ data collection, statistical analyses and the initial draft of the manuscript. LP, KL and GB performed the experiments and reviewed the manuscript. LZ, CY, and CL contributed to the data discussion, and edited the manuscript. HG and ZY are the guarantors of this work and, as such, had full access to all the data in the study and takes responsibility for the integrity of the data and the accuracy of the data analysis.

ACKNOWLEDGMENTS

This work was supported by the National Natural Science Foundation of China (Nos. 81771386, 21575105, 81400863, 81171306), and the Natural Science Foundation of Zhejiang Provincial (Nos. LY14H090014, LY15H180010, and LY16H180009).

REFERENCES

Barker-Haliski, M., and White, H. S. (2015). Glutamatergic mechanisms associated with seizures and epilepsy. *Cold Spring Harb. Perspect. Med.* 5:a022863. doi: 10.1101/cshperspect.a022863

Beckonert, O., Keun, H. C., Ebbels, T. M. D., Bundy, J. G., Holmes, E., Lindon, J. C., et al. (2007). Metabolic profiling, metabolomic and metabonomic procedures for NMR spectroscopy of urine, plasma, serum and tissue extracts. *Nat. Protoc.* 2, 2692–2703. doi: 10.1038/nprot.2007.376

Bogdanov, M., Matson, W. R., Wang, L., Matson, T., Saunders-Pullman, R., Bressman, S. S., et al. (2008). Metabolomic profiling to develop blood biomarkers for Parkinson's disease. *Brain* 131(Pt 2), 389–396. doi: 10.1093/brain/awm304

Buren, C., Parsons, M. P., Smith-Dijak, A., and Raymond, L. A. (2016). Impaired development of cortico-striatal synaptic connectivity in a cell culture model of Huntington's disease. *Neurobiol. Dis.* 87, 80–90. doi: 10.1016/j.nbd.2015.12.009

Chang, L. D., Munsaka, S. M., Kraft-Terry, S., and Ernst, T. (2013). Magnetic resonance spectroscopy to assess neuroinflammation and neuropathic pain. *J. Neuroimmune Pharmacol.* 8, 576–593. doi: 10.1007/s11481-013-9460-x

Chen, S. Q., Cai, Q., Shen, Y. Y., Xu, C. X., Zhou, H., and Zhao, Z. (2016). Hydrogen proton magnetic resonance spectroscopy in multidomain amnestic mild cognitive impairment and vascular cognitive impairment without dementia. *Am. J. Alzheimers Dis. Other Demen.* 31, 422–429. doi: 10.1177/1533317515628052

Chitty, K. M., Lagopoulos, J., Hickie, I. B., and Hermens, D. F. (2015). Hippocampal glutamatergic/NMDA receptor functioning in bipolar disorder: a study combining mismatch negativity and proton magnetic resonance spectroscopy. *Psychiatry Res.* 233, 88–94. doi: 10.1016/j.pscychresns.2015.05.002

Dawson, T. M., and Dawson, V. L. (2003). Molecular pathways of neurodegeneration in Parkinson's disease. *Science* 302, 819–822. doi: 10.1126/science.1087753

Delli Pizzi, S., Rossi, C., Di Matteo, V., Esposito, E., Guarnieri, S., Mariggio, M. A., et al. (2013). Morphological and metabolic changes in the nigro-striatal pathway of synthetic proteasome inhibitor (PSI)-treated rats: a MRI and MRS study. *PLoS ONE* 8:e56501. doi: 10.1371/journal.pone.0056501

Di Leo, M. A., Santini, S. A., Silveri, N. G., Giardina, B., Franconi, F., and Ghirlanda, G. (2004). Long-term taurine supplementation reduces mortality rate in streptozotocin-induced diabetic rats. *Amino Acids* 27, 187–191. doi: 10.1007/s00726-004-0108-2

Fasano, A., Daniele, A., and Albanese, A. (2012). Treatment of motor and non-motor features of Parkinson's disease with deep brain stimulation. *Lancet Neurol.* 11, 429–442. doi: 10.1016/S1474-4422(12)70049-2

Gallo, V., and Ghiani, C. A. (2000). Glutamate receptors in glia: new cells, new inputs and new functions. *Trends Pharmacol. Sci.* 21, 252–258. doi: 10.1016/S0165-6147(00)01494-2

Gao, H., Xiang, Y., Sun, N., Zhu, H., Wang, Y., Liu, M., et al. (2007). Metabolic changes in rat prefrontal cortex and hippocampus induced by chronic morphine treatment studied *ex vivo* by high resolution 1H NMR spectroscopy. *Neurochem. Int.* 50, 386–394. doi: 10.1016/j.neuint.2006.09.012

Gao, H. C., Zhu, H., Song, C. Y., Lin, L., Xiang, Y., Yan, Z. H., et al. (2013). Metabolic changes detected by *ex vivo* high resolution 1H NMR spectroscopy in the striatum of 6-OHDA-induced Parkinson's rat. *Mol. Neurobiol.* 47, 123–130. doi: 10.1007/s12035-012-8336-z

Groger, A., Bender, B., Wurster, I., Chadzynski, G. L., Klose, U., and Berg, D. (2013). Differentiation between idiopathic and atypical parkinsonian syndromes using three-dimensional magnetic resonance spectroscopic imaging. *J. Neurol. Neurosurg. Psychiatry* 84, 644–649. doi: 10.1136/jnnp-2012-302699

Grohm, J., Kim, S. W., Mamrak, U., Tobaben, S., Cassidy-Stone, A., Nunnari, J., et al. (2012). Inhibition of Drp1 provides neuroprotection *in vitro* and *in vivo*. *Cell Death Differ.* 19, 1446–1458. doi: 10.1038/cdd.2012.18

Hatano, T., Saiki, S., Okuzumi, A., Mohney, R. P., and Hattori, N. (2016). Identification of novel biomarkers for Parkinson's disease by metabolomic technologies. *J. Neurol. Neurosurg. Psychiatry* 87, 295–301. doi: 10.1136/jnnp-2014-309676

Hertz, L., Dringen, R., Schousboe, A., and Robinson, S. R. (1999). Astrocytes: glutamate producers for neurons. *J. Neurosci. Res.* 57, 417–428. doi: 10.1002/(SICI)1097-4547(19990815)57:4<417::AID-JNR1>3.0.CO;2-N

Jackson-Lewis, V., and Przedborski, S. (2007). Protocol for the MPTP mouse model of Parkinson's disease. *Nat. Protoc.* 2, 141–151. doi: 10.1038/nprot.2006.342

Jing, L., Luo, J., Zhang, M., Qin, W. J., Li, Y. L., Liu, Q., et al. (2011). Effect of the histone deacetylase inhibitors on behavioural sensitization to a single morphine exposure in mice. *Neurosci. Lett.* 494, 169–173. doi: 10.1016/j.neulet.2011.03.005

Kalia, L. V., and Lang, A. E. (2015). Parkinson's disease. *Lancet* 386, 896–912. doi: 10.1016/S0140-6736(14)61393-3

Lei, S., and Powers, R. (2013). NMR metabolomics analysis of Parkinson's Disease. *Curr. Metab.* 1, 191–209. doi: 10.2174/2213235X113019990004

Lewerenz, J., and Maher, P. (2015). Chronic glutamate toxicity in neurodegenerative diseases-what is the evidence? *Front. Neurosci.* 9:469. doi: 10.3389/fnins.2015.00469

Lewis, S. J., Shine, J. M., Duffy, S., Halliday, G., and Naismith, S. L. (2012). Anterior cingulate integrity: executive and neuropsychiatric features in Parkinson's disease. *Mov. Disord.* 27, 1262–1267. doi: 10.1002/mds.25104

Lien, Y. H., Shapiro, J. I., and Chan, L. (1991). Study of brain electrolytes and organic osmolytes during correction of chronic hyponatremia. Implications for the pathogenesis of central pontine myelinolysis. *J. Clin. Invest.* 88, 303–309. doi: 10.1172/JCI115292

Liu, K., Ye, X. J., Hu, W. Y., Zhang, G. Y., Bai, G. H., Zhao, L. C., et al. (2013). Neurochemical changes in the rat occipital cortex and hippocampus after repetitive and profound hypoglycemia during the neonatal period: an *ex vivo* H-1 magnetic resonance spectroscopy study. *Mol. Neurobiol.* 48, 729–736. doi: 10.1007/s12035-013-8446-2

Ma, Y., Johnston, T. H., Peng, S., Zuo, C., Koprich, J. B., Fox, S. H., et al. (2015). Reproducibility of a Parkinsonism-related metabolic brain network in non-human primates: a descriptive pilot study with FDG PET. *Mov. Disord.* 30, 1283–1288. doi: 10.1002/mds.26302

Nagy, C. L., Bernard, M. A., and Hodes, R. J. (2012). National institute on aging at middle ageuits past, present, and future. *J. Am. Geriatr. Soc.* 60, 1165–1169. doi: 10.1111/j.1532-5415.2012.03994.x

Niranjan, R. (2014). The role of inflammatory and oxidative stress mechanisms in the pathogenesis of Parkinson's Disease: focus on astrocytes. *Mol. Neurobiol.* 49, 28–38. doi: 10.1007/s12035-013-8483-x

Sako, W., Abe, T., Izumi, Y., Harada, M., and Kaji, R. (2016). The ratio of N-acetyl aspartate to glutamate correlates with disease duration of amyotrophic lateral sclerosis. *J. Clin. Neurosci.* 27, 110–113. doi: 10.1016/j.jocn.2015.08.044

Smith, M. L., King, J., Dent, L., Mackey, V., Muthian, G., Griffin, B., et al. (2014). Effects of acute and sub-chronic L-dopa therapy on striatal L-dopa methylation and dopamine oxidation in an MPTP mouse model of Parkinsons disease. *Life Sci.* 110, 1–7. doi: 10.1016/j.lfs.2014.05.014

Subramaniam, S. R., and Chesselet, M. F. (2013). Mitochondrial dysfunction and oxidative stress in Parkinson's disease. *Prog. Neurobiol.* 106, 17–32. doi: 10.1016/j.pneurobio.2013.04.004

Van Laar, V. S., Roy, N., Liu, A., Rajprohat, S., Arnold, B., Dukes, A. A., et al. (2015). Glutamate excitotoxicity in neurons triggers mitochondrial and endoplasmic reticulum accumulation of Parkin, and, in the presence of N-acetyl cysteine, mitophagy. *Neurobiol. Dis.* 74, 180–193. doi: 10.1016/j.nbd.2014.11.015

Wen, P., Li, M., Xiao, H., Ding, R., Chen, H., Chang, J., et al. (2015). Low-frequency stimulation of the pedunculopontine nucleus affects gait and the neurotransmitter level in the ventrolateral thalamic nucleus in 6-OHDA Parkinsonian rats. *Neurosci. Lett.* 600, 62–68. doi: 10.1016/j.neulet.2015.06.006

Zhang, Z., Zeng, Q., Liu, Y., Li, C., Feng, D., and Wang, J. (2014). Assessment of the intrinsic radiosensitivity of glioma cells and monitoring of metabolite ratio changes after irradiation by 14. 7-T high-resolution (1)H MRS. *NMR Biomed.* 27, 547–552. doi: 10.1002/nbm.3091

Zheng, H., Zhao, L., Xia, H., Xu, C., Wang, D., Liu, K., et al. (2015). NMR-based metabolomics reveal a recovery from metabolic changes in the striatum of 6-OHDA-induced rats treated with basic fibroblast growth factor. *Mol. Neurobiol.* 53, 6690–6697. doi: 10.1007/s12035-015-9579-2

Zhou, B., Yuan, F. Z., He, Z., and Tan, C. L. (2014). Application of proton magnetic resonance spectroscopy on substantia nigra metabolites in Parkinson's disease. *Brain Imaging Behav.* 8, 97–101. doi: 10.1007/s11682-013-9251-2

Conflict of Interest Statement: The authors declare that the research was conducted in the absence of any commercial or financial relationships that could be construed as a potential conflict of interest.

frontiers in Neurology

ORIGINAL RESEARCH
published: 03 July 2018
doi: 10.3389/fneur.2018.00496

Predictive Factors for Early Initiation of Artificial Feeding in Patients With Sporadic Creutzfeldt-Jakob Disease

*Pei-Chen Hsieh, Han-Tao Li, Chun-Wei Chang, Yih-Ru Wu and Hung-Chou Kuo**

Department of Neurology, Linkou Chang Gung Memorial Hospital, College of Medicine, Chang Gung University, Taipei, Taiwan

Background: Akinetic mutism has often been used as the predictor of sporadic Creutzfeldt-Jacob disease (sCJD) endpoints, but it may be difficult for general physcians to assess. Nasogastric (NG) tube insertion is indicated for many neurodegenerative diseases with a clinical course of swallowing failure, and can be more easily identified than akinetic mutism by general physicians. Therefore, the aim of this study was to identify whether there are predictive factors for early initiation of artificial feeding in patients with sCJD who require enteral nutrition due to swallowing failure.

Methods: We retrospectively reviewed the medical records of all patients diagnosed with probable sCJD who were admitted to the neurology ward at a medical center in Taiwan from January 2002 to July 2017. We used Pearson's chi-squared test to detect the correlation of initial symptoms, neurological signs, brain magnetic resonance imaging (MRI), electroencephalography (EEG), and increased levels of 14-3-3 protein in cerebrospinal fluid (CSF) analysis. The Cox proportional hazards model was used to detect prognostic factors for early initiation of NG tube insertion in sCJD patients.

Results: The onset age ranged from 51 to 83 years, and mostly ranged from 60 to 79 years. Akinetic mutism was correlated with pyramidal tract signs, myoclonus, and extrapyramidal signs. Furthermore, myoclonus was revealed to be associated with pyramidal tract signs. Multivariate Cox regression analysis showed that myoclonus and elevated CSF levels of 14-3-3 protein are predictive of early NG insertion.

Conclusions: Increased levels of 14-3-3 protein in CSF and the presence of myoclonus at diagnosis are predictive of early swallowing difficulty and indicate rapid deterioration in probable sCJD. In addition to akinetic mutism, early initiation of artificial feeding can be used to predict early deterioration in sCJD.

Keywords: creutzfeldt-jakob disease, artificial feeding, pognosis, myoclonus, akinetic mutism

OPEN ACCESS

Edited by:
Chaur-Jong Hu,
Taipei Medical University, Taiwan

Reviewed by:
Chien Tai Hong,
Taipei Medical University, Taiwan
Xifei Yang,
Shenzhen Center for Disease Control and Prevention, China

****Correspondence:***
Hung-Chou Kuo
kuo0426@adm.cgmh.org.tw

Specialty section:
This article was submitted to Neurodegeneration, a section of the journal Frontiers in Neurology

Received: *16 January 2018*
Accepted: *07 June 2018*
Published: *03 July 2018*

Citation:
Hsieh P-C, Li H-T, Chang C-W, Wu Y-R and Kuo H-C (2018) Predictive Factors for Early Initiation of Artificial Feeding in Patients With Sporadic Creutzfeldt-Jakob Disease. Front. Neurol. 9:496. doi: 10.3389/fneur.2018.00496

INTRODUCTION

The annual global incidence rate of sporadic Creutzfeldt-Jakob disease (sCJD) is approximately 1–1.5 cases per million people (1). In Taiwan, the incidence rate is 0.55 cases per million people per year. The pathogenesis of sCJD remains unclear. There are variable clinical symptoms and signs in sCJD. The median survival duration for patients with sCJD is 4–6 months (2, 3), but Asian populations may have longer survival (4, 5). Longer survival has been associated with younger age, female gender, absence of CSF 14-3-3 protein and type 2a prion protein,

sharp-wave complexes on EEG, and MV form in codon 129 PRNP human gene (6, 7). Survival has been found to be prolonged in patients who received tube feeding after they reached the state of akinetic mutism (8).

Our patients were genotyped at codon 129 of the PRNP gene and all were methionine homozygotes (MM) from 1998 to 2007, and the type was referred to as myoclonic type of sCJD (5, 9). sCJD is a rapidly progressive dementia that leads to decreased level of consciousness and cortical impairment which causes unsafe swallowing. The use of a nasogastric (NG) tube is a risk factor for mortality in advanced dementia (10–12). The initiation of artificial feeding indicates that patients have lost the ability to perform activities of daily living (ADL) and the disease has progressed to the final stage (13, 14). Although other studies have used akinetic mutism as the predictor for sCJD endpoints, it is difficult for general physicians to assess in patients whose consciousness level is impaired (4, 15, 16). Dysphagia is used for prognosis in spinal and bulbar muscular atrophy but there is a lack of reliable clinical markers for dysphagia assessment (17–19). The requirement for initiation of feeding tube insertion is easier to identify than detection of swallowing failure by a general physician or even a caregiver.

Although tube feeding may prolong survival in sCJD, the initiation time of artificial feeding may be a more suitable endpoint than akinetic mutism. Therefore, the goal of this study was to determine if there are predictive factors for early NG tube feeding.

METHODS

We retrospectively reviewed the medical charts of all patients diagnosed with probable sCJD and admitted to the neurology ward from January 2002 to July 2017 at Chang Gung Memorial Hospital. All of the cases were submitted by physicians who diagnose sCJD and were reviewed by the neurology, neuroradiology, and neuropathology experts of the CJD Surveillance Unit (CJDSU) at the Taiwan Neurological Society. We had a total of 35 probable sCJD patients. We included patients whose initial symptoms occurred within 2 months of admission and who could have a neurological examination with a Glasgow coma scale (GCS) score of 15 out of 15. We excluded a patient who had a history of progressive supranuclear palsy that made it difficult to identify initial neurological symptoms. Data were collected at baseline included gender, age, time of admission, cerebrospinal fluid (CSF) with 14-3-3 proteins, presence of high signal on diffusion-weighted images of magnetic resonance imaging (MRI), periodic sharp wave complex (PSWC) in electroencephalography (EEG) findings, NG tube insertion time, initial presentation, and abnormal neurological examination at admission. Results of CSF 14-3-3 protein assay data were obtained through collaboration with the Taiwan Prion Disease Pathology Surveillance Center. Clinical signs and symptoms that were assessed by neurologists included cognitive impairment (memory impairment, visual spatial dysfunction, apraxia, aphasia, and akinetic mutism), visual disturbance (visual field defect, visual hallucination, complex visual disturbance), cerebellar disturbance (ataxic gait, limbs dysmetria), pyramidal dysfunction (hemiparesis, spasticity, hyperreflexia, positive Babinski sign), extrapyramidal dysfunction (rigidity, bradykinesia, dystonia, dyskinesia), myoclonus, and seizure. NG tube insertion was performed when a patient was assessed by a clinical physician as having decreased level of consciousness or severe cognitive impairment that caused poor intake. The date of NG insertion was recorded according to medical record. The protocol was approved by the institutional review board of Chang Gung Memorial Hospital (IRB No.: 201701320B0).

Statistical Analysis

The time from admission to NG insertion of all patients were compared with age, sex, neurological signs, the elevation of CSF 14-3-3 protein, and brain MRI findings. Four patients did not have the records of NG insertion times because of loss to follow-up. We used Pearson's test was used to estimate the correlation of initial symptoms, clinical neurological signs, MRI image findings, and 14-3-3 proteins in CSF. For the cumulative incidence of NG tube insertion, the Kaplan–Meier method was used for overall analysis and each of the above features was stratified. The Cox proportional hazards model was used to identify the prognostic factors for the duration from onset to

TABLE 1 | Baseline demographic and clinical characteristics of sCJD patients.

Patients with sCJD	***n* = 30**	**(%)**
SEX		
Female	12	43
Male	18	57
Age of Onset ± SD (year)	67.7 ± 9.3	
Median (year)	68.5	
Range (year)	51-83	
AGE AT DIAGNOSIS (YEAR)		
40–49	0	
50–59	6	20
60–69	12	40
70–79	9	28
80–89	3	10
Initial symptom to admission ± SD (day)	27.5 ± 12	
CLINICAL MANIFESTATIONS AT DISEASE ONSET (%)		
Cognitive impairment	10	33
Visual disturbance	11	37
Gait disturbance	11	37
Speech disturbance	8	27
Increased 14-3-3 protein in CSF (%)	22/30	73
PSWC in Initial EEG (%)	10/30	33
BRAIN MRI FINDINGS		
Cortical involvement	14/30	47
Cortical and basal ganglia involvement	16/30	53

CSF, Cerebrospinal fluid; EEG, electroencephalography; MRI, magnetic resonance imaging; PSWC, periodic sharp wave complex; sCJD, sporadic Creutzfeldt-Jakob disease.

NG tube dependence, and the backward selection method in multivariate analysis was used to assess the independent effects of the investigated factors. Statistical significance was selected using the selection method at $P < 0.05$ in univariate regression analyses**.** We used the Wald test to estimate hazard ratios (HRs) and 95% confidence intervals (CIs), and we used Pearson's chi-squared test to detect the correlation of neurological signs at admission, imaging findings, 14-3-3 proteins in CSF, and initial PSWC on EEG. Statistical analyses were performed using SPSS version 22.

RESULTS

Thirty patients with probable sCJD admitted from January 2002 to July 2017 were included in the study. Basic characteristics are summarized in **Table 1**. The onset age ranged from 51 to 83 years, and mostly ranged from 60 to 79 years. The median age at diagnosis was 68.5 years. Female patients accounted for 43% of the patients in this study. Increased levels of CSF 14-3-3 protein were found in 22 of 30 patients. The PSWC of initial EEG was 33%. Among all patients, 47% had the characteristic brain MRI findings indicating cortical ribbon signs and 53% had the MRI findings indicating both cortical and basal ganglia involvement (**Table 1**). The initial symptoms of cognitive impairment, visual disturbance, unsteadiness, and speech disturbance were present in 43, 37, 37, and 27% of the patients, respectively. The most common neurological sign during admission was visual spatial dysfunction, which was followed by myoclonus and cerebellar and extrapyramidal dysfunction (**Figure 1**).

Correlations Among Variables at Diagnosis

The Pearson's x^2 test was used to assess correlation between neurological signs and variables, and the variables included basal ganglia and cortical involvement on brain MRI, PSWC on initial EEG, increased 14-3-3 protein in CSF, sex, and age. In addition, the neurological signs were also compared with each other. Both basal ganglia and cortical involvement on brain MRI were significantly correlated with akinetic mutism ($P <$ 0.01). Akinetic mutism was correlated with abnormal pyramidal and extrapyramidal signs and myoclonus. Furthermore, myoclonus was associated with pyramidal tract signs. **Figure 2** shows correlations between investigative tests and neurological signs and between variables at diagnosis. An

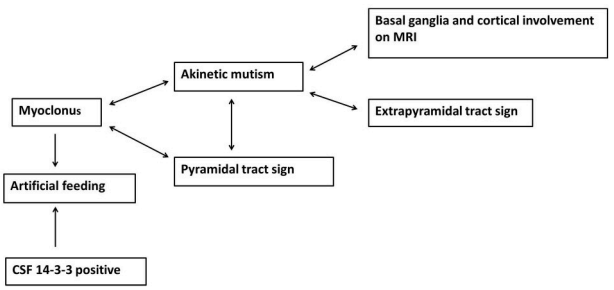

FIGURE 2 | The association between neurological signs and brain MRI findings as well as myoclonus and detectable 14-3-3 protein in CSF leading to early artificial feeding in sporadic Creutzfeldt-Jakob disease.

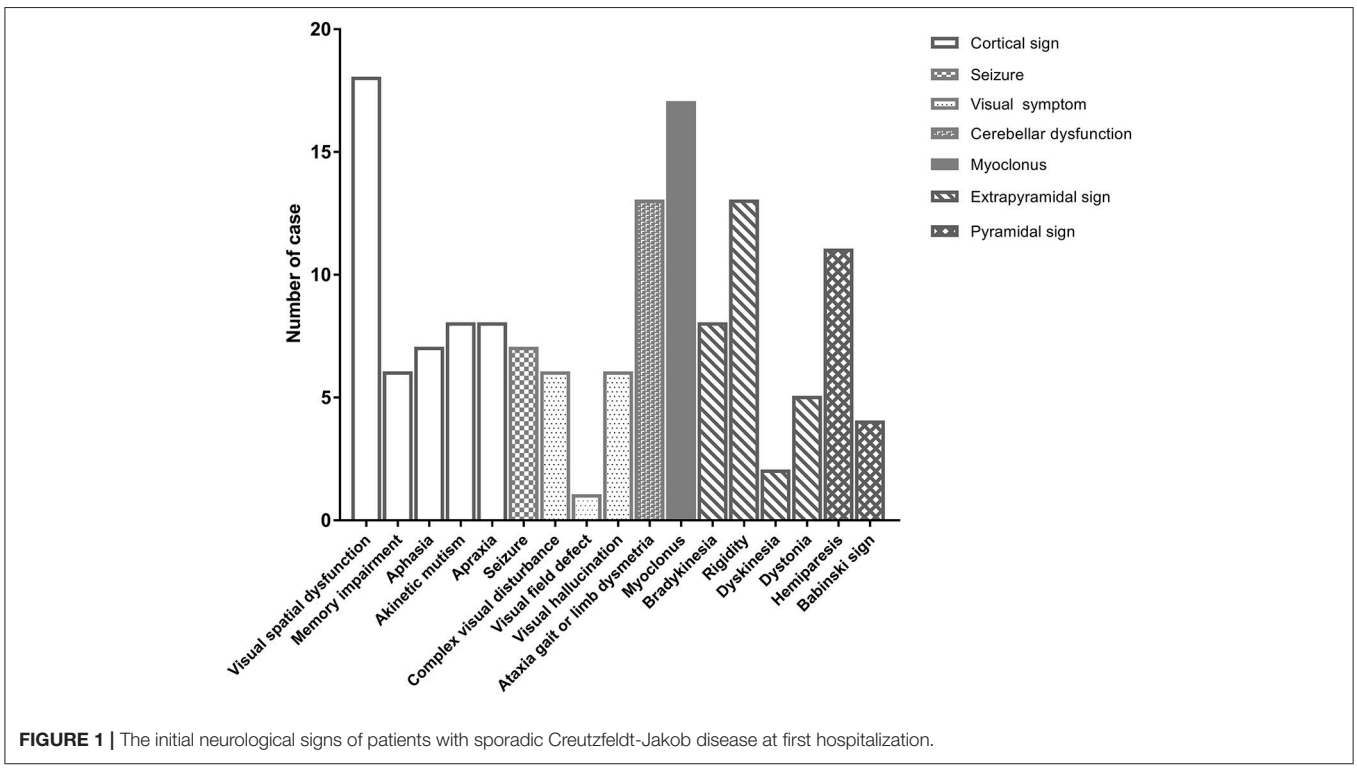

FIGURE 1 | The initial neurological signs of patients with sporadic Creutzfeldt-Jakob disease at first hospitalization.

association was revealed between myoclonus, akinetic mutism, and pyramidal tract dysfunction. Furthermore, myoclonus and detectable CSF 14-3-3 protein might lead to early use of artificial feeding.

Relationships Between Clinical Signs and Symptoms and NG Tube Insertion Time

The median time of NG tube insertion was 46.4 days after the onset of the initial symptom. **Table 2** shows a univariate Cox regression analysis of gender, age, PSWC in EEG, MRI with both basal ganglia and cortical involvement, elevation of CSF 14-3-3 protein, and neurological signs during initial hospitalization. The result demonstrated significant differences in the CSF 14-3-3 protein, myoclonus, pyramidal dysfunction, extrapyramidal dysfunction, and akinetic mutism. These were attributed to NG tube insertion. Patients with increased 14-3-3 protein in CSF were found to have 6.5 times higher risk of early NG tube insertion. No significant differences were found in the characteristic findings of sCJD on EEG and brain MRI with both cortex and basal ganglia involvement. The median periods from first hospitalization to NG tube insertion in myoclonus and CSF analysis were 10 and 19 days, respectively. **Figure 3** shows the cumulative incidences of artificial feeding in sCJD patients with (3A) myoclonus and (3B) 14-3-3 protein in CSF.

DISCUSSION

Swallowing requires coordination of multiple bulbar muscles and relatively clear consciousness (14). NG tube insertion is globally used for many neurological patients who suffer from swallowing failure and poor nutrition, and swallowing failure indicates that the patient's condition has reached the end of life in many neurodegenerative diseases (13). Therefore, NG tube feeding is a predictive factor of mortality in advanced dementia (12). On the other hand, feeding tube insertion increases the survival of CJD patients due to better supportive care (8).

Creutzfeldt-Jacob disease is a prion disease that can present as irreversible rapidly progressive dementia, accompanied by myoclonus, pyramidal tract, extrapyramidal tract, or cerebellar involvement (20). Most of the patients with decreased level of consciousness or severe cognitive dysfunction need NG tube feeding for nutrition support during disease progression. In Chinese culture and Taiwan's health insurance system, the majority of patients receive intensive life-sustaining treatment, and some even continue the treatment until there is irreversible advanced neurological disorder. Unlike akinetic mutism, NG tube insertion makes it easier for clinical physicians to detect patients with severe neurodegenerative disease. Furthermore, the time until death of patients with NG tube feeding can be influenced by underlying comorbidities such as aspiration pneumonia or other infectious diseases. NG tube insertion caused by swallowing failure is an early sign of poor outcome in patients with dementia syndromes. Increased 14-3-3 protein in CSF has been considered as an indicator of rapid neuronal damage (7). Our study found that the presence of myoclonus and elevated levels of CSF 14-3-3 protein led to a rapid deterioration of the patient's condition and the consequent need for enteral nutrition. According to Nakatani et al. akinetic mutism is the neurological symptom of sCJD endpoint. Cerebellar disturbance and psychiatric symptoms increase the risk of akinetic mutism. Myoclonus is a potential contributing factor of akinetic mutism and exercise-induced seizures, and myoclonus and myoclonic seizures are associated with pyramidal dysfunction (16). In our study, akinetic mutism was associated

TABLE 2 | Univariate and multivariate regression analyses of the day of nasogastric tube insertion.

Variables	HR	Univariate *P*-value	95% CI		HR	Multivariate *P*-value	95% CI	
			Lower	Upper			Lower	Upper
Gender: male	1.29	0.539	0.574	2.887				
Age at diagnosis > 65 (years)	1.40	0.426	0.613	3.180				
PWSC in EEG	1.76	0.203	0.738	4.181				
Cortical and basal ganglia involvement	1.77	0.188	0.767	4.117				
Increase in CSF 14-3-3 protein	2.85	0.039**	1.056	7.669	6.529	0.003**	1.928	22.109
CLINICAL SIGNS								
Myoclonus	5.61	0.001**	2.027	15.511	18.51	< 0.001**	4.875	70.279
Cognitive dysfunction	0.55	0.430	0.126	2.417				
Pyramidal dysfunction	4.08	0.007**	1.466	11.356				
Extrapyramidal dysfunction	2.72	0.029*	1.109	6.658				
Cerebellar sign	1.07	0.868	0.474	2.419				
Cortical visual dysfunction	0.98	0.953	0.423	2.249				
Akinetic mutism	4.19	0.009**	1.438	12.215				
Seizure	1.73	0.287	0.632	4.706				

*EEG, electroencephalography; MRI, magnetic resonance imaging; PSWC, periodic sharp wave complex; *p < 0.05, **p < 0.01.*

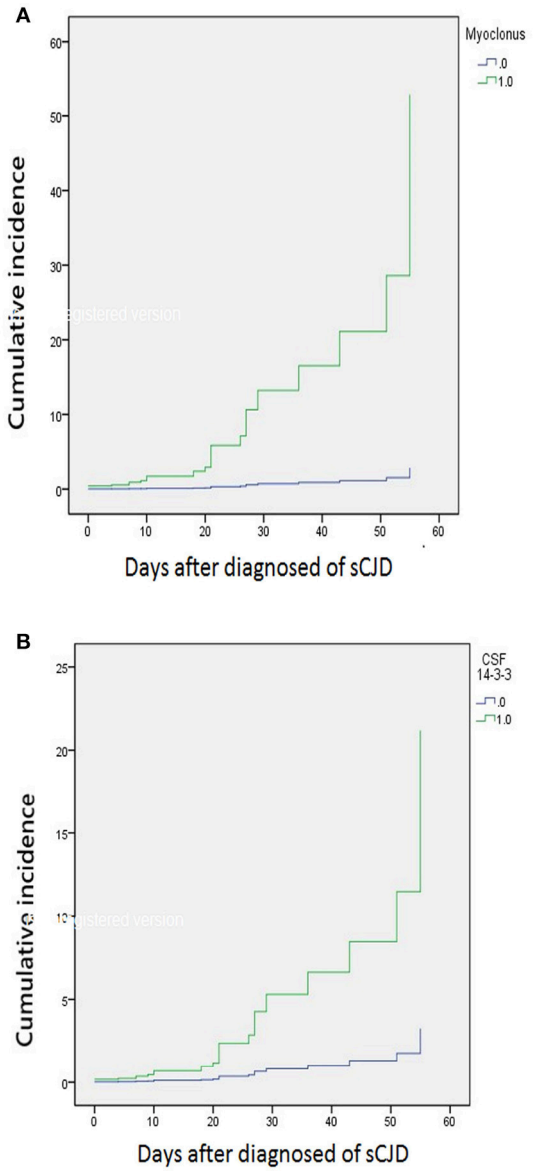

FIGURE 3 | Stratified cumulative incidence of artificial feeding in **(A)** myoclonus and **(B)** 14-3-3 protein in CSF at diagnosis of sporadic Creutzfeldt-Jakob disease.

with both cortical and basal ganglia involvement on brain MRI, pyramidal dysfunction, myoclonus, and extrapyramidal signs, indicating that neocortex and subcortical structures may be severely involved when akinetic mutism occurs. Therefore, since myoclonus, akinetic mutism, and pyramidal tract dysfunction are closely related, we may predict that the risk of swallowing failure increases when a patient presents with myoclonus.

Myoclonus in sCJD can present as irregular or rhythmic positive and negative jerky movements (21–23). It occurs in 82–100% of CJD patients and can be a focal or generalized pattern during the disease course, especially in the majority of advanced forms of all genotypes (24, 25). The presence of myoclonus has been considered to originate in the brainstem or thalamus area (15). Periodic rhythmic synchronized myoclonus has been suspected due to a hyperexcitable cortico-subcortical loop (26, 27). Furthermore, myoclonus occurred more frequently and earlier in MM type at codon 129 of the prion protein gene compared to other codon 129 polymorphism (9, 28). This genotype was considered to have the shortest survival compared to MV and VV forms of the human PRNP gene (7, 9). According to Iwasaki et al. CJD patients who have early onset of myoclonus, rapid disease progression to the akinetic mutism state, and PSWC on EEG were associated with relatively poor prognosis (8).

In conclusion, the dependence on artificial feeding could be a time point to predict the prognosis for CJD patients. The presence of myoclonus in CJD patients increases the risk of the need for artificial feeding and indicates an early irreversible dependence in daily activities.

AUTHOR CONTRIBUTIONS

P-CH wrote the initial manuscript and statistical analysis. H-TL collected data of all of the sCJD patients. P-CH, C-WC, Y-RW, and H-CK involve in conception and design and analysis and interpretation of data. H-CK also gave revision of manuscript for important intellectual content.

ACKNOWLEDGMENTS

This study was partially supported by a grant from Chang Gung Memorial Hospital, Taipei, Taiwan (CMRPG3G0431).

REFERENCES

1. World Health Organization. *WHO Manual for Surveillance of Human Transmissible Spongiform Encephalopathies Including Variant Creutzfeldt-Jakob Disease* (2003). Geneva: World Health Organization.
2. Parchi P, Giese A, Capellari S, Brown P, Schulz-Schaeffer W, Windl O, et al. Classification of sporadic Creutzfeldt-Jakob disease based on molecular and phenotypic analysis of 300 subjects. *Ann Neurol.* (1999) 46:224–33.
3. Ladogana A, Puopolo M, Croes EA, Budka H, Jarius C, Collins S, et al. Mortality from Creutzfeldt-Jakob disease and related disorders in Europe, Australia, and Canada. *Neurology* (2005) 64:1586–91. doi: 10.1212/01.WNL.0000160117.56690.B2
4. Nagoshi K, Sadakane A, Nakamura Y, Yamada M, Mizusawa H. Duration of prion disease is longer in Japan than in other countries. *J Epidemiol.* (2011) 21:255–62. doi: 10.2188/jea.JE20100085
5. Lu CJ, Sun Y, Chen SS. Incidence of Creutzfeldt-Jakob disease in Taiwan: a prospective 10-year surveillance. *Eur J Epidemiol.* (2010) 25:341–7. doi: 10.1007/s10654-010-9446-4
6. Puopolo M, Ladogana A, Almonti S, Daude N, Bevivino S, Petraroli R, et al. Mortality trend from sporadic Creutzfeldt-Jakob disease (CJD) in Italy, 1993-2000. *J Clin Epidemiol.* (2003) 56:494–9. doi: 10.1016/S0895-4356(02)00606-6
7. Pocchiari M, Puopolo M, Croes EA, Budka H, Gelpi E, Collins S, et al. Predictors of survival in sporadic Creutzfeldt-Jakob disease and other

human transmissible spongiform encephalopathies. *Brain* (2004) 127:2348–59. doi: 10.1093/brain/awh249
8. Iwasaki Y, Akagi A, Mimuro M, Kitamoto T, Yoshida M. Factors influencing the survival period in Japanese patients with sporadic Creutzfeldt-Jakob disease. *J Neurol Sci.* (2015) 357:63–8. doi: 10.1016/j.jns.2015.06.065
9. Iwasaki Y. Creutzfeldt-Jakob disease. *Neuropathology* (2017) 37:174–88. doi: 10.1111/neup.12355
10. Sarkar P, Cole A, Scolding NJ, Rice CM. Percutaneous endoscopic gastrostomy tube insertion in neurodegenerative disease: a retrospective study and literature review. *Clin Endosc.* (2017) 50:270–8. doi: 10.5946/ce.2016.106
11. Mitchell SL, Kiely DK, Lipsitz LA. The risk factors and impact on survival of feeding tube placement in nursing home residents with severe cognitive impairment. *Arch Intern Med*. (1997) 157:327–32.
12. Alvarez-Fernandez B, García-Ordoñez MA, Martínez-Manzanares C, Gómez-Huelgas R. Survival of a cohort of elderly patients with advanced dementia: nasogastric tube feeding as a risk factor for mortality. *Int J Geriatr Psychiatry* (2005) 20:363–70. doi: 10.1002/gps.1299
13. Mitchell SL, Teno JM, Kiely DK, Shaffer ML, Jones RN, Prigerson HG, et al. The clinical course of advanced dementia. *N Engl J Med.* (2009) 361:1529–38. doi: 10.1056/NEJMoa0902234
14. Harwood RH. Feeding decisions in advanced dementia. *J R Coll Physicians Edinb*. (2014) 44:232–7. doi: 10.4997/JRCPE.2014.310
15. Iwasaki Y, Mimuro M, Yoshida M, Kitamoto T, Hashizume Y. Survival to akinetic mutism state in Japanese cases of MM1-type sporadic Creutzfeldt-Jakob disease is similar to Caucasians. *Eur J Neurol.* (2011) 18:999–1002. doi: 10.1111/j.1468-1331.2010.03185.x
16. Nakatani E, Kanatani Y, Kaneda H, Nagai Y, Teramukai S, Nishimura T, et al. Specific clinical signs and symptoms are predictive of clinical course in sporadic Creutzfeldt-Jakob disease. *Eur J Neurol.* (2016) 23:1455–62. doi: 10.1111/ene.13057
17. Banno H, Katsuno M, Suzuki K, Tanaka S, Suga N, Hashizume A, et al. Swallowing markers in spinal and bulbar muscular atrophy. *Ann Clin Transl Neurol*. (2017) 4:534–43. doi: 10.1002/acn3.425
18. Kertscher B, Speyer R, Palmier M, Plant C. Bedside screening to detect oropharyngeal dysphagia in patients with neurological disorders: a systematic review. *Dysphagia* (2014) 29:204–12. doi: 10.1007/s00455-013-9490-9
19. Walshe M. Oropharyngeal dysphagia in neurodegenerative disease. *J Gastroenterol Hepatol Res*. (2014) 3:1265–71. doi: 10.6051/j.issn.2224-3992.2014.03.408-2
20. Ironside JW, Ritchie DL, Head MW. Prion diseases. *Handb Clin Neurol.* (2017) 145:393–403. doi: 10.1002/9780470015902.a0000426
21. Panzica F, Canafoglia L, Franceschetti S, Binelli S, Ciano C, Visani E, et al. Movement-activated myoclonus in genetically defined progressive myoclonic epilepsies: EEG-EMG relationship estimated using autoregressive models. *Clin Neurophysiol.* (2003) 114:1041–52. doi: 10.1016/S1388-2457(03)00066-X
22. Shibasaki H, Motomura S, Yamashita Y, Shii H, Kuroiwa Y. Periodic synchronous discharge and myoclonus in Creutzfeldt-Jakob disease: diagnostic application of jerk-locked averaging method. *Ann Neurol*. (1981) 9:150–6. doi: 10.1002/ana.410090208
23. Shibasaki, H. Neurophysiological classification of myoclonus. *Neurophysiol Clin.* (2006) 36:267–9. doi: 10.1016/j.neucli.2006.11.004
24. Brown P, Cathala F, Castaigne P, Gajdusek C. Creutzfeldt-Jakob disease: clinical analysis of a consecutive series of 230 neuropathologically verified cases. *Ann Neurol.* (1986) 20:597–602. doi: 10.1002/ana.410200507
25. Burger LJ, Rowan AJ, Goldensohn ES. Creutzfeldt-Jakob disease. An electroencephalographic study. *Arch Neurol*. (1972) 26:428–33.
26. Binelli S, Agazzi P, Canafoglia L, Scaioli V, Panzica F, Visani E, et al. Myoclonus in Creutzfeldt-Jakob disease: polygraphic and video-electroencephalography assessment of 109 patients. *Mov Disord.* (2010) 25:2818–27. doi: 10.1002/mds.23397
27. Shibasaki H, Neshige R, Hashiba Y. Cortical excitability after myoclonus: jerk-locked somatosensory evoked potentials. *Neurology* (1985) 35:36–41.
28. Hashimoto T, Iwahashi T, Ishii W, Yamamoto K, Ikeda S. EEG-EMG polygraphic study of dystonia and myoclonus in a case of Creutzfeldt-Jakob disease. *Epilepsy Behav Case Rep.* (2015) 4:30–2. doi: 10.1016/j.ebcr.2015.05.002

Conflict of Interest Statement: The authors declare that the research was conducted in the absence of any commercial or financial relationships that could be construed as a potential conflict of interest.

The reviewer CH and handling Editor declared their shared affiliation.

frontiers in Neurology

MINI REVIEW
published: 18 April 2018
doi: 10.3389/fneur.2018.00265

Role of Neuroimaging as a Biomarker for Neurodegenerative Diseases

Soichiro Shimizu, Daisuke Hirose, Hirokuni Hatanaka, Naoto Takenoshita, Yoshitsugu Kaneko, Yusuke Ogawa, Hirofumi Sakurai and Haruo Hanyu*

Department of Geriatric Medicine, Tokyo Medical University, Tokyo, Japan

It has recently been recognized that neurodegenerative diseases are caused by common cellular and molecular mechanisms including protein aggregation and inclusion body formation. Each type of neurodegenerative disease is characterized by the specific protein that aggregates. In these days, the pathway involved in protein aggregation has been elucidated. These are leading to approaches toward disease-modifying therapies. Neurodegenerative diseases are fundamentally diagnosed pathologically. Therefore, autopsy is essential for a definitive diagnosis of a neurodegenerative disease. However, recently, the development of various molecular brain imaging techniques have enabled pathological changes in the brain to be inferred even without autopsy. Some molecular imaging techniques are described as biomarker in diagnostic criteria of neurodegenerative disease. Magnetic resonance imaging (MRI), single photon emission computed tomography (SPECT), positron emission tomography (PET), and amyloid imaging are described in the diagnostic guidelines for Alzheimer's disease in the National Institute on Aging-Alzheimer's Association. MRI, dopamine transporter (DAT) imaging, and ^{123}I-metaiodobenzyl-guanidine (MIBG) myocardial scintigraphy listed in the guidelines for consensus clinical diagnostic criteria for dementia with Lewy bodies are described as potential biomarkers. The Movement Disorder Society Progressive Supranuclear Palsy Study Group defined MRI, SPECT/PET, DAT imaging, and tau imaging as biomarkers. Other diagnostic criteria for neurodegenerative disease described neuroimaging findings as only characteristic finding, not as biomarker. In this review, we describe the role of neuroimaging as a potential biomarker for neurodegenerative diseases.

Keywords: amyloid, biomarker, DAT, dementia, MIBG, neuroimaging, tau

OPEN ACCESS

Edited by:
Chaur-Jong Hu,
Taipei Medical University, Taiwan

Reviewed by:
Chaoyang Li,
Wuhan Institute of Virology (CAS), China
Andy Wai Kan Yeung,
University of Hong Kong, Hong Kong

****Correspondence:***
Soichiro Shimizu
soichiroshimizu@gmail.com

Specialty section:
This article was submitted to Neurodegeneration, a section of the journal Frontiers in Neurology

Received: *25 January 2018*
Accepted: *04 April 2018*
Published: *18 April 2018*

Citation:
Shimizu S, Hirose D, Hatanaka H, Takenoshita N, Kaneko Y, Ogawa Y, Sakurai H and Hanyu H (2018) Role of Neuroimaging as a Biomarker for Neurodegenerative Diseases. Front. Neurol. 9:265. doi: 10.3389/fneur.2018.00265

INTRODUCTION

Each neurodegenerative disease type is characterized by the specific protein that aggregates. Recently, extensive research has been performed on disease-modifying therapies for neurodegenerative diseases (i.e., Alzheimer's disease, tauopathies, etc.), which are expected to be developed in the near future. Simple and practical biomarkers specific for each neurodegenerative disease are urgently required for their accurate diagnosis and facilitate the development of disease-modifying interventions. A recent study demonstrated the potential clinical utility of plasma biomarkers in predicting brain amyloid-β burden (1). However, in daily clinical setting, plasma biomarkers are not available yet and analyzing the cerebrospinal fluid (CSF) of all patients may be difficult (2–4).

In many diagnostic criteria for neurodegenerative disease, characteristic findings in neuroimaging are mentioned. Moreover, only few recent diagnostic criteria for neurodegenerative diseases

have mentioned neuroimaging techniques as biomarkers that can estimate pathological changes occurring in the brains of neurodegenerative disease patients (2, 3, 5, 6).

The current mini-review addresses the roles of neuroimaging techniques described as biomarkers on diagnostic criteria for individual neurodegenerative diseases as research topics. Even though there were numerical findings of neuroimaging technique of neurodegenerative disease, we omitted those of not described in diagnostic criteria. For example, about prion disease, hyperintensity in cortex and basal ganglia on FLAIR and DWI are widely known as characteristic magnetic resonance imaging (MRI) finding of prion disease in daily clinical setting. However, this characteristic MRI finding is not described in diagnostic criteria for prion disease which is widely used (7).

In this review, we defined the characteristic neuroimaging findings described in diagnostic criteria from Level A and B based on evidence level as follows:

Level A: able to use the research criteria; described as biomarkers in diagnostic criteria.
Level B: supportive biomarker of clinical diagnosis; described as supportive biomarkers for research criteria in diagnostic criteria.
Level C: supportive of clinical diagnosis; not described as biomarkers but characteristic finding in diagnostic criteria.

Table 1 shows a summary of neuroimaging techniques used as biomarkers, as described in various diagnostic criteria.

Magnetic Resonance Imaging

Magnetic resonance imaging is one of the most widely used neuroimaging techniques for the diagnosis of neurodegenerative diseases. However, among the diagnostic criteria for neurodegenerative diseases, only two diagnostic guidelines, namely, for Alzheimer disease (AD) (2, 3) and for dementia with Lewy bodies (DLB) (5) state characteristic MRI findings as biomarkers.

The National Institute on Aging-Alzheimer's Association (NIA-AA) diagnostic guidelines for AD state disproportionate atrophy on structural MRI in the medial, basal, and lateral temporal lobes, as well as the medial parietal cortex, as a biomarker of neuronal degeneration or injury (2, 3) (Level A).

The latest diagnostic guidelines of DLB (5) state the absence of or minimal atrophy of the medial temporal lobe on MRI as a supportive biomarker that is consistent with DLB, which assists in the diagnostic evaluation, but does not have clear diagnostic specificity (Level B). Hippocampus is strongly correlated at autopsy with tangles rather than plaque or Lewy body-associated pathology (8). Many studies reported the coexistence of DLB and AD pathology in patients. Most patients with DLB also demonstrate AD pathology (5, 9). Therefore, it should be emphasized that if patients have medial temporal lobe atrophy, DLB should not be denied.

The movement disorder society (MDS) clinical diagnostic criteria for progressive supranuclear palsy (PSP) that has recently been established state a characteristic MRI finding, namely, predominant midbrain atrophy relative to the pons, as a supportive feature, but not a biomarker of PSP (10) (Level C). On the other hand, the MDS-endorsed PSP Study Group classified various neuroimaging techniques into five classes of biomarkers for Richardson's syndrome (PSP-RS) and the other variant syndromes of PSP (vPSP), which were defined by evidence levels. However, to our knowledge, the top two level evidence biomarkers (i.e., 5: definitive and 4: supportive of pathological diagnosis) have not been described in the literature. On the other hand, characteristic MRI findings on PSP are described in detail as classified biomarkers (level 1: research tool, level 2: supportive of clinical diagnosis, and level 3: supportive of early clinical diagnosis) for individual PSP clinical subtypes (Levels A–C). Although details have been omitted from this review, basal ganglia and thalamic atrophy, and rates of whole-brain and midbrain atrophy are mentioned as representative examples of biomarkers for PSP-RS, and midbrain

TABLE 1 | Summary of neuroimaging techniques used as biomarkers.

Imaging technique	Disease	Evidence level	Actual description in diagnostic criteria
MRI	AD	A	Atrophy in temporal lobe sand medial parietal cortex
	DLB	B	Absence of or minimal medial temporal lobe atrophy
	PSP[a]	A–C	Characteristic image findings described for each subtype
SPECT/PET	AD	A	Hypometabolism in temporoparietal cortex
	DLB	B	Hypoperfusion/metabolism in occipital lobe and posterior cingulate island sign on FDG-PET
	PSP[a]	A–C	Frontal lobe hypoperfusion, frontal lobe and midbrain hypometabolism, and frontal hypometabolism
DAT imaging	DLB	A	Reduced dopamine transporter uptake in basal ganglia
	PSP[a]	A–C	Reduced striatal DAT/D2 receptor and reduced brain stem DAT
MIBG	DLB	A	Abnormal (low uptake) on MIBG myocardial scintigraphy
Amyloid PET	AD	A	Positive PET amyloid imaging
Tau PET	PSP[a]	B	THK5351 uptake in midbrain and globus pallidus
			[^{18}F]AV-1451 uptake in midbrain, thalamus, basal ganglia, and dentate nucleus of the cerebellum

[a]Not described in diagnostic criteria, but defined as a biomarker by the MDS-endorsed PSP Study Group.
Evidence levels are different depend on clinical subtypes.
MRI, magnetic resonance imaging; SPECT, single photon emission computed tomography; PET, positron emission tomography; DAT imaging, dopamine transporter imaging; MIBG, ^{123}iodine-metaiodobenzylguanidine myocardial scintigraphy; AD, Alzheimer's disease; DLB, dementia with Lewy bodies; PSP, progressive supranuclear palsy; MDS, movement disorder society; FDG, ^{18}fluorodeoxyglucose.
Level A: able to use the research criteria; described as biomarkers in diagnostic criteria.
Level B: supportive biomarker of clinical diagnosis; described as supportive biomarkers for research criteria in diagnostic criteria.
Level C: supportive of clinical diagnosis; not described as biomarkers but characteristic finding in diagnostic criteria.

atrophy is mentioned as a biomarker of vPSP. Furthermore, it is noteworthy that not only structural MRI findings but also findings displayed on functional MRI and diffusion tensor imaging are described. Details of the MRI findings are described elsewhere (6).

Other diagnostic criteria for neurodegenerative diseases also describe characteristic findings on MRI, but there are no descriptions of biomarkers. Frontotemporal lobar degeneration (FTLD) has three clinical subtypes (11), which demonstrate various pathological changes (e.g., FTLD-tau, FTLD-TDP, FTLD-UPS, and FTLD-FUS FTLD-ni) (12). The diagnostic criteria for FTLD that is most commonly used (11) mentions MRI findings of individual clinical subtypes as characteristics, rather than as biomarkers (Level C). As FTLD is caused by various pathological changes, it is difficult to consider neuroimaging data, including those from MRI, as biomarkers. Recent diagnostic criteria for the behavioral variant of frontotemporal dementia (bvFTD) (13) mentioned frontal or anterior temporal atrophy displayed on MRI or computed tomography as characteristic findings suggesting a diagnosis of bvFTD.

A second consensus statement on the diagnosis of multiple system atrophy (MSA) mentioned atrophy displayed on MRI of the putamen, middle cerebellar peduncle, pons, or cerebellum as an additional feature suggestive of MSA-P or MSA-C, but not as a biomarker (14) (Level C).

However, many past studies showed, coexistence of several pathological changes is not rare in elderly patients (5, 9, 15). Therefore, existence of individual pathological change is suggested due to the above MRI characteristic findings, however, it should be noted that coexistence of other pathological changes cannot be denied.

Single Photon Emission Computed Tomography (SPECT) and Positron Emission Tomography (PET)

Recently, among the nuclear medicine imaging techniques, SPECT and PET have been used for the diagnosis of neurodegenerative diseases in the daily clinical setting and are the most commonly used new neuroimaging techniques.

The NIA-AA diagnostic guidelines for AD describe decreased ^{18}fluorodeoxyglucose (FDG) uptake on PET in the temporoparietal cortex as a biomarker of neuronal degeneration or injury (2, 3) (Level A).

The most recent diagnostic criteria for DLB (5) mentioned hypoperfusion/hypometabolism by SPECT/PET in the occipital lobe and the posterior cingulate island sign on FDG-PET imaging as supportive biomarkers (Level B). An autopsy-confirmed study suggested that FDG-PET occipital hypometabolism was able to differentiate DLB from AD with high accuracy (16). Larger studies on patients earlier in the course of the disease suggested a sensitivity (70%) and specificity (74%) slightly lower than required for an indicative biomarker, although better than that reported for SPECT (65 and 64%, respectively) (17, 18). On the other hand, our past study showed that there was no significant perfusion differences in medial occipital lobe between AD and DLB (19). In any case, compared with dopamine transporter (DAT) imaging ^{123}Iodine-metaiodobenzylguanidine (MIBG) cardiac scintigraphy described below, occipital hypoperfusion has low sensitivity and specificity. Therefore, it is understandable that it stayed in only one of the supportive biomarker with most resent diagnostic criteria. Relative preservation of the metabolic activities of the posterior cingulate cortex and midcingulate cortex on FDG-PET (the cingulate island sign) has been described in DLB (20), associated with less concurrent neurofibrillary pathology, but with no difference in amyloid-beta (Aβ) load relative to AD (21).

In the recent MDS clinical diagnostic criteria for PSP, predominant midbrain hypometabolism relative to the pons displayed on FDG-PET is described as a supportive feature, rather than a biomarker (10) (Level C). On the other hand, the MDS PSP Study Group defined SPECT frontal hypoperfusion as a level 1 biomarker (research tool), FDG-PET frontal and midbrain hypometabolism as a level 2 biomarker (supportive of clinical diagnosis), and FDG-PET frontal hypometabolism as a class 3 biomarker (supportive of early clinical diagnosis) for PSP-RS (6) (Levels A–C).

Recent diagnostic criteria for bvFTD (13) stated frontal or anterior temporal hypoperfusion or hypometabolism displayed on PET or SPECT as characteristic neuroimaging data suggestive of bvFTD (Level C). This criteria states that functional imaging changes may provide additional sensitivity, suggesting that behavioral and functional abnormalities may precede structural imaging changes in bvFTD.

The second consensus statement on MSA stated hypometabolism on FDG-PET in the putamen, brainstem, and cerebellum as additional features of possible MSA-P and hypometabolism on FDG-PET in the putamen as an additional feature of possible MSA-C, rather than as biomarkers (14) (Level C).

Dopamine Transporter Imaging

DAT imaging use a ligand that binds to the presynaptic dopamine transporter, can be used to analyze the integrity of the nigrostriatal projection pathway. ^{123}I-2β-carbomethoxy-3β-(4-iodophenyl)-*N*-(3-fluoropropyl) nortropane (^{123}I-FP-CIT) is the ligand for DAT-SPECT that is most widely used. ^{123}I-FP-CIT has been used in a large number of trials to identify the *in vivo* loss of dopamine transporters in the striatum of patients with presynaptic parkinsonism (22, 23). Therefore, Parkinson syndrome including Parkinson's disease (PD) that has the dysfunction of the nigrostriatal projection pathway showed reduced DAT uptake. In other words, DAT imaging is not suitable for differentiation of presynaptic Parkinson syndrome. Therefore, the recent clinical diagnostic criteria for PD by the MDS did not mention DAT imaging as biomarker or characteristic imaging finding of PD (24). DAT imaging requires attention to use in the following cases, patients with an infarction in the basal ganglia, patients who are unable to stop the use of medications that affect DAT uptake (e.g., cocaine, amphetamines, bupropion, selective serotonin reuptake inhibitors, etc.) (25).

However, DAT imaging is useful for differentiating DLB from other dementias. The latest diagnostic guidelines of DLB state reduced dopamine transporter (DAT) uptake in the basal ganglia displayed on SPECT or PET as indicative biomarkers (5) (Level A). However, there are no biomarkers available for the clinical

diagnosis of Lewy body-associated pathology. DAT imaging was described as a useful indirect method for determining Lewy body-associated pathology. Reduced DAT uptake in the basal ganglia has been confirmed by SPECT or PET imaging. The utility of DAT imaging in distinguishing DLB from AD is well established, with a sensitivity of 78% and a specificity of 90% (26).

In the recent MDS clinical diagnostic criteria for PSP, postsynaptic striatal dopaminergic degeneration, as demonstrated for example by ^{123}I-iodobenzamide (IBZM)-SPECT or ^{18}F-desmethoxyfallypride (DMFP)-PET, is described as a supportive feature rather than as a biomarker (10) (Level C). However, the MDS PSP Study Group defined reduced striatal DAT/D2 receptor levels and reduced brainstem DAT levels as level 2 biomarkers for PSP-RS (Level B), and reduced striatal DAT as a level 1 biomarker for some types of vPSP (6) (Level A).

The second consensus statement on the diagnosis of MSA states presynaptic nigrostriatal dopaminergic denervation displayed on SPECT or PET as an additional feature suggestive of MSA-P, but not as a biomarker (14) (Level C).

^{123}Iodine-Metaiodobenzylguanidine Myocardial Scintigraphy

MIBG is a physiologic analog of noradrenaline used to determine the location, integrity, and function of postganglionic noradrenergic neurons. Lewy body disease including DLB and PD presents an impairment of adrenergic function and consequently an abnormal MIBG myocardial syntigraphy (27). MIBG myocardial scintigraphy requires attention to patients with heart disease, diabetes, or thyroid disease, or patients taking any drugs known to affect the accumulation of MIBG (28).

The latest diagnostic guidelines of DLB state abnormal (low uptake) MIBG myocardial scintigraphy as an indicative biomarker (5) (Level A). MIBG myocardial scintigraphy quantifies postganglionic sympathetic cardiac innervation, which is reduced in Lewy body disease (27, 29). The sensitivity and specificity values of MIBG myocardial scintigraphy for discriminating probable DLB from probable AD rise from 69 and 87%, respectively, in severely demented patients to 77 and 94%, respectively, in mildly demented patients (30).

The recent clinical diagnostic criteria for PD by the MDS described the presence of either olfactory loss or cardiac sympathetic denervation on MIBG myocardial scintigraphy as supportive criteria, but not as a biomarker (24) (Level B).

In MSA, which is an α-synucleinopathy similar to PD, the diagnostic criteria (14) also does not state MIBG myocardial scintigraphy as supportive diagnostic criteria (Level C). The reason is that there is no consensus on the usefulness of MIBG myocardial scintigraphy for diagnosing MSA. Many reports using MIBG myocardial scintigraphy have shown preserved sympathetic postganglionic neurons in MSA, in contrast to in PD (31). On the other hand, some studies have shown denervation in patients with MSA displayed on MIBG myocardial scintigraphy (32).

Aβ Imaging

Interest in the use of Aβ imaging for the diagnosis of AD has been increasing. Aβ imaging is a tool expected to be new possibilities for the early detection, intervention, and prevention of AD. NIA-AA diagnostic guidelines for AD showed that biomarkers of brain Aβ protein deposition are low CSF Aβ42 and positive PET amyloid imaging (2, 3) (Level A). In addition, the diagnostic criteria do not specify the particular amyloid imaging tracer to be used. Studies with ^{11}C-Pittsburgh compound-B (^{11}C-PiB), the first and most widely studied PET Aβ ligand, indicated that Aβ imaging may enable the earlier diagnosis of AD (33, 34). However, owing to the 20-min half-life of ^{11}C, ^{11}C-PiB can only be used in large PET centers with their own on-site cyclotron and radiopharmacy facilities. ^{18}F is a more suitable radioisotope for widespread clinical use as its longer half-life of 110 min enables distribution from a production site to multiple PET centers. Recently, ^{18}F-labeled tracers have been developed, which are starting to be used clinically. The actual ^{18}F-labeled tracers being used are as follows: flutemetamol (GE Healthcare), florbetapir (Amyvid, Eli Lilly), florbetaben (Neuraceq, Piramal Imaging), and ^{18}F-AZD4694 (recently renamed NAV4694) (Astra-Zeneca, Navidea) are derived from stilbene. The above ^{18}F-labeled tracers except NAV4694 have been approved by the Food and Drug Administration. Correlations have been shown between levels of biomarker CSF Aβ42 and PET signals using ^{11}C-PiB as a tracer for Aβdeposits in the brain (35) and comparable studies have been performed for ^{18}F-labeled amyloid tracers (36, 37). A systematic review found no marked differences in the diagnostic accuracy among flutemetamol, florbetapir, and florbetaben (38). These three tracers perform better when used to differentiate between patients with AD and healthy controls. Furthermore, a study showed that NAV4694 displays high cortical binding and low nonspecific white matter binding in AD patients (39).

On the other hand, NIA-AA diagnostic guidelines for AD described, "guidelines do not advocate the use of AD biomarker tests for routine diagnostic purposes at the present time" (2, 3). At the present time, amyloid imaging should be used for research criteria of AD, taking into consideration that it is not possible at all facilities. Further studies using amyloid imaging are required to identify the tracer with the highest sensitivity and specificity, and to identify the positioning of Aβ imaging in clinical use. However, we believe that amyloid imaging, particularly ^{18}F-labeled tracers, contribute to the early diagnosis of AD.

Tau Imaging

The advances of molecular imaging in recent years have led to the development of promising tau-specific PET tracers. In recent years, hot topics were shifted from general neuroimaging to molecular imaging of the neurodegeneration related to tau protein (40).

Unfortunately, tau imaging has not been stated as a biomarker in any diagnostic criteria for neurodegenerative diseases. However, the MDS PSP study group defined two tau-specific tracers (i.e., ^{18}F-THK5351 and ^{18}F-AV1451) as a biomarker of PSP-RS (6) (Level B). Because very few articles have been published on this subject, it has been suggested to have low reliability.

However, tau imaging is expected to become an important biomarker of tau pathology in the future. There are six different isoforms of tau, formed by alternative mRNA splicing of the microtubule-associated protein tau (*MAPT*) gene. More importantly, the inclusion or exclusion of exon 10 results in either 4 repeats (4R) or 3 repeats (3R) of the microtubule-binding domain

being transcribed in the tau protein, respectively (41). The 3R/4R ratio is 1:1 under physiological conditions and in patients with AD, tangle predominant senile dementia, and chronic traumatic encephalopathy. 3R isoforms are dominant in FTD and 4R isoforms are dominant in corticobasal degeneration, PSP, and argyrophilic grain disease (42).

The radiotracers used to image tau neurofibrillary tangle deposition in living AD patient brains are ^{18}F-FDDNP (43), ^{18}F-AV1451 (44), ^{11}C-PBB3 (45), and ^{18}F-THK5351 (46). These tracers are now available for clinical assessment of patients with various tauopathies, including AD, as well as in healthy subjects.

However, PET tracers used for tau imaging still have some problems that remain to be resolved. These tracers often show "off-target" binding. Recently, it has become clear that these tracers detected the distribution of not only tau but also other proteins (47). For example, ^{18}F-THK5351 has been confirmed to also bind to monoamine oxidase B (48). Moreover, ^{18}F-AV1451 is well known to bind to calcifications, iron, melanin, and blood vessels (49). Therefore, further studies of a large number of patients, with consideration of the results of pathological analyses are required. Even considering the above issues, we believe that with further research, tau imaging will become a useful biomarker in the near future.

CONCLUSION

In this review, we introduced the various neuroimaging techniques described in the current diagnostic criteria for neurodegenerative diseases and the possibility of new neuroimaging techniques as biomarkers. We believe that further advances in these neuroimaging techniques will lead to useful biomarkers that can accurately predict the pathological changes occurring in various neurodegenerative diseases.

ETHICS STATEMENT

All procedures performed in the studies involving human participants were in accordance with the ethical standards of the institutional or national research committee and with the 1964 Helsinki declaration and its later amendments or comparable ethical standards. Informed consent: informed consent was obtained from all individual participants included in the study.

AUTHOR CONTRIBUTIONS

SS, DH, Hi.H, NT, YK, and YO wrote the manuscript. HS and Ha.H critically reviewed the manuscript.

ACKNOWLEDGMENTS

We are grateful to the medical editors of the Department of International Medical Communications of Tokyo Medical University for reviewing the manuscript.

REFERENCES

1. Nakamura A, Kaneko N, Villemagne VL, Kato T, Doecke J, Doré V, et al. High performance plasma amyloid-β biomarkers for Alzheimer's disease. *Nature* (2018) 554(7691):249–54. doi:10.1038/nature25456
2. Jack CR, Albert MS, Knopman DS, McKhann GM, Sperling RA, Carrillo MC, et al. Introduction to the recommendations from the National Institute on Aging-Alzheimer's Association workgroups on diagnostic guidelines for Alzheimer's disease. *Alzheimers Dement* (2011) 7(3):257–62. doi:10.1016/j.jalz.2011.03.004
3. McKhann GM, Knopman DS, Chertkow H, Hyman BT, Jack CR, Kawas CH, et al. The diagnosis of dementia due to Alzheimer's disease: recommendations from the National Institute on Aging-Alzheimer's Association workgroups on diagnostic guidelines for Alzheimer's disease. *Alzheimers Dement* (2011) 7(3):263–9. doi:10.1016/j.jalz.2011.03.005
4. Shaw LM, Vanderstichele H, Knapik-Czajka M, Clark CM, Aisen PS, Petersen RC, et al. Cerebrospinal fluid biomarker signature in Alzheimer's disease neuroimaging initiative subjects. *Ann Neurol* (2009) 65:403–13. doi:10.1002/ana.21610
5. McKeith IG, Boeve BF, Dickson DW, Halliday G, Taylor JP, Weintraub D, et al. Diagnosis and management of dementia with Lewy bodies: fourth consensus report of the DLB consortium. *Neurology* (2017) 89(1):88–100. doi:10.1212/WNL.0000000000004058
6. Whitwell JL, Höglinger GU, Antonini A, Bordelon Y, Boxer AL, Colosimo C, et al. Radiological biomarkers for diagnosis in PSP: where are we and where do we need to be? *Mov Disord* (2017) 32(7):955–71. doi:10.1002/mds.27038
7. WHO. *WHO Manual for Strengthening Diagnosis and Surveillance of Creutzfeldt-Jakob Disease*. Geneva, switzerland (1998).
8. Burton EJ, Barber R, Mukaetova-Ladinska EB, Robson J, Perry RH, Jaros E, et al. Medial temporal lobe atrophy on MRI differentiates Alzheimer's disease from dementia with Lewy bodies and vascular cognitive impairment: a prospective study with pathological verification of diagnosis. *Brain* (2009) 132(Pt 1):195–203. doi:10.1093/brain/awn298
9. Ballard C, Ziabreva I, Perry R, Larsen JP, O'Brien J, McKeith I, et al. Differences in neuropathologic characteristics across the Lewy body dementia spectrum. *Neurology* (2006) 67(11):1931–4. doi:10.1212/01.wnl.0000249130.63615.cc
10. Höglinger GU, Respondek G, Stamelou M, Kurz C, Josephs KA, Lang AE, et al. Clinical diagnosis of progressive supranuclear palsy: the movement disorder society criteria. *Mov Disord* (2017) 32(6):853–64. doi:10.1002/mds.26987
11. Neary D, Snowden JS, Gustafson L, Passant U, Stuss D, Black S, et al. Frontotemporal lobar degeneration: a consensus on clinical diagnostic criteria. *Neurology* (1998) 51(6):1546–54. doi:10.1212/WNL.51.6.1546
12. Mackenzie IR, Neumann M, Bigio EH, Cairns NJ, Alafuzoff I, Kril J, et al. Nomenclature and nosology for neuropathologic subtypes of frontotemporal lobar degeneration: an update. *Acta Neuropathol* (2010) 119(1):1–4. doi:10.1007/s00401-009-0612-2
13. Rascovsky K, Hodges JR, Knopman D, Mendez MF, Kramer JH, Neuhaus J, et al. Sensitivity of revised diagnostic criteria for the behavioural variant of frontotemporal dementia. *Brain* (2011) 134(Pt 9):2456–77. doi:10.1093/brain/awr179
14. Gilman S, Wenning GK, Low PA, Brooks DJ, Mathias CJ, Trojanowski JQ, et al. Second consensus statement on the diagnosis of multiple system atrophy. *Neurology* (2008) 71(9):670–6. doi:10.1212/01.wnl.0000324625.00404.15
15. Toledo JB, Cairns NJ, Da X, Chen K, Carter D, Fleisher A, et al. Clinical and multimodal biomarker correlates of ADNI neuropathological findings. *Acta Neuropathol Commun* (2013) 2013(1):65. doi:10.1186/2051-5960-1-65
16. Minoshima S, Foster NL, Sima AA, Frey KA, Albin RL, Kuhl DE. Alzheimer's disease versus dementia with Lewy bodies: cerebral metabolic distinction with autopsy confirmation. *Ann Neurol* (2001) 50(3):358–65. doi:10.1002/ana.1133
17. Lobotesis K, Fenwick JD, Phipps A, Ryman A, Swann A, Ballard C, et al. Occipital hypoperfusion on SPECT in dementia with Lewy bodies but not AD. *Neurology* (2001) 56(5):643–9. doi:10.1212/WNL.56.5.643
18. O'Brien JT, Firbank MJ, Davison C, Barnett N, Bamford C, Donaldson C, et al. 18F-FDG PET and perfusion SPECT in the diagnosis of Alzheimer and Lewy body dementias. *J Nucl Med* (2014) 55(12):1959–65. doi:10.2967/jnumed.114.143347

19. Shimizu S, Kanetaka H, Hirao K, Fukasawa R, Namioka N, Hatanaka H, et al. Neuroimaging for diagnosing dementia with Lewy bodies: what is the best neuroimaging technique in discriminating dementia with Lewy bodies from Alzheimer's disease? *Geriatr Gerontol Int* (2017) 17(5):819–24. doi:10.1111/ggi.12794
20. Lim SM, Katsifis A, Villemagne VL, Best R, Jones G, Saling M, et al. The 18F-FDG PET cingulate island sign and comparison to 123I-beta-CIT SPECT for diagnosis of dementia with Lewy bodies. *J Nucl Med* (2009) 50(10):1638–45. doi:10.2967/jnumed.109.065870
21. Graff-Radford J, Murray ME, Lowe VJ, Boeve BF, Ferman TJ, Przybelski SA, et al. Dementia with Lewy bodies: basis of cingulate Island sign. *Neurology* (2014) 83(9):801–9. doi:10.1212/WNL.0000000000000734
22. Benamer TS, Patterson J, Grosset DG, Booij J, de Bruin K, van Royen E, et al. Accurate differentiation of parkinsonism and essential tremor using visual assessment of [123I]-FP-CIT SPECT imaging: the [123I]-FP-CIT study group. *Mov Disord* (2000) 15(3):503–10. doi:10.1002/1531-8257(200005)15:3<503::AID-MDS1013>3.0.CO;2-V
23. Booij J, Speelman JD, Horstink MW, Wolters EC. The clinical benefit of imaging striatal dopamine transporters with [^{123}I]FP-CIT SPET in differentiating patients with presynaptic parkinsonism from those with other forms of parkinsonism. *Eur J Nucl Med* (2001) 28:266–72. doi:10.1007/s002590000460
24. Postuma RB, Berg D, Stern M, Poewe W, Olanow CW, Oertel W, et al. MDS clinical diagnostic criteria for Parkinson's disease. *Mov Disord* (2015) 30(12):1591–601. doi:10.1002/mds.26424
25. Djang DS, Janssen MJ, Bohnen N, Booij J, Henderson TA, Herholz K, et al. SNM practice guideline for dopamine transporter imaging with 123I-ioflupane SPECT 1.0. *J Nucl Med* (2012) 53:154–63. doi:10.2967/jnumed.111.100784
26. McKeith I, O'Brien J, Walker Z, Tatsch K, Booij J, Darcourt J, et al. Sensitivity and specificity of dopamine transporter imaging with 123I-FP-CIT SPECT in dementia with Lewy bodies: a phase III, multicentre study. *Lancet Neurol* (2007) 6(4):305–13. doi:10.1016/S1474-4422(07)70057-1
27. Treglia G, Cason E. Diagnostic performance of myocardial innervation imaging using MIBG scintigraphy in differential diagnosis between dementia with Lewy bodies and other dementias: a systematic review and a meta-analysis. *J Neuroimaging* (2012) 22(2):111–7. doi:10.1111/j.1552-6569.2010.00532.x
28. Solanski KK, Bomanji J, Moyes J, Mather SJ, Trainer PJ, Britton KE. A pharmacological guide to medicines which interfere with the biodistribution of radiolabelled meta-iodobenzylguanidine (MIBG). *Nucl Med Commun* (1992) 13:513–21. doi:10.1097/00006231-199207000-00006
29. Nakajima K, Okuda K, Yoshimura M, Matsuo S, Wakabayashi H, Imanishi Y, et al. Multicenter cross-calibration of I-123 metaiodobenzylguanidine heart-to-mediastinum ratios to overcome camera-collimator variations. *J Nucl Cardiol* (2014) 21(5):970–8. doi:10.1007/s12350-014-9916-2
30. Yoshita M, Arai H, Arai T, Asada T, Fujishiro H, Hanyu H, et al. Diagnostic accuracy of 123I-meta-iodobenzylguanidine myocardial scintigraphy in dementia with Lewy bodies: a multicenter study. *PLoS One* (2015) 10(3):e0120540. doi:10.1371/journal.pone.0120540
31. Courbon F, Brefel-Courbon C, Thalamas C, Alibelli MJ, Berry I, Montastruc JL, et al. Cardiac MIBG scintigraphy is a sensitive tool for detecting cardiac sympathetic denervation in Parkinson's disease. *Mov Disord* (2003) 18(8):890–7. doi:10.1002/mds.10461
32. Nagayama H, Hamamoto M, Ueda M, Nagashima J, Katayama Y. Reliability of MIBG myocardial scintigraphy in the diagnosis of Parkinson's disease. *J Neurol Neurosurg Psychiatry* (2005) 76(2):249–51. doi:10.1136/jnnp.2004.037028
33. Rowe CC, Ng S, Ackermann U, Gong SJ, Pike K, Savage G, et al. Imaging beta-amyloid burden in aging and dementia. *Neurology* (2007) 68(20):1718–25. doi:10.1212/01.wnl.0000261919.22630.ea
34. Klunk WE, Engler H, Nordberg A, Wang Y, Blomqvist G, Holt DP, et al. Imaging brain amyloid in Alzheimer's disease with Pittsburgh compound-B. *Ann Neurol* (2004) 55(3):306–19. doi:10.1002/ana.20009
35. Weigand SD, Vemuri P, Wiste HJ, Senjem ML, Pankratz VS, Aisen PS, et al. Transforming cerebrospinal fluid Aβ42 measures into calculated Pittsburgh compound B units of brain Aβ amyloid. *Alzheimers Dement* (2011) 7(2):133–41. doi:10.1016/j.jalz.2010.08.230
36. Schipke CG, Koglin N, Bullich S, Joachim LK, Haas B, Seibyl J, et al. Correlation of florbetaben PET imaging and the amyloid peptide Aß42 in cerebrospinal fluid. *Psychiatry Res* (2017) 265:98–101. doi:10.1016/j.pscychresns.2016.10.011
37. Toledo JB, Bjerke M, Da X, Landau SM, Foster NL, Jagust W, et al. Nonlinear association between cerebrospinal fluid and florbetapir F-18 β-amyloid measures across the spectrum of Alzheimer disease. *JAMA Neurol* (2015) 72(5):571–81. doi:10.1001/jamaneurol.2014.4829
38. Morris E, Chalkidou A, Hammers A, Peacock J, Summers J, Keevil S. Diagnostic accuracy of (18)F amyloid PET tracers for the diagnosis of Alzheimer's disease: a systematic review and meta-analysis. *Eur J Nucl Med Mol Imaging* (2016) 43(2):374–85. doi:10.1007/s00259-015-3228-x
39. Rowe CC, Pejoska S, Mulligan RS, Jones G, Chan JG, Svensson S, et al. Head-to-head comparison of 11C-PiB and 18F-AZD4694 (NAV4694) for β-amyloid imaging in aging and dementia. *J Nucl Med* (2013) 54(6):880–6. doi:10.2967/jnumed.112.114785
40. Yeung AW, Goto TK, Leung WK. The changing landscape of neuroscience research, 2006-2015: a bibliometric study. *Front Neurosci* (2017) 11:120. doi:10.3389/fnins.2017.00120
41. Niblock M, Gallo JM. Tau alternative splicing in familial and sporadic tauopathies. *Biochem Soc Trans* (2012) 40(4):677–80. doi:10.1042/BST20120091
42. Liu F, Gong CX. Tau exon 10 alternative splicing and tauopathies. *Mol Neurodegener* (2008) 3:8. doi:10.1186/1750-1326-3-8
43. Shoghi-Jadid K, Small GW, Agdeppa ED, Kepe V, Ercoli LM, Siddarth P, et al. Localization of neurofibrillary tangles and beta-amyloid plaques in the brains of living patients with Alzheimer disease. *Am J Geriatr Psychiatry* (2002) 10(1):24–35. doi:10.1097/00019442-200201000-00004
44. Chien DT, Bahri S, Szardenings AK, Walsh JC, Mu F, Su MY, et al. Early clinical PET imaging results with the novel PHF-tau radioligand [F-18]-T807. *J Alzheimers Dis* (2013) 34(2):457–68. doi:10.3233/JAD-122059
45. Maruyama M, Shimada H, Suhara T, Shinotoh H, Ji B, Maeda J, et al. Imaging of tau pathology in a tauopathy mouse model and in Alzheimer patients compared to normal controls. *Neuron* (2013) 79(6):1094–108. doi:10.1016/j.neuron.2013.07.037
46. Harada R, Okamura N, Furumoto S, Furukawa K, Ishiki A, Tomita N, et al. 18F-THK5351: a novel PET radiotracer for imaging neurofibrillary pathology in Alzheimer disease. *J Nucl Med* (2016) 57(2):208–14. doi:10.2967/jnumed.115.164848
47. Kikuchi A, Okamura N, Hasegawa T, Harada R, Watanuki S, Funaki Y, et al. In vivo visualization of tau deposits in corticobasal syndrome by 18F-THK5351 PET. *Neurology* (2016) 87(22):2309–16. doi:10.1212/WNL.0000000000003375
48. Ng KP, Pascoal TA, Mathotaarachchi S, Therriault J, Kang MS, Shin M, et al. Monoamine oxidase B inhibitor, selegiline, reduces 18F-THK5351 uptake in the human brain. *Alzheimers Res Ther* (2017) 9(1):25. doi:10.1186/s13195-017-0253-y
49. Choi JY, Cho H, Ahn SJ, Lee JH, Ryu YH, Lee MS, et al. "Off-target" 18F-AV-1451 binding in the basal ganglia correlates with age-related iron accumulation. *J Nucl Med* (2018) 59(1):117–20. doi:10.2967/jnumed.117.195248

Conflict of Interest Statement: The authors declare that the research was conducted in the absence of any commercial or financial relationships that could be construed as a potential conflict of interest.

frontiers in Neuroscience

ORIGINAL RESEARCH
published: 08 June 2018
doi: 10.3389/fnins.2018.00384

Pretreatment With Risperidone Ameliorates Systemic LPS-Induced Oxidative Stress in the Cortex and Hippocampus

Md. Mamun Al-Amin[1], Md. Faiyad Rahman Choudhury[1], Al Saad Chowdhury[1], Tahsinur Rahman Chowdhury[1], Preeti Jain[1], Mohsin Kazi[2], Musaed Alkholief[2], Sultan M. Alshehri[2] and Hasan Mahmud Reza[1]**

[1] Department of Pharmaceutical Sciences, North South University, Dhaka, Bangladesh, [2] Department of Pharmaceutics, College of Pharmacy, King Saud University, Riyadh, Saudi Arabia

OPEN ACCESS

Edited by:
Jean-Noël Octave,
Université catholique de Louvain,
Belgium

Reviewed by:
Ghulam Md Ashraf,
King Abdulaziz University,
Saudi Arabia
Zhiyun Wei,
Brigham and Women's Hospital,
United States
Annie Andrieux,
CEA Grenoble, France

***Correspondence:**
Mohsin Kazi
mkazi@ksu.edu.sa
Hasan Mahmud Reza
hasan.reza@northsouth.edu

Specialty section:
This article was submitted to Neurodegeneration, a section of the journal Frontiers in Neuroscience

Received: 27 December 2017
Accepted: 22 May 2018
Published: 08 June 2018

Citation:
Al-Amin MM, Choudhury MFR, Chowdhury AS, Chowdhury TR, Jain P, Kazi M, Alkholief M, Alshehri SM and Reza HM (2018) Pretreatment With Risperidone Ameliorates Systemic LPS-Induced Oxidative Stress in the Cortex and Hippocampus. Front. Neurosci. 12:384. doi: 10.3389/fnins.2018.00384

Risperidone (RIS), an atypical antipsychotic has been found to show anti-inflammatory effect against lipopolysaccharide (LPS)-induced inflammation. *In vitro* study has revealed that RIS inhibits the LPS-induced reactive oxygen species (ROS) formation. We investigated the antioxidant effects of RIS on LPS-induced oxidative stress markers in *Swiss albino* mice. Ten weeks old male *Swiss albino* mice (30 ± 2 g) were pretreated with either distilled water (control) or RIS (3 mg/kg) for 7 days. On day 8, animals were challenged with a single dose of LPS (0.8 mg/kg) while control animals received distilled water only. The animals were sacrificed after 24 h of LPS administration and tissue samples were collected. RIS administration significantly ($p < 0.05$) reduced the LPS-induced elevated levels of lipid peroxidation product malondialdehyde (MDA), advanced protein oxidation products, and nitric oxide (NO) in the cortex. Catalase (CAT) and superoxide dismutase (SOD) levels were also diminished while the level of glutathione (GSH) was enhanced. Hippocampus data showed that RIS significantly ($p < 0.05$) reduced the LPS-induced increased levels of MDA and NO, and SOD activity. Our results suggest that LPS-induced neuronal oxidative damage can be alleviated by the pretreatment with RIS and the effect is shown presumably by scavenging of the ROS by risperidone as an antioxidant.

Keywords: brain, psychiatric disease, oxidative stress, risperidone, LPS

INTRODUCTION

The brain is a specialized restricted region separated by blood–brain barrier (BBB). Endothelial cells, astrocytes, and microglial cells are the vital elements that conserve the features of BBB. Endothelial cells create a tight junction and electrical resistance of BBB, thus selectively permitting external substances to penetrate through. On the other hand, astrocytes and microglial cells provide a distinct immune mechanism to the brain. However, under inflammatory state, BBB becomes leaky and allows the access of undesirable components, such as immune cells, inflammatory molecules, and albumin to the brain. Entrance of pro-inflammatory cytokines; tumor necrosis factor-alpha (TNF-α), interleukin-6 (IL-6) has been shown to be associated with the progression of Parkinson's disease (Smith et al., 2012), Alzheimer's disease (Minagar et al., 2002), and

schizophrenia (O'Brien et al., 2008; Al-Amin and Reza, 2014). Inflammatory cytokines (IL-1 or IL-6, TNF-α); nitric oxide (NO); and reactive oxygen species (ROS) may also mediate neurodegeneration (Gebicke-Haerter, 2001; Vallieres et al., 2002). Under inflammatory condition, microglia becomes activated resulting in the release of cytotoxic mediators; such as NO, TNF-α, IL-1β, and ROS. Overproduction of these mediators has been found to be toxic to the neurons which leads to neuronal death (Cui et al., 2012).

Inflammatory agents such as LPS (lipopolysaccharide) has been used to simulate a range of brain diseases; depression (Medeiros et al., 2015), schizophrenia (Zhu et al., 2014a), autism (Kirsten et al., 2015), Parkinson's disease (Sharma and Nehru, 2015), Alzheimer's disease (El-Sayed and Bayan, 2015) in rodents. LPS is a major component of the cell wall of gram negative bacteria and a potent activator of the inflammatory response, particularly of microglia. LPS at a dose of 1 g/ml (intraperitoneal injection) enhances the permeability of the BBB and increases the production of ROS in the brain (Zhao et al., 2014; Yu et al., 2015). While, most of the studies have discussed the inflammatory mechanism of LPS, several studies have explained LPS-induced oxidative damage in the brain (Noworyta-Sokolowska et al., 2013). For example, ROS formation is accelerated by LPS, which causes a significant alteration in NO, malondialdehyde (MDA), GSH, superoxide dismutase (SOD), and CAT levels in brain disease (Sharma and Nehru, 2015). Previous studies have shown that an increased level of pro-inflammatory cytokines (e.g., TNF-α, INF-γ, and IL-6) can be the basis of formation of ROS, MDA, AOPP, CAT, SOD, and GSH (Zhang et al., 2003; Rukmini et al., 2004; Yao et al., 2006; Dean et al., 2009).

Peripheral systemic administration of LPS has shown to produce neuro-inflammation and oxidative stress in the brain (Ho et al., 2015). Single-dose of LPS is adequate to stimulate the production of inflammatory cytokines; IL-1β, IL-6, and TNF-α in the prefrontal cortex and hippocampus (Sulakhiya et al., 2014; Ho et al., 2015; Li et al., 2015). Previous research has indicated that a single dose of systemic LPS could enhance the production of MDA – a lipid peroxidation marker, nitrite- a reactive nitrogen species marker, while reduce GSH level in the rat (Shukla et al., 2008). On the other hand, RIS, a second generation atypical antipsychotic, which is prescribed for the treatment of schizophrenia, schizoaffective disorders, bipolar disorders, and behavioral irritability in autistic patients, was used to improve the situation given that the anti-inflammatory activity of RIS is mediated through the reduction of TNF-α, INF-γ, and IL-6 (Al-Amin et al., 2013; MacDowell et al., 2013; Ajami et al., 2014), and prevention of microglial activation (Zhu et al., 2014b). The antioxidant effect of RIS has been reported previously. *In vitro* human U937 cell culture study by Chen et al. (2013) revealed that RIS inhibits LPS-induced ROS formation. A recent study on first episode drug naïve schizophrenic patient demonstrates that 11 weeks-long treatment with RIS lowers lipid peroxidation (Noto et al., 2015). Moreover, RIS treatment reduces elevated SOD level in schizophrenic patient (Zhang et al., 2012). In animal model of schizophrenia, RIS has been found to enhance the level of GSH, while reduce SOD and MDA (Stojković et al., 2012) levels. Neuroprotective properties exhibited by RIS could be attributed to microglial activation or antioxidant maintenance mechanisms in the cerebral cortex and hippocampus (Yan et al., 2014). The aim of this study was to investigate the effect of risperidone (RIS) on the LPS-induced oxidative stress in the prefrontal cortex and hippocampus.

MATERIALS AND METHODS

Animals

Male *Swiss albino* (10 weeks old weighing 30–32 g) mice ($n = 24$) were obtained and 6 mice per cage (Tecniplast, Italy) were housed in humidity controlled environment at a temperature of 25 ± 1°C on a 12 h light/day cycle, with liberal access to food and water. Prior to the testing, the mice were allowed to get habituated to the testing rooms for 1 week. The mice were divided into four groups; Ctrl (control) ($n = 6$), LPS (lipopolysaccharide, I.P.) ($n = 6$), RIS (risperidone) ($n = 6$), and RIS+LPS (risperidone + LPS) ($n = 6$). RIS was administered at a dose of 3 mg/kg once daily, for 7 days. LPS (*Escherichia coli*, Sigma Aldrich), was administered only once on day 8 at a concentration of 0.8 mg/kg with the water for injection (WFI). All experimental procedures were approved by the institutional ethical committee, North South University (NSU/PHA/2014/133-046), Dhaka, Bangladesh. Animals were handled in accordance with the international principles guiding the usage and handling of experimental animals (United States National Institute for Health Publication, 1985).

Preparation of RIS and LPS

Risperidone powder (99.8%) was obtained as a gift from General Pharmaceuticals, Ltd., Dhaka, Bangladesh. RIS was dissolved in distilled water and administered orally at a dose of 3 mg/kg (O'Sullivan et al., 2014). LPS (10 μg/μl) (Zhu et al., 2014b) was dissolved in WFI and a single dose was administered via IP route. The concentration of the administered risperidone dose was 900 μg/ml. The control animals received 100 μl of distilled water orally. LPS group received LPS at a dose of 0.8 mg/kg body weight. The working concentration of LPS was 240 μg/mL. LPS + Risperidone group received LPS (0.8 mg/kg) and Risperidone (3 mg/kg). Risperidone group received risperidone at a dose of 3 mg/kg.

Tissue Collection

Mice were euthanized using 200 μl of ketamine (50 mg/ml, ACI Pharmaceuticals, Ltd., Bangladesh). The animals were sacrificed by decapitation. The entire brain was rapidly removed cautiously and kept in a Petri dish on ice. Then cortex, hippocampus regions were dissected from the brain. Liver tissue was also collected. Homogenate of various brain regions, 10% (w/v) were prepared in phosphate buffer saline (PBS) (10 mM, pH 7.0) using Ultra-Turrax T25 (United States) homogenizer. Homogenized tissue samples were sonicated at 5 s cycle for 30 s using an ultrasonic processor and centrifuged at 10,000 rpm (RCF 11200) for 10 min. The supernatant was diluted with 0.1x PBS buffer and preserved in −20°C. The clear supernatants were collected for the biochemical analysis.

Biochemical Test

The following biochemical tests were conducted in triplicate.

Determination of the Level of MDA

Lipid peroxidation was evaluated colorimetrically as described previously (Niehaus and Samuelsson, 1968). Briefly, 0.1 ml of tissue homogenate (Tris-HCl buffer, pH 7.5) was treated with 2 ml of (1:1:1 ratio) TBA-TCA-HCl reagent (2-thiobarbituric acid 0.37%, 0.25 N HCl and 15% TCA) and placed in water bath (70°C) for 15 min and cooled. The absorbance of clear supernatant was measured against reference blank at a wavelength of 535 nm. The level of MDA was measured by using standard curve and expressed as nmol/mg of tissue.

Determination of the Level of APOP

Determination of advanced protein oxidation products (APOPs) was carried out spectrophotometrically as described by Witko-Sarsat et al., 1996). Concisely, 50 µl of plasma, which was diluted 1:2 with PBS and chloramine T (0–100 µmol/l) were used for the preparation of calibration curve. PBS was used as blank. One hundred µl of 1.16 M potassium iodide and 50 µl of acetic acid were added to each well and absorbance was measured immediately at a wavelength of 340 nm. Concentration of APOP was expressed as µmol/mg of tissue.

Determination of the Level of NO

Nitric oxide was assayed according to the method described by Tracey et al. (1995). In this assay, Griess-Illosvoy reagent was modified by using naphthyl ethylene diaminedihydrochloride (0.1% w/v) instead of 1-napthylamine (5%). The reaction mixture (3 ml) containing brain homogenates (1.5 ml) and PBS (1.5 ml) was incubated at 25°C for 15 min. Rest of the process was followed as described previously (Al-Amin et al., 2015). A pink colored chromophore was formed in diffused light. The absorbance was measured at a wavelength of 540 nm against the corresponding blank. NO level was determined by using standard curve and expressed as nmol/mg of tissue.

Determination of the Activity of CAT

The activity of catalase enzyme was assayed spectrometrically at a wavelength of 240 nm (Sinha, 1972). The reaction mixture (1.5 ml) contained 1.0 ml of 0.01 M phosphate buffer (pH 7.0), 0.1 ml of tissue homogenate (supernatant) and 0.4 ml of 2 M H_2O_2. The reaction was stopped by the addition of 2.0 ml of dichromate-acetic acid reagent (5% potassium dichromate and glacial acetic acid were mixed in 1:3 ratio). The activity of catalase was expressed as the percent change in absorption between initial and subsequent at 1 min interval.

Determination of the Activity of SOD

The activity of SOD was assayed by a modified procedure by Ma et al. (2010). Briefly, 300 µL of reaction mixture contained 50 mM sodium phosphate (pH 7.8), 13 mM methionine, 75 mM nitrobluetetrazolium (NBT), 2 mM riboflavin, 100 mM EDTA, and 20 µl of plasma. The change in absorbance of the sample was then recorded at a wavelength of 560 nm after the production of blue formazan. The activity of SOD was determined as changes of absorption between initial and subsequent at 30 s interval divided by initial absorption. Results were expressed as percentage activity of SOD enzyme.

Determination of the Level of GSH

Glutathione in the brain was evaluated based on the method described by Ellman (1959). Briefly, 1 ml of plasma was added with 2.7 ml of phosphate buffer (0.1 M, pH 8) and 0.2 ml of 5, 5-dithio-bis (2-nitrobenzoic acid). The color developed was determined immediately at 412 nm. Results of glutathione assay was expressed as µmol/mg of protein.

Data Analysis

All the biochemical tests were carried out in triplicate and data were represented as mean ± SEM (standard error of mean). One-way ANOVA was conducted followed by suitable *post hoc* test to analyze the main effect of treatment on the dependent variables among four treatment groups. Oxidative stress markers (MDA, APOP, NO, GSH, CAT, and SOD) were considered as dependent variables. All analyses were carried out in SPSS 16, and graphs were prepared using GraphPad prism (version 6.0, GraphPad Software, Inc.). The difference was considered significant when p-value was at least less than 0.05.

RESULTS

Effect of Risperidone on Lipid Peroxidation (MDA)

There was a significant main effect of risperidone treatment on MDA level [$F_{(3,20)} = 10.04$, $p < 0.001$] in the prefrontal cortex (**Figure 1A**). *Post hoc* multiple comparison test indicated an increased level of MDA in the LPS group ($M = 62.67$, $SD = 13.15$) than the control ($M = 35.11$, $SD = 5.72$), LPS+RIS ($M = 59.17$, $SD = 1.64$) and RIS ($M = 47.67$, $SD = 12.78$) groups.

There was a noticeable main effect of treatment on MDA level [$F_{(3,20)} = 6.70$, $p = 0.002$] in the hippocampus (**Figure 1B**) also. *Post hoc* analysis exhibited an increased level of MDA in the LPS ($M = 60.67$, $SD = 0.73$) than the control ($M = 47.00$, $SD = 9.83$) group. Interestingly, LPS+RIS ($M = 52.33$, $SD = 3.28$) group had a lower level of MDA than LPS ($M = 60.67$, $SD = 0.73$) group. However, there was no significant effect of treatment on MDA [$F_{(3,18)} = 2.75$, $p = 0.07$] level in the liver (**Figure 1C**).

Effect of Risperidone on Advanced Protein Oxidation Product (APOP)

There was a significant main effect of treatment on APOP [$F_{(3,20)} = 7.66$, $p < 0.001$] in the prefrontal cortex (**Figure 2A**). *Post hoc* analysis showed an enhanced level of AOPP in the LPS ($M = 144.7$, $SD = 12.86$) than the control ($M = 100.2$, $SD = 23.71$) group. LPS+RIS ($M = 113.8$, $SD = 18.56$), group showed a lower level of MDA than LPS ($M = 144.7$, $SD = 12.84$) group indicating effectiveness of risperidone treatment.

The noticeable main effect of treatment on AOPP [$F_{(3,20)} = 4.63$, $p < 0.01$] in the hippocampus is shown in **Figure 2B**. *Post hoc* test displayed an elevated level of AOPP

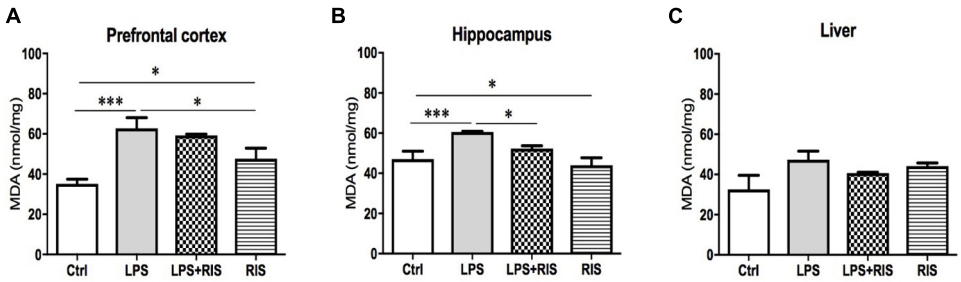

FIGURE 1 | Effect of various treatments on the level of lipid peroxidation (MDA). Groups are Ctrl (control), LPS (lipopolysaccharide), LPS+RIS (lipopolysaccharide + risperidone), and RIS (risperidone). The level of MDA was assayed from the prefrontal cortex **(A)**, hippocampus **(B)**, and liver **(C)** tissues. Values are represented as mean ± SEM. *Post hoc* multiple comparison test namely, "Newman–Keuls" test was used to compare between groups. $n = 6$ per group. $^{*}p < 0.05$, $^{**}p < 0.01$, $^{***}p < 0.001$.

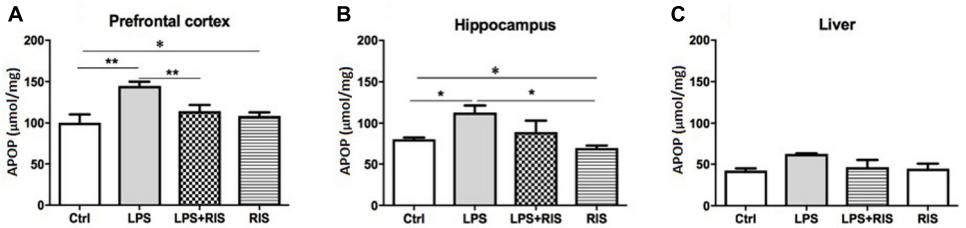

FIGURE 2 | Effect of various treatments on the level of advanced protein oxidation products (APOPs). Groups are Ctrl (control), LPS (lipopolysaccharide), LPS+RIS (lipopolysaccharide + risperidone), and RIS (risperidone). The level of AOPP was determined from the prefrontal cortex **(A)**, hippocampus **(B)**, and liver **(C)** tissues. Values are represented as mean ± SEM. *Post hoc* multiple comparison test namely, "Newman–Keuls" test was used to compare between groups. $n = 6$ per group. $^{*}p < 0.05$, $^{**}p < 0.01$, $^{***}p < 0.001$.

in the LPS ($M = 112.3$, $SD = 21.44$) than control ($M = 80.33$, $SD = 4.92$), LPS+RIS ($M = 89.17$, $SD = 34.25$), and RIS ($M = 69.50$, $SD = 7.66$) groups. No significant main effect of treatment on AOPP in the liver [$F_{(3,18)} = 2.67$, $p = 0.07$] was observed (**Figure 2C**).

Effect of Risperidone on Nitric Oxide (NO)

A significant main effect of RIS treatment on NO [$F_{(3,20)} = 15.28$, $p < 0.001$] level was observed in the prefrontal cortex (**Figure 3A**). *Post hoc* analysis showed an enhanced level of NO in the LPS ($M = 7.72$, $SD = 3.07$) than the control ($M = 1.84$, $SD = 0.19$) group. LPS+RIS ($M = 4.23$, $SD = 0.88$) group showed a decreased level of NO than LPS ($M = 7.72$, $SD = 3.07$) group.

There was a noticeable main effect of treatment on NO [$F_{(3,20)} = 259.2$, $p < 0.001$] level in the hippocampus (**Figure 3B**). *Post hoc* test disclosed an increased level of NO in the LPS group ($M = 7.60$, $SD = 0.61$) as compared to control ($M = 1.83$, $SD = 0.38$). LPS+ RIS ($M = 3.02$, $SD = 0.34$) group mice showed a diminished level of NO than LPS ($M = 7.60$, $SD = 0.61$) only group. As shown in **Figure 3C**, a significant main effect of treatment on NO [$F_{(3,19)} = 32.74$, $p < 0.001$] was observed in the liver also. *Post hoc* study showed a higher level of NO in the LPS ($M = 6.80$, $SD = 0.32$) than the control ($M = 3.55$, $SD = 1.19$) group. However, no significant difference was found between LPS+RIS ($M = 6.48$, $SD = 0.23$) and LPS mice groups.

Effect of Risperidone on Catalase (CAT) Level

The main effect of treatment on CAT was noteworthy [$F_{(3,17)} = 53.59$, $p < 0.001$] in the prefrontal cortex (**Figure 4A**). *Post hoc* analysis indicated an increased level of CAT in the LPS ($M = 85.50$, $SD = 3.83$) than the control ($M = 11.69$, $SD = 2.36$) group. Importantly, LPS+ RIS ($M = 29.73$, $SD = 11.16$) mice had a reduced level of CAT than LPS ($M = 85.50$, $SD = 3.83$) only group.

There was no significant main effect of treatment on CAT [$F_{(3,20)} = 2.58$, $p = 0.08$] in the hippocampus (**Figure 4B**). However, there was an obvious main effect of treatment on CAT [$F_{(3,19)} = 9.68$, $p < 0.001$] in the liver (**Figure 4C**). *Post hoc* multiple comparison analysis exhibited a higher activity of CAT in the LPS ($M = 65.34$, $SD = 2.55$) than control ($M = 17.48$, $SD = 3.85$), LPS+RIS ($M = 51.78$, $SD = 19.26$) and RIS ($M = 55.67$, $SD = 22.59$) groups.

Effect of Risperidone on Superoxide Dismutase (SOD) Level

Risperidone treatment showed a significantly strong main effect on SOD level [$F_{(3,20)} = 36.32$, $p < 0.001$] in the prefrontal cortex (**Figure 5A**). *Post hoc* analysis exhibited an increased SOD level in the LPS ($M = 21.43$, $SD = 0.61$) than the control ($M = 11.69$, $SD = 2.37$) group. LPS+RIS ($M = 14.86$, $SD = 2.91$) mice showed a significantly lower level of SOD than LPS

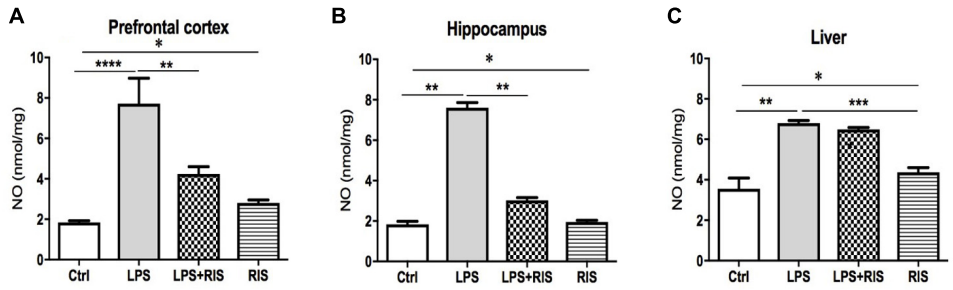

FIGURE 3 | Effect of various treatments on the level of nitric oxide (NO). Groups are Ctrl (control), LPS (lipopolysaccharide), LPS+RIS (lipopolysaccharide + risperidone), and RIS (risperidone). NO was measured from the prefrontal cortex **(A)**, hippocampus **(B)**, and liver **(C)** tissues. Values are represented as mean ± SEM. *Post hoc* multiple comparison test namely, "Newman–Keuls" test was used to compare between groups. $n = 6$ per group. $^{*}p < 0.05$, $^{**}p < 0.01$, $^{***}p < 0.001$, $^{****}p < 0.0001$.

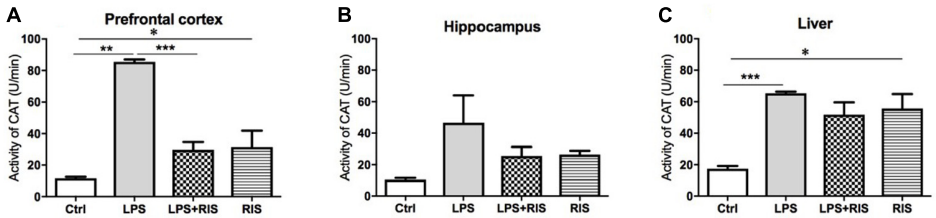

FIGURE 4 | Effect of various treatments on the activity of catalase (CAT). Groups are Ctrl (control), LPS (lipopolysaccharide), LPS+RIS (lipopolysaccharide + risperidone), and RIS (risperidone). CAT activity was measured from the prefrontal cortex **(A)**, hippocampus **(B)**, and liver **(C)** tissues. Values are represented as mean ± SEM. *Post hoc* multiple comparison test namely, "Newman–Keuls" test was used to compare between groups. $n = 6$ per group. $^{*}p < 0.05$, $^{**}p < 0.01$, $^{***}p < 0.001$.

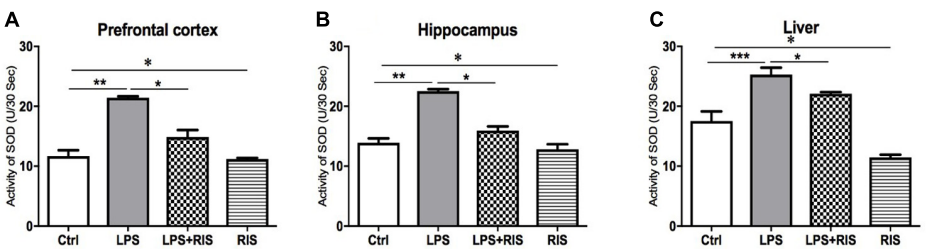

FIGURE 5 | Effect of various treatments on the activity of superoxide dismutase (SOD). Groups are Ctrl (control), LPS (lipopolysaccharide), LPS+RIS (lipopolysaccharide + risperidone), and RIS (risperidone). SOD activity was measured from the prefrontal cortex **(A)**, hippocampus **(B)**, and liver **(C)** tissues. Values are represented as mean ± SEM. *Post hoc* multiple comparison test namely, "Newman–Keuls" test was used to compare between groups. $n = 6$ per group. $^{*}p < 0.05$, $^{**}p < 0.01$, $^{***}p < 0.001$.

($M = 21.43$, $SD = 0.61$) which demonstrates the effectiveness of the treatment.

The main effect of treatment on SOD [$F_{(3,20)} = 40.94$, $p < 0.001$] level in the hippocampus is shown in **Figure 5B**. *Post hoc* analysis exhibited a significantly higher SOD level in the LPS ($M = 22.54$, $SD = 0.78$) than control ($M = 13.92$, $SD = 1.75$). Interestingly, LPS+RIS ($M = 15.94$, $SD = 0.24$) mice showed a lower SOD activity than LPS ($M = 22.54$, $SD = 0.78$) mice. There was a noticeable main effect of treatment on SOD [$F_{(3,20)} = 34.81$, $p < 0.001$] in the liver (**Figure 5C**). *Post hoc* test revealed a significant elevation of SOD in LPS group ($M = 25.30$, $SD = 2.79$) than the control ($M = 17.54$, $SD = 3.91$). By contrasts, LPS+RIS ($M = 22.08$, $SD = 0.70$) group showed a reduced SOD level than LPS group.

Effect of Risperidone on the Level of Glutathione (GSH)

There was a significant main effect of treatment on GSH [$F_{(3,20)} = 4.19$, $p = 0.018$] level in the prefrontal cortex (**Figure 6A**). *Post hoc* multiple comparison analysis displayed a reduced level of GSH in the LPS ($M = 131.5$, $SD = 2.74$) group than the control ($M = 158.2$, $SD = 5.49$). By contrasts, LPS+RIS ($M = 151.8$, $SD = 17.72$) mice showed a higher glutathione level than LPS mice.

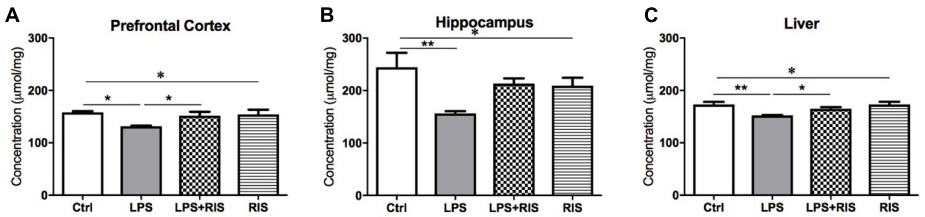

FIGURE 6 | Effect of various treatments on the level of glutathione (GSH). Groups are Ctrl (control), LPS (lipopolysaccharide), LPS+RIS (lipopolysaccharide + risperidone), and RIS (risperidone). GSH was measured from the prefrontal cortex **(A)**, hippocampus **(B)**, and liver **(C)** tissues. Values are represented as mean ± SEM. *Post hoc* multiple comparison test namely, "Newman–Keuls" test was used to compare between groups. $n = 6$ per group. $^{*}p < 0.05$, $^{**}p < 0.01$, $^{***}p < 0.001$.

There was a noticeable main effect of treatment on GSH [$F_{(3,20)} = 4.75$, $p = 0.011$] level in the hippocampus (**Figure 6B**). *Post hoc* test revealed a significantly reduced level of GSH in the LPS ($M = 156.3$, $SD = 10.60$) than the control ($M = 244.3$, $SD = 67.65$) group. Moreover, LPS+RIS ($M = 213.0$, $SD = 24.55$) mice showed no significant difference than LPS treated mice.

There was a significant main effect of treatment on GSH [$F_{(3,20)} = 5.86$, $p = 0.004$] level in the liver (**Figure 6C**). *Post hoc* test displayed a significant reduction of GSH in LPS ($M = 152.3$, $SD = 1.37$) than control ($M = 173.0$, $SD = 12.68$). In addition, LPS+RIS ($M = 165.0$, $SD = 7.64$) mice showed a significantly higher level of GSH than LPS mice.

DISCUSSION

The present study was designed to evaluate the neuroprotective effect of risperidone pre-treatment on the acute peripheral LPS-induced oxidative damage in different regions of the brain in *Swiss albino* mice. We found that the level of oxidative damage in the prefrontal cortex and hippocampus were markedly enhanced following intraperitoneal LPS administration. However, pretreatment with risperidone improved most of the oxidative stress parameters in the hippocampus and cortex.

Our results showed that LPS causes a significant detrimental effect on the prefrontal cortex and hippocampus by increasing the breakdown of lipids and proteins. Moreover, LPS enhanced the level of NO and diminished the level of glutathione. In response to this damage, the level of antioxidant enzymes, catalase and SOD were elevated It is possible that the administration of LPS increased the activity of antioxidant enzymes in the brain regions. Our results are consistent with the previous findings (Al-Amin et al., 2013; MacDowell et al., 2013; Cauwels et al., 2014; Jia et al., 2014; Su et al., 2014; Zhang et al., 2015). We also found that RIS treatment reduces LPS-induced increased MDA level in the hippocampus but not in the liver. Also, LPS+RIS group showed reduction in LPS-induced increase in NO levels in the hippocampus and cortex. These results are consistent with the studies performed on RIS (Shioda et al., 2012). Furthermore, LPS+RIS improved the level of AOPP in the cortex and hippocampus. Our results indicate that RIS treatment increased the level of glutathione in the cortex and liver, which is in agreement with a previous study (Stojković et al., 2012).

The effect of RIS treatment on the level of glutathione in LPS-induced neuroinflammatory model has not been studied in the past. However, a previous study reported that LPS reduces the level of glutathione (Yamada et al., 2006). In addition, RIS could reverse phencyclidine-induced reduced glutathione levels in the rat brain (Stojković et al., 2012). Consistent with this finding, we also report that RIS may reverse LPS-induced reduced glutathione levels.

Upon analyzing the levels of the antioxidant enzymes catalase and SOD, we found that RIS pretreatment improves the activity of catalase in the cortex and hippocampus.

Our observation that the level of SOD was improved in the brain is consistent with several previous studies (Zhang et al., 2012; Yan et al., 2014). All these findings taken together, asserts that pretreatment with RIS can rescue the LPS-induced oxidative stress in the brain.

The damaging effect of LPS due to oxidative stress in the brain has been demonstrated in the previous studies as well (Shukla et al., 2008; Del Angel-Meza et al., 2011; Tomaz et al., 2014; Ho et al., 2015). The organelle that encounters the oxidative stress most is the mitochondria. Mitochondria produce energy by the breakdown of glucose with the help of oxygen. It is noted that the brain requires almost 20% of the total oxygen intake to produce energy. Mitochondria in the neural cells are constantly producing highly reactive free radicals as by product during the metabolic processes. The excess amount of free radicals may cause the damage to proteins, lipids and even the neural function (Lohr, 1991; Lohr and Browning, 1995). Unfortunately, neural cells are poorly equipped to defend against oxidative damage (Mahadik and Mukherjee, 1996). The underlying reason of this poor defensive system is due to the sensitivity of lipids to the free radicals, failure of adult neurons to reproduce and compensate destroyed DNA and poor activity of antioxidant enzymes namely glutathione, catalase, and SOD (Cohen, 1984). Impaired antioxidant defense system has been reported to be associated with neuropsychiatric diseases (Lohr, 1991; Lohr and Browning, 1995; Salim, 2014), such as, schizophrenia (Li et al., 2006), autism (McGinnis, 2004), depression (Michel et al., 2012), bipolar mood disorder (Erdem et al., 2014). In this study, treatment with risperidone showed decrease in the LPS-induced high levels of oxidative markers in the distinct brain regions. We report that the administration of RIS in LPS-induced stress model might be promising in improving the deficits due to oxidative stress.

Accumulating evidences suggest the neuroprotective potential of RIS (Lauterbach et al., 2010) via antioxidant immunomodulatory activity. A study with 22 schizophrenic patients demonstrated that RIS possesses significant antioxidant activity (Gilca et al., 2014). Moreover, RIS treatment lowers lipid peroxidation on 51 first episode schizophrenic patients treated with risperidone for 11 weeks. Noto et al. (2015), suggested that RIS enhances antioxidant defense against lipid peroxidation possibly through PON1 (paraoxonase 1) antioxidant enzyme. Immunomodulatory potential of RIS was observed when given with celecoxib as an add-on therapy in schizophrenia (Müller et al., 2002). Animal model of gerbil stroke revealed that post-treatment with RIS provides neuroprotection presumably via attenuation of microglial activation as well as maintenance of the antioxidants (Yan et al., 2014). RIS also shows the antioxidant activity by lowering the glutathione level in phencyclidine-treated rat brain (Stojković et al., 2012). RIS has also been found effective in preventing microglia activation and improves behavioral deficits when LPS was administered directly to the hippocampus in neonatal rats (Zhu et al., 2014b).

In this study, LPS was administered only once on day 8. We have observed that acute LPS administration increased immobility time in the behavioral test. We have not incorporated behavioral data in this study since acute LPS administration causes immediate effect on behavioral level. We have conducted open field test and tail suspension test; both tests have shown a significant increase in immobile phase following LPS administration (data not shown) as consistent with the previous studies (Frenois et al., 2007; O'Connor et al., 2008). LPS at a dose of 25, 50, 100, or 1000 μg/kg caused suppressed behavior in the open field test (Yirmiya et al., 1994), while LPS at 0.63 or 1.25 μg/kg exhibited diminished locomotor activity at 2 h (Dunn and Swiergiel, 2005), reduced distance traveled at 6 h and poor exploration behavior in 24 h (Biesmans et al., 2013). It is noted that we used 0.8 mg/kg (800 μg/kg) (El-Sayed and Bayan, 2015) single dose to induce behavioral impairment. LPS at a dose of 1 and 5 μg/kg once dose has been shown to produce long immobility time in the TST (Dunn and Swiergiel, 2005).

Lipopolysaccharide directly enhances the production of inflammatory cytokines. Therefore, the determination of the cytokines in this study could have provided insights into the effect of RIS in the LPS-induced impairment at the molecular level. Despite this limitation, our study is novel in some respects. To the best of our knowledge, this study is the first to report the role of RIS in the LPS-induced six oxidative stress markers in the two important brain regions that are involved in cognitive function, learning and memory formation. Moreover, liver data provided additional evidence on overall condition besides the brain. Our findings further support the hypothesis that RIS possesses a significant antioxidant property that could be studied further in details. There are several possible explanations in favor of the current outcomes (i) RIS may regulate the production of GSH, CAT, and SOD to combat against ROS, (ii) RIS might diminish the formation of ROS, (iii) RIS, itself is involved in neutralizing the already formed ROS, (iv) RIS is possibly associated with the regulation of GSH, SOD, and CAT forming genes. Future work can be undertaken to gain insight into the mechanisms underlying the antioxidant activity of RIS in improving the stress condition induced by LPS.

CONCLUSION

The present study was designed to determine the effect of risperidone on systemic LPS-induced oxidative damage in the specific brain regions and liver. The study has demonstrated that risperidone is effective in reversing LPS-mediated behavioral impairment and subsequent oxidative stress. In conclusion, our findings suggest that risperidone may possess some neuro-protective effects through reduction of oxidative stress parameters. The results of this research support the notion that RIS diminishes the production of ROS possibly through the regulation of antioxidant enzymes in the brain. We further propose that RIS may contribute to the improvement in brain diseases due to its protective effects against the endotoxin-linked oxidative damage in the brain.

AUTHOR CONTRIBUTIONS

MAA-A and HMR participated in the design of the experimental work. MAA-A, MFRC performed experiments and analyzed the data. ASC and TRC provided technical support. PJ and HMR contributed to preparation, editing and critically revising the manuscript for important intellectual content. MK, MA and HMR corrected drafts and obtained the funding. SMA contributed in the manuscript during the revision period and shared his experience in editing the manuscript. All authors read and approved the final manuscript.

ACKNOWLEDGMENTS

The authors are very grateful to the Deanship of Scientific Research and Research Centre, College of Pharmacy, King Saud University, Riyadh, Saudi Arabia for their funding and support.

REFERENCES

Ajami, A., Abedian, F., Hamzeh Hosseini, S., Akbarian, E., Alizadeh-Navaei, R., and Taghipour, M. (2014). Serum TNF-alpha, IL-10 and IL-2 in schizophrenic patients before and after treatment with risperidone and clozapine. *Iran. J. Immunol.* 11, 200–209.

Al-Amin, M. M., Rahman, M. M., Khan, F. R., Zaman, F., and Mahmud Reza, H. (2015). Astaxanthin improves behavioral disorder and oxidative stress in prenatal valproic acid-induced mice model of autism. *Behav. Brain Res.* 286, 112–121. doi: 10.1016/j.bbr.2015.02.041

Al-Amin, M. M., and Reza, H. M. (2014). Neuroinflammation: contemporary anti-inflammatory approaches. *Neurosciences* 19, 87–92.

Al-Amin, M. M., Uddin, M. M. N., and Mahmud Reza, H. (2013). Effects of antipsychotics on the inflammatory response system of patients with schizophrenia in peripheral blood mononuclear cell cultures. *Clin. Psychopharmacol. Neurosci.* 11, 144–151. doi: 10.9758/cpn.2013.11.3.144

Biesmans, S., Meert, T. F., Bouwknecht, J. A., Acton, P. D., Davoodi, N., De Haes, P., et al. (2013). Systemic immune activation leads to neuroinflammation and sickness behavior in mice. *Mediators Inflamm.* 2013:271359. doi: 10.1155/2013/271359

Cauwels, A., Bultinck, J., De Zwaef, R., Vandendriessche, B., Magez, S., and Brouckaert, P. (2014). Nitric oxide production by endotoxin preparations in TLR4-deficient mice. *Nitric Oxide* 36, 36–43. doi: 10.1016/j.niox.2013.11.001

Chen, M. L., Wu, S., Tsai, T. C., Wang, L. K., and Tsai, F. M. (2013). Regulation of macrophage immune responses by antipsychotic drugs. *Immunopharmacol. Immunotoxicol.* 35, 573–580. doi: 10.3109/08923973.2013.828744

Cohen, G. (1984). Oxy-radical toxicity in catecholamine neurons. *Neurotoxicology* 5, 77–82.

Cui, Y. Q., Jia, Y. J., Zhang, T., Zhang, Q. B., and Wang, X. M. (2012). Fucoidan protects against lipopolysaccharide-induced rat neuronal damage and inhibits the production of proinflammatory mediators in primary microglia. *CNS Neurosci. Ther.* 18, 827–833. doi: 10.1111/j.1755-5949.2012.00372.x

Dean, O. M., van den Buuse, M., Bush, A. I., Copolov, D. L., Ng, F., Dodd, S., et al. (2009). A role for glutathione in the pathophysiology of bipolar disorder and schizophrenia? Animal models and relevance to clinical practice. *Curr. Med. Chem.* 16, 2965–2976. doi: 10.2174/092986709788803060

Del Angel-Meza, A. R., Dávalos-Marín, A. J., Ontiveros-Martinez, L. L., Ortiz, G. G., Beas-Zarate, C., Chaparro-Huerta, V., et al. (2011). Protective effects of tryptophan on neuro-inflammation in rats after administering lipopolysaccharide. *Biomed. Pharmacother.* 65, 215–219. doi: 10.1016/j.biopha.2011.02.008

Dunn, A. J., and Swiergiel, A. H. (2005). Effects of interleukin-1 and endotoxin in the forced swim and tail suspension tests in mice. *Pharmacol. Biochem. Behav.* 81, 688–693. doi: 10.1016/j.pbb.2005.04.019

Ellman, G. L. (1959). Tissue sulfhydryl groups. *Arch. Biochem. Biophys.* 82, 70–77. doi: 10.1016/0003-9861(59)90090-6

El-Sayed, N. S., and Bayan, Y. (2015). Possible role of resveratrol targeting estradiol and neprilysin pathways in lipopolysaccharide model of Alzheimer disease. *Adv. Exp. Med. Biol.* 822, 107–118. doi: 10.1007/978-3-319-08927-0_12

Erdem, M., Akarsu, S., Pan, E., and Kurt, G. Y. (2014). Bipolar disorder and oxidative stress. *J. Mood Disord.* 4, 70–79. doi: 10.5455/jmood.20131205063815

Frenois, F., Moreau, M., O'Connor, J., Lawson, M., Micon, C., Lestage, J., et al. (2007). Lipopolysaccharide induces delayed FosB/DeltaFosB immunostaining within the mouse extended amygdala, hippocampus and hypothalamus, that parallel the expression of depressive-like behavior. *Psychoneuroendocrinology* 32, 516–531. doi: 10.1016/j.psyneuen.2007.03.005

Gebicke-Haerter, P. J. (2001). Microglia in neurodegeneration: molecular aspects. *Microsc. Res. Tech.* 54, 47–58. doi: 10.1002/jemt.1120

Gilca, M., Piriu, G., Gaman, L., Delia, C., Iosif, L., Atanasiu, V., et al. (2014). A study of antioxidant activity in patients with schizophrenia taking atypical antipsychotics. *Psychopharmacology* 231, 4703–4710. doi: 10.1007/s00213-014-3624-0

Ho, Y. H., Lin, Y. T., Wu, C. W., Chao, Y. M., Chang, A. Y., and Chan, J. Y. (2015). Peripheral inflammation increases seizure susceptibility via the induction of neuroinflammation and oxidative stress in the hippocampus. *J. Biomed. Sci.* 22:46. doi: 10.1186/s12929-015-0157-8

Jia, M., Jing, Y., Ai, Q., Jiang, R., Wan, J., Lin, L., et al. (2014). Potential role of catalase in mice with lipopolysaccharide/D-galactosamine-induced fulminant liver injury. *Hepatol. Res.* 44, 1151–1158. doi: 10.1111/hepr.12220

Kirsten, T. B., Queiroz-Hazarbassanov, N., Bernardi, M. M., and Felicio, L. F. (2015). Prenatal zinc prevents communication impairments and BDNF disturbance in a rat model of autism induced by prenatal lipopolysaccharide exposure. *Life Sci.* 130, 12–17. doi: 10.1016/j.lfs.2015.02.027

Lauterbach, E. C., Victoroff, J., Coburn, K. L., Shillcutt, S. D., Doonan, S. M., and Mendez, M. F. (2010). Psychopharmacological neuroprotection in neurodegenerative disease: assessing the preclinical data. *J. Neuropsychiatry Clin. Neurosci.* 22, 8–18. doi: 10.1176/appi.neuropsych.22.1.8

Li, H.-C., Chen, Q.-Z., Ma, Y., and Zhou, J.-F. (2006). Imbalanced free radicals and antioxidant defense systems in schizophrenia: a comparative study. *J. Zhejiang Univ. Sci. B* 7, 981–986. doi: 10.1631/jzus.2006.B0981

Li, R., Zhao, D., Qu, R., Fu, Q., and Ma, S. (2015). The effects of apigenin on lipopolysaccharide-induced depressive-like behavior in mice. *Neurosci. Lett.* 594, 17–22. doi: 10.1016/j.neulet.2015.03.040

Lohr, J. B. (1991). Oxygen radicals and neuropsychiatric illness. Some speculations. *Arch. Gen. Psychiatry* 48, 1097–1106. doi: 10.1001/archpsyc.1991.01810360061009

Lohr, J. B., and Browning, J. A. (1995). Free radical involvement in neuropsychiatric illnesses. *Psychopharmacol. Bull.* 31, 159–165.

Ma, L., Liu, J., Li, N., Wang, J., Duan, Y., Yan, J., et al. (2010). Oxidative stress in the brain of mice caused by translocated nanoparticulate TiO2 delivered to the abdominal cavity. *Biomaterials* 31, 99–105. doi: 10.1016/j.biomaterials.2009.09.028

MacDowell, K. S., García-Bueno, B., Madrigal, J. L., Parellada, M., Arango, C., Micó, J. A., et al. (2013). Risperidone normalizes increased inflammatory parameters and restores anti-inflammatory pathways in a model of neuroinflammation. *Int. J. Neuropsychopharmacol.* 16, 121–135. doi: 10.1017/S1461145711001775

Mahadik, S. P., and Mukherjee, S. (1996). Free radical pathology and antioxidant defense in schizophrenia: a review. *Schizophr. Res.* 19, 1–17. doi: 10.1016/0920-9964(95)00049-6

McGinnis, W. R. (2004). Oxidative stress in autism. *Altern. Ther. Health Med.* 10, 22–36.

Medeiros, I. U., Ruzza, C., Astha, L., Guerrini, R., Romão, P. R. T., Gavioli, E. C., et al. (2015). Blockade of nociceptin/orphanin FQ receptor signaling reverses LPS-induced depressive-like behavior in mice. *Peptides* 72, 95–103. doi: 10.1016/j.peptides.2015.05.006

Michel, T. M., Pulschen, D., and Thome, J. (2012). The role of oxidative stress in depressive disorders. *Curr. Pharm. Des.* 18, 5890–5899. doi: 10.2174/138161212803523554

Minagar, A., Shapshak, P., Fujimura, R., Ownby, R., Heyes, M., and Eisdorfer, C. (2002). The role of macrophage/microglia and astrocytes in the pathogenesis of three neurologic disorders: HIV-associated dementia, Alzheimer disease, and multiple sclerosis. *J. Neurol. Sci.* 202, 13–23. doi: 10.1016/S0022-510X(02)00207-1

Müller, N., Riedel, M., Scheppach, C., Brandstätter, B., Sokullu, S., Krampe, K., et al. (2002). Beneficial antipsychotic effects of celecoxib add-on therapy compared to risperidone alone in schizophrenia. *Am. J. Psychiatry* 159, 1029–1034. doi: 10.1176/appi.ajp.159.6.1029

Niehaus, W. G., and Samuelsson, B. (1968). Formation of malonaldehyde from phospholipid arachidonate during microsomal lipid peroxidation. *Eur. J. Biochem.* 6, 126–130. doi: 10.1111/j.1432-1033.1968.tb00428.x

Noto, C., Ota, V. K., Gadelha, A., Noto, M. N., Barbosa, D. S., Bonifácio, K. L., et al. (2015). Oxidative stress in drug naive first episode psychosis and antioxidant effects of risperidone. *J. Psychiatr. Res.* 68, 210–216. doi: 10.1016/j.jpsychires.2015.07.003

Noworyta-Sokolowska, K., Gorska, A., and Golembiowska, K. (2013). LPS-induced oxidative stress and inflammatory reaction in the rat striatum. *Pharmacol. Rep.* 65, 863–869. doi: 10.1016/S1734-1140(13)71067-3

O'Brien, S. M., Scully, P., and Dinan, T. G. (2008). Increased tumor necrosis factor-alpha concentrations with interleukin-4 concentrations in exacerbations of schizophrenia. *Psychiatry Res.* 160, 256–262. doi: 10.1016/j.psychres.2007.11.014

O'Connor, J. C., Lawson, M. A., André, C., Moreau, M., Lestage, J., Castanon, N., et al. (2008). Lipopolysaccharide-induced depressive-like behavior is mediated by indoleamine 2,3-dioxygenase activation in mice. *Mol. Psychiatry* 14, 511–522. doi: 10.1038/sj.mp.4002148

O'Sullivan, D., Green, L., Stone, S., Zareie, P., Kharkrang, M., Fong, D., et al. (2014). Treatment with the antipsychotic agent, risperidone, reduces disease severity in experimental autoimmune encephalomyelitis. *PLoS One* 9:e104430. doi: 10.1371/journal.pone.0104430

Rukmini, M. S., D'Souza, B., and D'Souza, V. (2004). Superoxide dismutase and catalase activities and their correlation with malondialdehyde in schizophrenic patients. *Indian J. Clin. Biochem.* 19, 114–118. doi: 10.1007/BF02894268

Salim, S. (2014). Oxidative stress and psychological disorders. *Curr. Neuropharmacol.* 12, 140–147. doi: 10.2174/1570159X11666131120230309

Sharma, N., and Nehru, B. (2015). Characterization of the lipopolysaccharide induced model of Parkinson's disease: role of oxidative stress and neuroinflammation. *Neurochem. Int.* 87, 92–105. doi: 10.1016/j.neuint.2015.06.004

Shioda, K., Nisijima, K., Kasai, M., Yoshino, T., and Kato, S. (2012). Risperidone attenuates the increase of extracellular nitric oxide and glutamate levels in

serotonin syndrome animal models. *Neurosci. Lett.* 528, 22–26. doi: 10.1016/j.neulet.2012.08.083

Shukla, R., Tyagi, E., and Kumar, R. (2008). Protective effect of COX and NOS inhibitors on LPS induced oxidative stress in rat. *Ann. Neurosci.* 15, 6–10. doi: 10.5214/ans.0972.7531.2008.150102

Sinha, A. K. (1972). Colorimetric assay of catalase. *Anal. Biochem.* 47, 389–394. doi: 10.1016/0003-2697(72)90132-7

Smith, A. J., Das, A., Ray, K. S., and Banik, N. L. (2012). Role of pro-inflammatory cytokines released from microglia in neurodegenerative diseases. *Brain Res. Bull.* 87, 10–20. doi: 10.1016/j.brainresbull.2011.10.004

Stojković, T., Radonjić, N. V., Velimirović, M., Jevtić, G., Popović, V., Doknić, M., et al. (2012). Risperidone reverses phencyclidine induced decrease in glutathione levels and alterations of antioxidant defense in rat brain. *Prog. Neuropsychopharmacol. Biol. Psychiatry* 39, 192–199. doi: 10.1016/j.pnpbp.2012.06.013

Su, Z., Mo, Z., Liao, J.-B., Feng, X.-X., Liang, Y.-Z., Zhang, X., et al. (2014). Usnic acid protects LPS-induced acute lung injury in mice through attenuating inflammatory responses and oxidative stress. *Int. Immunopharmacol.* 22, 371–378. doi: 10.1016/j.intimp.2014.06.043

Sulakhiya, K., Kumar, P., Jangra, A., Dwivedi, S., Hazarika, N. K., Baruah, C. C., et al. (2014). Honokiol abrogates lipopolysaccharide-induced depressive like behavior by impeding neuroinflammation and oxido-nitrosative stress in mice. *Eur. J. Pharmacol.* 744, 124–131. doi: 10.1016/j.ejphar.2014.09.049

Tomaz, V. S., Cordeiro, R. C., Costa, A. M., de Lucena, D. F., Nobre Júnior, H. V., de Sousa, F. C., et al. (2014). Antidepressant-like effect of nitric oxide synthase inhibitors and sildenafil against lipopolysaccharide-induced depressive-like behavior in mice. *Neuroscience* 268, 236–246. doi: 10.1016/j.neuroscience.2014.03.025

Tracey, W. R., Tse, J., and Carter, G. (1995). Lipopolysaccharide-induced changes in plasma nitrite and nitrate concentrations in rats and mice: pharmacological evaluation of nitric oxide synthase inhibitors. *J. Pharmacol. Exp. Ther.* 272, 1011–1015.

Vallieres, L., Campbell, I. L., Gage, F. H., and Sawchenko, P. E. (2002). Reduced hippocampal neurogenesis in adult transgenic mice with chronic astrocytic production of interleukin-6. *J. Neurosci.* 22, 486–492. doi: 10.1523/JNEUROSCI.22-02-00486.2002

Witko-Sarsat, V., Friedlander, M., Capeillere-Blandin, C., Nguyen-Khoa, T., Nguyen, A. T., Zingraff, J., et al. (1996). Advanced oxidation protein products as a novel marker of oxidative stress in uremia. *Kidney Int.* 49, 1304–1313. doi: 10.1038/ki.1996.186

Yamada, H., Arai, T., Endo, N., Yamashita, K., Fukuda, K., Sasada, M., et al. (2006). LPS-induced ROS generation and changes in glutathione level and their relation to the maturation of human monocyte-derived dendritic cells. *Life Sci.* 25, 926–933. doi: 10.1016/j.lfs.2005.05.106

Yan, B. C., Park, J. H., Ahn, J. H., Kim, I. H., Park, O. K., Lee, J.-C., et al. (2014). Neuroprotection of posttreatment with risperidone, an atypical antipsychotic drug, in rat and gerbil models of ischemic stroke and the maintenance of antioxidants in a gerbil model of ischemic stroke. *J. Neurosci. Res.* 92, 795–807. doi: 10.1002/jnr.23360

Yao, J. K., Leonard, S., and Reddy, R. (2006). Altered glutathione redox state in schizophrenia. *Dis. Markers* 22, 83–93. doi: 10.1155/2006/248387

Yirmiya, R., Rosen, H., Donchin, O., and Ovadia, H. (1994). Behavioral effects of lipopolysaccharide in rats: involvement of endogenous opioids. *Brain Res.* 648, 80–86. doi: 10.1016/0006-8993(94)91908-9

Yu, H. Y., Cai, Y. B., and Liu, Z. (2015). Activation of AMPK improves lipopolysaccharide-induced dysfunction of the blood-brain barrier in mice. *Brain Inj.* 29, 777–784. doi: 10.3109/02699052.2015.1004746

Zhang, X. Y., Cao, J. B., Zhang, L. M., Li, Y. F., and Mi, W. D. (2015). Deferoxamine attenuates lipopolysaccharide-induced neuroinflammation and memory impairment in mice. *J. Neuroinflammation* 12:20. doi: 10.1186/s12974-015-0238-3

Zhang, X. Y., Zhou, D. F., Cao, L. Y., Chen, D. C., Zhu, F. Y., and Wu, G. Y. (2003). Blood superoxide dismutase level in schizophrenic patients with tardive dyskinesia: association with dyskinetic movements. *Schizophr. Res.* 62, 245–250. doi: 10.1016/S0920-9964(02)00352-3

Zhang, X. Y., Zhou, D. F., Shen, Y. C., Zhang, P. Y., Zhang, W. F., Liang, J., et al. (2012). Effects of risperidone and haloperidol on superoxide dismutase and nitric oxide in schizophrenia. *Neuropharmacology* 62, 1928–1934. doi: 10.1016/j.neuropharm.2011.12.014

Zhao, Z., Hu, J., Gao, X., Liang, H., and Liu, Z. (2014). Activation of AMPK attenuates lipopolysaccharide-impaired integrity and function of blood-brain barrier in human brain microvascular endothelial cells. *Exp. Mol. Pathol.* 97, 386–392. doi: 10.1016/j.yexmp.2014.09.006

Zhu, F., Zhang, L., Ding, Y. Q., Zhao, J., and Zheng, Y. (2014a). Neonatal intrahippocampal injection of lipopolysaccharide induces deficits in social behavior and prepulse inhibition and microglial activation in rats: implication for a new schizophrenia animal model. *Brain Behav. Immun.* 38, 166–174. doi: 10.1016/j.bbi.2014.01.017

Zhu, F., Zheng, Y., Ding, Y., Liu, Y., Zhang, X., Wu, R., et al. (2014b). Minocycline and risperidone prevent microglia activation and rescue behavioral deficits induced by neonatal intrahippocampal injection of lipopolysaccharide in rats. *PLoS One* 9:e93966. doi: 10.1371/journal.pone.0093966

Conflict of Interest Statement: The authors declare that the research was conducted in the absence of any commercial or financial relationships that could be construed as a potential conflict of interest.

Advantages of publishing in Frontiers

OPEN ACCESS
Articles are free to read for greatest visibility and readership

FAST PUBLICATION
Around 90 days from submission to decision

HIGH QUALITY PEER-REVIEW
Rigorous, collaborative, and constructive peer-review

TRANSPARENT PEER-REVIEW
Editors and reviewers acknowledged by name on published articles

Frontiers
Avenue du Tribunal-Fédéral 34
1005 Lausanne | Switzerland

Visit us: www.frontiersin.org
Contact us: info@frontiersin.org | +41 21 510 17 00

REPRODUCIBILITY OF RESEARCH
Support open data and methods to enhance research reproducibility

DIGITAL PUBLISHING
Articles designed for optimal readership across devices

FOLLOW US
@frontiersin

IMPACT METRICS
Advanced article metrics track visibility across digital media

EXTENSIVE PROMOTION
Marketing and promotion of impactful research

LOOP RESEARCH NETWORK
Our network increases your article's readership